INFORMATION TO USERS

Order Number 9313839

Burial depth and lithofacies control of stylolite development in the Mississippian Salem Limestone, Illinois Basin

Losonsky, George, Ph.D.

University of Cincinnati, 1992

U·M·I
300 N. Zeeb Rd.
Ann Arbor, MI 48106

BURIAL DEPTH AND LITHOFACIES CONTROL OF STYLOLITE DEVELOPMENT IN THE MISSISSIPPIAN SALEM LIMESTONE, ILLINOIS BASIN

A Dissertation submitted to the

Division of Graduate Studies and Research
of the University of Cincinnati

in partial fulfillment of the
requirements of the degree of

DOCTOR OF PHILOSOPHY

in the Department of Geology
of the College of Arts and Sciences

1992

by

George Losonsky

A.B., Oberlin College, 1980

M.S., University of Cincinnati, 1983

Committee Chair: Dr. Wayne A. Pryor

UNIVERSITY OF CINCINNATI

November 13 , 19 92

I, George Losonsky ,
hereby submit this as part of the requirements for the degree of:

Doctor of Philosophy

in Geology Department

It is entitled Burial Depth and Lithofacies Control of Stylolite Development in the Mississippian Salem Limestone, Illinois Basin.

Approved by:

ABSTRACT

Stylolites in twelve stratigraphic sections of the Salem Limestone, distributed throughout the Illinois Basin, provide clues to their origin and development. Chemical and X-ray diffraction analyses reveal that stylolite seam material contains organic matter and clay minerals too sparse or absent in the host limestone to be considered solely as insoluble residue. Stylolite distribution in various lithofacies suggests that stylolites develop along thin sedimentary layers rich in organic matter and clay minerals. Stylolite density (vertical distribution) mimics the distribution of organic-rich sedimentary layers: sparse but thick in grainstone, and abundant but thin in packstone and wackestone. Many stylolites grade laterally into organic-rich layers, or hummocky seams. Thicknesses of stylolite caps and hummocky seams are approximately equal in the same host rock, but hummocky seams tend to be more laterally continuous. Stylolite density in packstone increases with burial depth, whereas hummocky seam density decreases. Hummocky seam thickness does not change with depth. Stylolite column height in grainstone, which is sparse in hummocky seams, increases with depth, whereas stylolite density does not increase. This list of observations supports the hypothesis that stylolites develop along pre-existing, organic-rich layers, or hummocky seams, rather than nucleating in pure host rock and creating

organic-rich seams as accumulations of insoluble residue. Volumetric calculations indicate that the contribution of stylolites to pore-filling cement is 5 to 25 percent throughout the Illinois Basin.

Acknowledgements

I thank Dr. Wayne Pryor for accepting the position of advisory committee chairperson. I thank him and the entire advisory committee, including Drs. John Grover, Warren Huff, and Frank Meeks, for their advice and encouragement. I thank my family for their patience and moral support.

TABLE OF CONTENTS

List of Figures

List of Plates

List of Appendices

CHAPTER 1

INTRODUCTION

This dissertation describes and analyzes bedding-parallel stylolites in the Mississippian-aged Salem Limestone of the Illinois Basin in southern Illinois and Indiana (Figure 1). Previous studies in Mississippian-aged rocks of the Appalachian Basin (Losonsky, 1983a, 1983b) have shown that bedding-perpendicular (tectonic) stylolites develop along pre-existing, regularly spaced fracture planes or joints formed during previous tectonic stress episodes (Losonsky, 1985).

With this conclusion in mind, a major purpose of this study is to establish whether bedding-parallel stylolites also develop along pre-existing surfaces or are solely the product of passive accumulation of insoluble residues along planes of dissolution. Correlations between stylolite density (abundance) and stylolite seam thickness on one hand, and various depositional, lithological, mineralogical and paleontological parameters on the other, presented in this dissertation, suggest that bedding-parallel stylolites in the Salem Limestone develop along thin sedimentary layers rich in organic matter and clay minerals. It appears that only part of a typical stylolite seam consists of insoluble residue. Calculation of the volume of rock dissolved along

Figure 1.

Location map of the Illinois Basin, showing locations of outcrops and cores used in this dissertation.

SALEM LIMESTONE OUTCROP AND CORE LOCATIONS

With Depths to Top of Salem Formation, in Feet (Outcrop Depths are Zero)

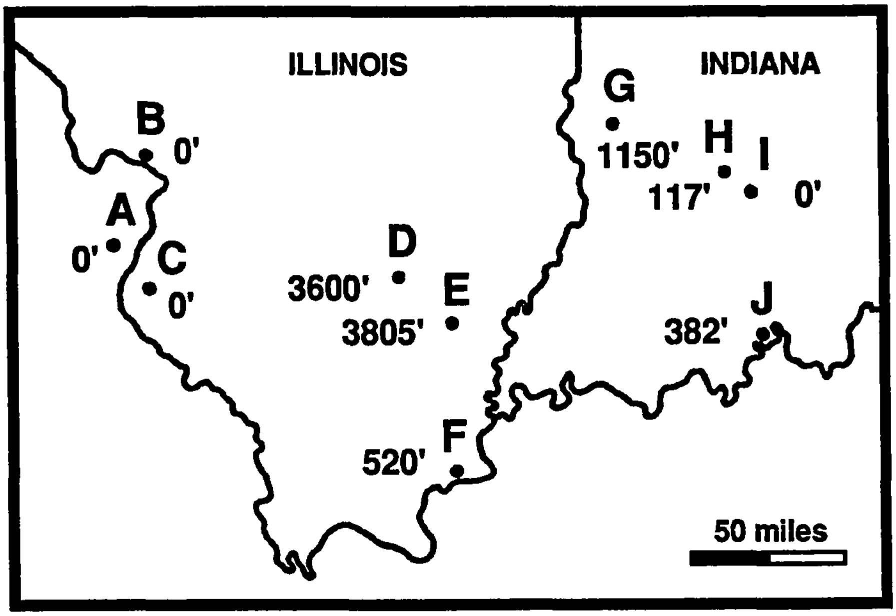

a stylolite must take into account the fraction of the stylolite seam that represents sedimentary deposition.

Definition of a Stylolite

In the numerous definitions of stylolites that have appeared in the literature since the earliest references in the nineteenth century (see Bibliography), two issues emerge: are the columnar protrusions necessary features of stylolites; and does "stylolite" refer to the individual columns or to the entire surface containing the columns?

The recent literature is in agreement over the latter point: "stylolite" refers to the entire surface, and not to the individual columnar protrusion (e.g., Wanless, 1979). Less clear is the resolution of the former dispute, but there appears to be a general trend in the past 20 years of accepting noncolumnar, wavy or hummocky surfaces as stylolites, provided they contain a film of clay or organic matter (e.g., Wanless, 1979; see Bibliography). In the case of bedding-perpendicular (tectonic) stylolites, even smooth, clay-lined surfaces have been referred to as stylolites, under the assumption that they represent an evenly spaced "solution cleavage," (e.g., Nickelsen, 1972; Alvarez et al., 1978).

This study uses the term "stylolites" to refer to surfaces with clearly developed, columnar or serrate protrusions, regardless of the thickness or distribution of clay or organic matter along the surfaces. In contrast, this study uses the term "hummocky seams" to refer to non-serrate, non-columnar, undulose surfaces characterized by the presence of a film or thin layer of clay or organic matter.

This usage avoids any genetic connotation in the term "stylolite" while remaining true to the originally intended meaning of the term, which derives from the greek word "stylos," meaning "column."

Field Classification of Stylolites

A practical field classification of stylolites focusses on three aspects of stylolite morphology: (1) geometry of stylolite columns, (2) symmetry of stylolite columns, and (3) shape of stylolite caps (Figure 2).

Shape and size define the geometry of a stylolite column. The shape can be (1) cylindrical, (2) conical, or (3) serrate. In addition, some stylolite-like seams exhibit hummocky shapes, but lack well-defined columns. Such features are referred to as "hummocky seams."

A cylindrical column, like a cylindrical fold, possesses an axis of rotational symmetry, everywhere at a constant distance from the walls of the column (Figure 2).

A conical column also possesses an axis of rotational symmetry, but the walls of the column converge toward a point. Such a column resembles a cone with truncated apex (Figure 2).

A serrate column has a point, or peak, instead of a cap. It is essentially a conical column, with walls extending to the apex of the cone. A row of serrate columns resembles the teeth of a saw (Figure 2).

The field description of stylolite column geometry includes column shape as well as size. Column size is measured in terms of the column height and width. Column height is measured along the axis of symmetry--connecting the base and cap of the column. Column width is measured at the base of the column. For serrate columns, the base is defined in cross section as the line connecting adjacent peaks and troughs (upward and downward pointing teeth; Figure 2).

An unusual stylolite column shape is that of a compound, or stacked, stylolite. Such a stylolite has the

Figure 2.

List of symbols and stylolite classification scheme, showing idealized stylolite morphologies and symmetries observed in the Salem Limestone, Illinois Basin. This figure serves as legend to Plates 1-12.

LIST OF SYMBOLS AND STYLOLITE CLASSIFICATION SCHEME

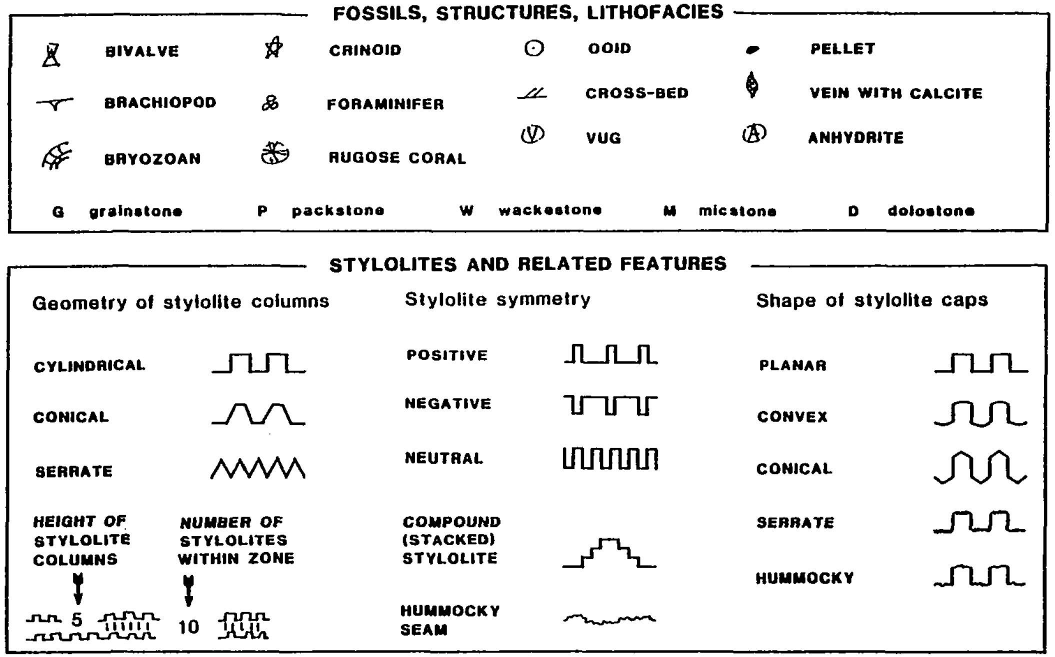

cross-sectional shape of a stepped pyramid, with the distance between the axis of symmetry and the column wall decreasing with distance in steps from the base of the column (Figure 2).

Stylolite symmetry refers to the distribution of variously sized columns relative to the plane perpendicular to the rotational axes of the columns. This distribution determines the stratigraphic direction in which stylolite columns appear to point. Asymmetry exits only if adjacent columns are unequal in width. The narrower columns point either upward or downward, stratigraphically. A stylolite may exhibit (1) neutral symmetry, (2) positive asymmetry, or (3) negative asymmetry.

A symmetrical stylolite either (1) has columns of equal width, so that columns do not appear to point in any direction; or (2) has columns of unequal width, but they appear to point randomly upward or downward (Figure 2).

Positive asymmetry requires that the majority of narrow columns points in the stratigraphically upward direction (Figure 2). The "majority" must be well over 50%, since asymmetry must be obvious visually.

Negative asymmetry requires that the majority of narrow columns points stratigraphically downward (Figure 2). Again, the "majority" must include significantly more than 50%, making the asymmetry visually immediately evident.

Finally, the morphology of stylolite caps is a useful refinement of the field description of a stylolite. Stylolite caps constitute the crests and troughs of stylolite columns. They may be (1) planar, (2) convex, (3) conical, (4) serrate, or (5) hummocky.

Planar caps are flat and smooth. Convex caps are also smooth, but bulge outward, away from the bases of the columns. Conical caps define cones, with apices also pointing outward. Serrate caps resemble miniature serrate stylolites, confined to the cap of an individual stylolite column. Hummocky caps, in turn, resemble miniature hummocky seams (Figure 2).

If field preservation does not allow clear distinction between convex and conical caps, or between serrate and hummocky caps, the classification of cap morphologies becomes threefold: (1) planar, (2) convex to conical, and (3) hummocky to serrate.

Detailed Features of Stylolites

A detailed tracing of a stylolite seam in the Salem Limestone (Figure 3) illustrates some important features of stylolite composition and morphology. The tracing was made from a mosaic of photomicrographs taken from a thin section. The host rock, a packstone, contains two or three partially overlapping seams, defined mainly by dark, organic and clay-rich material shown in black. The same material in the host packstone is also shown in black. Large crystals or crystal clusters of clear calcite are outlined, but unshaded, both along the stylolite and in the host rock.

The stylolite seam consists of 50% to 100% dark material, composed of clay and organic matter. The remainder is clear calcite. Given the sparse distribution of pockets of dark material in the host rock, it seems unlikely that all the dark material along the stylolite represents insoluble residue. A common hypothesis is that the height of stylolite columns reflects the amount of rock dissolved (e.g., Stockdale, 1920). Yet the amount of dark material within individual columns is far less than necessary to account for the thick stylolite seams. This suggests that the thick lenses of dark material within stylolite seams are largely primary, depositional in nature.

Figure 3.

Detailed tracing of stylolite from photomicrograph of thin section of packstone from the Salem Limestone formation. Organic material and clays are shown in black, both along the stylolite and in the host rock. Large crystals or crystal clusters of clear calcite are outlined, but unshaded.

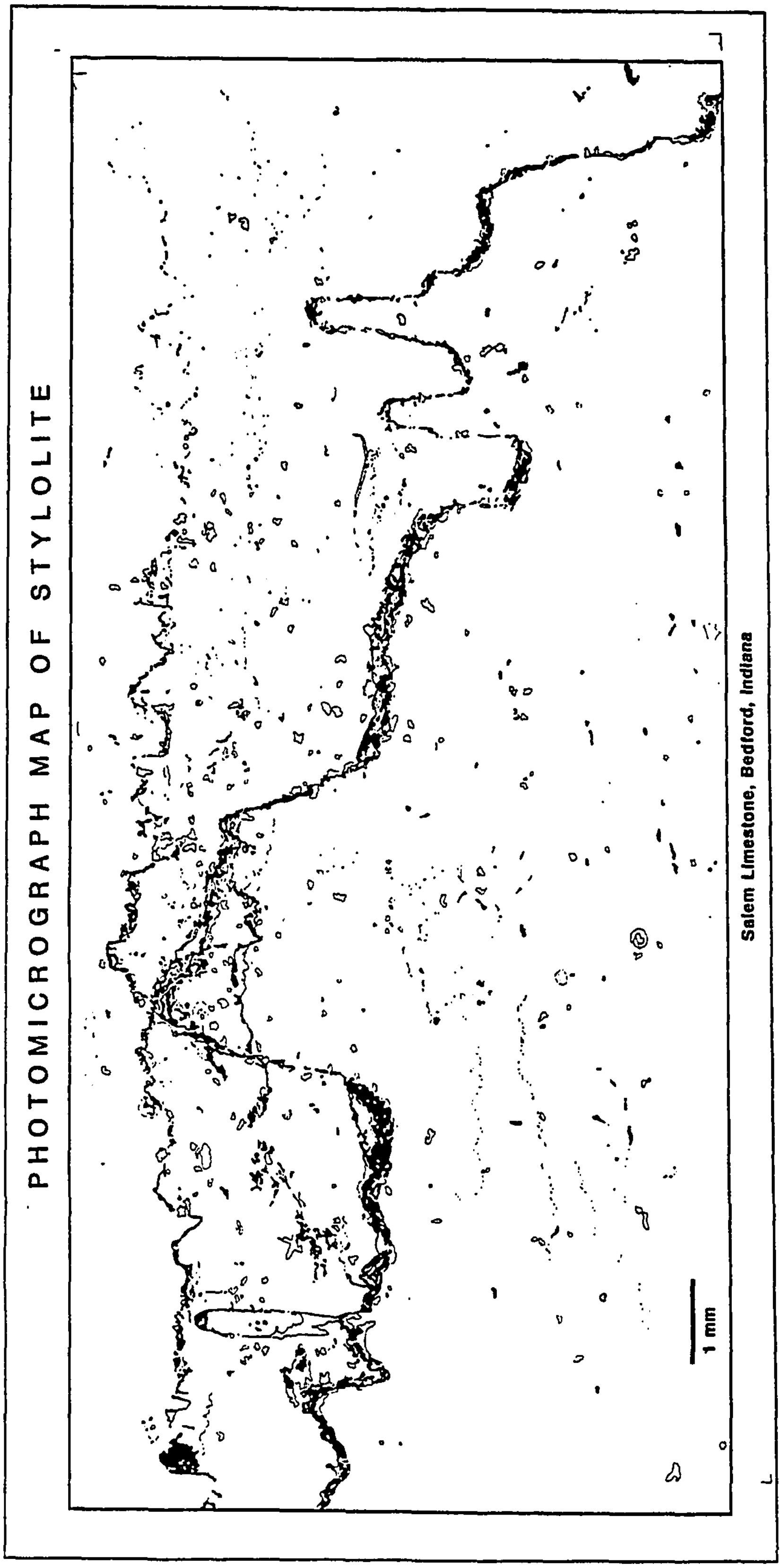
PHOTOMICROGRAPH MAP OF STYLOLITE
Salem Limestone, Bedford, Indiana
1 mm

Sedimentary deposition of dark material apparently occurred not only along stylolite seams, but in surrounding rock as well, as illustrated by the numerous examples of horizontally aligned groups, or chains, of dark pockets throughout the photomicrograph field of view (Figure 3).

Coarse, clear calcite is sparse within most stylolite seams. The high concentration of calcite, a relatively soluble mineral, within some long segments of stylolite seams, however, casts doubt on the hypothesis that stylolites form solely by pressure-induced dissolution (pressure solution)--a hypothesis championed by many geologists (e.g., Stockdale, 1920; Heald, 1953; Dunnington, 1954; Wanless, 1979; Finkel and Wilkinson, 1990). Under this hypothesis, calcite found within stylolite seams would represent precipitate from solutions produced by earlier pressure solution.

A certain amount of post-depositional rearrangement of grains is indicated by the near-vertical alignment of particles along the sides of stylolite columns. In many cases, calcite crystals and clay or organic matter particles are oriented almost vertically (Figure 3). Apparently, some form of rearrangement has occurred along the column walls, either by shearing and rotation, or dissolution and reprecipitation along the fissures that constitute stylolite column walls.

In summary, the observations presented above suggest that stylolites form along preexisting, organic-rich and clay-rich seams, which later became physically disjointed due to dissolution along the caps and walls of stylolite columns. Dissolution along a stylolite may be induced by pressure at grain contacts, or by depressed pH levels due to the presence of organic matter.

Composition of Stylolite Seam Material

Stylolite seams are rich in organic matter and clay minerals. Chemical analysis of stylolite seam material for organic carbon content indicates that the seams contain up to 20% organic carbon. Limestone, particularly grainstone, with relatively small amounts of organic material commonly contains stylolites with thick, organic-rich column caps. If the caps represented only insoluble residue, with no preexisting, depositional material, and if stylolite column heights represent minimum amounts of rock shortening due to dissolution along the stylolites, then the columns would have to be many times longer than they commonly are in order to account for all of the organic carbon contained within the clay caps. Thus, the high organic content of stylolite seam material suggests that the seams originated as thin, organic-rich sedimentary layers within the rock, along which some of the adjacent rock dissolved during burial diagenesis.

X-ray diffraction analyses (Appendix A) of stylolite seam material and immediately adjacent host rock reveals that the seams contain clay minerals not included in the host limestone, suggesting a depositional origin for the seams. These minerals include chlorite, gibbsite, halloysite, and montmorillonite. Clay minerals found in both host limestone and stylolite seams belong to the illite group. Other phyllosilicates occurring in both host and seam include talc and other micas. The minerals common to host rock and stylolite seam suggest that at least part of the seam represents insoluble residue.

Illite is a very common clay mineral in marine substrates. High cation content in seawater, particularly of Ca^{++}, combined with relatively alkaline conditions with pH values of 5 between 9, can cause the replacement of kaolinite by illite. This is because kaolinite is a silica-depleted and aluminum-oxide-rich clay compared to illite, and silica is soluble at pH values between 5 and 9, whereas metal oxides are only slightly soluble within the same pH range (Grim, 1968). Thus, the lack of kaolinite, combined with the abundance of illite are consistent with marine origin of both stylolite seams and host limestone.

Illite has been found to be the most abundant clay mineral in calcareous marine and lagoonal sediments, whereas kaolinite is more indicative of lacustrine and fluvial origin (Pryor and Glass, 1961). Association of illite with deep marine and kaolinite with shallow marine sediments has also been suggested (Hayes, 1962). The lack of smectite, however, should not be attributed to specific depositional or diagenetic factors, since smectite is generally absent from pre-Mesozoic rocks (Grim, 1968).

Illite is the dominant clay mineral in saline shales, which supports the hypothesis that stylolite seams originate as thin "shale breaks" of depositional origin.

Talc, another mineral common to both host rock and stylolite seam, is a secondary mineral resulting from a very low-grade metamorphic, or diagenetic, reaction in which dolomite, chert and water combine to form talc, calcite and carbon dioxide:

$$3CaMg(CO_3)_2 + 4SiO_2 + H_2O = Mg_3Si_4O_{10}(OH)_2 + 3CaCO_3 + 3CO_2 \quad (1)$$

This reaction occurs between 150° and 250° C. Above

250° C, talc would react with calcite to form tremolite, dolomite, water and carbon dioxide. Tremolite was not found in either host rock or stylolite seam. Alternatively, the talc could be of detrital origin.

Micas, especially lithium-rich biotite and margarite, occur in both host rock and stylolite seam. Since the metamorphic regimes associated with the formation of the micas are not within the range of primary, nonrecrystallized limestone constituting the Salem Limestone, the micas are interpreted as being detrital in origin.

Clay minerals occurring only in the stylolite seam and not in surrounding host rock include chlorite, gibbsite, halloysite, and smectite.

Illite is replaced by chlorite via diagenetic reaction in a marine environment (Grim, 1968). If the stylolite seam were originally deposited as a thin shale layer in a relatively quiet, low-energy environment, slow burial of the seam might allow ample time for this reaction to take place. More rapidly buried sediment such as grainstone, a typical host rock of stylolites, might not experience the necessary duration of exposure to seawater to allow illite to become replaced by chlorite, particularly in a near-shore, meteoric-marine mixing-zone. Chlorite is a common minor constituent of marine and lagoonal sediment (Pryor and Glass, 1961), and it has been found to be especially common in rocks deposited at intermediate depths, between the kaolinite-dominated, near-shore environment and the illite-dominated, deep marine environment (Hayes, 1962). Thus, the presence of chlorite in stylolite seam material and not in host rock may reflect different depositional environments of the seam and host, even though the chlorite may not be a primary mineral. The occurence in stylolite seams of secondary minerals associated with depositional environments contrasting with those attributed to the host rock strengthens the hypothesis that the seams represent original, depositional material.

The absence of gibbsite, the product of weathering of clay-bearing limestone, in host rock in spite of its presence in stylolite seam material further supports the notion that the seam has a different depositional origin than the host rock, rather than simply representing insoluble residue. The gibbsite may be a detrital mineral that found its way exclusively into thin layers of shale. Halloysite, although it is a relatively insoluble clay mineral found in stylolite seam material, should not be considered an insoluble residue, since it is absent in host rock. Both halloysite and montmorillonite, a clay mineral frequently associated with bentonite deposits, are probably detrital minerals that were deposited exclusively in "shale breaks" that later became stylolite seams.

Tectosilicate distribution between stylolite seams and host rock, like clay mineral distribution, appears to argue against a purely residual origin of seam material. Whereas low quartz and nepheline, a silica-deficient feldspathoid mineral, occur in both seam and host, chabazite, a rhombohedral, calcium-aluminum tectosilicate, occurs exclusively in the stylolite seam. In association with chlorite, quartz and mica, all of which occur in seam material, chabazite indicates diagenetic temperatures of up to 170° C.

The minerals rhomboclase and corrensite also occur only in stylolite seam material, and not in adjacent host limestone, further corroborating the evidence in favor of depositional, pre-burial origin of at least some of the seam material.

Two minerals were found only in host rock adjacent to stylolite seams investigated by X-ray diffraction analysis. These were dolomite and rhodocrosite. Small amounts of calcite detected in seam material probably constitute contamination of the seam sample by host rock, thus representing sampling error. The lack of dolomite in the seam samples suggests that dolomite, though less soluble than calcite, dissolves during stylolite development. Similarly, rhodocrosite apparently dissolves during stylolite development. These observations indicate that stylolites develop under burial diagenetic conditions, instead of near-surface temperature and pressure.

Stylolite-Host Rock Relationships

One of the goals of this study is the correlation of stylolite growth parameters, such as stylolite density, column height, and seam thickness, to detailed lithologic and paleontologic features of host rock immediately above and below the stylolites. Chapter 5 describes these correlations, which are based on detailed observations of 820 feet of stratigraphic section. In general, poor grain-sorting and high organic content are the two most important rock characteristics that cause stylolites to thrive, provided that thin, clay-rich shaley layers (shale breaks) are present to nucleate stylolitic dissolution processes.

Basin-Wide Trends

At the megascopic scale lies the relationship of stylolites to burial depth and regional facies trends, described in Chapter 6. The most surprising result of this study is the observation that lithologic characteristics of the host rock determine the sensitivity of stylolite development to burial depth. Stylolite density, or vertical spacing, increases with burial depth only in packstone, but not appreciably in grainstone, wackestone or micstone. Stylolite column height, however, increases with depth mainly in grainstone. These observations underscore the notion that overburden stresses alone do not drive stylolite growth.

Comparison of the volume of rock contained within stylolite columns throughout the Illinois Basin to current porosity and estimated initial porosity indicates that reprecipitation of rock dissolved along stylolites accounts for 5% of pore-filling cement in grainstone, and 25% in packstone.

CHAPTER 2

SURVEY OF RECENT LITERATURE ON STYLOLITES

Following is a survey of topics dominating the stylolite literature since 1970. The survey covers references included in Appendix A, the annotated bibliography of stylolite-related geologic literature. The annotated bibliography includes references dating back to 1879.

There is broad consensus among geologists that the morphologies--shapes and sizes--and distributions of stylolites are related to host rock lithology. Several workers have argued that stylolites form preferentially along preexisting discontinuities in rock, such as fractures and lithologic contacts. One reason for this may be the abundance of fluids along such surfaces, and several workers have addressed the question of the effect of fluid chemistry on stylolitization. In addition to fluid chemistry, the lithic state of a rock also influences stylolite growth: cementation and mineralogical stabilization during early diagenesis can promote or inhibit stylolitization during later, burial diagenesis. Of course, the literature abounds with examples of cementation associated with stylolites, but several workers presented examples of stylolites that appear to have formed later than pore-filling cement.

This leads to the question of the role of stylolites in rock compaction and porosity reduction. Although it is clear that stylolites have reduced the porosity and permeability of many potential reservoir formations (e.g., Meyers, 1980; Mossop, 1972), other formations exhibit secondary porosity and fracturing developed preferentially within stylolite seams (e.g., Nelson, 1981; Bissell, 1972).

Finally, stylolites themselves can act both as barriers to and conduits for fluid migration, thus greatly affecting reservoir quality.

Lithology Affects Stylolite Development

The occurrence, morphology and distribution of stylolites depend on host lithology. Micrite-rich reef carbonates deposited in low-energy environments are typically stylolitized, whereas grainy, micrite-poor deposits remain free of stylolites in a Devonian reef (Wong, 1983). Weyl (1959) indicated that stylolites tend to form along clay-rich beds. The prevalence of sutured seams (stylolites) in clean limestone, especially grainstones, with a low content of clay, platy silt and organic material, and of non-sutured seams (including individual seams as well as swarms of seams, called "horsetails") in muddy, impure limestones, especially wackestones and micstones, has been documented in various Paleozoic limestone of the United States by Wanless (1983, 1979), Buxton and Sibley (1981), and Mossop (1972). The same correlation between stylolite shape and purity of limestone has been observed among bedding-perpendicular, tectonic stylolites (Losonsky, 1983a, b; Geiser and Sansone, 1981; Alvarez et al., 1978). Small amounts of clay or silt appear to be necessary, however, even for the formation of sutured seams, as has been suggested in a model by Bayly (1986).

Stylolites seem to be less common in dolomite than in limestone, but some examples have been documented. Braithwaite (1986) has noted that they tend to occur in cluster, and that they are associated with zones of broken, collapsed dolomite crystals. Stylolites postdate pervasive dolomitization in Middle Precambrian stromatolites (Ricketts, 1983), whereas stylolites are truncated and partly obliterated by post-stylolitic dolomite crystals in Devonian dolomites of east-central California (Zenger, 1983).

The effect of cementation on stylolite morphologies and distributions is less clear, possibly because it can be difficult to distinguish between pre-stylolitic cement and post-stylolitic cement. In a Devonian limestone from Michigan, high-amplitude stylolites occur in well-cemented grainstone, whereas non-sutured seams occur in poorly cemented packstones and wackestones (Buxton and Sibley, 1981). On the other hand, in a Devonian reef in Australia, low-amplitude, widely spaced stylolites are associated with strong early cementation, whereas high-amplitude, closely spaced stylolites are associated with little or no early cementation (Playford, 1980).

Differences in stylolite spacing in grainstones and mudstones might be explained by the fact that in coarser rock the pressure of overburden or of tectonic forces is divided among fewer contact points so that threshold forces for stylolitization would be lower (Bathurst, 1983). This may explain why stylolites are more common in grainstones than in micstones. Early descriptions of stylolites in the literature are in coarse-grained limestone (Stockdale, 1920; Irving, 1904) and sandstone (Price, 1934; Tarr, 1916).

Alternatively, stylolite spacing may reflect the spacing of inhomogeneities or discontinuities in rock (Gratier, 1983). Dolomite crystals or crystal clusters would behave as rigid inclusions within limestone, stimulating pressure solution in adjacent limestone (Schofield, 1983). Large fossils or concretions, and masses of chert may serve the same purpose (Bathurst, 1983). Even soft but insoluble inclusions within soluble rock might promote pressure solution in their vicinity (Losonsky, 1985). Lithologic boundaries are especially prone to stylolitization (Sellier, 1983; Buxton and Sibley, 1981; Wanless, 1979; see also references cited in Nelson, 1983). Indeed, any preexisting surface, such as a crack or joint, that is coated with micrite, carbonaceous matter, or clays, or that can retain water during compaction, is especially likely to become stylolitized (Bathurst, 1983, 1975).

Pore-Fluid Chemistry Affects Stylolite Development

The latter point--that water retention promotes stylolite formation--opens the issue of the influence of pore-fluid chemistry on stylolitization. Direct correlations between fluid composition and pressure solution have usually been made with reference to sutured grain contacts. In Mississippian limestone of New Mexico, for example, the degree of saturation of groundwater with respect to calcite was the controlling factor over the intensity of intergranular pressure solution (Meyers and Hill, 1983). Meteoric water, which has low magnesium concentrations, has allowed intergranular pressure solution to occur within highly porous, shallow-buried (120 meters) limestones of southern Florida (Halley and Schmoker, 1983),and meteoric water has been reported to accelerate pressure solution, compared to marine fluids, in chalks (Scholle, 1977;

Neugebauer, 1973).

Inhibitive effects on intergranular pressure solution and stylolitization include dryness of pores, and to coating of pore walls with oil or hydrophobic organic compounds, preventing contact between grains and pore fluids (Scholle and Halley, 1983; Gratier, 1983; Scholle, 1977; Dunnington, 1967).

Studies of Jurassic limestones in the Paris Basin and in Arkansas have shown that pre-burial, meteoric cementation and mineralogical stabilization tend to stabilize the rocks and retard or prevent later stylolitization (Purser, 1983, 1978; Scholle and Halley, 1983; Wagner and Matthews, 1982; Moore and Druckman, 1981). Conversely, the absence of significant pre-burial diagenesis opens the door to substantial pressure solution, both intergranular and along stylolites, during later burial (Moore and Druckman, 1981). Meteoric water can stabilize a limestone during pre-burial diagenesis, thus inhibiting pressure solution during later burial, but also promote pressure solution in a limestone if it permeates the pores during burial diagenesis.

Early marine cementation may also help stabilize a limestone. For example, differential compaction of a Devonian reef in Australia is attributed to the localized, stylolite-inhibiting effect of early submarine cementation (Playford, 1980).

Stylolites Promote Cementation

Having discussed how cements affect stylolites, we now turn to stylolite-derived cements. The literature abounds with examples of stylolites associated with low-porosity (high-cementation) zones, suggesting that material dissolved along stylolites reprecipitated locally, usually as pore-filling, sparry calcite cement. Some examples include carbonates of the Middle East (Koepnick, 1983; Dunnington, 1954); Jurassic limestones of the Paris Basin (Purser, 1983) and of Arkansas (Wagner and Matthews, 1982); Devonian reefs of Alberta, Canada (Wong, 1983; Wong and Oldershaw, 1981; Mossop, 1972) and of Australia (Playford, 1980); in various Paleozoic carbonates of the United States (Wanless, 1983, 1979); and elsewhere (see references cited in Nelson, 1983). Specifically, it has been reported that stylolites are numerous where porosity is in the range of 1 - 7%, whereas they occur rarely where porosity is in the range of 10 - 35% (Sellier, 1983).

Stylolites occur only in the middle of isolated, non-porous bands of rock, surrounded by highly porous, poorly cemented or non-cemented rock. In some cases, the cements are zoned, and youngest cement zones become wider away from the stylolites, suggesting that cementation began close to the stylolites, and moved away from the stylolites as pores close to it became filled (Wong, 1983; Wagner and Matthews, 1982; Wong and Oldershaw, 1981).

Carbon isotopes can also supply evidence that carbonate dissolved along stylolites constitutes part of the local, pore-filling cement. For example, Purser (1983) found that, in the vicinity of stylolites, carbon isotopes of sparitic cement and of enclosing sediments are equivalent.

The low solubility of calcium carbonate in typical subsurface waters provides a strong argument for the necessity of carbonate dissolution at stylolites and sutured grain contacts as the sources of pore-filling cement. It has been calculated that 10,000 to 50,000 pore volumes of water would be needed to fill pores with externally derived cement, i.e., in the absence of local dissolution and reprecipitation (e.g., Scholle and Halley, 1983).

Cementation Promotes Stylolite Development

Several authors have suggested that by cementing their host rock, stylolites promote their own continued growth. Well-cemented portions of limestone behave as rigid, structurally resistant blocks, causing stress concentrations, and hence, pressure solution, along their boundaries (Gratier, 1983; Sellier, 1983; Wanless, 1983, 1979).

Another feedback mechanism has been proposed by Merino et al. (1983), in which local porosity maxima, where the equilibrium chemical potential of components from dissolved rock in the pore fluid are highest, self-amplify because of the diffusive gradient away from the dissolution sites. This process would continue until neighboring rock becomes clogged with new cement, which is consistent with the observations cited above. The process would also generate evenly-spaced stylolites, because precipitation of freshly dissolved cement in rock near the original dissolution sites--the local porosity maxima--would create new chemical potential gradients, and hence, new diffusion gradients toward the precipitation sites. Thus, evenly spaced stylolites, such as those described by Simpson (1985) in an homogeneous, Lower Carboniferous limestone in South Wales, need not have formed along original bedding planes or other lithologic discontinuities or inhomogeneities. Instead, the stylolites create a form of "pseudo-bedding."

If stylolites form in porous rock, and if they fill those pores with cement during their growth, it seems possible that a point may be reached when the host rock is saturated with stylolite-derived cement and stylolite growth stops. Why dissolution along stylolites stops is as poorly understood as why it begins. Stylolites have been reported to cut even the youngest generations of cement in Lower Ordovician limestones of Nevada (Gillet, 1983)p; in Mississippian skeletal limestones of New Mexico (Meyers and Hill, 1983; Meyers, 1980); and in Middle Jurassic limestones of the Paris Basin (Purser, 1983). In some cases, it is believed that stylolites were initiated after intergranular pores had been almost completely filled with cement (e.g., Meyers and Hill, 1983), whereas in other cases, dissolution on stylolites is also the source of material for part of the pore-occluding, late sparitic cement (e.g., Purser, 1983). The latter case supports the notion of stylolite "cannibalism:" cement formed during early stages of stylolitization may later be consumed by the same stylolite that liberated the cementing material (Gillet, 1983).

Furthermore, thin, short stylolites may be consumed by larger ones, especially in bedding-oblique ("tectonic") stylolites (e.g., Losonsky, 1983a; Geiser and Sansone, 1981; Nickelsen, 1972). This leads to the concept of coalescence of microstylolite swarms to create single, thick stylolites.

The terminations of many stylolites are surrounded by microstylolite swarms, suggesting that stress concentrations at the terminations lead to enhanced pressure solution, allowing the stylolites to grow in length (Fletcher and Pollard, 1981).

Stylolites Contribute to Rock Compaction

By reducing the volume of rock, stylolites and sutured grain contacts contribute to rock compaction. Before pressure solution begins, however, most rocks experience mechanical compaction, including reorientation, breakage and plastic deformation of grains, accompanied by dewatering (Bathurst, 1983; Scholle, and Halley, 1983; Meyers, 1980; Dunnington, 1954). This is followed by pressure solution, first along grain contacts, and later along stylolites (Bathurst, 1983; Moore and Druckman, 1981).

The depths of overburden at which pressure solution becomes effective have been variously reported to be as shallow as 100 meters (330 feet) for microstylolitic limestones of Guam (Schlanger, 1964), or 120 meters (390 feet) for pressure solution along grain contacts in highly porous limestones of southern Florida (Halley and Schmoker, 1983); and as deep as 600 meters (2000 feet) in carbonates of the Middle East (Dunnington, 1967) and in chalks of the North Sea (Neugebauer, 1973; see also other citations in

Scholle and Halley, 1983).

The relative importance of mechanical and chemical compaction in reducing porosity is variable. In general, mechanical compaction reduces porosity as much as 80% from initial values in uncompacted sediment, to 30 - 35%. Porosity can be further reduced to as little as 5% by chemical compaction (Bathurst, 1983; Scholle and Halley, 1983).

Chemical compaction can be the dominant factor contributing to porosity reduction, such as in carbonates of southern Florida, in which porosity ranges from 45% near the surface to 25 - 30% at a depth of 800 meters (2600 feet) (Halley and Schmoker, 1983).

Lithology also affects the role of different compaction mechanisms. In Silurian carbonate clinothems of east-central Indiana, mudstones have suffered 50% compaction due to dewatering, but only 8% thinning due to stylolites; lithofacies consisting of alternating grainstones and mudstones show only 13% compaction due to dewatering, and 17% thinning due to stylolites (Devaney et al., 1986). In other rocks, mechanical compaction reportedly accounts for 1/3 to 1/2 of the total porosity loss in mudstones, but smaller fractions in grainstones and packstones (Scholle and

Halley, 1983). In Mississippian skeletal limestones of New Mexico, mechanical breakage is unimportant, while intergranular pressure solution increases with compaction intensity (Meyers and Hill, 1983). Apparently, the relative importance of chemical compaction is greater in grain-supported rocks than in mud-supported rocks.

One must be careful, though, in distinguishing between mechanical and chemical compaction, because physical compaction of sediment rich in organic matter produces stylolite-like lenses of organic material (Pratt, 1982). This has been demonstrated experimentally by Shinn et al. (1977). An especially tricky scenario arises when early diagenetic, non-stress-related dissolution of carbonate minerals around burrows, followed by physical collapse of the burrows, forms clay microseams that may later serve as nuclei for pressure solution (Eller, 1983).

Mechanical and chemical compaction need not be separate processes. In Devonian dolomites of the United States and Canada, stylolites are associated with mechanical breakage and collapse of dolomite grains; this may, in turn, lead to local stress concentrations and to continued stylolitization (Braithwaite, 1986).

Stylolites Affect Reservoir Quality

We have seen that as part of the compaction a carbonate rock undergoes during burial, stylolites help reduce porosity and bed thickness. Porosity reduction typically decreases permeability, which, in turn, makes oil recovery difficult (Dunnington, 1967). In Lower Cretaceous, oil-rich carbonates of Abu Dhabi (United Arab Emirates), reservoir quality is moderate to poor where stylolites are numerous, whereas it is moderate to good where stylolites are sparse (Alsharhan, 1985).

Individual stylolites can form barriers to fluid migration. If they develop after hydrocarbon entrapment, however, no porosity occlusion occurs because hydrocarbons coat and poison potential nucleation sites for calcite growth (Koepnick, 1983). Even without concomitant cementation stylolites can act as barriers to fluid migration because their insoluble residues are likely to be impermeable. Conversely, in the absence of significant accumulations of residue, stylolites can serve as drains or zones of fluid circulation (Sellier, 1983). Thus, by affecting flow patterns in reservoir rocks, stylolites may influence hydrocarbon accumulation (Dunnington, 1967).

Finally, stylolites may also be responsible for the creation of secondary porosity. In carbonate reservoirs of the Delaware Basin, Texas, stylolites are associated with oomoldic porosity and gash fractures, which decrease in abundance away from the stylolites (Mazullo, 1981). This secondary porosity counteracts the effects of compaction.

Conclusion

The shapes, sizes, and distributions of stylolites affect reservoir quality. The chareacter of these stylolites is controlled by host lithofacies and fluid chemistry, and thus tied to the depositional and diagenetic environments. A better understanding of the relationships between stylolites and the depositional and diagenetic history of their host rocks should improve our ability to predict the occurrence of stylolites in carbonate reservoirs; to estimate their effects on reservoir quality; and, with the known distribution of stylolites, to interpret the depositional and diagenetic history of the host rock.

CHAPTER 3

STRATIGRAPHY

Detailed stratigraphic sections contain the bulk of the data used in this study of stylolites across the Illinois Basin. I described 820 feet of Salem Limestone, distributed among 8 cores and 4 outcrops. I described 3 outcrops in western Illinois and eastern Missouri (in the St. Louis metropolitan area); 5 cores in central and southern Illinois; 2 cores in central and western Indiana; and 1 outcrop in south central Indiana (Figure 1, Chapter 1).

The vertical resolution of the stratigraphic sections ranges from 1 to 3 inches. I described the sections in 4-foot intervals, using 14x and 20x hand lenses, mineral oil to enhance resolution, and 2% hydrochloric acid with alizarin red stain to distinguish calcite and dolomite. I measured outcrops using a hand level, Jacob's staff, and spray paint, marking 1-foot intervals on the outcrop surface. I measured cores in groups of 2 boxes, or 5 feet, marking 1-foot intervals on the cores.

This chapter describes each of the 10 stratigraphic sections depicted in Plates 1 through 10 (Appendix B). The sections define a west-to-east traverse across the Illinois

Basin, beginning with section A in Missouri, and ending with section J in Indiana. Stratigraphic sections K and L are not depicted in Appendix B. Figures 4 and 5 show the stratigraphic relationship of the Salem Limestone to other Mississippian formations in the Illinois Basin.

Graphs indicating grain size and grain sorting accompany each stratigraphic section (Appendix B). The stratigraphic data are the basis for the graphs shown in the chapter on stylolite-host rock relationships (Chapter 5), and for the contour diagrams shown in the chapter on basin-wide analysis (Chapter 6).

Characteristics described in the stratigraphic sections include lithofacies, prominent fossils, minerals, sedimentary structures, grain size, sorting, and stylolites. Four basic lithotypes dominate various parts of most of the stratigraphic sections: grainstone, packstone, wackestone to micstone, and dolomicstone to dolopackstone. Rock sequences exhibiting up-section increases in micrite content, starting with grainstone at the bottom, ranging through packstone and wackestone, and ending with micstone and, in some cases, dolostone and even shale at the top, are characteristic of the Salem Limestone. Previous students of the Salem Limestone recognized that these sequences represent shoaling-upward depositional cycles (Cluff, 1984; Lamborg,

Figure 4.

Stratigraphic column of Middle Mississippian formations in the Illinois Basin. Thicknesses are typical of the center of the basin. After Pryor and others, 1991.

Middle Mississippian Formations of the Illinois Basin

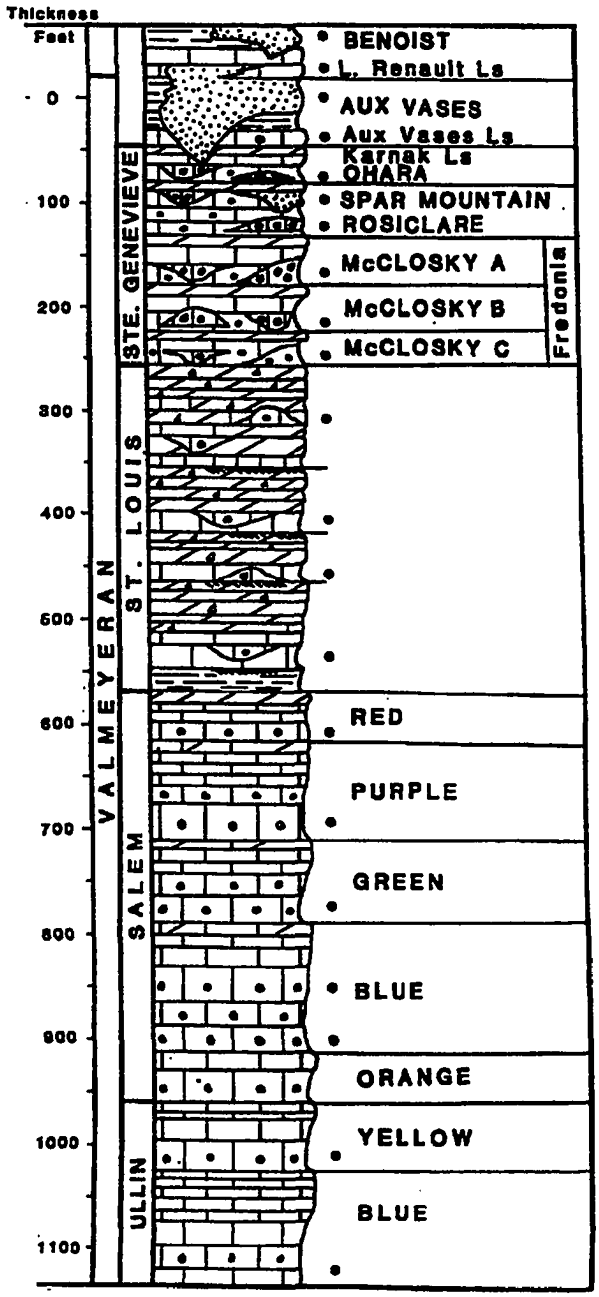

Figure 5.

West-to-east cross section of Mississippian formations in the Illinois Basin. Letters indicate locations of outcrops and cores described in this chapter (see Figure 1, Chapter 1). The eastern limb of the basin was compiled with the help of resistivity and spontaneous potential logs in southwestern Indiana.

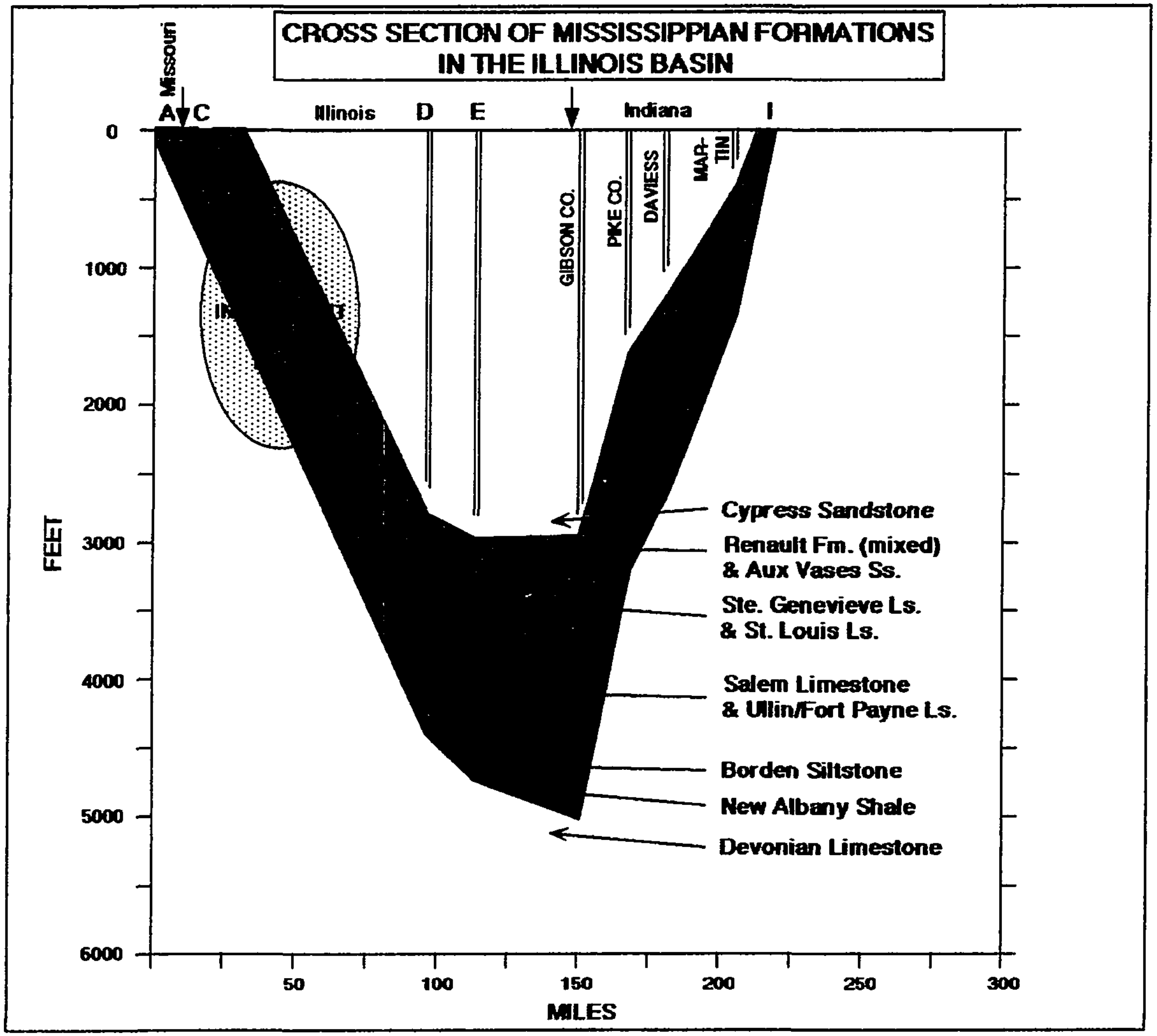
CROSS SECTION OF MISSISSIPPIAN FORMATIONS
IN THE ILLINOIS BASIN
Missouri
A
C
Illinois
D
E
Indiana
I
GIBSON CO.
PIKE CO.
DAVIESS
MAR-
TIN
FEET
0
1000
2000
3000
4000
5000
6000
50
100
150
200
250
300
MILES
Cypress Sandstone
Renault Fm. (mixed)
& Aux Vases Ss.
Ste. Genevieve Ls.
& St. Louis Ls.
Salem Limestone
& Ullin/Fort Payne Ls.
Borden Siltstone
New Albany Shale
Devonian Limestone

1986). The term deposequence refers to a depositional sequence representing such a cycle (Figure 6).

This study uses a simplified version of Cluff's (1984) shoaling-upward cycle, in order to consistently relate stratigraphic sections distributed over a large area. The depocycle is divided into two parts--a high-energy lower part and a low-energy upper part. The high-energy regime probably represents oolite shoals, whereas the low-energy regime probably represents lagoons and tidal flats (Cluff, 1984; Pryor and others, 1991).

The corresponding deposequence consists of a "clean," micrite-poor lower part, overlain by a "muddy," micrite-rich upper part. The lower part typically consists of cross-bedded, oolitic, skeletal grainstone and oolitic, skeletal packstone. The upper part typically consists of vuggy, bioturbated, pelletal, skeletal wackestone and packstone, locally with anhydrite crystals and shale partings, as well as massive, sucrosic dolostone. For simplicity, the two parts of a deposequence are referred to as the lower subsequence ("L" in Plates 1-10) and the upper subsequence ("U"). The lowest deposequence within a particular stratigraphic section is referred to as the first deposequence, and the deposequences are numbered in ascending stratigraphic order.

Figure 6.

Representative stratigraphic column of a shoaling-upward depositional sequence, or deposequence, in Middle Mississippian formations in the Illinois Basin. Units A and B constitute a lower subsequence, and units C, D, F, and G constitute an upper subsequence. From Pryor and others, 1991.

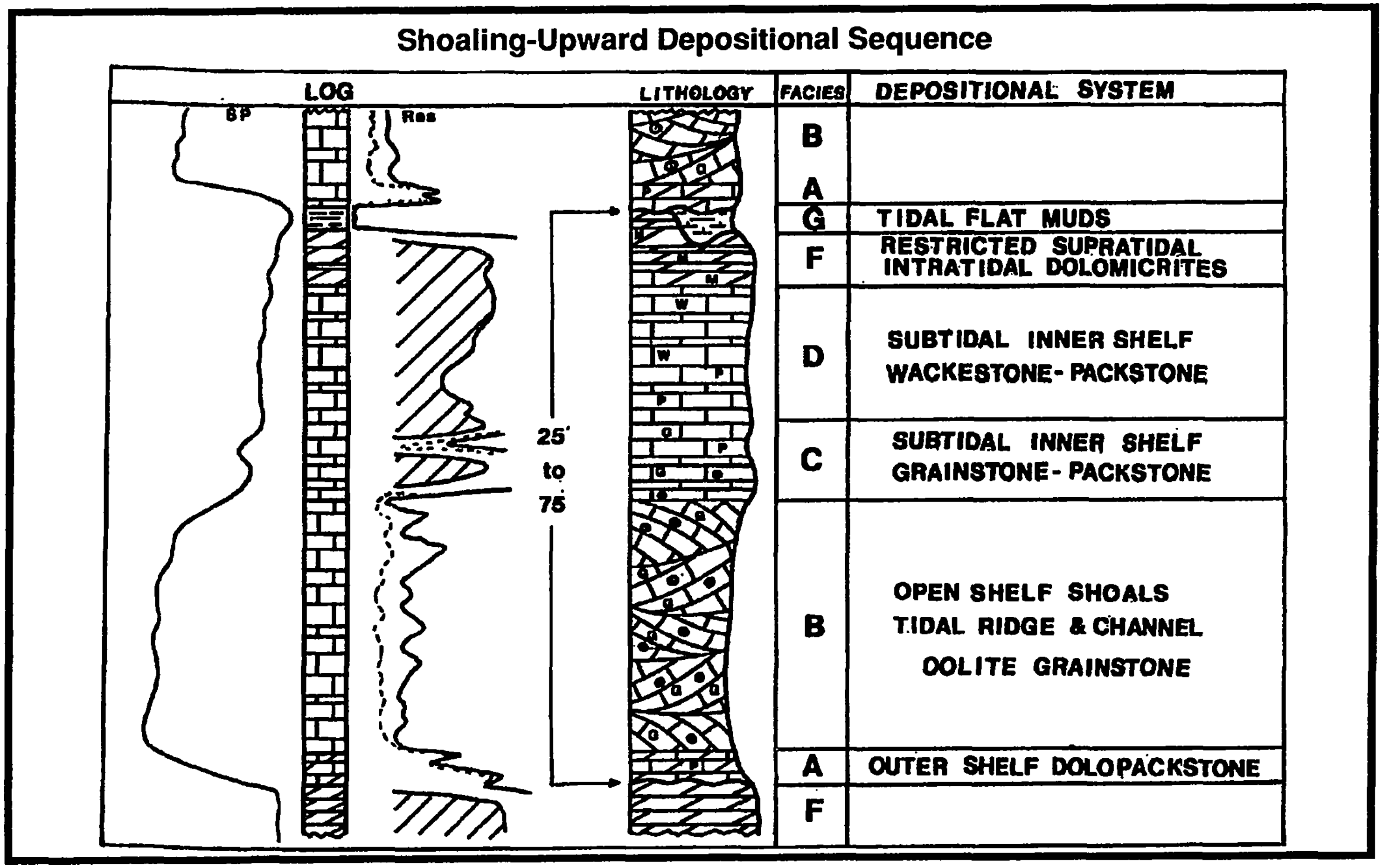
Shoaling-Upward Depositional Sequence
LOG
SP
Res
LITHOLOGY
FACIES
DEPOSITIONAL SYSTEM
B
A
G
TIDAL FLAT MUDS
F
RESTRICTED SUPRATIDAL
INTRATIDAL DOLOMICRITES
D
SUBTIDAL INNER SHELF
WACKESTONE-PACKSTONE
C
SUBTIDAL INNER SHELF
GRAINSTONE-PACKSTONE
25' to 75'
B
OPEN SHELF SHOALS
TIDAL RIDGE & CHANNEL
OOLITE GRAINSTONE
A
OUTER SHELF DOLOPACKSTONE
F

Ooids, foraminifers and echinoderms dominate the grainstone and some of the packstone in lower subsequences in the Salem Limestone. Brachiopods, Pelecypods and Corals occur mainly in the wackestones and some of the packstones in upper subsequences. Bryozoans occur throughout the Salem Limestone.

Pyrite, anhydrite and chert occur sporadically throughout the Salem. Micritic facies, particularly wackestones and micstones, commonly contain small (<0.5 mm) pyrite crystals or crystal aggregates, as well as small (<5 mm) anhydrite crystals or concretions. Some grainstones and packstones contain chert nodules or thin (<5 cm) chert lenses.

Cross-bedding, flaser bedding, organic laminae and vugs are common in some lithofacies in the Salem Limestone. Cross-bedded grainstone characterizes lower subsequences in the Salem Limestone (Cluff, 1984). Flaser bedding and organic laminae, often associated with the same rock, characterize much of the wackestone and some of the packstone in upper subsequences. The laminae are typically thin (<1 mm), and short (<10 cm), but they form dense networks of organic material, particularly in the vicinity of some stylolites. Finally, vugs, found in wackestones and micstones, range in diameter from about 2-200 mm, and they are also typical of upper subsequences in the Salem Limestone.

Grain size and sorting also distinguish the lower from the upper subsequences. Typically, lower subsequences are well sorted and fine upward, from coarse (500-710 microns) to medium fine (177-500 microns). In contrast, upper subsequences are typically poorly sorted, ranging in grain size from very fine micrite (<100 microns) to very coarse fossil fragments (>2000 microns).

Some deposequences include a transition zone between the lower and upper subsequences, consisting of thin beds characteristic of both subsequences. Interbedded, thin- to medium-bedded packstone and wackestone constitute a typical transition zone.

Stylolites occur throughout the Salem Limestone, in all 4 major lithofacies, across the Illinois Basin. Their distribution and development is the subject of Chapters 6 and 7. Morphological data collected as part of the stratigraphic descriptions include the heights and widths of individual stylolite columns, the thicknesses of fillings lining the tops, bottoms, and sides of stylolite columns, the shapes and symmetries of stylolite columns, and the shapes and sizes of serrations found along flat, smooth stylolite segments between individual stylolite columns.

Many stylolites are associated with smooth, wavy or hummocky seams of clay and organic material--the same material that constitutes the stylolite fillings. Some hummocky seams even contain a few isolated, stylolite-like columns. I included the locations and thicknesses of hummocky seams in the stratigraphic descriptions.

Two of the described outcrops--one at the eastern edge and one at the western edge of the Illinois Basin--afforded both vertical and horizontal control of stylolites. These outcrops yielded information on stylolite lengths, inter-stylolitic relationships, and relationships between stylolites and lithofacies. Detailed maps of these outcrops are presented in Appendix B (Plates 11 and 12), and they are discussed in Chapter 4.

A. Kirkwood, MO., Roadcut

Location

The westernmost stratigraphic section (Plate 1) is based on a roadcut west of St. Louis, Missouri, along northbound Interstate Highway 270, just north of the junction with Interstate Highway 44, and just south of the

Kirkwood Exit. The outcrop is located in Township 44 North, Range 6 East, Section 14, in St. Louis County, Missouri. A moderate, south-dipping grade in the highway, and a wide bench half way up the roadcut provide very good conditions for measuring the stratigraphic section.

Stratigraphy

The section is 69 feet thick, exposing 46 feet of Salem Limestone, and is underlain by 23 feet of Ullin Limestone (Figure 4). The Salem Limestone in this section consists of 57% grainstone, 11% packstone, 2% wackestone, 17% dolostone, and 13% shale, distributed among 3 upward shoaling depositional sequences. The lowest deposequence is only 7 feet thick, but it is overlain by a pair of 20-foot deposequences.

The lower 7 feet of the section represent the thin, first deposequence. Cross-bedded, moderate-grained, well-sorted, skeletal grainstone with fragments of crinoids and bryozoans constitute the 2-foot thick, lower subsequence. The grainstones contain chert lenses. Fine-grained, poorly sorted, sucrosic dolomicstone and dolowackestone, overlain by cherty, skeletal packstone and wackestone containing bryozoans, pelecypods and brachiopods, and a thin shale parting, constitute the upper subsequence.

Figure 7.

Two complete deposquences within the Salem Limestone, exposed in the Kirkwood roadcut, along northbound Interstate Highway 270, approximately 10 mi west of St. Louis, Missouri, and just south of the Kirkwood exit. The lower arrow shows the contact between the Salem Limestone and the underlying Ullin Limestone. The upper arrow points toward the stratigraphic horizon of a prominent, isolated stylolite within cross-bedded grainstone in the lower part of the second deposequence, 33 ft above the base of the Salem Limestone.

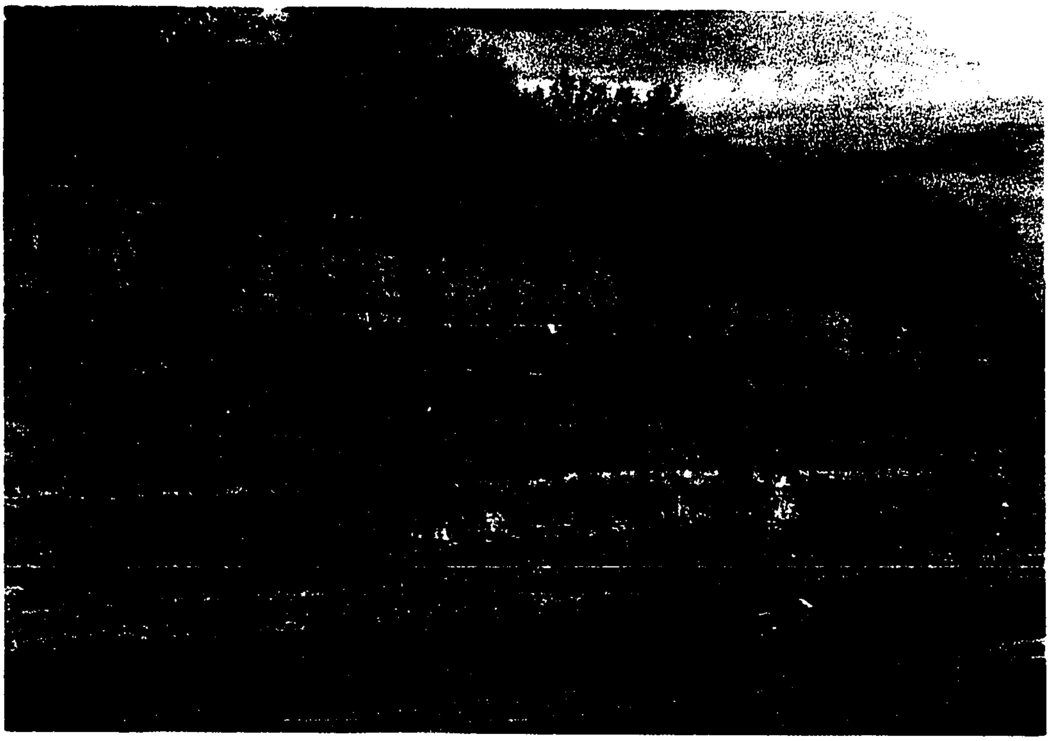

The 20-foot thick, second deposequence consists of two halves, corresponding to the lower and upper parts of the deposequence. The lower subsequence is a massive, cross-bedded, fining-upward, moderately to poorly sorted oolitic, skeletal grainstone with foraminifers, fragments of crinoids and bryozoans, and a few brachiopods. The upper subsequence consists of 4 feet of shale, overlain by 6 feet of locally vuggy and organic-rich, sucrosic dolomicstone, with a thin (6-inch) bed of cherty, skeletal packstone in the middle, and two shale partings near the top.

The third deposequence is only partially exposed. Massive, cross-bedded, fining-upward, mostly well-sorted, locally cherty and stylolitic, oolitic, skeletal grainstone constitutes the bulk (16 feet) of the exposed section, and it represents the complete lower subsequence. It is capped by 4 feet of massive, sucrosic dolomicstone, representing a portion of the upper subsequence.

Stylolites

A prominent, negatively asymmetrical stylolite occurs in the grainstone of the lower subsequence of the third deposequence. The stylolite columns are 20 mm tall, and point downwards.

Microstylolites with columns or serrations shorter than 1 mm, occur in the grainstones of the lower subsequences of the second and third deposequences. These stylolites follow the cross-bedding.

Individual hummocky seams with local serrations or small columns mark the boundaries between deposequences. Small columns, several mm tall, and pronounced undulations with wavelengths of 5 to 10 cm, characterize the hummocky seam at the base of the third deposequence.

Summary

Well-developed deposequences are a distinguishing feature of the Kirkwood section. Clearly contrasting grainstones and shales or dolomicstones occur below and above the boundaries between the lower and upper subsequences, respectively. Hummocky seams mark the upward transitions from micritic to nonmicritic rock at the boundaries between deposequences.

The Salem Limestone at the Kirkwood section is underlain by shale of the Ullin Limestone, and is capped by an erosional surface. The shale beneath the Salem indicates that the base of the Salem represents the base of a deposequence.

A paucity of well-developed stylolites is balanced by a wealth of microstylolites in the Kirkwood section. Stylolites occur mainly, and perhaps exclusively, in grainstones of this stratigraphic section.

B. Riehl Quarry, Madison Co., IL

Location

The Riehl Quarry is the northernmost of the sections along the western rim of the Illinois Basin, and it is the only quarry face that I describe in detail (Plate 2). The Riehl Quarry is an abandoned quarry west of Alton, Missouri, along Indiana State Route 3. It is located in Township 6 North, Range 10 West, Section 31, in Madison County, Illinois. The well-weathered wall of this abandoned quarry exposes lithologic contrasts clearly, but stylolites are easily overlooked. Collinson and others (1979, p. 62) claim that this quarry "represents the best exposed and thickest section of the Salem Limestone in western Illinois." The quarry was used by Weller (1906) to define the Salem in western Illinois (Collinson and others, 1979, p.62; also Treworgy and others, 1979, p.20).

Stratigraphy

The Riehl Quarry exposes 50 feet of Salem Limestone, overlain by several feet of St. Louis Limestone (Figures 5 and 6). The section contains 27% grainstone, 38% packstone, 14% wackestone to micstone, 12% dolostone, and 9% shale, distributed rather unevenly between two deposequences. The first is 36 feet thick, whereas the second is only 14 feet thick.

The first deposequence comprises the lower 36 feet of the section. Three feet of massive dolopackstone at the very base of the section are suggestive of the top of a deposequence, similar to the one found at the base of the Kirkwood roadcut. Locally cross-bedded, coarse-grained, well-sorted, oolitic, skeletal grainstone, with foraminifers, crinoids and bryozoans, grading locally into dolograinstone and dolopackstone, characterizes the bottom 12 feet of the lower subsequence. Massive, medium-grained, well-sorted, locally oolitic, skeletal packstone and grainstone, with bryozoans and some crinoids and foraminifers, dominate the overlying 15 feet of the lower subsequence.

Thin-bedded, locally shaley, medium- to fine-grained, moderately sorted, pelletal, skeletal packstone and

Figure 8.

Complete section of Salem Limestone exposed at the abandoned Riehl Quarry, in Madison County, Illinois. The lower arrow indicates a shale bed, 35 ft above the base of the Salem Limestone, which coincides with the base of the quarry wall. The upper arrow indicates the stratigraphic horizon of an exceptionally large stylolite, located 46 ft above the base of the Salem Limestone. The stylolite has columns that are 100 mm tall.

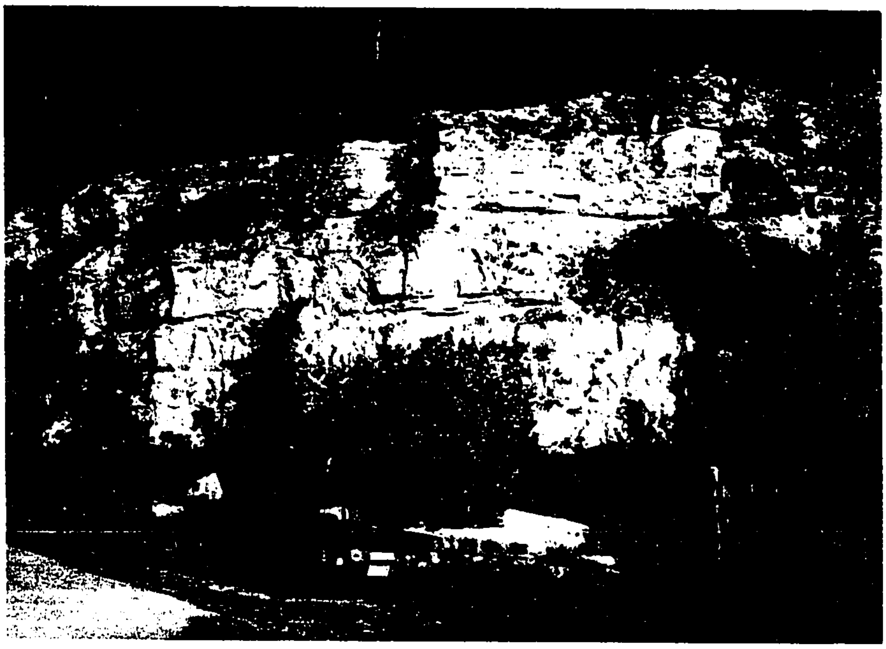

Figure 9.

View of Salem Limestone in the wall of the abandoned Riehl Quarry, in Madison County, Illinois. The lower arrow points toward a stylolitic zone at the base of the Salem Limestone. The upper arrow points toward cross-bedded, non-stylolitic packstone, 20 ft above the base of the Salem Limestone.

wackestone, with pelecypods, bryozoans, crinoids, and some rugose corals, interbedded with organic-laminated, sucrosic dolowackestone and dolopackstone, and grading upward into 5 feet of dolomitic shale, constitute the 9-foot thick, upper subsequence.

The second deposequence consists of two almost equally thick parts, reminiscent of the top deposequence in the Kirkwood section (Section A). The lower subsequence is 6 feet thick, and consists of a medium-bedded (1.5 ft) to massive, fining upward (from very coarse to moderate grain size), poorly to moderately sorted sequence of pelletal, skeletal rudstone, packstone and dolopackstone, with foraminifers, bryozoans, and crinoids.

The upper subsequence is 8 feet thick, starting with a 6-inch shale at the bottom. This overlain by massive, locally vuggy micstone and wackestone, with scattered fragments of crinoids, pelecypods, and horn corals.

Stylolites

Symmetrical stylolites with even, 1-foot spacing occur in grainstone at the bottom of the lower part of the first deposequence. The heights of columns decrease in ascending stratigraphic order, starting at the bottom with 25 mm in the first stylolite, and decreasing upward to 7 mm or less in the fourth stylolite, which grades laterally into a hummocky seam. Macroscopic stylolites are notably absent in the massive packstones of the first deposequence. An isolated, symmetrical stylolite with 100-mm tall columns occurs in a wackestone in the upper subsequence of the second deposequence. Weathering of the quarry wall precludes positive identification of microstylolites.

The series of 1-foot-spaced stylolites in at the bottom of the first deposequence is overlain by a series of 1-foot-spaced hummocky seams. Well-sorted grainstones to packstones host the hummocky seams, whereas poorly-sorted grainstones, grading locally into dolograinstones, host the stylolites. Three hummocky seams are underlain by another hummocky seam that grades laterally into a stylolite; this in turn, is underlain by three stylolites.

A hummocky seam with locally developed stylolitic columns marks the boundary between the two deposequences.

Summary

The two deposequences that comprise the Salem in the Riehl Quarry section are different in several respects. The first is much thicker (36 feet) and better developed. It contains a complete suite of lithofacies, from oolitic grainstones in the lower part, to dolomicstone and shale in the upper part. Rudstone in the lower part distinguishes the second deposequence, which is thin (14 feet) and lacks grainstones.

Shale provides a clear boundary between the two deposequences, and a thin bed of shale also marks the boundary between the lower and upper subsequences of the second deposequence.

The Salem Limestone is sandwiched between two shales in the Riehl Quarry. The Warsaw Shale lies below the base, and several feet of shale or shaley micstone belonging to the St. Louis Limestone lie above the top of the Salem. It appears that the shale at the base of the St. Louis Limestone is a continuation of the upper subsequence of the second deposequence in the Salem Limestone.

An interesting, 6-foot thick, ascending, evenly-spaced (1 foot) series of stylolites and hummocky seams occurs near the base of the section. Moderately tall (15-25 mm) columns in stylolites at the bottom of the series grade upward into short columns (7 mm), which, in turn, give way to hummocky seams with no columns. A very large stylolite near the top of the section is of dubious origin. A hummocky seam marks the boundary between the two deposequences.

C. Columbia, Mo., Roadcut

Location

The Columbia roadcut (Plate 3) is the southernmost of all outcrops described in this study. The roadcut through Illinois State Route 3, 1 mile south of the town of Columbia (about 10 miles south of St. Louis), is located in Township 1 South, Range 10 West, Section 31, in Monroe County, Illinois.

The Salem Limestone is exposed on either side of a southward ascending stretch of the road. Access to the lower 14 feet of the section, exposed only on the western side of the road, is difficult, since the base of the Salem, marked by a protruding ledge of gray packstone, occurs about 10 feet above the base of the roadcut. The upper 30 feet of the Salem are well-exposed, with easy access on either side of the road, just south of a minor intersection.

The underlying Ullin Limestone and Warsaw Shale (in descending order) are also exposed along this roadcut. The sequence of Valmeyeran age rocks exposed here is not considered to be typical for western Illinois (Collinson and others, 1979, p. 77).

Stratigraphy

The Columbia roadcut exposes 64 feet of Salem Limestone, consisting of 13% grainstone, 66% packstone, 15% wackestone to micstone, and 6% dolostone. These are evenly distributed among three deposequences of roughly equal thickness (Figures 7 and 8).

The first deposequence is 25 feet thick, and its lower and upper subsequences are 14 and 11 feet thick, respectively. In the lower subsequence, 4 feet of massive, cross-bedded, medium- to coarse-grained, well-sorted, oolitic, skeletal grainstone and packstone are overlain by 10 feet of thin-bedded (<0.5 ft), lenticular, cross-bedded, medium-grained, well-sorted, locally oolitic, skeletal packstone to grainstone, with bryozoans, crinoids, and locally, brachiopods or ooids. Massive to thin-bedded and lenticular, organic-laminated, locally cherty, vuggy, or load-casted, skeletal wackestone to dolowackestone, with crinoids and brachiopods, and micstone to dolomicstone, comprise the upper subsequence.

A gradual transition between the lower and upper subsequences characterizes the 22-foot thick second

Figure 10.

Basal 13 ft of Salem Limestone, and underlying Warsaw Limestone, in Columbia roadcut, along southbound Illinois State Route 3, near Columbia, Illinois (approximately 10 mi south of St. Louis). The lower arrow indicates the base of the Salem Limestone, marked by gray, echinodermal packstone and foraminiferal grainstone. Upper arrow indicates stratigraphic horizon of isolated stylolite within lenticular, cross-bedded packstone, 8 ft above the base of the Salem Limestone.

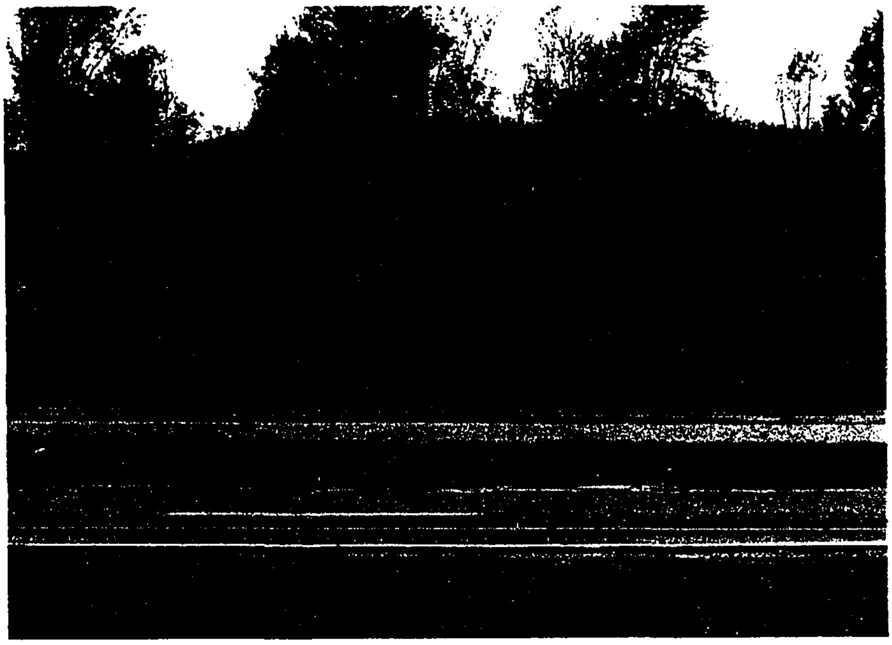

Figure 11.

Salem Limestone in Columbia roadcut, along southbound Illinois State Route 3, near Columbia, Illinois. The arrow indicates the contact between cross-bedded, oolitic packstone and overlying massive, pelletal packstone. The contact is located in the lower part of the second deposequence, 30 ft above the base of the Salem Limestone.

deposequence. Massive, cross-bedded, medium-grained and moderately sorted, oolitic, skeletal packstone in the lower 8 feet of the deposequence clearly belong to the lower subsequence. Cherty, organic-laminated micstones to wackestones with crinoid fragments in the upper 4 feet of the sequence clearly belong to the upper subsequence.

The intervening 10 feet of massive to thin-bedded, locally cross-bedded, locally cherty, pelletal, skeletal, interbedded packstone and wackestone, with bryozoans, brachiopods, and some rugose corals, apparently represent a transition zone between the lower and upper subsequences. The actual boundary between two subsequences may be placed quite arbitrarily in the middle of this zone.

Only 17 feet of the lower subsequence of the third deposequence are exposed below the erosion surface. Interbedded, massive to medium-bedded (1 foot), cross-bedded, medium-grained, well-sorted, oolitic, locally pelletal, skeletal grainstone, with bryozoans and crinoids, and massive, medium-grained, moderately- to well-sorted, locally cherty, pelletal, skeletal packstone, with fragmented brachiopods, bryozoans and crinoids, comprise the lower subsequence.

Stylolites

Symmetrical and asymmetrical stylolites, with columns 10 to 20 mm tall, occur at irregular vertical intervals in packstone and grainstone in the lower subsequences of the first and third deposequences, and in wackestone and micstone in the upper subsequence of the second deposequence. Negatively asymmetrical stylolites occur within packstone and micstone. A positively asymmetrical stylolite occurs at a contact between grainstone and overlying packstone, 3 feet from the base of the section. Its columns point upward, into packstone.

Cross-beds host microstylolites in massive grainstone at the base of the section, but not in thin-bedded packstone near the top of the lower subsequence of the first deposequence. Organic laminae exhibit serrated morphology, suggestive of microstylolites, in wackestone in the upper subsequence of the first deposequence, but organic laminae are smooth in cherty dolomicstone higher in the same deposequence.

Hummocky seams form contacts between thin, lenticular, cherty micstone in the upper subsequence of the first deposequence, but not in the thin, lenticular, locally stylolitic, packstone of the lower subsequence. Packstones in the third deposequence, and in the transition zone within the second deposequence, are hosts for fairly regularly spaced (0.5-1 foot) hummocky seams. A hummocky seam in grainstone, 5 feet below the erosion surface, exhibits locally developed, short (a few mm) columns.

Summary

Thin, lenticular bedding in the first deposequence is the most unusual aspect of the Columbia roadcut. A 10-foot thick transition zone, dominated by packstone, between the upper and lower subsequences of the second deposequence, is another distinguishing feature of this section. Although the lower subsequence of the third deposequence appears typical of lower subsequences, the upper subsequence is not exposed, and may belong to the overlying, St. Louis Limestone (as is the case in the Riehl Quarry, Section B). Abundant chert also characterizes the Columbia roadcut.

Stylolite development apparently fared better in massive to medium-bedded, non-cross-bedded packstone to grainstone in the lower subsequences of the first and third deposequences, than in either the lenticular, thin-bedded, cross-bedded packstone to grainstone in the lower subsequence of the first deposequence, or the large-scale cross-bedded packstone in the lower subsequence of the second deposequence. Organic laminae are associated with stylolites and microstylolites in wacekstones to micstones throughout the section.

Microstylolites developed along cross-beds at the bottom of the section. Thin-bedded, lenticular, cherty micstone to wackestone hosts many hummocky seams in the first deposequence.

D. Roy Reed # 5 Core, Wayne Co., IL

Location

The westernmost core used in this study, the Roy Reed #5 core (Plate 4), was drilled by the Farrar Oil Company in Township 1 South, Range 5 East, Section 27, in Wayne County, Illinois. The core contains 56 feet of continuous Salem Limestone, at a depth of 3600 to 3656 feet. The core is 4 inches in diameter, contains a minimal number of breaks, and provides an excellent opportunity to study the vertical distribution of stylolites at significant burial depth.

The Roy Reed #5 core was previously described by Lamborg (1986). A major difference between her description and mine is that I consider the degree of dolomitization in the upper part of the section to be insufficient to warrant the name "dolostone."

Stratigraphy

The 56-foot thick Roy Reed #5 core contains 53% grainstone, 46% packstone, 1% wackestone to micstone, and no true dolostone. These rock types are unevenly distributed between two deposequences recognizable in the section. The first deposequence is 27 feet thick, and contains most of the grainstone in the section. The cored portion of the second deposequence is 29 feet thick, and includes most of the packstones in the section. A deposequence boundary 17 feet below the top of the core is conceivable, but unlikely.

Although the absence of wackestone and micstone in the 27-foot thick first deposequence makes the delineation of the upper and lower subsequences difficult, bedding thickness, micrite content, and even stylolite density clearly divide the deposequence into two parts. Massive, cross-bedded, medium-grained, moderately- to well-sorted, oolitic, skeletal grainstones, with foraminifers, and crinoid and bryozoan fragments, constitute the 18-foot thick, lower subsequence. Thin- to medium-bedded, locally small-scale cross-bedded, fining-upward, coarse- to fine-grained, poorly- to moderately sorted, locally oolitic or pelletal, skeletal packstones and grainstones, with rugose corals, bryozoans, and crinoid fragments, constitute the 9-foot thick, upper subsequence.

Only the lower 9 feet of the 29-foot thick second deposequence clearly belong to the lower subsequence. Massive, cross-bedded, locally lenticular, medium-grained, moderately- to poorly-sorted, oolitic, skeletal grainstones and packstones, with foraminifers, bryozoans and crinoids, comprise those 9 feet of the lower subsequence. The remaining 20 feet appear to be a transition zone between the upper and lower parts (as in the Riehl Quarry section). Thin-bedded to locally massive, medium- to fine-grained, moderately sorted, locally oolitic or pelletal, skeletal packstones to wackstones and packstones to grainstones, with rugose corals, pelecypods, foraminifera, crinoids and bryozoans, and with locally developed anhydrite concretions, characterize the transition zone. A true, upper subsequence of the second deposequence is not included in the core.

Stylolites

Stylolites of various shapes and sizes abound in the Roy Reed #5 Core. The lower subsequences of both deposequences contain isolated, 5-foot spaced stylolites with columns 10 to 30 mm tall. Well-developed, symmetrical to negatively asymmetrical stylolites with stacked or pyramid-shaped columns attaining heights of up to 30 mm, occur within packstones in the lower subsequences of both deposequences and in the transition zone in the second deposequence. A positively asymmetrical stylolite, with 20-mm tall columns featuring conical caps, occurs within grainstone in the lower subsequence of the first deposequence.

Zones of closely spaced, symmetrical and asymmetrical stylolites characterize the upper subsequence of the first deposequence, and the transition zone of the second deposequence. Two such zones, each 1 foot thick, adorn packstone to grainstone in the upper part of the first deposequence. Stylolites within those zones are spaced as closely as 10mm, with columns only 1 to 5 mm tall. Most of the stylolites are symmetrical, although both negatively and positively asymmetrical stylolites exist in the zones.

Cross-beds host microstylolites in grainstone in the lower subsequence of the second deposequence. The microstylolites follow along individual, moderately dipping cross-laminations.

Several hummocky seams occur within packstones to grainstones in the transitional zone of the second deposequence.

Summary

Poorly defined, poorly balanced deposequences characterize the Roy Reed #5 core. In the absence of significant quantities of wackestone, micstone, or dolostone, the upper subsequences may be distinguished by decrease in bedding thickness, appearance of pelecypods, corals, and anhydrite, lack of cross-bedding, and the occurrence of zones of closely-spaced stylolites.

Grainstone dominates the first deposequence, whereas packstone dominates the second. The second deposequence contains a very thick transition zone. Individual, widely-spaced stylolites with stacked, pyramid-shaped columns are an outstanding feature of lower subsequences, whereas zones of many, closely-spaced stylolites, some with very short columns, are characteristic of upper subsequences and transition zones within the Roy Reed #5 core.

Microstylolites occur along cross-laminations and hummocky seams; these are comparatively rare in this section, and occur mainly in the transition zone.

E. Gray Estate #8 Core, White Co., IL

Location

The Gray Estate #8 core (Plate 5), drilled by MEPCO (Moore Engineering and Production Company) in Township 3 South, Range 8 East, Section 30, in White County, Illinois, is the deepest core used in this study. It contains almost 24 feet of Salem Limestone from a depth of 3805 to 3829 feet. This continuous, 4-inch core provides a unique opportunity to observe a dense array of stylolites at depth.

Stratigraphy

All but the upper 1 foot of the 23.5-foot thick, Gray Estate #8 core constitutes an upper subsequence. Lithologic correlation suggests that this subsequence belongs to the second deposequence identified in the Illinois C-1830 core, as indicated in Section F, below. The core contains no true grainstone, 45% packstone, 51% wackestone to micstone, and no true dolostone.

Medium- to thin-bedded, organic-laminated, poorly sorted, locally pelletal, skeletal wackestone and packstone, with pelecypods, crinoids, bryozoans, rugose corals, and, locally, foraminifera, as well as anhydrite concretions, dominate the portion of the upper subsequence exposed in this core.

The upper foot of the core consists of medium-bedded, coarse- to fine-grained, moderately-sorted, oolitic, skeletal packstone to grainstone, with foraminifers, and fragments of crinoids and bryozoans. This rock appears to belong to the lower subsequence.

Stylolites

Individual stylolites are spaced as much as 1 foot apart, in packstone and wackestone near the top of the core. Several of the stylolites have stacked columns, up to 40 mm tall, and they are symmetrical. A negatively asymmetrical stylolite occurs within packstone, 4 feet from the top of the core.

Zones of very closely spaced (5-10 mm) stylolites abound in poorly sorted packstone and wackestone throughout most of the core. The zones are 10 to 50 mm wide (vertically), and the distance between zones is approximately equal to the widths of the zones. A typical zone contains 3 or 4 stylolites. Stylolite zones alternate with individual stylolites in the lower half of the core.

The absence of well-developed stylolites in three massive, 2-foot thick beds of wackestone to packstone is conspicuous. Two of the beds occur in the lower 5 feet of the core, and one of them occurs 10 feet below the top of the core. Fine grain size and good sorting distinguish these massive beds from the very poorly sorted packstones and wackestones which host the dense stylolite zones elsewhere in the core.

Microstylolites occur in every part of the core: between stylolite zones; between individual, isolated stylolites; and even along organic laminae within the otherwise non-stylolitic, massive beds.

Hummocky seams are conspicuous only in a 1.5-foot thick bed of wackestone near the bottom of the core.

Summary

Wackestone and packstone comprising the bulk of the Gray Estate #8 core are indicative of an upper subsequence. The upper 1 foot of packstone to grainstone probably represents the base of a lower subsequence.

Zones of closely spaced stylolites are ubiquitous in coarse-grained, poorly sorted packstone and wackestone, but only a few microstylolites, and no macroscopic stylolites (with columns at least 1mm tall) occur in fine-grained, well-sorted wackestones to packstones.

F. Illinois C-1830 Core, Hardin Co., IL

Location

The thickest section of Salem Limestone is also the southermost section, and it is contained in the C-1830 core (Plate 6), drilled by the Illinois Geological Survey, in Township 12 South, Range 8 East, Section 32, in Hardin County, Illinois. The core has several missing intervals, notably an 18-foot interval located 20 feet from the top of the core. This 2-inch core is not longitudinally cut, which makes description and measurement difficult.

Stratigraphy

The C-1830 core contains most of the Salem Limestone, over a 151-foot interval, at a depth of 520 to 671 feet. Packstone (44%) and wackestone (25%) dominate the section, whereas grainstone (6%) is a minor constituent, and true dolostone is absent. At least part of the missing 25% of the section may have contained shale. Fault breccia may also account for some of the missing intervals, which makes stratigraphic interpretation of the core somewhat tricky. Parts of 3 deposequences comprise this core. The first is less than 10 feet thick, and the other two deposequences each represent approximately half of the remainder of the section.

Three feet of medium-bedded to massive, brecciated, coarse-grained, moderately-sorted, skeletal packstone, with crinoid and bryozoan fragments, are overlain by 5 feet of thin-bedded to massive, organic-laminated, fine-grained, poorly sorted, skeletal wackestone, with crinoids, pelecypods, local foraminifera, and vertical calcite veins, in the first deposequence. The packstones constitute the lower subsequence, and the wackestones, the upper subsequence.

An 8-foot thick lower subsequence contrasts with a 70-foot thick upper subsequence within the second deposequence. Massive, medium-grained, well-sorted, oolitic, skeletal grainstone to packstone, with foraminifers, and vertical calcite veins, dominates the lower subsequence. The top of the last grainstone is the boundary between the lower and upper subsequences.

The upper subsequence of the second deposequence consists of alternating, 5- to 10-foot thick units of thin-to medium-bedded, organic-laminated, medium- to coarse-grained, poorly sorted, skeletal packstones to wackestones, with crinoids, bryozoans, pelecypods, corals, foraminifers, and densely packed stylolites; and massive, locally organic-laminated, fine-grained, well-sorted, skeletal wackestones to micstones, without stylolites. Thin shale beds occur within some of the packstones, at vertical intervals of about 15 feet.

Several missing intervals within the upper subsequence suggest the possibility that part of the section is repeated, but no clear stratigraphic evidence was found for such repetition. An 18-foot thick missing interval just 7 feet above the base of the third deposequence separates what is clearly the lower subsequence, below the missing interval, from the upper subsequence, above the missing interval. The true thickness of the lower subsequence is, hence, unknown, as is the thickness of the upper subsequence, which is truncated at the top of the core. The available 7 feet of the lower subsequence consist of massive, locally brecciated and vuggy, medium-grained, moderately-sorted, oolitic, skeletal grainstone to packstone, with crinoid fragments and vertical calcite veins.

The upper subsequence of the third deposequence is similar to that of the second deposequence, in that it contains alternating, 5- to 10-foot thick units of thin- to medium-bedded, coarse-grained, poorly-sorted, stylolitic packstone and massive, fine-grained, well-sorted, non-stylolitic wackestone and micstone. In contrast with the second deposequence, wackestones in the upper subsequence of the third deposequence contain numerous brachiopod and pelecypod fragments, in addition to bryozoans and crinoids, as well as local, organic laminae. The packstones to wackestones in the third deposequence contain crinoids, corals, brachiopods, bryozoans, organic laminae, and vertical calcite veins. A pair of shale partings, spaced closely--about 1 foot apart--occurs near the bottom, and an isolated shale parting occurs near the top, of the upper subsequence.

Stylolites

Only 6 prominent stylolites, with columns taller than 10 mm, occur in the C-1830 core. Notably, none of them developed within grainstone of lower subsequences in the core. The tallest columns, measuring 50 mm, are in a symmetrical stylolite within packstone to wackestone, 10 feet below the top of the section. Twenty feet below this stylolite, there is a symmetrical stylolite, with 50-mm tall columns and conical caps, also within packstone to wackestone. A symmetrical stylolite with 30-mm columns occurs within packstone to wackstone in the upper subsequence of the second deposequence, 20 feet above the base of the section. The only asymmetrical stylolite, with positive asymmetry, adorns the contact between overlying packstone, and underlying micstone to wackestone, 12 feet below the top of the section.

Stylolite zones are particularly abundant in the upper subsequence of the second deposequence. As many as 6 parallel stylolites occur within 0.5-foot thick intervals, in packstone, below and above a 4-inch thick shale bed near the middle of the upper subsequence. The stylolites are symmetrical, with 1 to 5 mm tall columns. The densest stack of stylolites, with 15 stylolites within a 1-foot thick packstone bed, occurs in a stylolite zone, 17 feet below the top of the second deposequence, less than 4 feet above a thin shale bed. The greatest number of closely spaced stylolites occurs just 2 feet above that zone, where 18 stylolites are regularly spaced within a 3-foot thick zone of stylolites.

Microstylolites are difficult to identify in this uncut core. Organic laminae in packstone in the first deposequence exhibit microserrations suggestive of microstylolites.

Hummocky seams, spaced at least 1 foot apart, occur in non-stylolitic, massive micstone and wackestone of the upper subsequences of the second and third deposequences of the Illinois C-1830 core.

Summary

The C-1830 core represents the thickest section of Salem Limestone described in this study. A thin deposequence at the bottom of the section is typical of many other sections of Salem Limestone. The two other deposequences are the thickest described in this study. A thin lower subsequence, and an upper subsequence consisting of alternating, poorly sorted, stylolitic packstones and nonstylolitic micstones and wackestones, characterize both deposequences.

A prominent stylolite with very tall columns occurs in wackestone to packstone near the top of the section. It is reminiscent of a similar stylolite in wackestone near the top of the Riehl Quarry section. Ubiquitous stylolite zones, with densely packed stylolites, are the dominant feature of this core. The particularly high stylolite density in the upper subsequence of the second deposequence suggests that this is the same portion of the Salem Limestone that constitutes the Gray Estate #8 core (Section E), at much greater depth (3200 feet deeper), and about 60 miles to the north.

G. Harry Siepman Farm Core, Sullivan Co., IN

Location

The northernmost section used in this study is also the westernmost and deepest section in Indiana (Plate 7). It was drilled by the Indiana Geological Survey on the Farm of Harry A. Siepman, in Township 9 North, Range 8 West, Section 30, in Sullivan County, Indiana. The core covers 38 feet of Salem Limestone. The core was drilled in the 1950's, and is preserved in discontinuous sections, with approximately 1 inch per foot missing in the upper half of the core and 2.5 inches per foot missing in the lower half of the core. The core is, hence, not ideal for measuring section, but it was the only deep (>1000 feet) core from Indiana available at the time of this study.

Stratigraphy

The Siepman Farm core contains 38 feet of Salem Limestone, from depths of 1188 to 1150 feet. Only the lower subsequence of one deposequence is represented in the core, which consists of 12% grainstone and 88% packstone, assuming that the numerous but short, missing intervals did not contain other lithotypes.

The lower 23 feet of the core contain massive, medium- to coarse-grained, moderately- to well-sorted, oolitic, skeletal packstone and packstone to grainstone, with fragments of crinoids, bryozoans, and, locally, pelecypods and brachiopods. The upper 15 feet of the core contains massive to medium-bedded, locally cross-bedded, locally organic-laminated or cherty, medium- to coarse-grained, moderately- to poorly-sorted, locally oolitic, skeletal packstone and grainstone, with foraminifers, crinoids, bryozoans, and some brachiopod fragments.

Stylolites

Figures 9 through 14 show a representative selection of stylolites in the Siepman Farm core, in ascending stratigraphic order.

Asymmetrical stylolites are common in the Siepman Farm core. The lower half of the core, where individual stylolites predominate, contains 3 negatively asymmetrical stylolites with 20-mm tall columns, spaced 3 to 8 feet apart, within packstone to grainstone. One of the stylolites features calcite veins oriented parallel to striae along the sides of columns, which are essentially vertical. Two negatively asymmetrical stylolites, with 2 and 5 mm tall columns, respectively, occur in the upper half of the core. One of them forms the contact between overlying grainstone and underlying packstone. A positively asymmetrical stylolite occurs 2.5 feet below the bottom of the core, with 10 mm tall columns. Three symmetrical stylolites, with columns ranging in height from 1 to 10mm, occur within packstone rich in organic laminations, with medium grain size and moderate sorting. Stylolites are notably absent in a 10-foot thick, massive bed of medium-grained, well-sorted packstone, in the middle portion of the core.

Two zones of closely-spaced stylolites occur within medium-grained, poorly-sorted packstone in the upper half of the core. One zone, located 9 feet below the top of the core, is 0.5 foot wide (vertically). It contains 3 stylolites with 7-mm tall columns. The other, located 2 feet below the first, is 0.5 foot wide and contains 6 stylolites with 10-mm tall columns. Organic laminae occur within both stylolite zones.

Microstylolites stand out only in association with organic laminae in packstone near the top of the core. Hummocky seams are not a characteristic feature of the Siepman Farm core.

Figure 12.

Cylindrical stylolite with conical caps and poorly developed negative asymmetry, located 1182 ft below ground surface in the Harry A. Siepman Farm Core (Sullivan County, Indiana), in Salem Limestone. The stylolite is overlain by medium-grained, moderately sorted, oolitic, crinoidal packstone to grainstone, and underlain by lenses of fine-grained, oolitic packstone to wackestone, embedded within fine- to coarse-grained, poorly sorted, echinodermal packstone to grainstone. Stylolite columns are 18 mm tall and 15 mm wide, with .75 mm thick caps. The columns exhibit striae, and they enclose coarse calcite spar. Neighboring stylolites are located 3 ft below and 7.5 ft above this one, which is fairly typical of lower-deposequence stylolite development (see text).

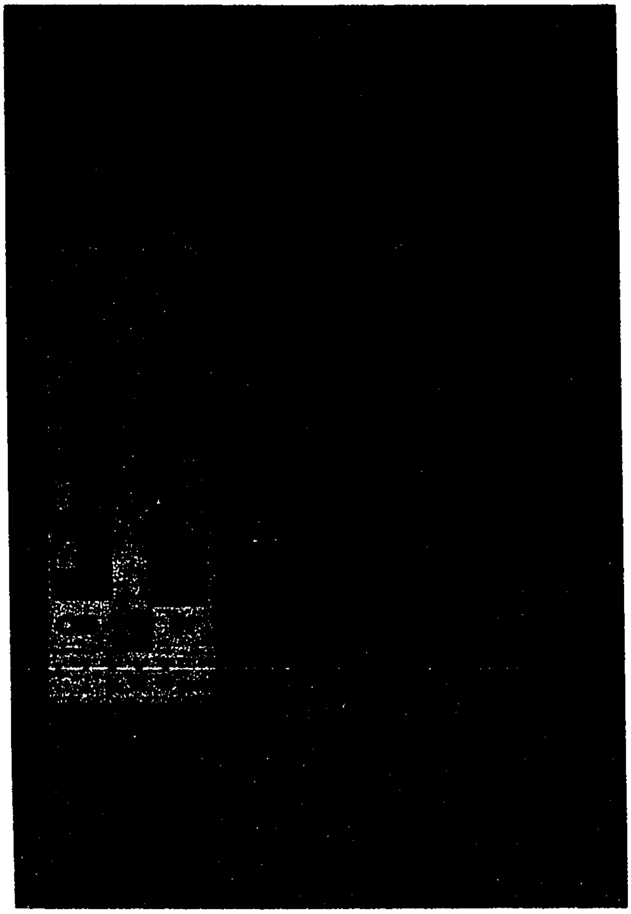

Figure 13.

Cylindrical stylolite with hummocky to serrated caps, located 1164.5 ft below ground surface in the Harry A. Siepman Farm Core (Sullivan County, Indiana), in Salem Limestone. Faintly laminated, medium-grained, well sorted, oolitic, crinoidal, bryozoan packstone surrounds the stylolite. Columns are striated, measuring 5 mm in height and width, and caps are .25 mm thick. Neighboring stylolites are located 9.5 ft below (see Figure 11) and 2 ft above (see Figure 13) this one.

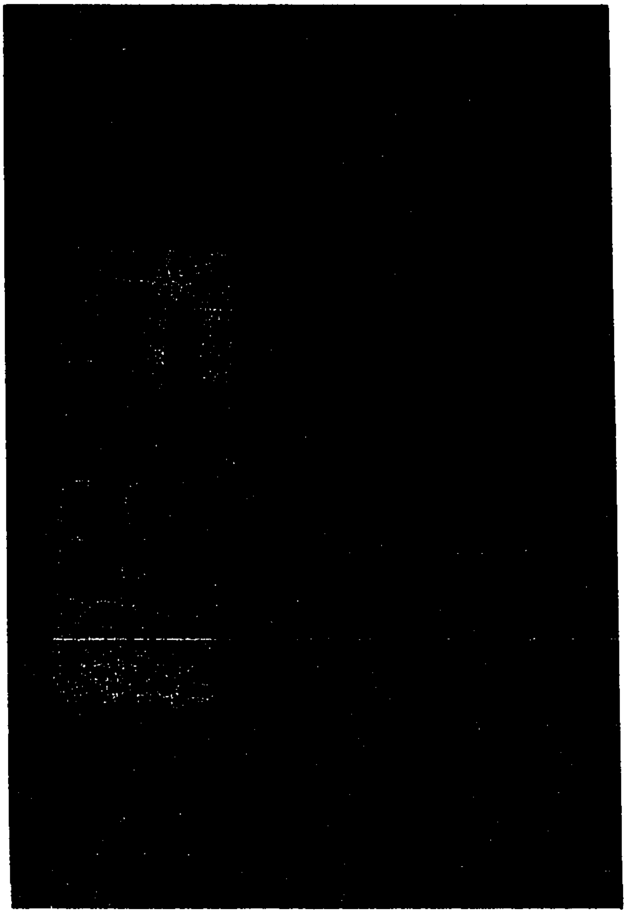

Figure 14.

Cylindrical stylolite with hummocky to serrated caps, located 1162.5 ft below ground surface in the Harry A. Siepman Farm Core (Sullivan County, Indiana), in Salem Limestone. Cross-laminated, medium-grained, well-sorted, oolitic, foraminiferal, echinodermal packstone to grainstone surrounds the stylolite. Columns are blocky -- 10 mm tall and wide, with, .5 mm thick caps. The Stylolite is parallel to the inclined lamination. Some columns are perpendicular to cross-lamination, whereas others are vertical. Neighboring stylolites occur 2 ft below (see Figure 12) and 1 ft above this one. The moderate vertical spacing and moderate, blocky column development is indicative of stylolite development in an organic-rich, thin-bedded transition zone between lower and upper deposequences in the Salem Limestone (see text).

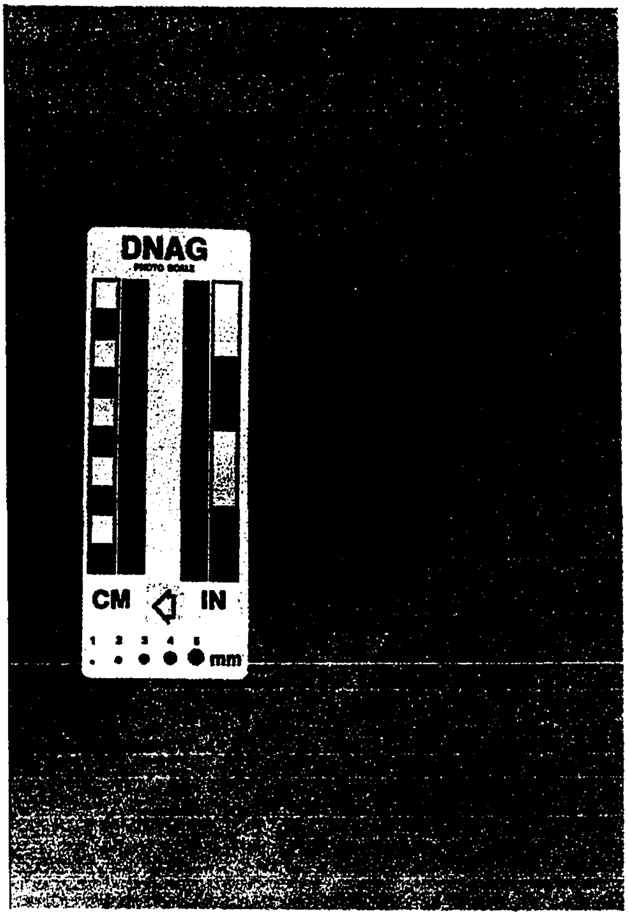
DNAG
PHOTO SCALE
CM
IN
1
2
3
4
5
mm

Summary

The Siepman Farm core contains the lower part of a single deposequence and includes only packstone and grainstone. The high organic content, thin bedding, and stylolite zones in the upper half of the core are suggestive of a transitional zone.

Massive, medium-grained, well-sorted packstones without organic laminations contain no stylolites. Massive to medium-bedded, medium- to coarse-grained, poorly sorted packstones contain individual stylolites, spaced 0.5 feet to more than 5 feet apart. Medium- to thin-bedded, organic-laminated, medium-grained, poorly- to moderately-sorted packstones contain stylolite zones, with many, closely spaced stylolites. Microstylolites occur along some organic laminae, particularly where macroscopic stylolites are absent.

H. George Armstrong Farm core, Lawrence Co., IN

Location

The shallowest of the cores used in this study was drilled by the Indiana Geologic Survey on the farm of George Armstrong, in Township 6 North, Range 2 West, Section 28, in

Lawrence County, Indiana (Plate 8). This 3-inch core offers a good, continous view of the Salem Limestone.

Stratigraphy

All 92 feet of Salem Limestone, between the contacts with the underlying Harrodsburg Limestone and the overlying St. Louis Limestone, constitute the Armstrong Farm core. A well-balanced and well-developed deposequence that makes up 76 feet of this core shows a broad representation of lithofacies. The core consists of 21% grainstone, 33% packstone, 15% wackestone, and 32% dolostone.

The first, 76-foot thick deposequence features almost equally thick lower (40 ft) and upper (36 ft) subsequences. The lower subsequence, itself, can be divided into 3 units. The lowest unit is 5 feet thick, and consists of medium-bedded, fine- to medium-grained, moderately- to poorly-sorted, skeletal packstone, with foraminifers, and crinoid, bryozoan, and some pelecypod fragments. This unit contains many stylolites. The second unit is 23 feet thick, and consists of massive, medium-grained, well-sorted, locally oolitic, skeletal grainstone to packstone, with foraminifers, and fragments of crinoids, bryozoans, and some brachiopods. The third, 12-foot thick unit is dominated by massive to medium-bedded, locally flaser-bedded and organic-laminated, fining-upward, medium- to fine-grained, well sorted, skeletal, sucrosic dolopackstone and packstone, with foraminifers and fragments of bryozoans and crinoids.

The upper subsequence of the first deposequence can also be divided into three units. The first, lowest unit is 12 feet thick, and consists of medium- to thin-bedded, locally flaser-bedded and vuggy, fine- to coarse-grained, well- to poorly-sorted, skeletal, sucrosic dolowackestone to dolomicstone, with fragments of crinoids and bryozoans and a few, thin interbeds of micstone, wackestone, packstone, and even grainstone. The second unit consists of 19 feet of massive, flaser-bedded, locally cherty, fine- to medium-grained, well- to locally poorly-sorted, skeletal, sucrosic dolowackestone and packstone, with foraminifers and crinoids. The third unit is 5 feet thick, and lithologically very similar to the first unit.

The 17-foot thick, second deposequence also consists of almost equally thick upper and lower subsequences. Massive, coarsening-upward, fine- to medium-grained, well- to moderately-sorted, locally pelletal, skeletal packstones, with foraminifers and bryozoans, constitute the 7-foot thick, lower subsequence. The 10-foot thick upper subsequence consists of six feet of massive to medium-bedded, organic-laminated, fine-grained, well-sorted, skeletal wackestone to micstone, with pelecypod fragments and foraminifers, grading upwards into 4 feet of massive to thin-bedded, fine- to medium-grained, moderately sorted, skeletal packstone, with crinoids, foraminifers, and pelecypods.

Stylolites

Figures 15 through 19 show a representative selection of stylolites in the Armstrong Farm core, in ascending stratigraphic order.

Individual stylolites with columns taller than 2 mm occur only in lower subsequences in the Armstrong Farm core. A symmetrical stylolite with 40-mm tall, stacked (pyramid-shaped) columns occurs within massive packstone in the lower subsequence of the second deposequence. A negatively asymmetrical stylolite, with 30-mm tall columns that feature conical caps, occurs within massive grainstone in the lower subsequence of the first deposequence. Another negatively asymmetrical stylolite, located 10 feet above the latter, has 10-mm tall, conical columns. Four symmetrical stylolites also occur in the lower subsequence of the first deposequence, with column heights ranging from 2 to 25 mm, and the columns of one of the stylolites are characterized by conical caps.

Figure 15.

Cylindrical stylolite with conical caps, located 207 ft below ground surface in the George Armstrong Farm Core (Lawrence County, Indiana), in Salem Limestone, 1.5 ft above the contact between the Salem and Harrodsburg Formations. The stylolite is overlain by fine-grained, well-sorted, foraminiferal, echinodermal packstone (P), and underlain by patches of micstone (M) embedded within medium-grained, well-sorted packstone (P). The well-developed columns of the stylolite (12mm tall and 6 mm wide, with .5 mm thick caps), and its isolated occurrence -- the closest stylolites are at least one ft away vertically -- are features typical of stylolites developed in lower parts of deposequences in the Salem Limestone (see text).

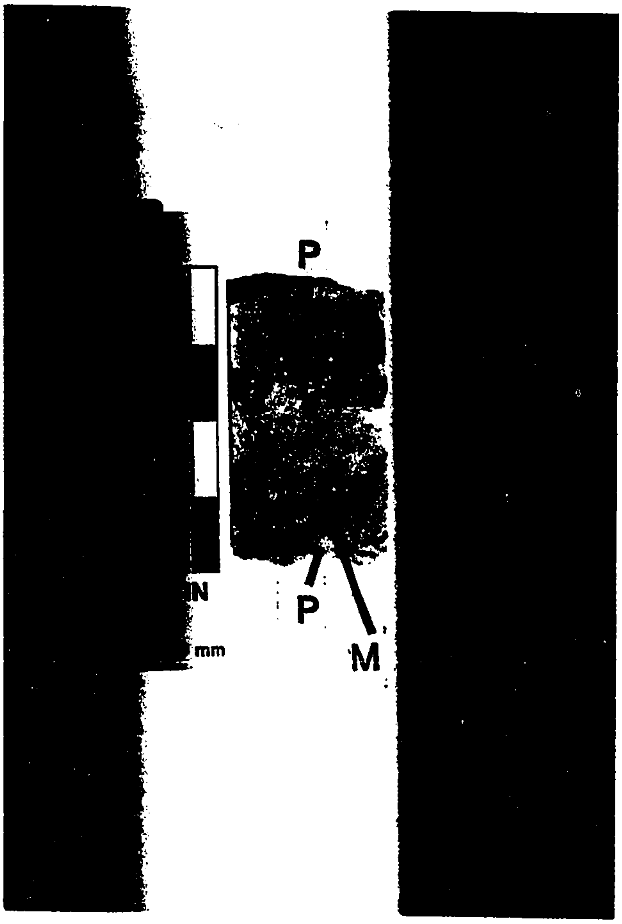
P
P
M
N
mm

Figure 16.

Cylindrical stylolite with conical caps and negative asymmetry, located 183.5 ft below ground surface in the George Armstrong Farm Core (Lawrence County, Indiana), in Salem Limestone, 25 ft above the base of the formation. The stylolite is overlain by fine-grained, well-sorted, foraminiferal, bryozoan grainstone (G), and underlain by medium-grained, moderately to poorly sorted, echinodermal, foraminiferal packstone (P). Striated columns are up to 30 mm tall and 8 mm wide, and the closest stylolite is six ft above the stylolite, typical of stylolites developed in lower parts of deposequences in the Salem Limestone (see text).

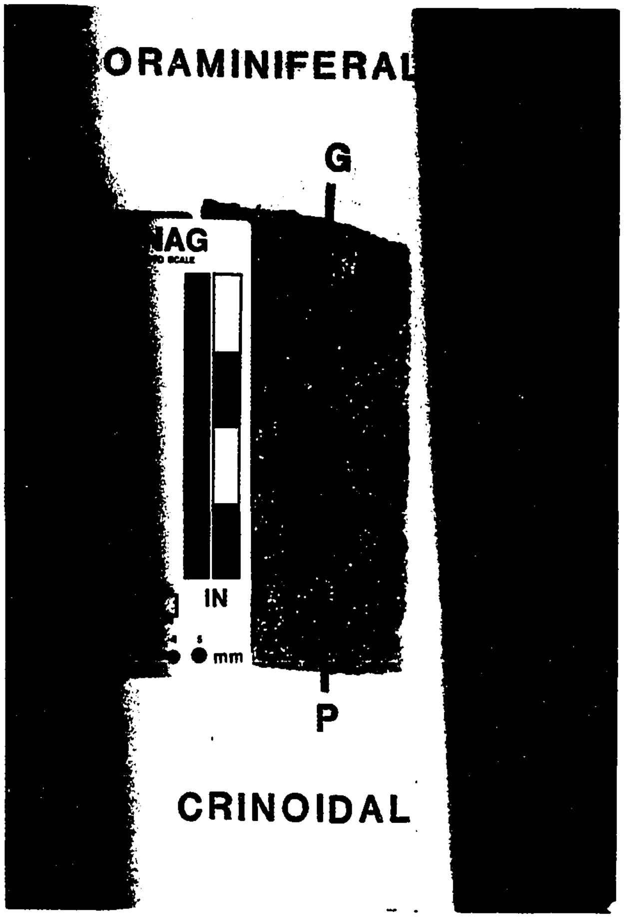
ORAMINIFERAL
G
IAG
IN
mm
P
CRINOIDAL

Figure 17.

Portion of large, 30 mm tall, conical stylolite column (arrow), accompanied by a dense network of hummocky to serrated seams, located 159.5 ft below ground surface in the George Armstrong Farm Core (Lawrence County, Indiana), in Salem Limestone, 49 ft above the base of the formation. The stylolite is overlain by flaser-bedded, fine-grained, moderately sorted, echinodermal, foraminiferal packstone and dolomicstone (DM), and underlain by spotty, flaser-bedded, fine- to medium-grained, poorly sorted, echinodermal, bryozoan, partially dolomitized packstone to wackestone (P/W). Organic laminae occur within and adjacent to the stylolite column. Individual hummocky seams are 1 mm thick. The interwoven network of organic, hummocky to serrated seams and columnar stylolite is typical of stylolitic zones developed in upper parts of deposequences in the Salem Limestone (see text).

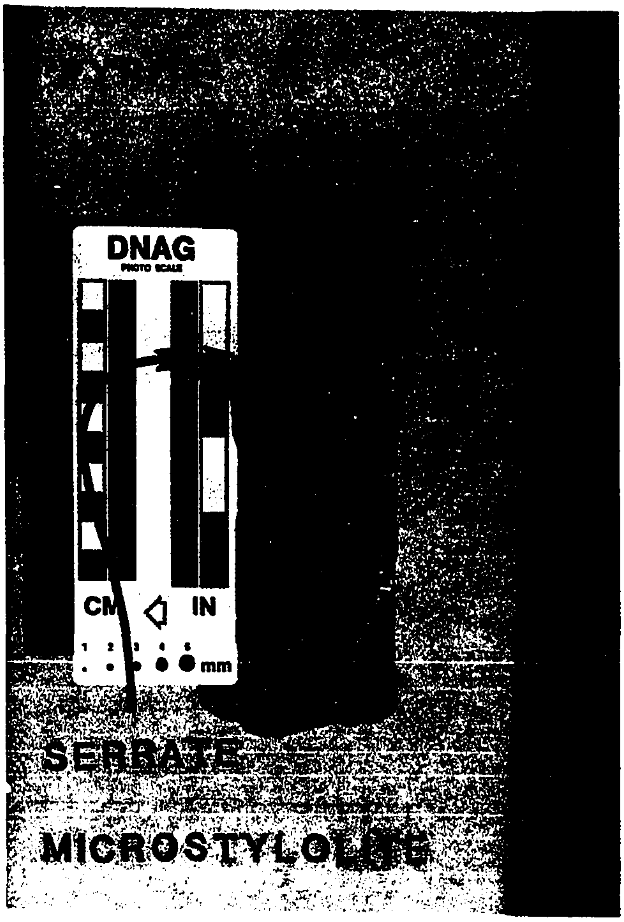
DNAG
PHOTO SCALE
CM
IN
1 2 3 4 5
mm
SERRATE
MICROSTYLOLITE

Figure 18.

Hummocky to serrated organic seams along the margins of chert lenses, located 142 ft below ground surface in the George Armstrong Farm Core (Lawrence County, Indiana), in Salem Limestone, 66.5 ft above the base of the formation. The seams and chert lenses are embedded in flaser-bedded dolowackestone. Serrations are up to 5 mm tall and 10 mm wide, and hummocky seams are commonly 1 mm thick. Zones of hummocky seams, lacking well-developed, columnar stylolites, are typical of dolomitic, upper parts of deposequences in the Salem Limestone (see text).

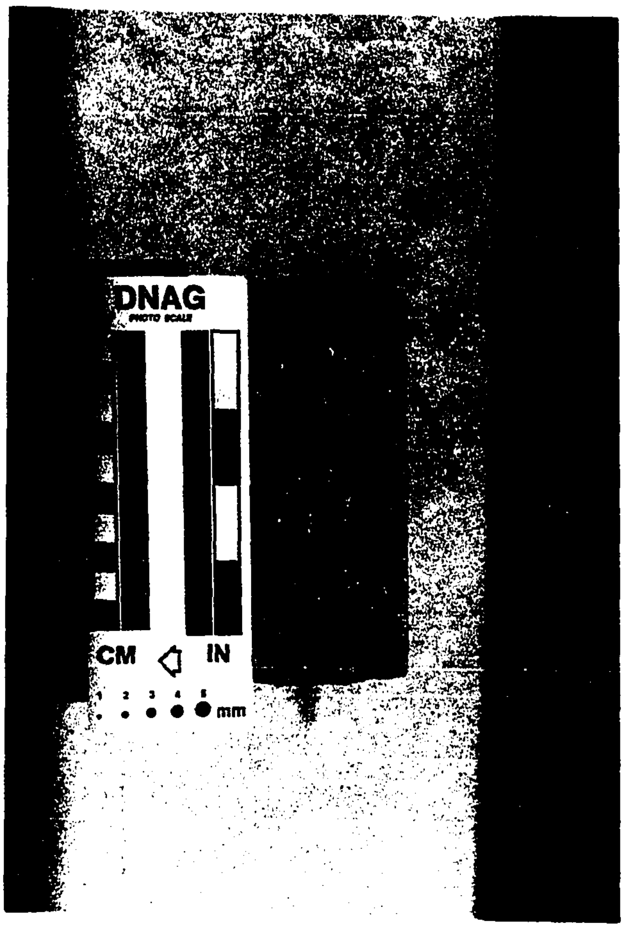
DNAG
CM
IN
mm

Figure 19.

Large, cylindrical stylolite with stepped (pyramidal) column, located 128 ft below ground surface in the George Armstrong Farm Core (Lawrence County, Indiana), in Salem Limestone, 80.5 ft above the base, and only 12.5 ft above the top of the formation. Fine- to medium-grained, moderately sorted, foraminiferal, bryozoan packstone surrounds the stylolite. The stylolite column measures 20 mm in height, and 40 mm in width at the base of the pyramid, which points downward. The column cap is 4 mm thick, but appears thicker in the photograph because the core broke apart along the stylolite. The closest neighboring stylolite is located 3.5 ft above this one, which is a good example of a well-developed, isolated stylolite within the lower part of a deposequence (see text).

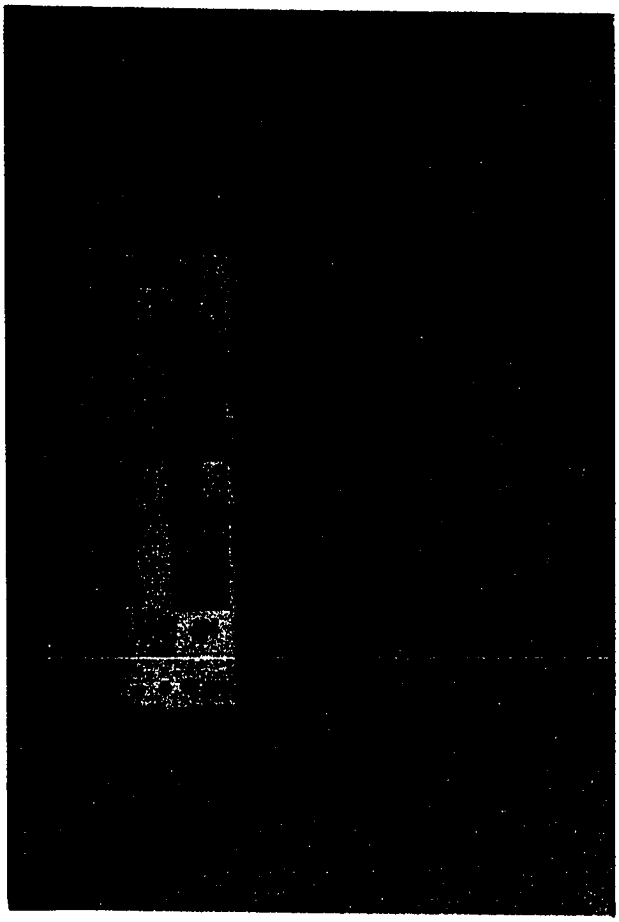

Most individual stylolites in upper subsequences in the George Armstrong Farm core are poorly developed, with short (1-2 mm) columns. Two stylolites in the second deposequence exemplify this pattern. Other stylolites in upper subsequences of the core occur in atypical lithologies. An example is the positively asymmetrical stylolite with 15-mm tall columns occurring within a thin (<0.5 foot), coarse-grained grainstone bed, located 3 feet above the base of the upper subsequence of the first deposequence.

An unusual stylolite zone in packstone 6 feet below the top of the first deposequence and overlain and underlain by dolowackestone, is defined by branching, symmetrical stylolites with 1-mm tall columns. A 2-inch thick stylolite zone, located in packstone near the middle of the upper subsequence of the first deposequence, hosts 4 stylolites, each with 1-mm tall columns. Another stylolite zone, located at the very bottom of the core, is about 0.5 feet thick and contains 7 laterally discontinuous stylolites with 1-mm tall conical columns. Such columns lend the stylolites a serrated appearance.

Microstylolites pervade the interbedded, thin-bedded, organic-laminated and flaser-bedded dolowackestones and packstones in the upper 5 feet of the upper subsequence of the first deposequence. An individual serrated microstylolite occurs 1 foot above the base of the same subsequence within a thin lense of packstone and enveloped by micstone.

The upper subsequences of both deposequences host numerous hummocky seams in packstone, wackestone and dolowackestone. Some of the seams exhibit small, isolated, conical columns.

Summary

The Armstrong Farm core features a thick, well-developed deposequence, containing a full suite of lithofacies ranging from massive grainstones in the lower subsequence to thin-bedded, organic-rich micstones and dolomicstones in the upper subsequence. The top of the lower subsequence is dolomitized, which is suggestive of a transitional zone.

Individual, isolated stylolites with tall columns characterize lower subsequences in this core, whereas stylolite zones containing microstylolites and stylolites with short columns characterize upper subsequences. Coarse- to medium-grained, poorly sorted rocks of all lithofacies host stylolites, whereas fine- to medium-grained, well-sorted rocks lack stylolites in both the upper and lower subsequences. Organic laminations are commonly associated with stylolites or microstylolites throughout the Armstrong Farm core.

I. Bedford, IN., Roadcut

Location

The thickest, most spectacular outcrop of the Salem Limestone described in this study is a roadcut along both sides of Indiana State Route 37, 1 mile north of Bedford, Lawrence County, Indiana, in Township 5 North, Range 1 West, Section 5 (Plate 9). The road ascends southward, exposing the complete Salem Limestone. Owing to the degree of weathering, stylolites are well defined, particularly on the northbound side.

Stratigraphy

The Bedford roadcut exposes 78 feet of Salem Limestone, representing an essentially complete section. It contains 29% grainstone, 38% packstone, 16% wackestone to micstone, and 17% dolostone (Figure 20). This broad palate of lithofacies is unevenly distributed between the first two deposequences, which are 41 feet and 34 feet thick, respectively, and make up the bulk of the section. Only 3 feet of the lower subsequence of a third deposequence are included at the top of the section, just below the erosion surface.

In the first deposequence a 35-foot thick lower subsequence contrasts with a 6-foot thick upper subsequence. The lower subsequence consists of two units. Medium- to thin-bedded, cross-bedded, fining-upward, medium- to fine-grained, poorly- to moderately-sorted, oolitic, skeletal grainstone and packstone, with foraminifers, and fragments of bryozoans, crinoids, and locally, brachiopods and gastropods, constitute the 20-foot thick, first (lower) unit. The boundary between the first and second units is concave-upward, resembling a large channel.

Massive, cross-bedded, coarse- to medium-grained, well-sorted, oolitic, skeletal packstone to grainstone, with foraminifers and fragments of bryozoans, crinoids, and brachiopods, constitute the 15-foot thick, second (upper) unit of the lower subsequence of the first deposequence.

Massive, locally flaser-bedded, vuggy, fine- grained, well- sorted, skeletal wackestone to micstone, with foraminifers, interbedded with medium-bedded, flaser-bedded, medium-grained, moderately-sorted, skeletal packstone, with

Figure 20.

Complete section of Salem Limestone, exposed in southerly view of west-facing roadcut along northbound Indiana State Route 37, just north of Bedford, Indiana. The leftmost arrow, shown in the lower left corner of the photograph, points toward planar, thin-bedded grainstone and packstone at the base of Salem Limestone. The middle arrow points toward large-scale cross-bedded packstone, filling a large channel in the lower part of the first deposequence. The rightmost arrow points toward massive micstone and dolostone in the upper part of the second deposequence.

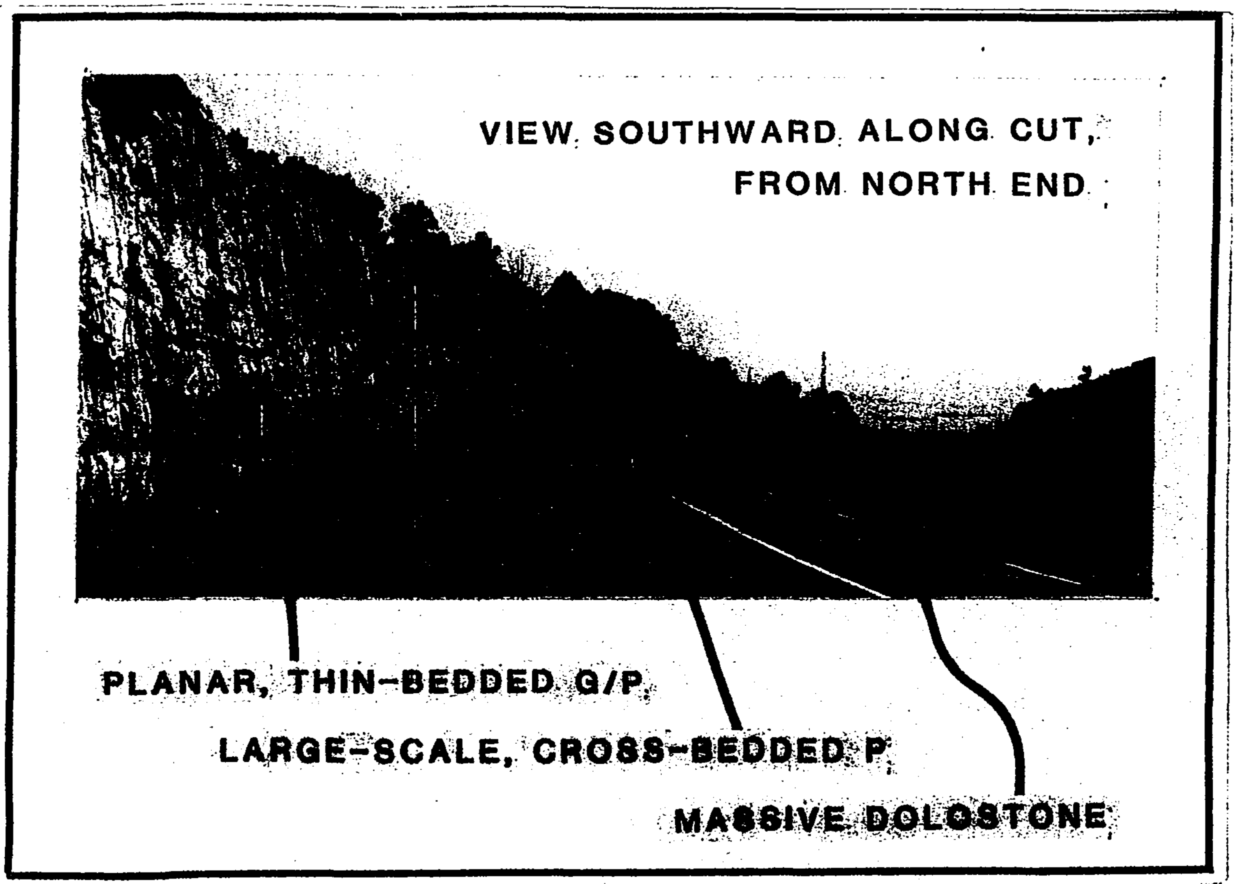
VIEW SOUTHWARD ALONG CUT,
FROM NORTH END
PLANAR, THIN-BEDDED G/P
LARGE-SCALE, CROSS-BEDDED P
MASSIVE DOLOSTONE

foraminifers, comprise the 6-foot thick, upper subsequence of the first deposequence.

Wackestone is the most common lithotype throughout the second deposequence, and grainstone is rare. The upper and lower subsequences are roughly equal in thickness. Medium- to thin-bedded, flaser-bedded, organic-laminated, medium-grained, moderately- to poorly- sorted, oolitic, skeletal packstone to grainstone, with foraminifers, and crinoid, bryozoan and pelecypod fragments, locally interbedded with medium-bedded, organic-laminated micstone, constitute the 16-foot thick, lower subsequence.

Massive to medium-bedded, locally flaser-bedded, fine-grained, well sorted, skeletal wackestone, dolowackestone, and micstone, with crinoids and pelecypods, interbedded with medium-bedded, medium- to coarse-grained, poorly-sorted, skeletal packstone, with brachiopods, foraminifers, crinoids and pelecypods, constitute the 18-foot thick, upper subsequence.

Finally, 3 feet of massive, medium-grained, moderately-sorted, oolitic, skeletal grainstone and packstone, with foraminifers and bryozoans, occur at the top of the roadcut. Apparently this belongs to the lower subsequence of an incomplete third deposequence at the top of the Salem

Limestone.

Stylolites

The largest stylolites in the Bedford roadcut, with the tallest columns, occur in medium- to coarse-grained, moderately- to poorly-sorted packstone and grainstone in the lower subsequences of the first two deposequences. Two positively asymmetrical stylolites, located 3 and 17 feet above the base of the section, have columns respectively 20 mm (with concave caps) and 50 mm (with serrated caps) tall. Packstone overlies both of the stylolites. The stratigraphically lower stylolite is underlain by grainstone, whereas the higher stylolite is underlain by packstone. Two negatively asymmetrical stylolites with 15 mm and 50 mm tall columns, respectively, occur within grainstone, 1 and 14 feet above the base of the section. The columns of both negatively asymmetrical stylolites have conical caps. Two symmetrical stylolites with 15 mm and 10 mm tall columns, respectively, occur within packstone, 5 and 27 feet above the base of the section. Both symmetrical stylolites have columns with serrated caps, and the stratigraphically higher stylolite has conical columns.

Stylolite zones characterize the upper subsequences of the first and second deposequences. The zones are 0.5- to 1-

foot thick, and they contain 3 or 4 stylolites, with 1- to 10-mm tall columns. Poorly- to moderately-sorted, organic-laminated packstone to wackestone typically hosts the stylolite zones. Stacked stylolites, with pyramid-shaped columns, occur in a stylolite zone at the top of the second deposequence.

Microstylolites grade into organic laminations in micstone to wackestone that hosts a stylolite zone, in the middle of the upper subsequence of the second deposequence.

Hummocky seams mark the boundaries between the upper and lower subsequence of the first and second deposequences, and they are common in packstone and wackestone in the upper subsequences of both deposequences. Hummocky seams with individual, isolated columns protruding from an otherwise smooth to hummocky surface occur in dolowackestone, and at contacts between dolowackestone and wackestone within the first 10 feet of the upper subsequence of the second deposequence.

Summary

The Bedford roadcut exhibits two full deposequences, each about 35 to 40 feet thick. The first has a well-developed lower subsequence, with a spectacular, massive, cross-bedded packstone lense cutting a deep channel into underlying, medium- to thin-bedded grainstone, and a very thin, poorly developed upper subsequence, with grainstone interrupting the micstone to wackestone unit. The second deposequence has roughly equally thick upper and lower subsequences, but the deposequence is poorly balanced, with much micstone and wackestone in the lower subsequence. In contrast with the massive bedding in the upper subsequences, the thin bedding in the lower subsequences of both deposequences is characteristic of the eastern rim of the Illinois Basin. Only a few feet of the lower subsequence of a third deposequence are included in the Bedford section of the Salem Limestone.

Well-developed, individual stylolites with columns 10 to 50 mm tall exhibit various asymmetrical forms in medium- to coarse-grained, poorly- to moderately-sorted rocks in lower subsequences. Positively asymmetrical stylolites occur within packstone or at contacts with overlying packstone and underlying grainstone. Negatively asymmetrical stylolites occur within grainstone, commonly with columns having pointed, conical caps. Stylolite zones, with many closely spaced stylolites with short columns, occur within poorly sorted, organic-laminated packstones to wackestones in upper subsequences. These rocks are generally dominated by non-stylolitic, well-sorted wackestones and micstones. Hummocky seams, with sparse, isolated columns, occur in dolostone in upper subsequences.

J. Mulzer Brothers Quarry Core, Crawford Co., IN

Location

The southernmost section in Indiana used in this study (Plate 10), is derived from a core drilled by the Indiana Geological Survey, in the Mulzer Brothers Quarry, in Township 4 South, Range 1 East, Section 25, in Crawford County, Indiana. The continuous, 3-inch core includes the entire Salem Limestone, and part of the overlying St. Louis Limestone. Stylolites are sparse in this micstone-dominated section.

Stratigraphy

The Mulzer Brothers core contains the only section of Salem Limestone used in this study with parts of 5 deposequences. The 118-foot long core is dominated by wackestone and micstone (81%), contains 14% packstone, and no grainstone or dolostone. Only 12 feet of the upper subsequence of the first deposequence are included in the core. The second, third, and fourth deposequences are complete, albeit poorly balanced, with an overabundance of micstone. They are 26 feet, 52 feet, and 13 feet thick, respectively. Finally, the 15-foot, fifth deposequence apparently continues upward into the St. Louis Limestone.

Massive, locally lenticular micstone and wackestone, with crinoid and bryozoan fragments, constituting the basal 12 feet of the core, represents the upper subsequence of the first deposequence. The lower subsequence is not included in the Salem Limestone.

The only well-balanced deposequence in the Mulzer Brothers core is the second, 26-foot thick deposequence, with a 14-foot thick lower subsequence, and a 12-foot thick upper subsequence. Medium-bedded to massive, oily, organic-laminated, fining upward, medium- to fine-grained, poorly- to moderately-sorted, locally pelletal, skeletal packstone to wackestone, with crinoid and bryozoan fragments, and with regularly spaced (1-2 feet) shale partings, constitutes the lower subsequence. A single, massive micstone bed with a few lenses of wackestone (with bryozoans and brachopods) constitutes the entire upper subsequence.

A very thin (3 feet) lower subsequence, and a thick (23 feet) upper subsequence characterize the third deposequence. The lower subsequence consists of medium-bedded, oily, fine- to medium-grained, moderately sorted, locally pelletal, skeletal packstone, with crinoid, bryozoan, and brachiopod fragments. The upper subsequence consists of 17 feet of massive, locally organic-laminated or cherty, micstone and skeletal wackestone, with locally large (>5 mm) brachiopods and crinoids, and with pelecypods and rugose corals. This is overlain by 6 feet of medium-bedded, locally lenticular, normally-faulted, organic-laminated, skeletal wackestone to micstone, with crinoids, foraminifers, pelecypods, and rugose corals.

The fourth, 13-foot thick deposequence also contains a very thin (3 feet) lower subsequence consisting of medium- to thin-bedded, organic-laminated, fine-grained, well-sorted, skeletal packstone, with foraminifers, brachiopods, and crinoid fragments, and with thin shale partings between beds, just as in the lower subsequence of the second deposequence. Massive, locally pelletal micstone to wackestone, with vertical calcite veins and some foraminifers and crinoids, comprises the upper subsequence of the fourth deposequence.

Massive to medium-bedded, organic-laminated, fine-grained, well-sorted, foraminiferal packstone, with thin shale partings between beds, and with crystalline calcite lining some of the organic laminae, constitutes the 4-foot thick, lower subsequence of the fifth deposequence. Massive to thin-bedded, locally organic-laminated or cherty, locally pelletal, skeletal wackestone to micstone, with bryozoans, foraminifers, pelecypods, and rugose corals, constitutes the 11 feet of the upper subsequence which lie at the top of the Salem Limestone.

Stylolites

Stylolites are rare in the Mulzer Brothers Quarry core, probably due to oil accumulation (Figure 21).

A symmetrical stylolite, with 50-mm tall columns featuring hummocky caps, marks the boundary between the fourth and fifth deposequences. A negatively asymmetrical stylolite, with 7-mm tall columns, occurs within packstone, just 1 foot above the latter. A symmetrical stylolite with 15-mm tall columns occurs within wackestone, 5 feet below the top of the Salem Limestone.

A 2-inch thick stylolite zone, containing 5 stylolites with 1-mm tall columns, occurs within packstone at the boundary between the upper and lower subsequences of the fourth deposequence.

Well-defined microstylolites either do not occur in the Mulzer Brothers core, or the dark, oily nature of much of

Figure 21.

Thick organic laminae (or hummocky seams), defining an organic-rich zone, located 481 ft below ground surface in the Mulzer Brothers Quarry Core (Crawford County, Indiana), in Salem Limestone, 99 ft below the contact between the Salem and St. Louis Formations. Fine-grained, crinoidal, bryozoan packstone to wackestone is host to the laminae or seams. The core is saturated with oily, hydrocarbon substance, suggesting that hydrocarbon coating of grains prevented stylolite development in this exceptionally thick section of the Salem Limestone.

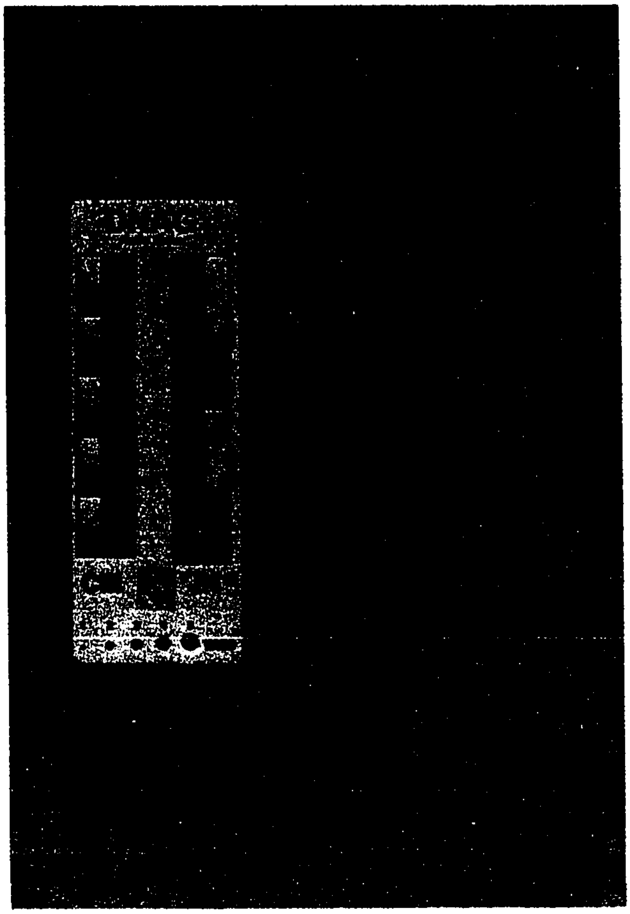

the core precludes their identification.

A hummocky seam occurs within wackestone, immediately above a thin shale parting, 2 feet below the top of the Salem Limestone. Some of the thin shale partings between packstone in the lower subsequences of the second, fourth, and fifth deposequences appear to grade laterally into hummocky seams.

Summary

Poorly developed, thin, oily lower subsequences with no grainstone, overlain by thick, oily upper subsequences with massive micstone to wackestone, characterize the Salem Limestone in the Mulzer Brothers core. Shale partings, instead of stylolites, commonly mark the contacts between packstone beds in lower subsequences.

A paucity of stylolites distinguishes the Mulzer Brothers core. Stylolites occur only in the less oily, upper 25 feet of the section, where a prominent stylolite and a stylolite zone mark the boundaries between the fourth and fifth deposequences, and between the upper and lower subsequences of the fourth deposequence, respectively. Microstylolites are rare or difficult to observe in the oily rock, and hummocky seams associated with thin shale partings are common in lower subsequences in the core.

K. Trainor #4 Core, Jasper Co., IL

Location

The Trainor #4 Core, drilled by the Unocal Oil Company, is one of two cores from Jasper County, Illinois--the northernmost part of Illinois represented in this study. The core has a diameter of 4 inches, and spans 46 feet of discontinuous Salem Limestone at a depth of 3300 to 3346 feet. 42% of the section missing; two to three foot sections alternate with equally thick, missing intervals. Because of the high percentage of missing section, the core is not included in the data set used in contouring basin-wide stylolite trends (Chapter 6).

Stratigraphy

The 26.5 feet of rock comprising the Trainor #4 core consist of 41% grainstone, 25% wackestone to micstone, 22% dolostone, and 12% packstone. All the grainstone and packstone is contained in the lower half of the section, and all the wackestone, micstone, and dolostone is contained in the upper half of the section. This distribution strongly suggests that the core represents a single deposequence.

The 46 foot stratigraphic span of the core may constitute the entire deposequence -- a possibility supported by the exact separation of grainstone and packstone in the lower 23 feet of section, and wackestone to micstone, as well as dolostone, in the upper 23 feet of section. Clearly, the lower 23 feet constitute the lower subsequence of the deposequence, and the upper 23 feet constitute the upper subsequence. Massive to cross-bedded, medium- to coarse-grained, poorly- to well-sorted, oolitic grainstone to packstone, with crinoids, foraminifers, and bryozoans, comprises much of the lower subsequence. Massive, organic-laminated and flaser-bedded, cherty micstone, wackestone, and dolostone, with locally developed anhydrite, comprises much of the upper subsequence. Shale may have occupied parts of the missing intervals of the section.

Stylolites

Figures 22 through 24 show typical stylolites and hummocky seams in the Trainor #4 core, in ascending stratigraphic order.

Stylolites and hummocky seams are spaced 0.5 to 2 feet apart in the lower subsequence. Most of the stylolites are symmetrical, with 10 to 20 mm columns. Conical caps surmount the 20-mm tall columns of a prominent, negatively

Figure 22.

Cherty, organic-laminated, microstylolitic wackestone and micstone, located 3308 ft below ground surface in the Trainor #4 Core (Jasper County, Illinois), in the Salem Limestone Formation. A hummocky seam bounds the bottom of the sample. Organic laminae are most abundant along the top and bottom of the sample, and not in the vicinity of the large chert nodule in the middle. The upper and lower boundaries of the chert nodule appear "truncated," but the boundaries are neither stylolitic nor truly hummocky. This suggests that the chert nodule, rather than being truncated, was stunted in its growth in both vertical directions, perhaps due to preexisting, thin, clay-rich or organic-rich layers that were impervious to silica in solution.

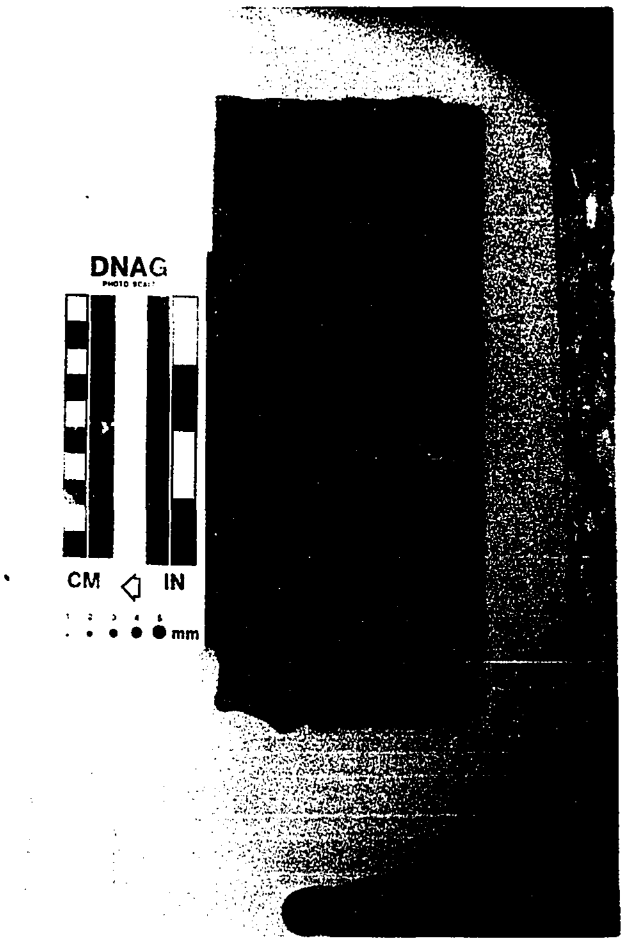
DNAG
CM
IN
mm

Figure 23.

Hummocky to serrated seam, located 3302 ft below ground surface in the Trainor #4 Core (Jasper County, Illinois), in Salem Limestone. The hummocky seams is overlain by locally cherty micstone, and underlain by organic-laminated, microstylolitic micstone, typical of upper parts of deposequences in the Salem Limestone. Serrations indicate incipient stylolitization of the organic-rich, hummocky seam, which is common at substantial depths, such as that of this sample.

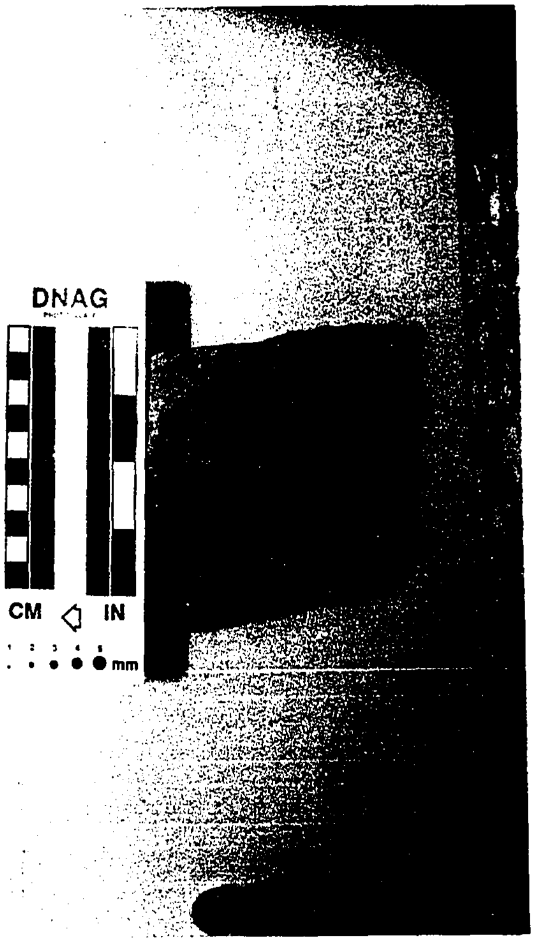
DNAG
CM
IN
mm

Figure 24.

Hummocky to columnar seam atop micstone to crinoidal wackestone, located 3300 ft below ground surface, at the top of the Trainor #4 Core (Jasper County, Illinois), in Salem Limestone. Organic laminations occur immediately adjacent to the hummocky seam. The large (20 mm tall), isolated column is typical of hummocky seams in matrix-dominated rock, such as micstone and, occasionally, dolostone, and is most commonly found in upper parts of deposequences in the Salem Limestone.

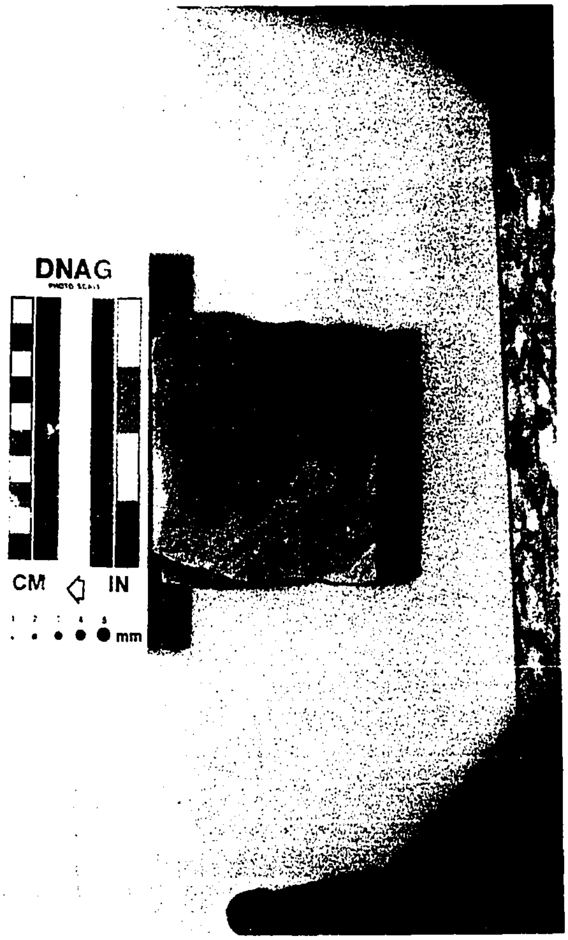
DNAG
CM
IN
mm

asymmetrical stylolite in packstone at a depth of 3325 feet. Stylolitic columns along hummocky seams are commonly 5 mm tall. A serrated seam, with 3 mm deep serrations, occurs near the bottom of the core, at the 3343 foot marker.

Hummocky to serrated seams, some with isolated stylolitic columns 10 to 20 mm tall and spaced 3 to 12 inches apart, are common in wackestone to micstone in the upper subsequence. Microstylolites occur throughout the upper subsequence and at the top of the lower subsequence in organic-laminated wackestone to micstone, particularly in the vicinity of hummocky to serrated seams. Dolostone contains sparse, hummocky seams and no microstylolites. Only one serrated seam was observed.

Summary

A single deposequence with equally thick upper and lower subsequences comprises the Trainor #4 core. Lithofacies clearly distinguish the upper and lower subsequences. Framework-supported, nondolomitic rock characterizes the lower subsequence, and micritic, matrix-supported, as well as dolomitic rock characterizes the upper subsequence.

Moderately spaced, well-developed columnar stylolites occur exclusively in the lower subsequence. In contrast, closely spaced, hummocky to serrated seams, locally accompanied by microstylolitic, organic laminae, are characteristic of the upper subsequence.

L. Unocal #2 Core, Jasper Co., IL

Location

The Unocal #2 core is the second of two cores drilled by the Unocal Oil Company in Jasper County, Illinois. The core spans 59 feet of discontinuous Salem Limestone at a depth of 3308.5 to 3367.5 feet, with 30% of the core consisting of rubble, and 8% of the core missing. Because of the thick sequence of rubble and the many interspersed, missing intervals, the core is not included in the data set used in contouring basin-wide trends of stylolite and lithofacies parameters.

Stratigraphy

The 54 feet of rock (including rubble) comprising the Unocal #2 core consist of 85% grainstone, 14% packstone, and 1% micstone. Dolostone is not present in the section. The almost complete lack of matrix-supported, micritic or dolomitic rock indicates that the section lacks an upper subsequence. The upper 30 feet of the section represent a transition zone. The missing intervals, each 0.5 to 1 foot thick, occur at regular intervals in the upper 30 feet of the section. A single micstone layer, 0.5 foot thick, occurs 2.5 feet below the top of the section. A 1.5 foot thick bed of packstone to wackestone caps the section. Bedding is thinner (0.5 to 1 foot) in the upper 30 feet of the section than in the lower 30 feet, where bedding is massive.

Most of the lower 30 feet of the section are dominated by massive, cross-bedded, medium-grained, moderately- to well-sorted, oolitic, skeletal grainstone, with foraminifers and crinoid fragments. The basal 5 feet of the section consist of medium-bedded to massive, planar-bedded, medium- to coarse-grained, poorly- to moderately-sorted, locally cherty, skeletal grainstone and packstone, with crinoids, foraminifers, bryozoans, corals, brachiopods, and locally developed pyrite concretions. Most of the overlying transition zone is characterized by planar, medium- to thin-bedded, fine- to coarse-grained, moderately- to poorly-sorted, skeletal grainstone to packstone and packstone to grainstone, with ooids, crinoids, foraminifers, bryozoans, brachiopods, pelecypods, corals, and with locally developed pyrite concretions.

Stylolites

Figures 25 through 32 show a representative suite of stylolitic and nonstylolitic lithofacies in the Unocal #2 core, in ascending stratigraphic order.

Large, isolated stylolites, with columns 30 mm tall or taller, and spaced 3 feet apart, occur at the base of the section, in planar-bedded, poorly sorted grainstone and packstone. Massive, cross-bedded, moderately sorted grainstone lacks stylolites. Stylolites are most abundant in the upper 30 feet of the section, where they are spaced 0.5 to 2 feet apart in medium- to thin-bedded, planar-bedded, poorly sorted grainstone and packstone. Some stylolites are asymmetrical and some are adorned by stacked columns. Columns of the stylolites are 5 to 30 mm tall.

Hummocky seams, with locally developed serrations, spikes, or isolated, stylolitic columns occur in packstone throughout the upper 20 feet of the section, or transition zone. Microstylolites accompany stylolites and hummocky seams in organic-laminated packstone in the upper 5 feet of the section.

Figure 25.

Symmetric, cylindrical stylolite (bar), with hummocky to serrated column caps, located 3366.5 ft below ground surface in the Unocal #2 core (Jasper County, Illinois), in Salem Limestone. Medium- to coarse-grained, poorly sorted, porous, skeletal grainstone to packstone, with crionoids, foraminifers, bryozoans and some brachiopod fragments, hosts the stylolite. Stylolite columns are up to 30 mm tall and 6 mm wide. The closest neighboring stylolite occurs 3 ft above this one, which is fairly typical of stylolites in lower parts of deposequences.

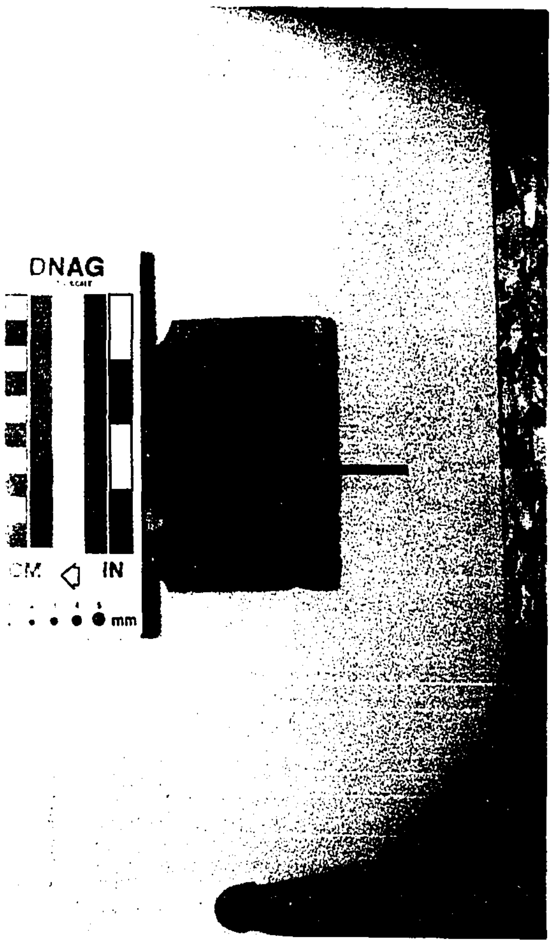
DNAG
IN
mm

Figure 26.

Cross-bedded, coarse-grained, well-sorted, relatively clean, oolitic, skeletal grainstone, with foraminifers, and crinoids, located 3344 ft below ground surface in the Unocal #2 core (Jasper County, Illinois), in the Salem Limestone Formation. The lack of organic laminae, hummocky seams and stylolites, along with the grain sorting, are diagnostic of grainstone associated with large-scale cross-bedding in lower parts of deposequences in the Salem Limestone.

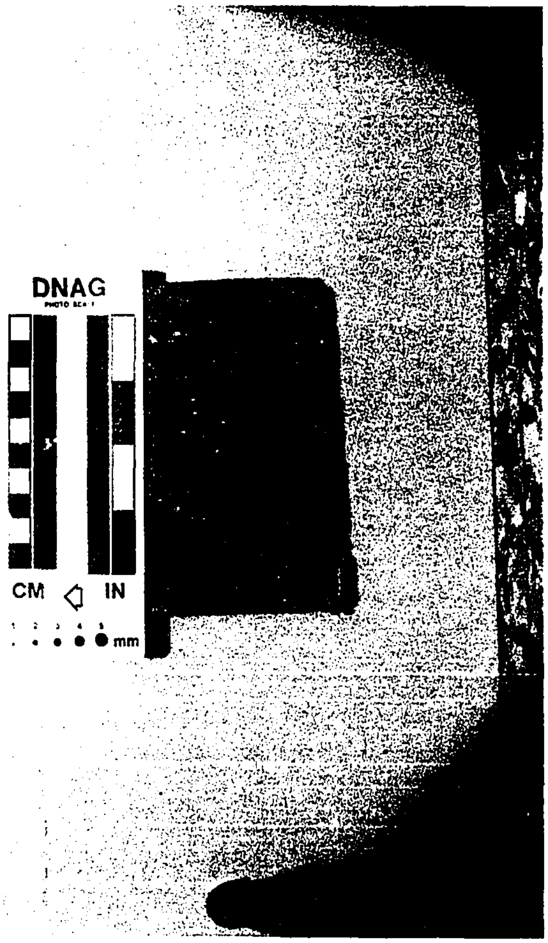
DNAG
CM
IN
mm

Figure 27.

Cross-bedded, medium-grained, well-sorted, oolitic, skeletal grainstone, with crinoids and formainifers, located 3336 ft below ground surface in the Unocal #2 core (Jasper County, Illinois), in the Salem Limestone Formation. Crinoid columnal plates and foraminirs contain sutured boundaries, but continuous microstylolites are lacking, which is consistent with the sample's location, in the lower part of a deposequence.

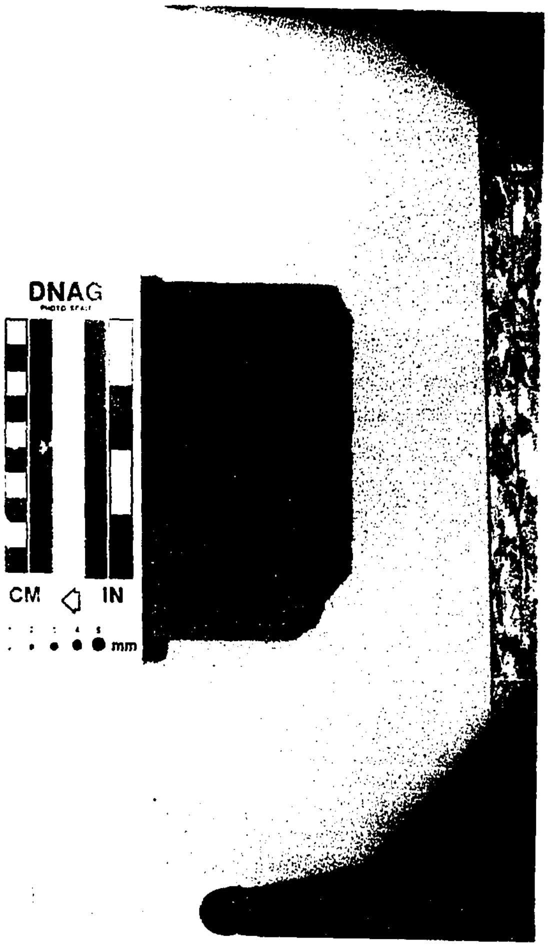
DNAG
CM
IN
mm

Figure 28.

Negatively asymmetric, cylindirical stylolite with compound (stacked) columns and conical caps, located 3330 ft below ground surface in the Unocal #2 core (Jasper County, Illinois), in the Salem Limestone Formation. Medium-grained, moderately sorted, oolitic, skeletal grainstone, with crinoids, foraminifers, and brachiopod fragments, hosts the stylolite. Rock underlying the stylolite grades partially into packstone. Stylolite columns are 20 mm tall and 6 mm wide. This stylolite exemplifies the predominance of negative asymmetry over positive asymmetry within grainstone.

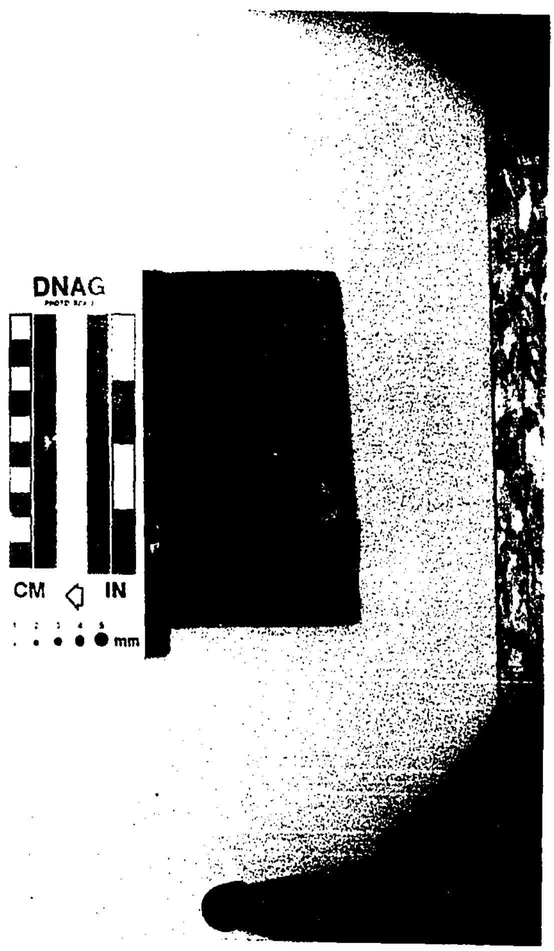
DNAG
CM
IN
mm

Figure 29.

Symmetric, cylindrical stylolite (bar) with compound (stacked) columns, located 3327.5 ft below ground surface in the Unocal #2 core (Jasper County, Illinois), in the Salem Limestone Formation. The stylolite is overlain by medium-grained, moderately sorted, oolitic, foraminiferal grainstone, and underlain by fine- to coarse-grained, poorly sorted, oolitic, skeletal grainstone to packstone, with crinoids, bryozoans, foraminifers, and corals. Stylolite columns are 30 mm tall and 20 mm wide at the base. Column walls contain appreciable amounts of filling material, suggesting that compound stylolite columns develop from a single, initial column that propagates preferrentially in the middle, leaving the edges of the inital column behind, as a "step."

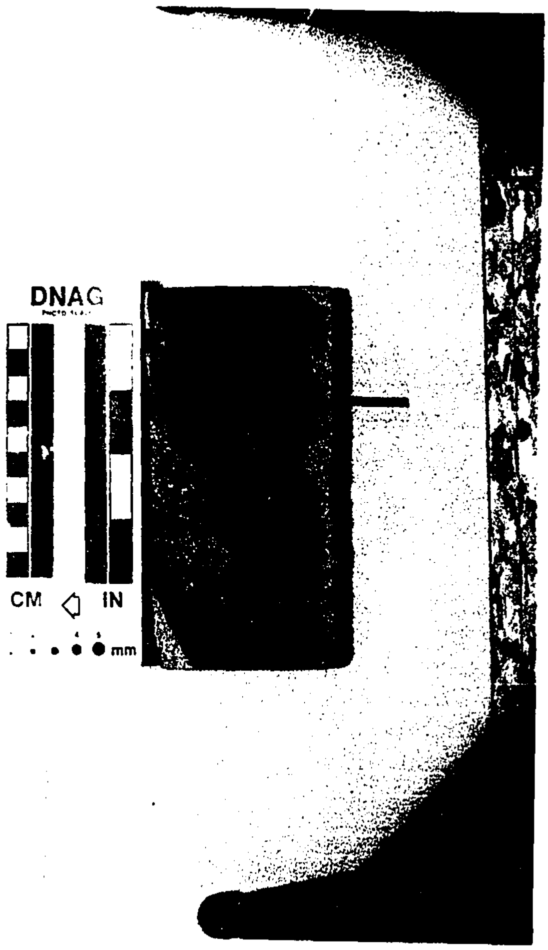
DNAG
CM
IN
mm

Figure 30.

Organic-laminated, pyritic, microstylolitic packstone, containing a hummocky seam with positively asymmetric, stylolitic spikes (bottom of sample), located 3313 ft below ground surface in the Unocal #2 core (Jasper County, Illinois), in Salem Limestone. Incipient stylolitization of hummocky seams is common at substantial burial depths such as that experienced by this sample, and it is most commonly found in upper or transitional parts of deposequences in the Salem Limestone.

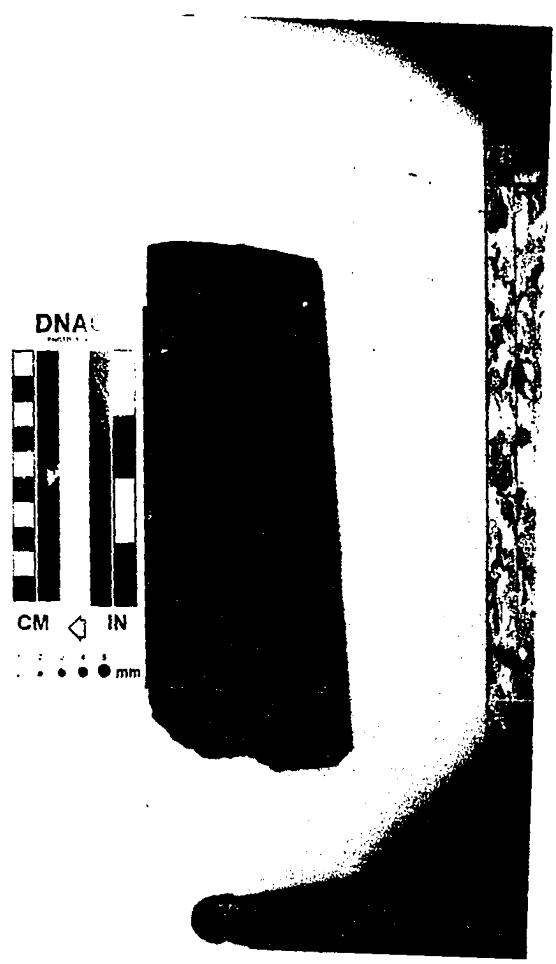
DNA
CM
IN
mm

Figure 31.

Pair of symmetric, cylindrical, locally compound stylolites (bars), located 3311.5 ft below ground surface in the Unocal #2 core (Jasper County, Illinois), in the Salem Limestone Formation. Cherty, organic-laminated micstone overlies the upper stylolite. Organic-laminated, microstylolitic, fine- to coarse-grained, poorly sorted, skeletal packstone, with fragments of crinoids, brachiopods and pelecypods, lies below the micstone. Stylolite columns are 5 mm tall and wide. Another pair of closely spaced stylolites occur 0.5 ft above this sample, suggesting that the stylolites represent fledgling stylolite zones, characteristic of transition zones between lower and upper parts of deposequences.

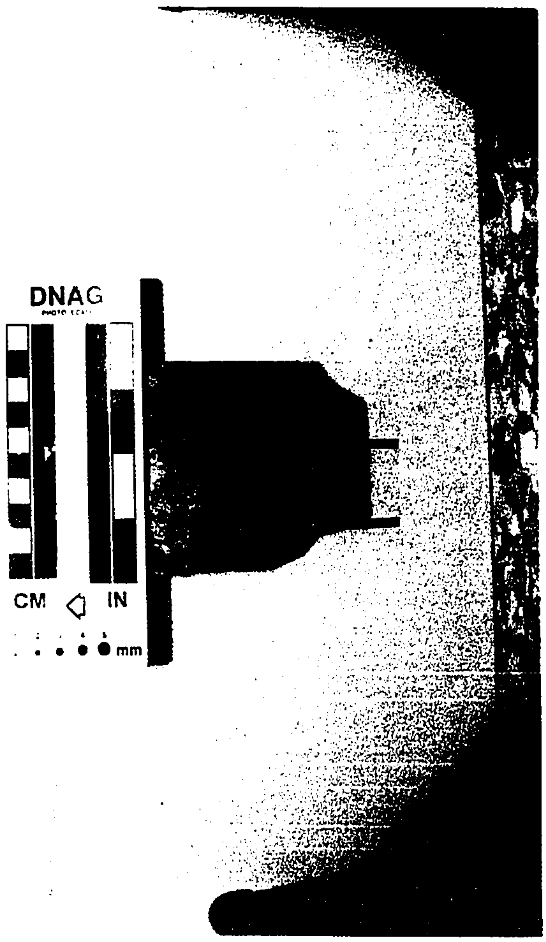
DNAG
CM
IN
mm

Figure 32.

Organic-laminated, microstylolitic, fine- to coarse-grained, poorly sorted, skeletal packstone, with crinoid and coral fragments, located 3311 ft below ground surface in the Unocal #2 core (Jasper County, Illinois), in the Salem Limestone Formation. The sample is bounded at the top and bottom edges by cylindrical stylolites, with columns that are 5 to 10 mm tall, and adorned by hummocky caps. The sample is underlain by the micstone in the sample shown in Figure 31.

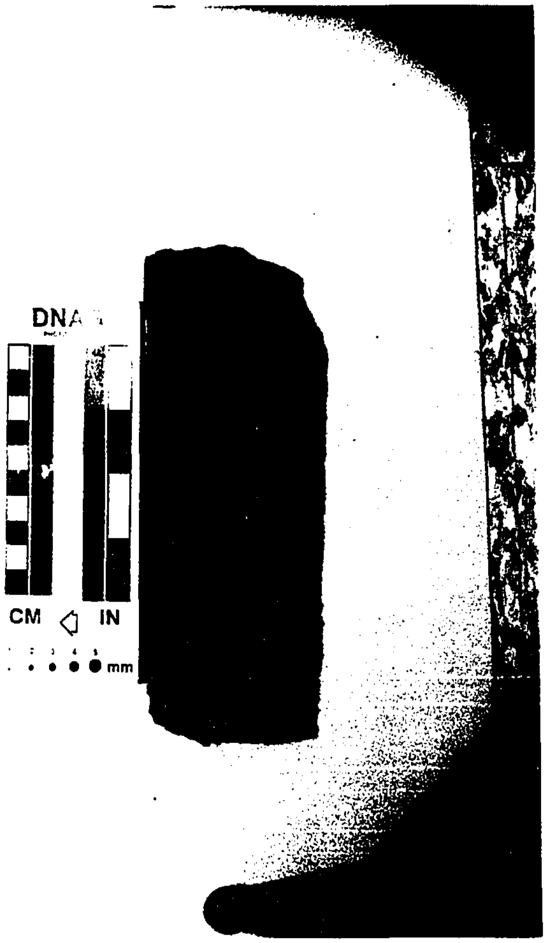
DNA
CM
IN
mm

Summary

The Unocal #2 Core represents an incomplete deposequence. The section contains a clearly defined, massive, cross-bedded lower subsequence, with large, isolated stylolites developed only in planar-bedded units. The part of the section overlying the massive, cross-bedded lower part of the deposequence is characterized by missing intervals (possibly representing shaley rock), increased micrite content, decreased bedding thickness, decreased sorting, and greater stylolite density, suggesting a transition zone overlain by an upper subsequence, not included in the core.

Summary and Conclusions

Stratigraphy

Across the Illinois Basin, from central Illinois to eastern Missouri, the Salem Limestone consists of a vertical succession of from 2 to 5, but typically 3, depositional sequences, or deposequences, representing upward shoaling depositional cycles. Each deposequence consists of a micrite-poor, cross-bedded or massive, grainstone- to packstone-dominated lower subsequence, and a micritic, locally dolomitic, wackestone- to micstone-dominated upper subsequence. The lower subsequence commonly contains ooids, foraminifers, and fragments of crinoids and bryozoans. The upper subsequence commonly contains organic laminations, pellets, and whole or fragmented bryozoans, brachiopods, pelecypods, and rugose corals. Transition zones between the upper and lower subsequences are significant in some sections of the Salem Limestone, and they are characterized by interbedded, thin-bedded packstone and wackestone.

The Salem Limestone ranges in thickness from under 50 feet in places along the eastern and western rims of the Illinois Basin, to over 100 feet in the central and southern regions of the Illinois Basin. Although typically 15 to 20 feet thick, deposequences can be as thick as 40 feet in the central and southern portions of the Illinois Basin. A very thin deposequence, measuring less than 10 feet, located at the top or bottom of the Salem Limestone, typically continues into the underlying or overlying formations. Its true thickness is therefore greater than 10 feet. Examples of deposequences containing the boundaries of the Salem Limestone include the tops of Sections C, H, and I; and the bottoms of Sections F and J.

The western rim of the Illinois Basin boasts well-defined, lithologically well-balanced deposequences, with grainstone and packstone in the lower parts, and wackestone, micstone, and shale in the upper subsequences. Clear boundaries between deposequences, marked by a sharp transition from underlying micstone to overlying grainstone, occur between the second and third deposequences in Sections A (the Kirkwood roadcut) and C (the Columbia roadcut). A sharp contrast between underlying shale and overlying packstone to rudstone highlights the boundary between the first and second deposequences in Section B, the Riehl Quarry wall. The second deposequences in sections A, the Kirkwood roadcut, and C, the Columbia roadcut, are perhaps the most well-defined deposequences of the Salem Limestone described in this study.

Although many deposequences along the eastern rim of the Illinois Basin are distinguished by their full range of lithofacies, these deposequences also tend to be poorly balanced, with thick lower subsequences overlain by very thin upper subsequences (e.g., the first deposequence of Section I, the Bedford roadcut) or with thin lower subsequences overlain by thick upper subsequences (e.g., the second deposequence of Section I, and the third and fifth deposequences in section J, the Mulzer Brothers Qarry core).

In the southern margin of the study, where the Salem Limestone is buried 500 feet deep, deposequences are thick, but poorly defined, with vague boundaries between deposequences, and thick transition zones between thin lower and upper subsequences. Examples include the second deposequence in Section F (Illinois core C-1830), and the first deposequence in Section J (Mulzer Brothers Quarry core).

Cores from the deep, central part of the Illinois Basin (also called the Fairfield Basin) cover only incomplete segments the Salem Limestone. The cores suggest that deposequences there are similar in character to those in the southern margin of the study area, and show poor definition. For example, vague boundaries occur between the two deposequences in Section D (Roy Reed #5 core), as well as between the upper and lower subsequences in both deposequences. The similarity between most of Section E (Gray Estate #8 core) and the thick transition zone in the middle of the second deposequence in Section F (Illinois core C-1830) suggests that Section E, itself, is part of a thick transition zone in a generally poorly defined deposequence. Bedding thickness, always a striking feature used naturally to define deposequences, is not always a dependable marker because it varies within lower subsequences, both vertically in the same section, and laterally between neighboring sections. Section C, the Columbia roadcut, for example, features an unusually thin-bedded, lenticular lower subsequence in the first deposequence and a more typical, massive and cross-bedded lower subsequence in the second deposequence. Compared laterally, the dominant lower deposequences of neighboring Sections A (Kirkwood roadcut), and B (Riehl Quarry wall) exhibit contrasting character. The second deposequence in Section A is massive, whereas the first deposequence in Section B is thin-bedded.

Stylolites

Prominent, individual stylolites, with vertical spacing greater than 1 foot, and columns more than 10 mm tall, typically occur in lower subsequences, in massive, coarse-grained, poorly-sorted grainstones and packstones. Examples include the lower subsequences of the third deposequences in Sections A (Kirkwood roadcut) and C (Columbia roadcut), and the lower subsequence of the second deposequence in Section B (Riehl Quarry wall).

Stylolite zones, less than 1 foot thick, containing many closely spaced (<1 inch) stylolites, with columns 1mm to 5mm tall, typically occur in upper subsequences, in medium- to thin-bedded, organic-laminated, medium- to coarse-grained, moderately- to poorly-sorted packstones to wackestones, typically interbedded with micstones and dolostones. Stylolite zones can be found in surface outcrops, such as in the upper subsequence of the second deposequence in Section I (Bedford roadcut), but they are best developed at depth, in Section E (Gray Estate #8 core), and in the upper subsequence of the second deposequence in Section F (Illinois core C-1830). These two cores contain vertical stacks of many 3- to 6-inch thick stylolite zones, separated by equally thick zones of nonstylolitized rock.

Microstylolites occur in different lithologic environments in upper and lower subsequences. In lower subsequences, they follow fine cross-laminations within cross-bedded units. In upper subsequences, they grade laterally into organic laminations, particularly adjacent to shale partings, and in some cases, within stylolite zones. Hummocky seams are most common in packstone to wackestone in the upper subsequences, particularly in shallow cores and surface outcrops. The upper subsequences of the second deposequences of both Section B (Riehl Quarry wall) and Section C (Columbia roadcut) exhibit good examples of hummocky seams.

Hummocky seams are less common at great depths, as in Sections D (Roy Reed #5 core), E (Gray Estate #8 core), or even F (Illinois Geol. Surv. C-1830 core). On the other hand, these deep sections contain more stylolites, mainly within stylolite zones in packstones of upper subsequences--

the same lithofacies that commonly hosts hummocky seams at shallow depths. This relationship between the occurrence of hummocky seams and stylolite zones suggests that hummocky seams in packstones in upper subsequences at shallow depths become stylolite zones at depth.

Partially "stylolitized" hummocky seams, with local, isolated columns protruding from an otherwise smooth to hummocky seam of organic material and clay, occurring in upper subsequences at intermediate depths, provide further support for the hypothesis that hummocky seams become stylolites at depth. The best examples are found in the 200-foot deep core of Section H (George Armstrong Farm core), which exhibits locally stylolitic hummocky seams in the upper subsequence of the first deposequence.

Since hummocky seams are sedimentary layers consisting of organic material and clay minerals, this hypothesis implies that at least some stylolites form along pre-existing depositional features.

Lateral continuity of stylolites and stylolite zones over distances up to 60 miles is suggested by several sections described in this study. Along the eastern rim of the Illinois Basin, a particular, 1-foot thick stylolite zone, including 2 to 4 stylolites with 1- to 5-mm tall columns, occurs in packstone immediately overlying massive micstone to wackestone, just 4 feet below the top of the Salem Limestone in both Sections H (Armstrong Farm core) and I (Bedford roadcut). This stylolite zone can therefore be traced over a distance of 20 miles in the NW-SE direction, from a height of 75 feet above the ground surface, to a depth of 120 feet below the surface. The same stylolite zone may also occur 60 miles southward, and 387 feet below the ground surface, to Section J, where a prominent stylolite with 15-mm tall columns occurs at the top of a wackestone bed, just 5 feet below the top of the Salem Limestone.

Along the western rim of the Illinois Basin, a prominent, individual stylolite with 20- to 100-mm tall columns occurs in the topmost deposequence, 10 feet above a unique, 5-foot thick shale bed in both Sections A (Kirkwood roadcut) and B (Riehl Quarry cut). The shale bed occurs in the middle s of both sections. The two sections are 40 miles apart along a NNE-SSW line. The same stylolite layer may also occur 50 miles southward, in Section C (Columbia roadcut), where an individual stylolite with 10-mm tall columns occurs 10 feet above a 5-foot thick, shaley micstone sequence, found within the middle of the section.

Stacks of stylolite zones can apparently be traced from the deep, central part of the Illinois Basin to the southern margin of the study area. A series of 3 or 4 overlying stylolite zones, each 3 to 6 inches thick, occurs within a 5-foot interval of packstone, just below a 4-inch thick shale bed in the middle of the upper subsequence of the second deposequence in Section F (Illinois Geol. Surv. C-1830 core). It is remarkably similar to a stack of stylolite zones occurring just below a 4-inch thick missing interval (probably shaley) in Section E (Gray Estate #8 core). The two zones are separated by 50 miles in a NS direction, and 3200 vertical feet.

Conclusions

Depositional cycles in the Salem Limestone manifest themselves as easily recognizable sequences of lithofacies, called deposequences. Across the Illinois Basin, the Salem Limestone includes 2 to 5 generally well-defined deposequences, each clearly divided into lower and upper subsequences. A high-energy environment, characteristic of oolite shoals, dominated during the deposition of massive, cross-bedded, oolitic, skeletal grainstone and packstone during the early phase of a typical depocycle. A low-energy environment, characteristic of lagoons and tidal flats, dominated during deposition of wackestone, micstone and dolostone, interbedded with thin-bedded, organic-rich packstone during the late phase of a typical depocycle. The resulting deposequence contains a full range of lithofacies, from micrite-poor, cross-bedded grainstones and packstones in the lower subsequence, to micrite-rich, organic-rich wackestones, micstones, dolostones, and, locally, packstones in the upper subsequence.

The boundary between the lower and upper subsequences of a deposequence can be sharp, as between micstone and grainstone, or gradual, covering a thick transition zone, with interbedded packstone and wackestone. A moderate-energy environment, characteristic of back-bar deposits, dominated during the deposition of thick, transition zone rock sequences in the middle phases of some depocycles. The resulting deposequences are poorly defined, in comparison to deposequences without significant transition zones.

Stylolites help define many deposequences because they are not randomly distributed throughout the Salem Limestone. Vertical spacing between stylolites, and the height of stylolite columns, both depend on stratigraphic position within deposequences. Prominent, individual stylolites, widely spaced and with tall columns, typically adorn grainstones and packstones in lower subsequences. Zones of densely packed stylolites with short columns typically occur in thin-bedded packstones and wackestones in upper subsequences.

CHAPTER 4

OUTCROP MAPS

Detailed maps of stylolites in two long roadcuts allow analysis of the effects of lateral facies changes on stylolite development in the Salem Limestone. The two maps represent occurrences on both the eastern and western margins of the Illinois Basin. The first roadcut described in this chapter is near Bedford, Indiana, and the second roadcut is near Columbia, Illinois, about 20 miles south of St. Louis, Missouri.

A mosaic of photographs served as the basis for each of the outcrop maps. Stylolites, stylolite zones, and hummocky seams were mapped directly on the photographs, and then transferred to the final copies of the maps.

A. Bedford, IN., Roadcut (Section I, Chapter 3)

Location

The roadcut along northbound Indiana State Route 37, one mile north of the city of Bedford, in Township 5 North, Range 1 West, Section 5, in Lawrence County, exposes an essentially complete section of the Salem Limestone. The roadcut is, on average, 25 feet tall, and approximately 1800 feet long, with a mild southward ascent of about 5 degrees.

In Plate 11 (Appendix C), the roadcut is divided into 3 segments, each 600 feet long. Weathering of the outcrop defines stylolites and lithofacies contacts. Stratigraphic section I, described in Chapter 3, was described at the Bedford, Indiana roadcut.

Facies Relationships

The southward ascending highway transects 8 major lithofacies boundaries in the Salem Limestone. The lithofacies do not simply overlie one another. Instead, lateral facies boundaries are exposed, especially in the northern and middle segments of the roadcut (the top and middle segments shown in Plate 11).

The 9 major lithofacies exposed in the roadcut constitute 3 depositional sequences (deposequences). The bottom of the first deposequence is located at the northern end of the roadcut. The bottom of the second deposequence is marked by a thin (2 to 3 ft) layer of packstone to grainstone, intersecting the ground surface at the southern end of the middle segment of the roadcut. This layer first occurs at the top of the roadcut near the midpoint of the northern segment. The bottom of the third deposequence is marked by a 3 to 4 foot thick layer of grainstone to packstone, located about 7 feet above the ground surface at the southern end of the outcrop. The layer first occurs at the top of the roadcut near the northern (left) end of the southern (bottom) segment.

The lower, high-energy subsequence of the first deposequence exhibits the best example of lateral lithofacies transition in the Bedford roadcut. Thinly interbedded, coarse-grained, poorly sorted grainstone and medium-grained, moderately sorted packstone characterize the northern (left) half of the northern (upper) segment of the roadcut, whereas massive, cross-bedded, coarse-grained, moderately- to well-sorted grainstone and packstone characterize the southern (right) half of that segment. A 100 foot wide, interfingering transition zone separates the two lithofacies near the midpoint of the northern segment.

The upper, low-energy subsequence of the first deposequence is represented by micritic and dolomitic lithofacies below the thin packstone to grainstone layer in the middle segment. A lateral facies transition between wackestone and micstone to the north (left) and interbedded dolostone and packstone-grainstone to the south (right) occurs about 75 feet north of the midpoint of the middle segment. For brevity, the latter lithofacies unit is labeled simply "dolostone," Plate 11.

The lower subsequence of the second deposequence is thin, and grades upward into a transition zone consisting of interbedded packstone and wackestone. This subsequence is exposed in the southern (right) half of the middle segment of the roadcut.

The upper subsequence of the second deposequence consists of massive, micritic and dolomitic rock, locally containing vugs and geodes. Clearly defined lateral facies transitions were not observed in this rock unit, which comprises the upper portion of the southern (right) half of the middle segment, dominating most of the southern (lower) segment of the roadcut.

The third deposequence, which occupies the upper portion of the southern (right) half of the southern (lower) segment of the roadcut, is the least carefully mapped of the three deposequences in the Bedford roadcut map because it does not intersect the ground surface. Furthermore, weathering is pronounced in the upper part of the roadcut and obscures many stylolites and lithofacies boundaries.

Stylolites

Columnar or serrated stylolites, hummocky seams, and hummocky seams with isolated stylolitic columns are mapped in Plate 11. The upper and lower boundaries of stylolite zones and hummocky seam zones--beds containing at least three stylolites or hummocky seams per foot--are mapped. A numeral indicates the number of stylolites or hummocky seams contained within the zone.

The lower subsequence of the first deposequence exhibits the clearest example of lateral lithofacies control over stylolite development. Columnar stylolites occur throughout the thinly interbedded, coarse- to medium-grained, poorly- to moderately sorted grainstone and packstone sequence north (left) of the lateral lithofacies boundary at the midpoint of the northern (upper) segment of the roadcut. The stylolites are 25 to 75 feet long, and many are aligned along particular horizons. Stylolites are sparse, almost nonexistent, in the massive, cross-bedded, well-sorted packstone and grainstone south (right) of the lateral lithofacies boundary.

Columnar stylolites are densely packed in packstone and grainstone within a unit of interbedded dolostone and packstone to grainstone, south (right) of a lateral lithofacies transition 75 feet north (left) of the midpoint of the middle segment of the roadcut. The stylolites are 25 to 50 feet long, and there are up to 3 stylolites per foot, vertically. Stylolites are rare in wackestone and micstone north (left) of the lateral lithofacies boundary. Hummocky seams are fairly common along the upper and lower boundaries of the wackestone-micstone unit.

Zones of stylolites and hummocky seams characterize the lower subsequence and transition zone of the second deposequence. Stylolite zones of 3 to 5 stylolites per foot extend laterally for 50 to 100 feet, and grade laterally into zones of hummocky seams with 3 to 5 seams per foot. Many of the hummocky seams contain isolated stylolitic columns. Although the map indicates that most of these zones occur within a 5-foot unit marked "wackestone-micstone," sandwiched between two thinner beds of packstone in the southern two-thirds of the middle segment of the roadcut, some of the stylolites actually occur within or along thin (several inches thick) beds of packstone within the 5-foot wackestone-micstone unit.

Stylolites are almost nonexistent in the upper subsequence of the second deposequence, which is dominated by massive, largely dolomitized micstone and wackestone. Several stylolites up to 25 feet long occur within the dolostone unit at the southern (right) end of the roadcut. Individual hummocky seams and hummocky seam zones, typically 1 foot thick and contain up to 5 hummocky seams, line the lower contact of the massive dolostone unit. Individual hummocky seams are up to 200 feet long and many contain isolated stylolitic columns. Most of the upper subsequence of the second deposequence, however, contains no hummocky seams. Several hummocky seams, 25 to 75 feet long, and a 100-foot long, 1-foot thick zone of 4 hummocky seams occur at the southern (right) end of the roadcut; some of these grade laterally into stylolites.

Individual stylolites, typically about 25 feet long, are found only in the lower subsequence of the third deposequence, and some grade laterally into hummocky seams and hummocky seam zones up to 100 feet in length and containing up to 4 seams. Nondolomitized micstone and wackestone of the upper subsequence of the third deposequence exhibit only hummocky seams, many with isolated stylolitic columns, and hummocky seams zones.

Summary

Lateral lithofacies transitions affect stylolite development in the Salem Limestone, as illustrated by the Bedford roadcut. In both the lower and upper subsequences of the first deposequence, stylolites occur preferentially within thinly bedded units separated laterally from massive units. In the lower subsequence, thin, interbedded packstone and grainstone, generally coarse-grained and poorly sorted, contains many stylolites, whereas massive, cross-bedded, medium-grained and moderately sorted grainstone and packstone located just south of that unit contains few stylolites. In the upper subsequence, thin, interbedded packstone to grainstone and dolostone contains stylolites and stylolite zones, mainly within the nondolomitic beds, whereas massive micritic rock located just north of the subsequence contains few stylolites.

The Bedford roadcut illustrates the preferred development of individual stylolites within thin-bedded, coarse-grained, poorly sorted grainstone and packstone in the lower subsequences on one hand; and of densely packed zones of stylolites and hummocky seams within thin-bedded micstone, wackestone and dolostone in upper subsequences. This pattern is recurrent throughout the Illinois Basin (Chapter 3).

B. St. Louis, MO, Roadcut

Location

Portions of the first and second deposequences of the Salem Limestone occur several miles south of the Kirkwood, Missouri roadcut, along northbound Interstate Highway 270, one mile south of the I-44 interchange, where they are exposed along a 20-foot tall, half-mile long roadcut (Plate 12). The highway is nearly horizontal, so that only about 20 vertical ft of Salem Limestone are exposed. The length of the roadcut, however, offers a good opportunity to study lateral changes in lithofacies in the Salem Limestone.

Facies Relationships

A prominent shale marks the top of the second deposequence identified in the Kirkwood roadcut about two miles to the north. It is continuous, horizontal and parallel to the highway across the entire length of the roadcut. The shale constitutes the upper subsequence of the second deposequence. It is 2 to 4 ft thick, and its base is 11 to 13 ft above the base of the roadcut.

The lower subsequence of the second deposequence consists of coarse packstone to grainstone in the northern (left) portion of the roadcut, grading laterally into poorly sorted, fine- to very coarse-grained packstone in the middle third of the roadcut. This, in turn, grades laterally into fine- to coarse-grained grainstone in the southern (right) portion of the roadcut.

Fine-grained dolopackstone and dolomicstone, grading laterally into fine-grained packstone and wackestone in the southern (right) third of the roadcut, represents the upper subsequence of the first deposequence, and defines the base of the outcrop.

Above the shale, a fine-grained packstone represents the lower subsequence of the third deposequence of the Salem Limestone. The section in the St. Louis roadcut is thus very similar to the one described in the Kirkwood roadcut, two miles to the north.

Stylolites

Columnar and serrated stylolites are most abundant in the poorly-sorted, fine- to very coarse-grained packstone of the lower subsequence of the second deposequence in the middle portion of the roadcut. Individual stylolites are spaced as closely as one ft, with columns up to 15 mm tall.

Stylolites tend to form clusters five ft wide vertically and 10 to 30 ft wide laterally. Left-lateral staggering of the stylolites is common, creating en echelon patterns of stylolites throughout the roadcut. The longest stylolites, up to 70 ft (21.3 m) long, mark lithofacies boundaries.

Well-sorted, coarse- or medium-grained grainstone and packstone in the northern and southern portions of the roadcut are relatively free of stylolites compared to the poorly-sorted packstone and grainstone in the middle portion. Dolopackstone and dolomicstone at the base of the roadcut also lack columnar or serrated stylolites. Several stylolites were observed in packstone at the top of the outcrop above the shale, but these are not necessarily representative of stylolite distribution in the upper portion of the roadcut, where access is limited.

Hummocky seams are more widely distributed across the roadcut than columnar or serrated stylolites. They commonly form zones of up to 15 closely spaced seams. These zones are up to 6 inches tall and at least 5 feet long. The longest zone of hummocky seams is 230 ft (48.7 m) long and marks the contact between packstone and grainstone in the lower middle portion of the outcrop.

As with many stylolites, hummocky seams in the St. Louis roadcut commonly form en echelon left-lateral patterns. Examples abound throughout the lower subsequence of the second deposequence in this raodcut. Hummocky seams occur within dolostone at the base of the roadcut, and they are particularly common along lithofacies boundaries throughout the roadcut.

Hummocky seams are conspicuously absent within clusters of columnar stylolites in packstone in the lower subsequence of the second deposequence. Hummocky seam distribution is mapped in detail in the lower 10 feet of the outcrop map. Above 10 feet, identification of hummocky seams was at least as difficult as identification of stylolites.

Summary

Relationships between lateral stylolite distribution and lithofacies boundaries in the St. Louis roadcut is in agreement with correlations between stylolite density and lithologic attributes identified in vertical sections of the Salem Limestone across the Illinois Basin. Stylolites are concentrated in poorly-sorted packstone to grainstone, and are rare in well-sorted grainstone and dolostone.

Hummocky seams are abundant in the same lithofacies where stylolites abound, but the hummocky seams occupy regions of those lithofacies not occupied by stylolites. This suggests that stylolites replace hummocky seams, which in turn serve as nucleation surfaces for stylolites.

The en echelon arrangement of stylolites and hummocky seams reflects the fact that stylolites and hummocky seams tend to occur along bedding planes, even in cross-bedded rock. Stylolite surfaces generally do not dip steeper than 5 to 10 degrees, and strongly cross-bedded facies typically lack stylolites.

Summary and Conclusions

The Bedford, Indiana, and Columbia, Illinois, roadcuts expose the essential, lithologic and stylolitic attributes of deposequences in the Salem Limestone. Lower subsequences are dominated by high-energy, cross-bedded deposits, including both thin-bedded and massive grainstones and packstones. Stylolites develop preferentially in the thin-bedded units, particularly where grain sorting is moderate to poor. The stylolites are typically isolated and feature tall columns. Upper subsequences are dominated by low-energy deposits, including thin-bedded wackestone, packstone, and massive, locally dolomitized micstone. Stylolites develop preferentially in thin-bedded, non-dolomitic wackestone and packstone. The stylolites typically occur in zones of many, closely spaced stylolites with short columns. Some grade laterally into hummocky seams.

The roadcuts--especially that at Bedford, Indiana--revealed up-section trends in lithologic and stylolitic characteristics of successive deposequences. These trends are summarized in Figure 33 for the Bedford, Indiana, roadcut. The left-hand diagram in Figure 33 represents up-section trends in overall lithologic compositions of successive deposequences, and the right-hand diagram represents overall stylolite densities of successive deposequences.

Up-section lithofacies compositions of deposequences reflect greater representation of lower subsequences in the first two deposequences (A and B in Figure 33), and greater representation of upper subsequences in the third and fourth deposequences (C and D in Figure 33). Grainstone, the dominant constituent of lower subsequences, constitutes 40% of the first two deposequences, but only 20% of the third and fourth deposequences. Wackestone and micstone, the dominant constituents of upper subsequences, are absent in the first deposequence, but constitute approximately 10% to 15% of the second and third deposequences and 35% of the fourth deposequence. Dolostone, typical of upper

Figure 33.

Lithofacies distribution and stylolite density within deposequences of the Bedford, Indiana roadcut, indicating up-section increase in stylolite density.

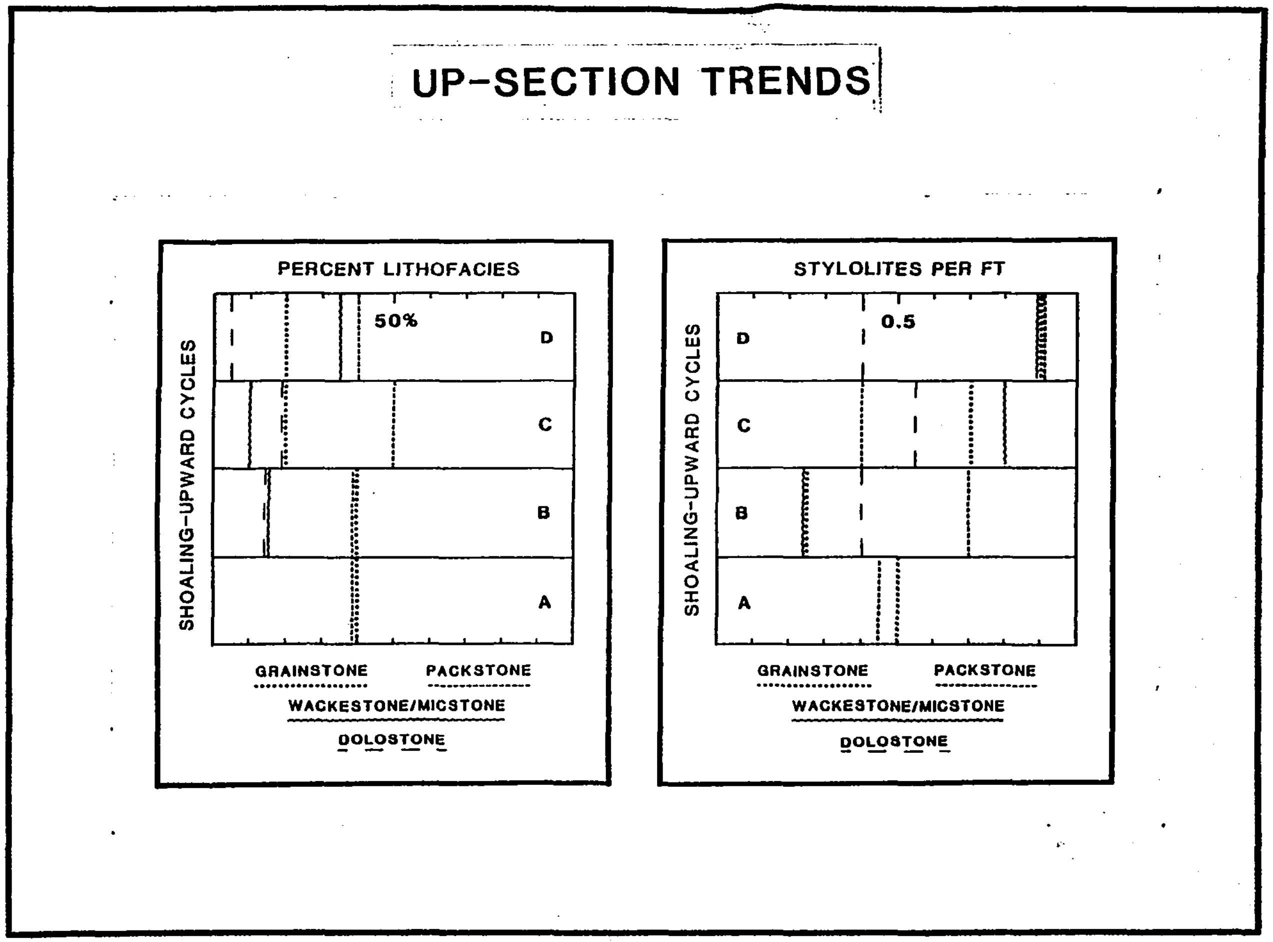
UP-SECTION TRENDS
PERCENT LITHOFACIES
50%
SHOALING-UPWARD CYCLES
D
C
B
A
GRAINSTONE
PACKSTONE
WACKESTONE/MICSTONE
DOLOSTONE
STYLOLITES PER FT
0.5
SHOALING-UPWARD CYCLES
D
C
B
A
GRAINSTONE
PACKSTONE
WACKESTONE/MICSTONE
DOLOSTONE

subsequences, constitutes 5 to 15% of the second, third, and fourth deposequences. Packstone is a significant component of both lower and upper subsequences. It is not surprising, therefore, that the percentage of packstone in each deposequence is approximately the same--40% to 50%--in all four deposequences.

Because the upper subsequences are most strongly represented in the stratigraphically highest deposequences and because stylolite zones (characterized by high stylolite density) develop preferentially in upper subsequences, the stylolite density is expected to increase in stratigraphically successive deposequences. This correlation is borne in by Figure 33. With the exception of dolostone, the stylolite density (stylolites per foot) in each lithofacies increases up-section. Stylolite density in grainstone and packstone is 0.4 to 0.5 stylolites per foot in the first deposequence and generally increases to 0.9 stylolites per foot in the fourth deposequence. Stylolite density in wackestone and micstone, which are absent in the first deposequence, is 0.2 to 0.3 stylolites per foot in the second deposequence and increases to 0.9 stylolites per foot in the fourth deposequence. Stylolite density in dolostone is 0.4 to 0.55 stylolites per foot in the second, third and fourth deposequences.

The increase in stylolite density up-section in each lithofacies appears to reflect the fact that in successive stratigraphic levels, greater proportions of each lithofacies occur in sedimentary settings conducive to stylolite development. Thus, packstone and wackestone are predominantly massive in the first deposequence, but they are thinly interbedded in the fourth deposequence.

In conclusion, stratigraphically successive deposequences in the Salem Limestone along the eastern rim of the Illinois Basin contain increasing proportions of upper subsequences, and an increasing abundance of stylolites and stylolite zones. This correlation between stratigraphic position within the Salem Limestone may complicate the correlation of lithologic and stylolitic characteristics with burial depth within the Illinois Basin. Further study, using a greater number of samples than available for this study, is required to substantiate those correlations.

CHAPTER 5

STYLOLITE-HOST ROCK RELATIONSHIPS

Close examination of the grain size, sorting, lithofacies, and fossil fauna of rock overlying and underlying 200 stylolites with various shapes and sizes, in the Salem Limestone at sections spanning the entire Illinois Basin, reveals interesting relationships between stylolites and their host rock. These relationships, in turn, help explain the patterns and mechanisms of stylolite development.

Stylolite-host rock relationships examined in the following sections include the following categories:

A. Frequencies of occurrence for symmetric and asymmetric stylolites within particular lithofacies and along lithofacies boundaries;

B. Height-to-width ratios of stylolite columns within particular lithofacies and along particular lithofacies boundaries;

C. Ratios of the heights of stylolite columns to the thickness of stylolite caps (the dark, organic-rich, clay-rich "filling" of a stylolite), in particular lithofacies and along lithofacies boundaries;

D. Average grain sizes adjacent to symmetric and asymmetric stylolites, and the difference in grain size between overlying and underlying rock adjacent to symmetric and asymmetric stylolites;

E. Degrees of grain sorting in overlying and underlying rock adjacent to symmetric and asymmetric stylolites;

F. Frequencies of occurrence of particular fossil fauna and organic laminations in overlying and underlying rock adjacent to symmetric and asymmetric stylolites; and

G. Average heights of the columns for symmetric and asymmetric stylolites adjacent to rock with predominance of particular fossil fauna and organic laminations.

Several conventions are used to simplify the following graphs. These conventions concern lithofacies and stylolite symmetry.

The abbreviations, "GR," "PK," "WK," and "DL" denote grainstone, packstone, wackestone, and dolostone, respectively.

Micstone is included in the wackestone category because the distinction between the two is based on an arbitrary cutoff point (concentration of "floating" grains), as opposed to a structural (grain-supported versus matrix-supported) or compositional (micrite matrix versus sparry calcite matrix; calcite versus dolomite) difference between lithotypes. Furthermore, wackestone and micstone are generally non-stylolitic, whereas packstone and grainstone host most stylolites and stylolite zones.

Dolostone includes all observed dolomitic lithofacies, such as dolomicstone, dolowackestone, and dolopackstone.

Three classes of stylolite symmetry are recognized in this chapter. These are, symmetric stylolites, positively asymmetric stylolites, and negatively asymmetric stylolites. A plus (+) sign denotes positively asymmetric stylolites; a minus (-) sign denotes negatively asymmetric stylolites; and zero (0) denotes symmetric stylolites (i.e., stylolites with zero asymmetry).

Positively asymmetric stylolites have columns that point or protrude generally upward into the overlying host rock. Negatively asymmetric stylolites have columns that point or protrude generally downward into the underlying host rock. Symmetric stylolites have columns pointing both upward and downward into the overlying and underlying host rock, with approximately equal frequency in both directions.

A. Stylolite-Lithofacies Relationships

The 4 by 4 matrix of graphs shown in Plate 13 represents the frequency of symmetric (0), positively asymmetric (+), and negatively asymmetric (-) stylolites within each of the four major lithofacies recognized in the Salem Limestone in this study, and along contacts between lithofacies. The four major lithofacies are: grainstone (GR), packstone (PK), wackestone to micstone (WK), and dolostone (DL).

Each of the 16 graphs in the matrix represents a lithofacies or contact between lithofacies. Lithofacies of host rock overlying a stylolite remains the same within each row, while the host rock underlying a stylolite remains the same within each column. The lithofacies of the host rock underlying a stylolite varies systematically, from left to right, in the order of increasing micrite content, with dolostone at the far end. The result is a matrix containing all possible relationships among the 4 lithofacies. Note that the main diagonal of the matrix contains the 4 cases in which a stylolite occurs within a single lithofacies.

As appropriate, the graphs show a dotted line and up to 3 rectangular zones, marked with different patterns. The height of the dotted line indicates the percentage of all stylolites observed and measured in this study that occur within the lithfacies or at the lithofacies boundary represented by the graph. The vertical axis represents percentage, from 0 to 100.

The thickness of each of the three patterned fields indicates the percentage of stylolites occurring within that lithofacies or lithofacies boundary that belong to one of the three symmetry categories, in the order positive asymmetry (+); no asymmetry (0), and negative asymmetry (-), from top to bottom.

Results

The 4 highest frequencies of stylolite occurrence are in the 4 graphs representing stylolites within the 4 lithofacies--that is, in the main diagonal of the matrix. The percentages of stylolites occurring within single lithofacies range from 6.75% (DL) to 43.5% (PK), whereas the percentages of stylolites occurring along lithfacies contacts range from 0% to 6%. The greatest fraction of stylolites occurs within packstone (43.5%), followed by grainstone (18%), wackestone-micstone (12.5%), and dolostone (6.75%). This means that twice as many stylolites develop within packstone than in any other lithofacies. Dolostone contains by far the fewest number of stylolites.

It appears that stylolites do not occur preferentially at lithofacies boundaries. Rather, they develop along surfaces within a lithofacies.

Of the 12 possible lithofacies contacts involving the 4 lithofacies recognized in the Salem Limestone only 4 hosted more than 1% each of all stylolites. All 4 combinations involve packstone, and none involve dolostone.
Contacts between packstone and overlying grainstone hosted 6% of all stylolites; between grainstone and overlying packstone, 5%; between wackestone and overlying packstone, 3.5%; and between packstone and overlying wackestone, 2.25%. All other combinations host 0 to 1% each of all stylolites. This means that both possible contacts involving grainstone and packstone host roughly 5% of all stylolites. Both possible contacts involving wackestone and packstone host roughly 2 to 3% of all stylolites.

These data indicate that the stratigraphic order of two lithofacies in contact does not influence the general development of stylolites, if stylolite symmetry is ignored. The preference of stylolites for packstone followed by grainstone and then wackestone, is clear. Stylolites also occur preferentially in single lithofacies, rather than at lithofacies boundaries, and tend not to occur in dolostone.

Symmetric stylolites represent the majority of stylolites within the 4 lithologies and along most lithologic contacts except grainstone-packstone, grainstone-wackestone, and packstone-dolostone contacts.

Symmetric stylolites represent more than 90% of stylolites occurring within wackestone-micstone and dolostone, along grainstone-dolostone contacts, and along contacts with dolostone overlying packstone, and with wackestone overlying packstone. Symmetric stylolites represent 60% to 80% of stylolites occurring within grainstone and packstone, and with packstone overlying wackestone. Symmetric stylolites represent 40% to 50% of stylolites along packstone-grainstone contacts. No symmetric stylolites occurred along contacts with packstone overlying dolostone. The remaining combinations--grainstone overlying dolostone, wackestone overlying grainstone, and wackestone-dolostone contacts--included no stylolites.

In general, symmetric stylolites predominate within and between matrix-supported, micritic and dolomitic lithofacies and are least predominant within and between framework-supported lithofacies. At contacts between framework-supported and matrix-supported lithofacies, symmetric stylolites predominate in most cases, particularly where matrix-supported rock overlies framework-supported rock. Conversely, symmetric stylolites tend not to develop at contacts where framework-supported rock overlies matrix-supported rock.

Asymmetric stylolites represent significant percentages of stylolites within grainstone and packstone, along grainstone-packstone contacts, along contacts with packstone overlying wackestone or dolostone, and with grainstone overlying wackestone. Since the grainstone, packstone, and combinations of both lithotypes host over 72% of all stylolites analyzed in this study, those two lithotypes, and contacts between them, are the most frequent carriers of asymmetric stylolites.

Positively asymmetric stylolites are most common at grainstone-packstone contacts. They constitute 55.5% of stylolites at contacts between grainstone and overlying packstone, 20% at contacts between packstone and overlying grainstone, 16.5% between wackestone and overlying packstone, 6.5% within packstone, and 6% within grainstone. Half of all stylolites found along contacts between dolostone and overlying packstone are also positively asymmetric, but the sample number is very small.

<u>Negatively asymmetric stylolites</u> are most common at contacts between packstone and overlying grainstone, where they constitute 30% of stylolites, but they are also found within grainstone, where they constitue 25%, within packstone, where they constitute 15.5%, and at contacts between wackestone and overlying packstone, where they constitute 16.5% of stylolites. All stylolites found at contacts between wackestone and overlying grainstone, and half of those found at contacts between dolostone and overlying packstone, are negatively asymmetric, but sample numbers at both types of contact are very small.

Negatively asymmetric stylolites are generally more common within a given lithfacies or along a given lithofacies contact than positively asymmetric stylolites. In general, negatively asymmetric stylolites are common, and predominate over positively asymmetric ones, at contacts where the underlying lithofacies contrasts with the overlying lithofacies either by being micrite-rich, or by being matrix-supported.

Conversely, positively asymmetric stylolites predominate over negatively asymmetric ones at contacts where the underlying lithofacies contrasts with the overlying lithofacies by being micrite-rich. Disregarding the lower half of the matrix, in which asymmetric stylolites are uncommon, leaves only the contact between grainstone and overlying packstone as an interface where positively asymmetric stylolites predominate over negatively asymmetric ones.

Interpretations

Textural contrast between lithofacies in contact has long been suggested as a driving force for stylolite development. Proponents of this idea maintain that "differential stresses" along bedding surfaces cause pressure solution, which leads to stylolite development. The data presented above do not support this model. Stylolites occur most frequently within a single lithofacies, and not at bedding surfaces between lithofacies.

The combination of framework support and micrite matrix is most favorable for stylolite development. This combination is found, of course, in packstone. Two possible advantages of packstone over grainstone may be related to the assumptions that pressure concentrations at grain contacts and porosity in adjacent rock are important conditions favoring stylolite development.

Since most grainstone may be well-cemented by the time that stylolites begin to form, packstone may be the only lithotype with significant pressure concentrations at grain-to-grain contacts. This would be true if in packstone the micrite matrix had low cohesive strength, and if in grainstone the sparry calcite cement had yield stresses similar to the framework grains. Another possible advantage of packstone over well-cemented grainstone is the possibility of a more permeable network of micropores within the micrite matrix, as opposed to the occluded pore regions in well-cemented grainstone.

Neither pressure concentrations at grain contacts nor microporosity within micrite matrix, however, can explain the fact that stylolites seldom pervade a rock, but instead are generally spaced vertically at distances 2 to 6 orders of magnitude greater than the average grain size.

A more likely influence in stylolite development that packstone has over grainstone is the greater abundance of shale partings, clay-rich seams, and organic laminations that occur within moderate-energy, behind-bar, packstone deposits, than within high-energy, oolite shoal, grainstone deposits. Such thin, organic- and clay-rich layers and laminations might easily serve as surfaces for stylolite development because of their high permeability parallel to the lamination, and a favorable chemistry (acidic, carbon dioxide-rich pore fluid).

The predominance of symmetric over asymmetric stylolites suggests that stylolite development is typically unaffected by gravity or by differential dissolution rates. Furthermore, the predominance of negatively asymmetric stylolites over positively asymmetric ones supports the idea that gravitational forces commonly are involved in asymmetric stylolite development, especially in cases where there is no lithologic difference between the overlying and underlying host rock.

The preference of positive asymmetry over negative asymmetry in stylolites along contacts between grainstone and overlying packstone is particularly interesting. Microporosity within micrite matrix in packstone may be the key to this asymmetry. The possible occlusion of porosity in the underlying grainstone, either before or during stylolite development, would make the micrite-rich (microporous) overlying packstone a more hospitable environment for the continued growth of stylolite columns. Only columns projecting upward into the more permeable packstone would grow to considerable heights, whereas columns projecting into the underlying, well-cemented grainstone would be stunted in their growth because of insufficient permeability.

A similar argument could be formulated with respect to pressure concentrations at grain-to-grain contacts, which would be greater in packstone, with soft, micrite matrix, than in well-cemented grainstone. Again, stylolite column growth upward into packstone would be favored.

The same mechanism may be responsible for the predominance of negatively asymmetric stylolites at contacts where grainstone overlies packstone.

Differences in the typical cementation history of grainstone overlying packstone, as opposed to grainstone underlying packstone, may provide the key to understanding the surprising abundance of positively asymmetric stylolites at contacts where grainstone overlies packstone. Grainstone overlying packstone may become less well cemented than grainstone underlying packstone. Occluded grainstone below a stylolite would prevent column growth downward, causing preferrential column growth upward, into microporous packstone. Porous grainstone above a stylolite, on the other hand, would allow column growth upward, and this growth would compete with downward growth into microporous packstone.

B. Height-to-Width Ratios of Stylolite Columns

The heighth and width of a typical column in each individual stylolite measured in this study is recorded as a data point on one of 3 graphs (Figures 34, 35 and 36), showing height, in mm, versus width, in mm. Each of the three graphs contains data from stylolites belonging to a particular subset of the 16 combinations of lithofacies represented by the matrix of stylolite-lithofacies relationships described in the previous section (Plate 13). In addition, Figure 37 shows a detail of Figure 34, near the origin of the graph.

The first graph represents the main diagonal of the matrix, where stylolites occur within each of the 4 recognized lithofacies (grainstone, packstone, wackestone-micstone, and dolostone). The second graph represents all lithofacies combinations except those involving dolostone. The third graph represents all lithofacies combinations containing dolostone.

Figure 34.

Scatter plot of height-to-width ratios of stylolite columns occurring within each of four lithofacies (grainstone, packstone, wackestone-micstone, and dolostone).

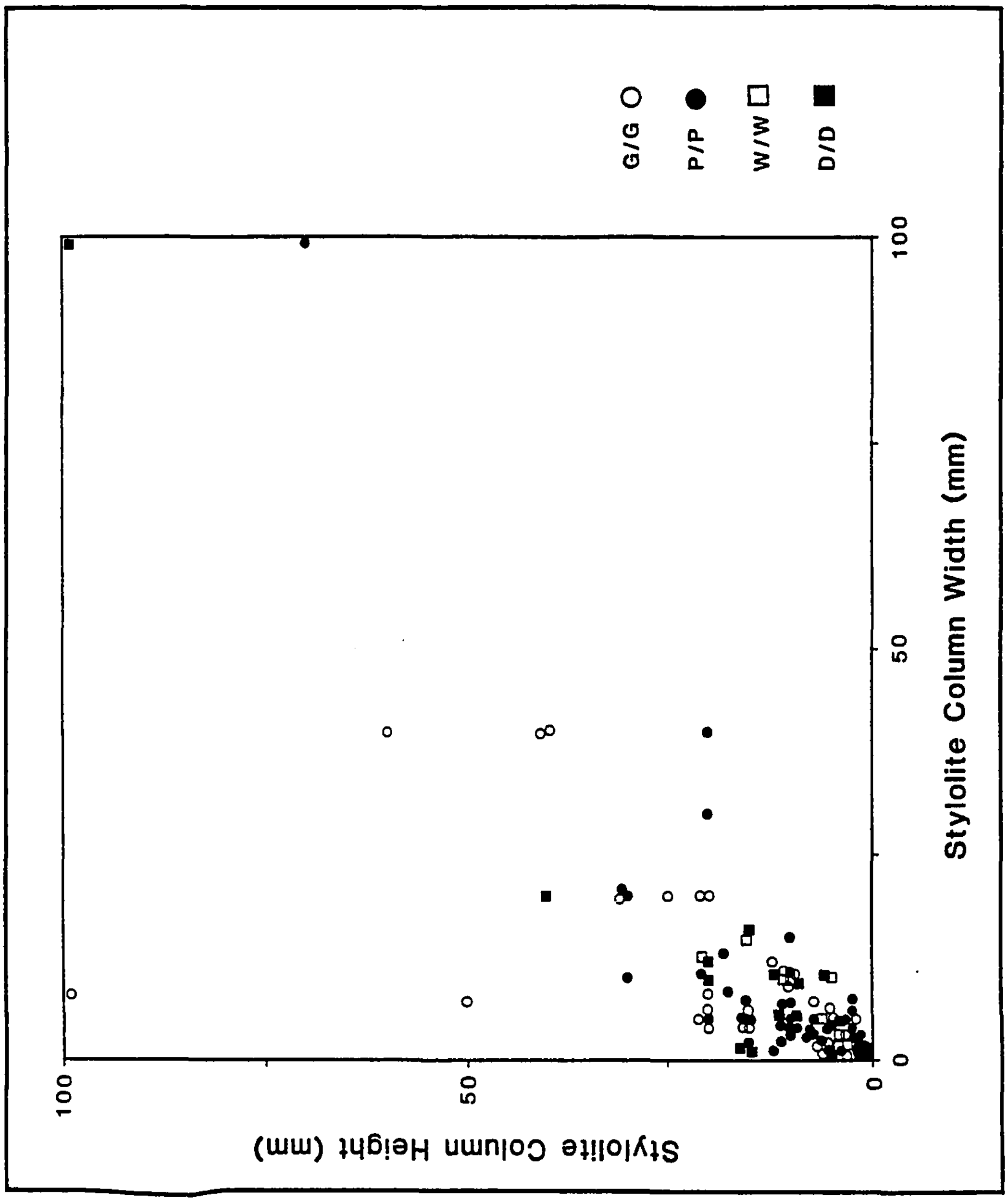

Stylolite Column Height (mm)
Stylolite Column Width (mm)
0
50
100
G/G
P/P
W/W
D/D

Figure 35.

Scatter plot of height-to-width ratios of stylolite columns occurring between contrasting lithofacies, excluding dolostone.

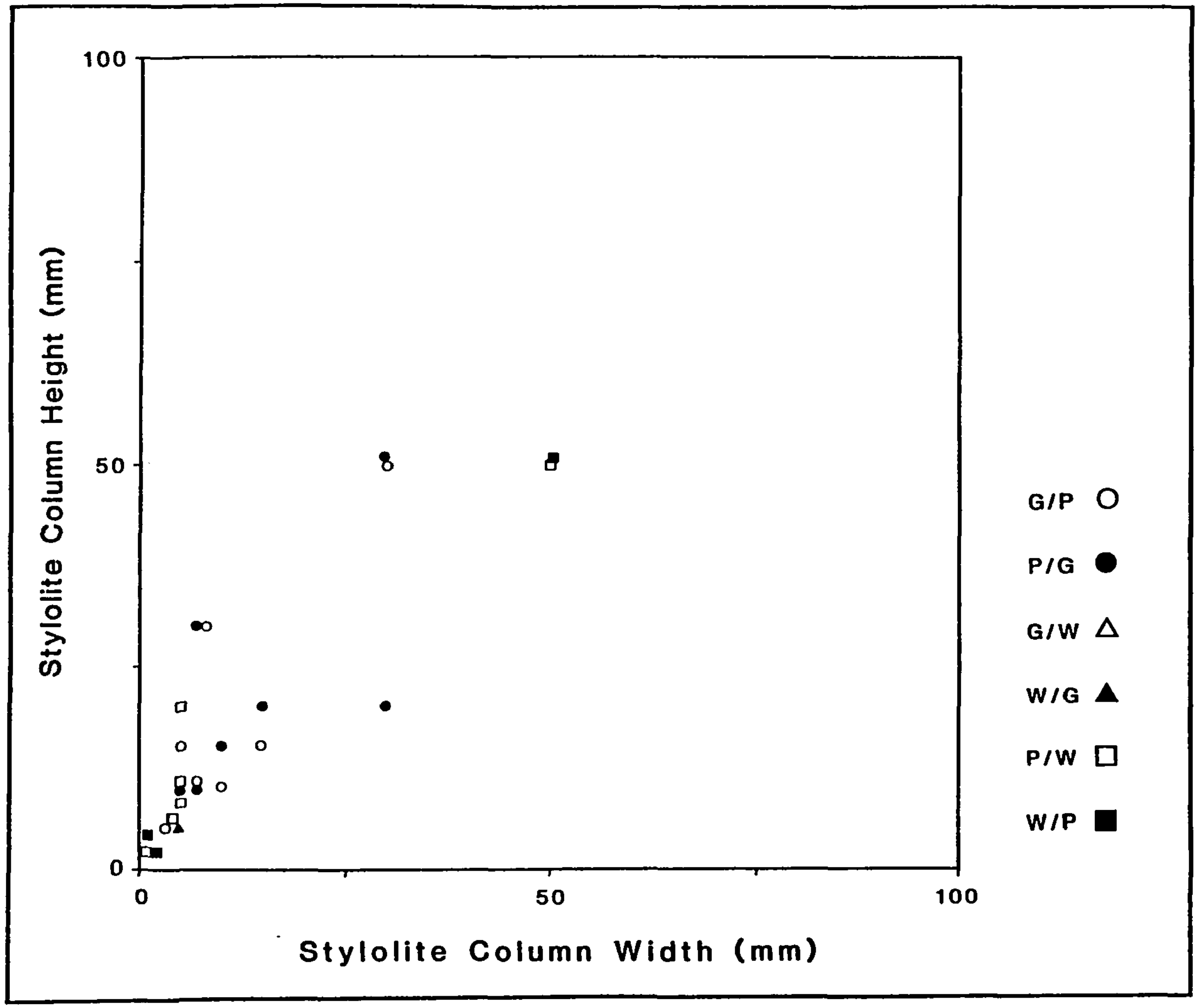
100
50
0
0
50
100
Stylolite Column Height (mm)
Stylolite Column Width (mm)
G/P
P/G
G/W
W/G
P/W
W/P

Figure 36.

Scatter plot of height-to-width ratios of stylolite columns occurring between dolostone and other, non-dolomitic lithofacies.

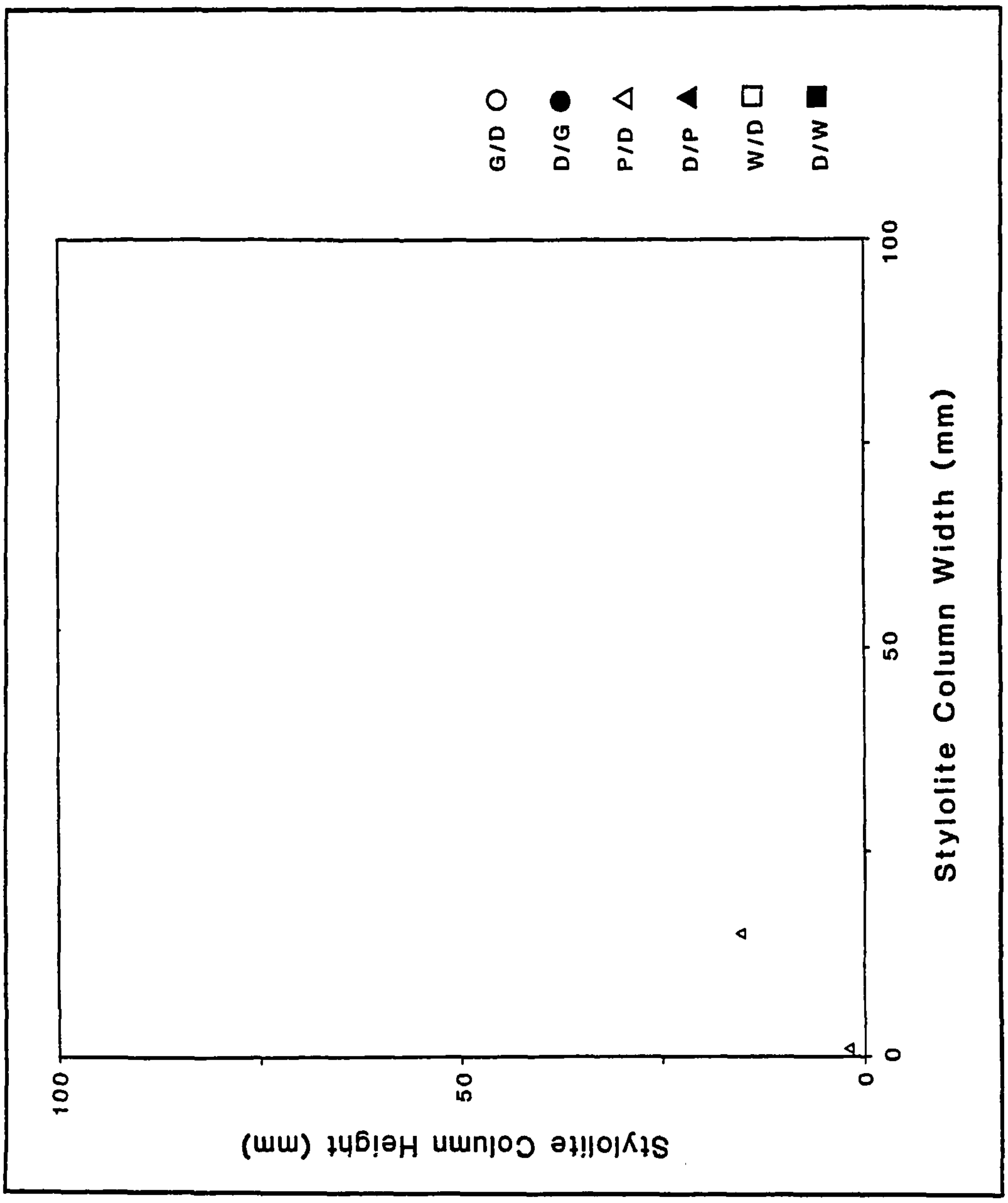
Stylolite Column Height (mm)
Stylolite Column Width (mm)
0
50
100
0
50
100
G/D
D/G
P/D
D/P
W/D
D/W

Figure 37.

Detail of the scatter plot shown in Figure 34, including points close to the origin of the axes.

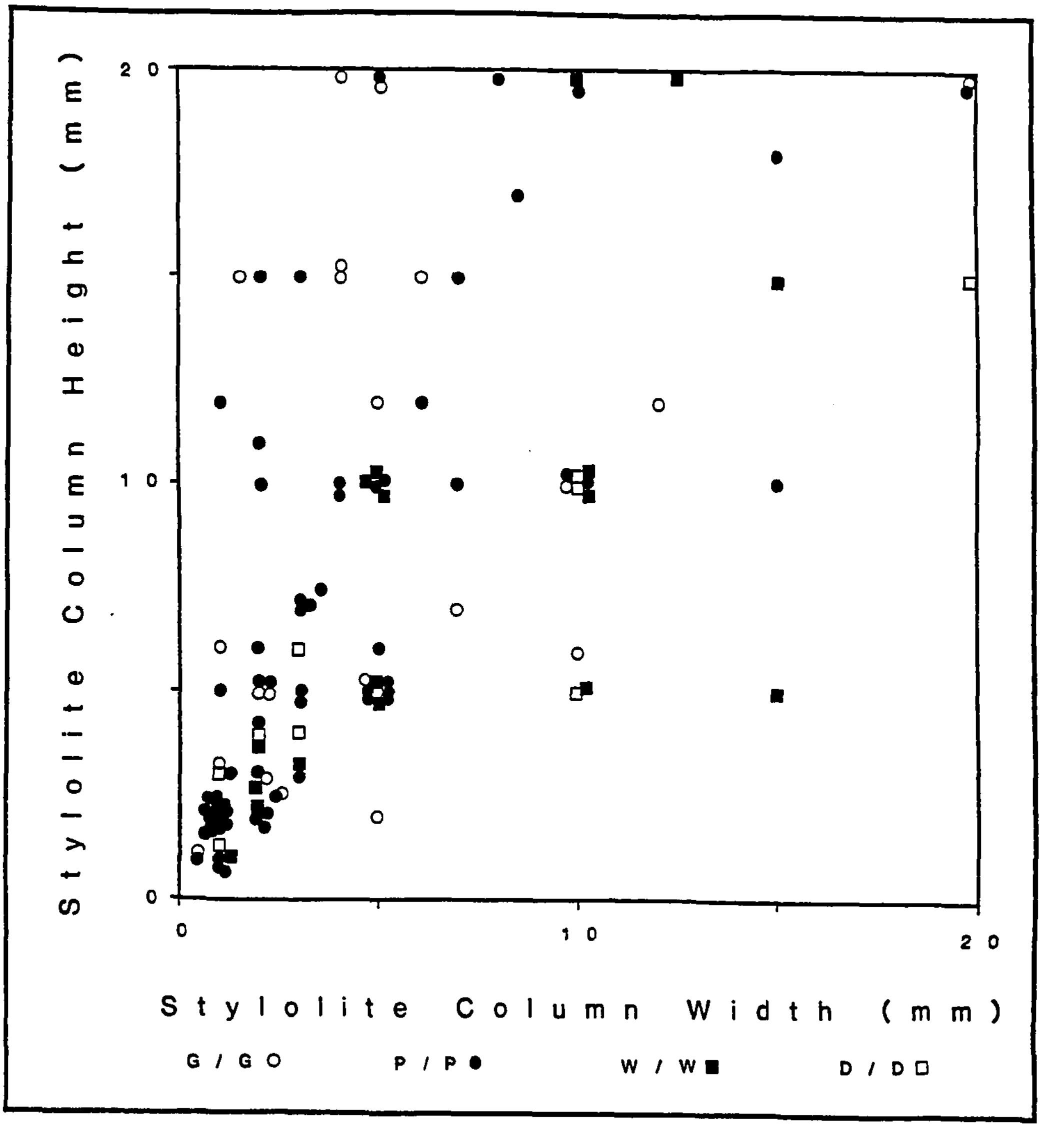
Stylolite Column Height (mm)
20
10
0
0
10
20
Stylolite Column Width (mm)
G/G ○
P/P ●
W/W ■
D/D □

Results

Although the data points for the 200 stylolites included in this survey show considerable scatter, there is a clear linear relationship between the heights and widths of stylolite columns.

The distribution of data points in Figure 34 (and its companion, Figure 37) reveals that the general range of height-to-width ratios (h/w) of stylolite columns in all 4 major lithotypes is from 1/3 to 10:

$$(1/3) \leq (h/w)_{G,P,W,D} \leq 10 \qquad (1)$$

About 80% to 90% of the data lie between 1 and 3:

$$1 \leq [(h/w)_{G,P,W,D}]_{maj.} \leq 3 \qquad (2)$$

The average height-to-width ratio, $\underline{h/w}$, based on the distribution of data points, is 2:

$$(\underline{h/w})_{G,P,W,D} \simeq 2 \qquad (3)$$

Grainstone and packstone have somewhat higher $\underline{h/w}$ values than wackestone and dololstone:

$$(\underline{h/w})_{G,P} \simeq 2 \qquad (4)$$

$$(\underline{h/w})_{W,D} \simeq 1 \qquad (5)$$

The tallest columns measured in grainstone and wackestone are 100 mm tall. In packstone, the maximum column height is 70 mm, and in dolostone, it is 20 mm. The widest columns measured packstone and wackestone are 100 mm wide. In grainstone, the maximum column width is 40 mm, and in dolostone, it is 20 mm. The growth potential of stylolites in dolostone appears to be limited to sizes smaller than 50 mm.

Data for stylolites along lithofacies contacts among grainstone, packstone, and wackestone, shown in Figure 35, are sparse. Along contacts between grainstone and packstone, and between packstone and wackestone, $\underline{h/w}$ is about 3/2, regardless of which lithofacies overlies the other:

$$(\underline{h/w})_{G/P,P/G,P/W,W/P} \simeq 1.5 \qquad (6)$$

There are too few data on contacts between grainstone and wackestone to be conclusive.

The maximum column height measured at grainston-packstone and packstone-wackestone contacts is 50 mm. The maximum column width is 50 mm at packstone-wackestone contacts, and 30 mm at grainstone-packstone contacts.

Only 2 data points are available for h/w ratios at lithofacies contacts involving dolostone, shown in Figure 36. Both points are for dolostone overlain by packstone, and they define a line with a slope of 1:

$$(\underline{h/w})_{P/D} \simeq 1 \qquad (7)$$

The maximum height and width of a stylolite column measured along a contact involving dolostone is 15 mm.

Interpretations

The data on heights and widths of stylolite columns may be interpreted in two contrasting ways. The data distribution may be viewed as being essentially random. Alternatively, a linear relationship may exist between column heights and widths.

Random data distribution would suggest that stylolite column growth is independent of column width. Even with this view of the data, one may recognize that Figure 37 suggests that there is a minimum column height which increases with column width. Perhaps column growth rate is proportional to column width, so that short, wide columns quickly grow in height. This would mean that the the rate of dissolution along a surface increases with its area. Alternatively, short, wide columns may be misidentified as hummocky seams.

Figures 34-37 can reasonably be viewed as displaying linear relationships between the heights and widths of stylolite columns. A 1:1 relationship between column heights and widths may result from the coalescence of short, narrow columns to forms tall, wide ones. This interpretation suffers from the sparseness of compound stylolites (small stylolites enclosed within large ones), but it is supported by serrated, micro-stylolitic caps of large columns. If one were to take the view that the width of a typical stylolite column remains unchanged during its period of growth, then the linear relationship between height and width would be interpreted in one of two ways. The 1:1 relationship may represent an preferred column shape, and columns may grow quickly in height to attain this shape, and continue to grow only very slowly to become taller than they are wide. Alternatively, stylolites with short, wide columns are misidentified as hummocky seams; and tall, narrow columns are rarely fully exposed in cross section because they are curved.

Differences between lithofacies have only minor effect on the heights and widths of stylolite columns. Stylolite columns in matrix-supported lithofacies--wackestone and dolostone--tend to be closer to square-shaped (h/w = 1), whereas stylolite columns in framework-supported rock--grainstone and packstone--tend to be rectangular (h/w = 2).

Differences in stylolite column dimensions among stylolites at the same type of lithofacies contact are greater than differences among stylolites at different types of lithofacies contacts. This suggests that other factors such as organic content, permeability, or duration of stylolite development all of which vary within a given lithofacies or between identical lithofacies units at different stratigraphic positions, strongly influence column size. For example, stylolites in packstone in the lower part of a deposection typically have taller columns than stylolites in packstone in the upper part of a deposection. An important difference between packstone in the two parts of a deposection is the organic content, which is much higher in the organic-laminated packstone in the upper part of a deposection.

The fact that no stylolite columns in dolostone attain the large sizes attained by some stylolite columns in nondolomitic lithofacies suggests that rock became dolomitized prior to or during stylolite development.

Alternatively, developing stylolites are affected by some characteristic of the rock that would later cause or facilitate dolomitization. The low frequency of stylolite occurrences in dolostone, combined with the small column size suggest that dolostone does not provide an environment amenable to stylolite development. The lower solubility of dolomite in seawater, compared to calcite, is one obvious explanation for the lack of stylolite development in dolostone.

C. Ratios of Column Heights to Cap Thicknesses

Plots showing the heights of stylolite columns and the thicknesses of the caps of the same columns are given in Figures 38 to 41.

Each point represents an individual stylolite in a paraticular lithologic setting. As in the previous section (Section B), Figure 38 includes data on stylolites located within each of the 4 lithofacies recognized in this study; Figure 39 includes data on stylolites located along contacts between nondolomitic lithofacies (grainstone, packstone, and wackestone-micstone); and Figure 40 includes data on stylolites located along contacts involving dolostone. Figure 41 shows the lower left corner of Figure 39 in greater detail.

Figure 38.

Scatter plot of the relationship between stylolite column heights and cap thicknesses in stylolites occurring within each of four lithofacies (grainstone, packstone, wackestone-micstone, and dolostone).

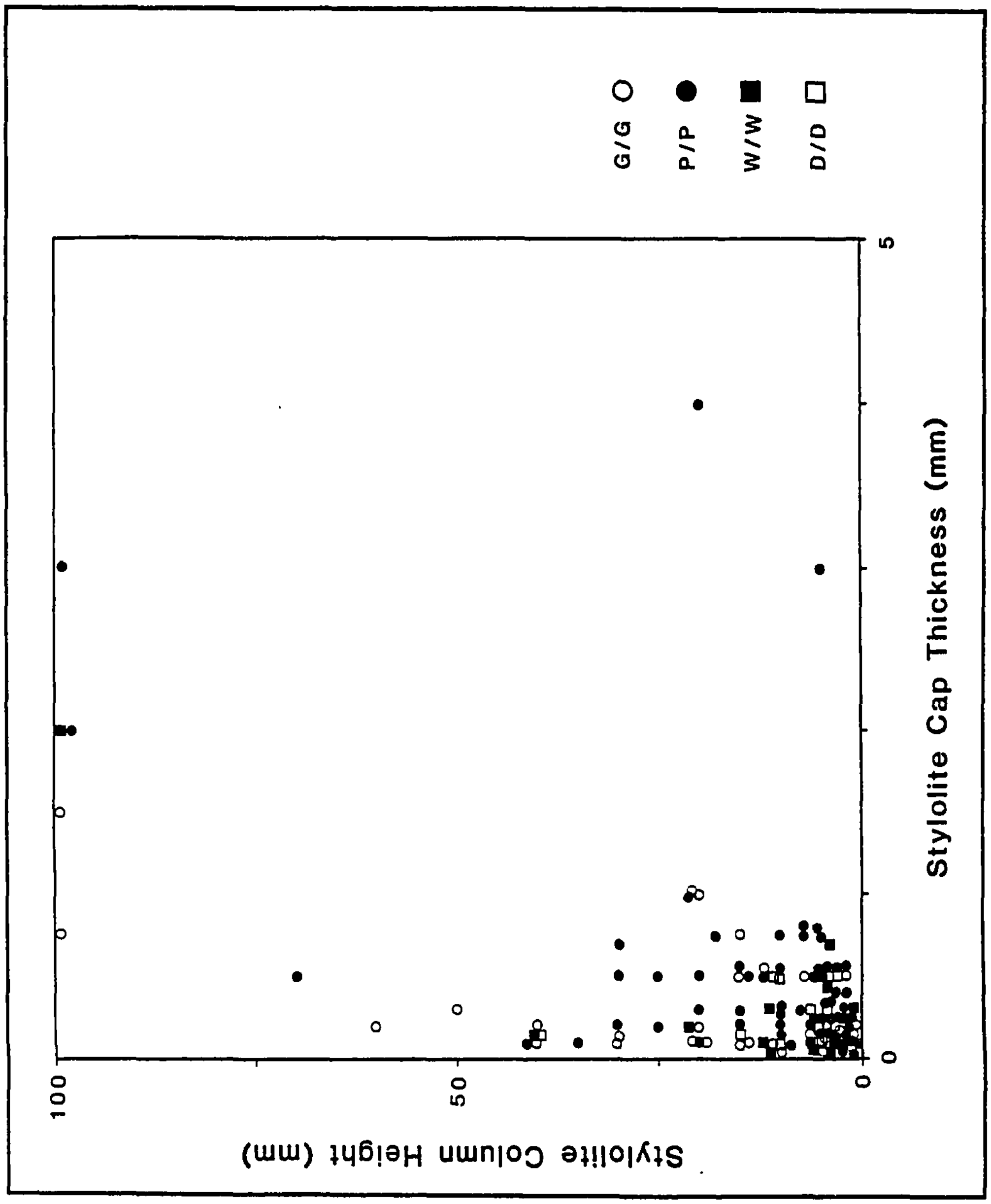

G/G
P/P
W/W
D/D
Stylolite Cap Thickness (mm)
0
5
Stylolite Column Height (mm)
100
50
0

Figure 39.

Scatter plot of the relationship between stylolite column heights and cap thicknesses in stylolites occurring between contrasting lithologies, excluding dolomite.

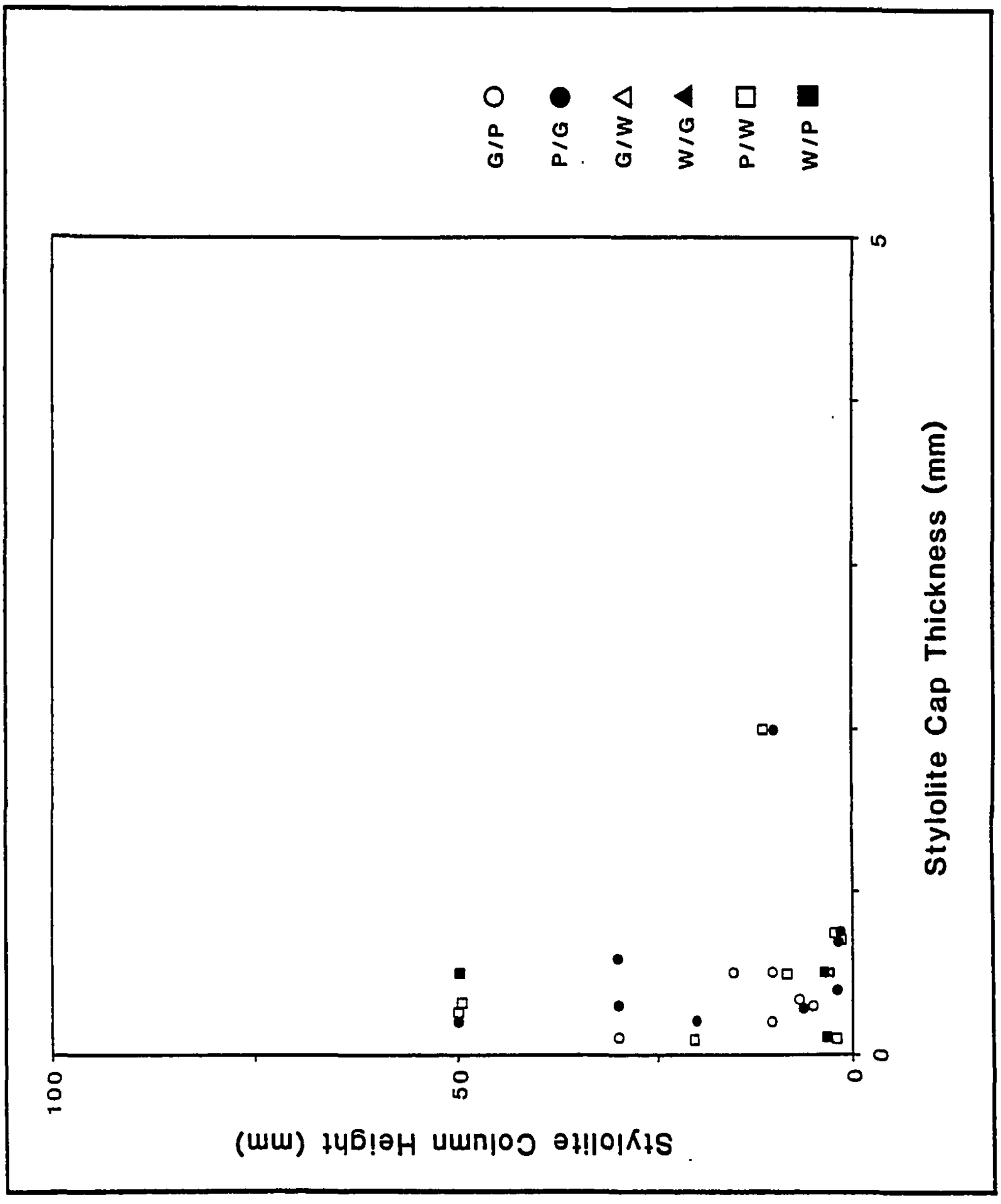

Stylolite Column Height (mm)
Stylolite Cap Thickness (mm)
100
50
0
0
5
G/P
P/G
G/W
W/G
P/W
W/P

Figure 40.

Scatter plot of the relationship between stylolite column heights and cap thicknesses in stylolites occurring between dolostone and other lithofacies.

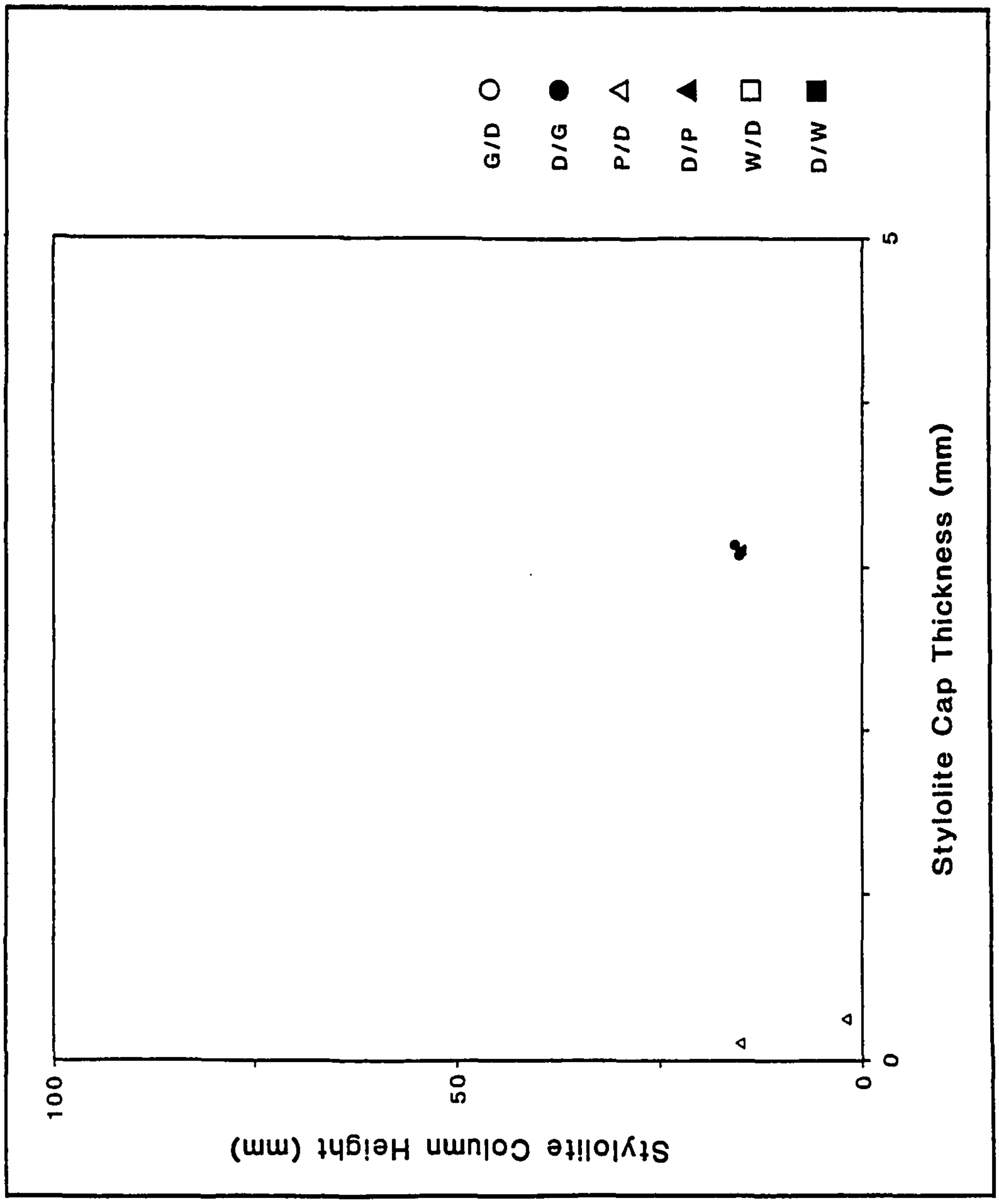

Stylolite Column Height (mm)
100
50
0
0
5
Stylolite Cap Thickness (mm)
G/D
D/G
P/D
D/P
W/D
D/W

Figure 41.

Detail of Figure 38, showing points close to the origin of the axes.

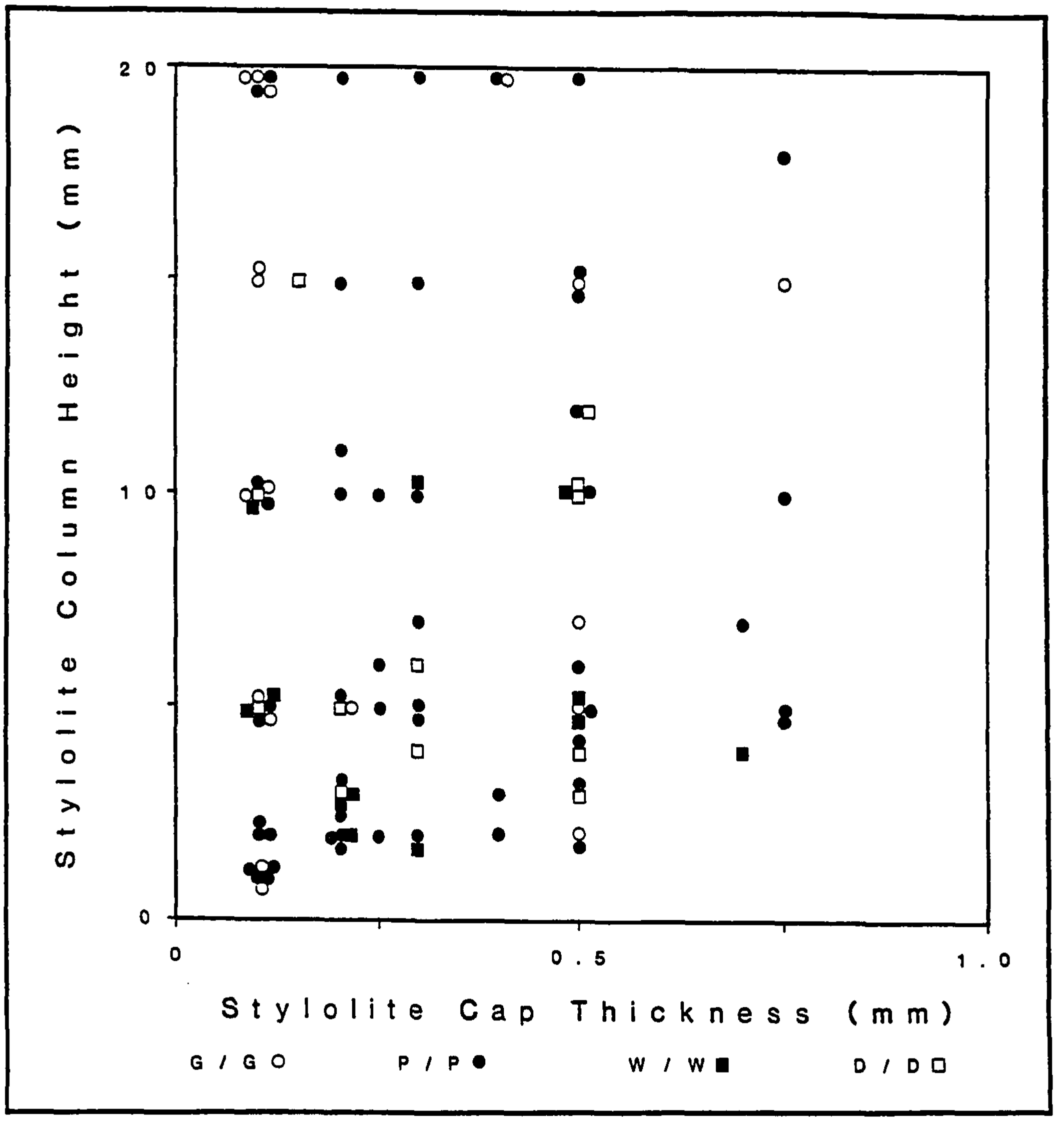
Stylolite Column Height (mm)
20
10
0
0
0.5
1.0
Stylolite Cap Thickness (mm)
G / G ○
P / P ●
W / W ■
D / D □

Results

There is no clear relationship between the heights of stylolite columns and the thicknesses of column caps. This holds within each of the sets of data, representing stylolites within particular lithofacies.

The majority of data points (>90%) for stylolites found within single lithfacies, shown in the first graph, occupy a rectangular region, with one corner at the origin, and extending horizontally to the 1 mm mark, and vertically to the 40 mm mark. Data points for all three nondolomitic lithofacies (grainstone, packstone, and wackestone-micstone) extend to the boundaries of this rectangle, and beyond. Data points for dolostone are completely contained within a smaller rectangle, extending horizontally to the 0.5 mm mark, and vertically to the 15 mm mark.

The majority of data points (<90%) for stylolites found along contacts between nondolomitic lithofacies, shown in the second graph, lie within a rectangular region, with one corner at the origin, and extending horizontally to the 0.5 mm mark, and vertically to the 50 mm mark. Data points involving all 3 nondolomitic lithfacies extend to the boundaries of this rectangle. Given the relative paucity of data points in this graph, one can only state that, within this rectangle, there is an even distribution of data points representing various combinations of contacts between nondolomitic lithofacies. There are, of course, no points for grainstone-wackestone contacts (see Figure [matrix of stylolites at lithofacies contacts]).

The third graph is marred by insufficient data, precluding any interpretation of relationships between column heights and column cap thickness.

Interpretations

Tall stylolite columns do not have thicker caps than short columns. This observation argues against the idea that stylolite caps consist of insoluble residue accumulated as the stylolite column grew, and that therefore the heights of stylolite columns should be proportional to the amount of material dissolved along the caps. If this model were true, there should be a linear (or other predictable) increase of cap thickness with column height.

The data on column height and cap thickness support the idea that the organic- and clay-rich material constituting the "filling" of a stylolite, and especially of its column caps, is largely a pre-existing, sedimentary deposit. The observations are consistent with the idea that stylolites formed along pre-existing shale breaks, clay seams, or organic laminations.

Greater average thicknesses of shale breaks, clay seams, or organic laminations within packstone than along packstone-grainstone interfaces could explain the apparently greater range of column cap thicknesses along stylolites within single lithofacies, as opposed to stylolites along lithofacies contacts.

Since the previous section (Section B) showed no systematic relation between column widths and lithofacies, differences in the rate or amount of stylolite column growth among lithofacies do not appear to be likely reasons for differences in column cap thicknesses.

Stylolites adjacent to dolostone tend to have shorter, narrower columns, with thinner caps than other stylolites. The lack of a systematic relationship between column heights and cap thicknesses within each of the data subgroups discussed in this section suggests that thin caps are, in general, not necessarily linked to smaller columns, as would be expected by the hypothesis of column growth, and cap thickening, by "pressure solution."

The linear relationship between column height and column width suggested in the previous section (Section B), in conjunction with petrographic evidence suggesting that column width remains constant during stylolite growth, supports the idea that column height depends on, or is pre-determined by, column width.

Since column width may be related linearly to column height, and column height is unrelated to cap thickness, I surmise that column width and cap thickness are unrelated. The main difference between dolostone (with short, narrow columns) and the 3 other lithofacies (with longer, wider columns) is mineralogical; porosities of the nondolomitic facies vary widely. It appears, hence, that rock mineralogy critically affects column size.

D. Grain Sizes in Stylolite Host Rock

An analysis of the relationship between stylolite symmetry or column height and the grain size of host rock helps determine the effect of rock texture on stylolite development.

Figures 42 and 43 show stylolite column height plotted against one of two grain size parameters with stylolite symmetry shown by the nature of the symbol. Of these, symmetric stylolites comprise the largest data set.

The abscissa in Figure 42 represents the average grain size in the host rock adjacent to a stylolite, including both overlying and underlying host rock. The ordinate represents stylolite column height up to 50 mm. This graph relates grain size to column size and includes more than 90% of stylolites measured in this study. It also serves to test the hypothesis that negatively asymmetric stylolite growth is driven by increased permeability below the stylolite and thus coarser average grain size.

The abscissa in the Figure 43 represents the difference between the average grain size above and below a stylolite. The ordinate represents stylolite column height. The stylolites included in this data set are identical to those included in Figure 42. This graph is a measure of the effect of grain size contrast across a stylolite on the symmetry of the stylolite, and also tests the hypothesis that stylolite column size is a function of the permeability contrast across a stylolite.

Results

Data points in the Figure 42 are scattered, revealing no systematic relation between average grain size and column

Figure 42.

Scatter plot of stylolite column height versus average grain size in adjacent host rock, for various stylolite symmetries.

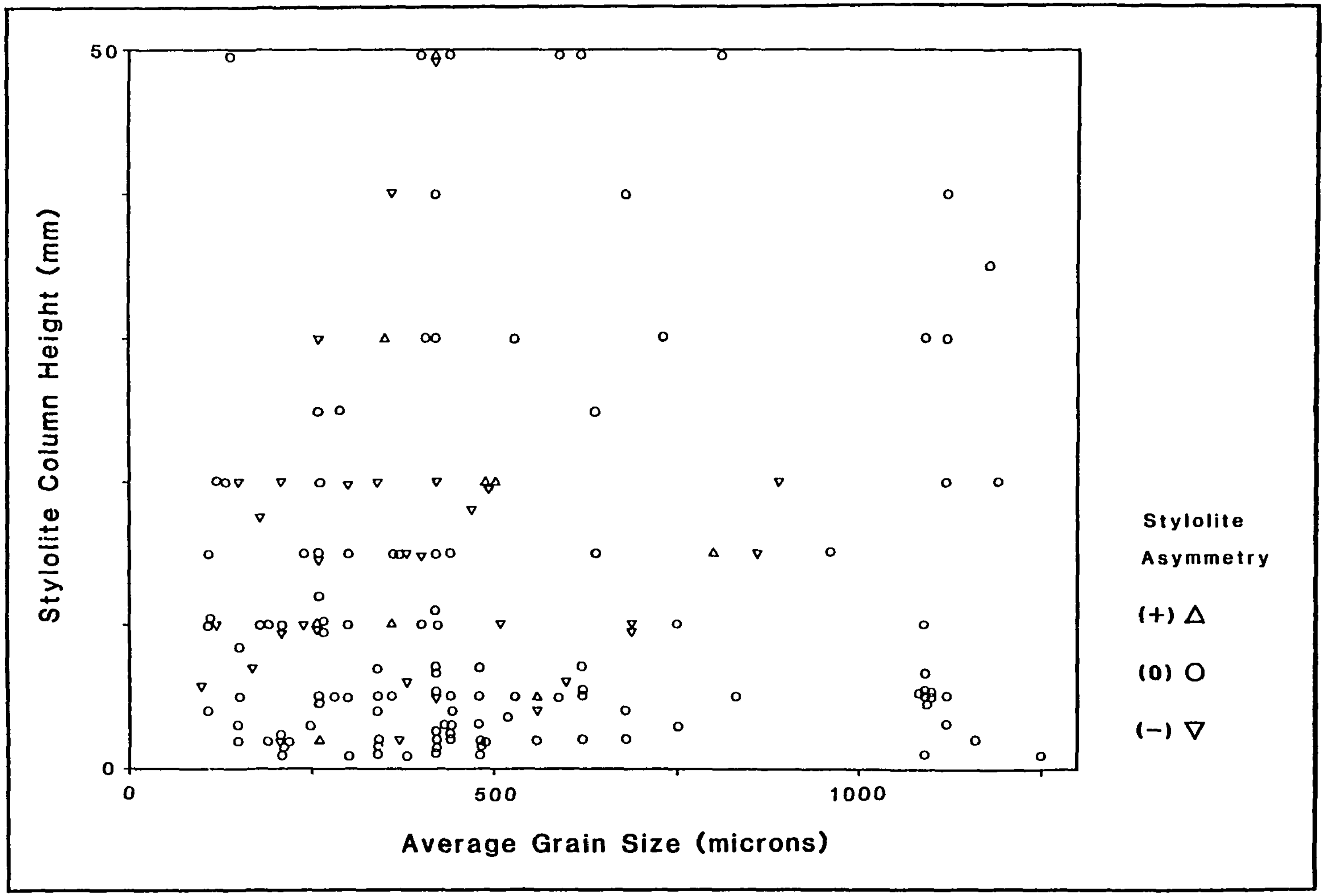
50
0
Stylolite Column Height (mm)
0
500
1000
Average Grain Size (microns)
Stylolite
Asymmetry
(+) △
(0) ○
(−) ▽

Figure 43.

Scatter plot of stylolite column height versus grain size contrast across a stylolite, for various stylolite symmetries.

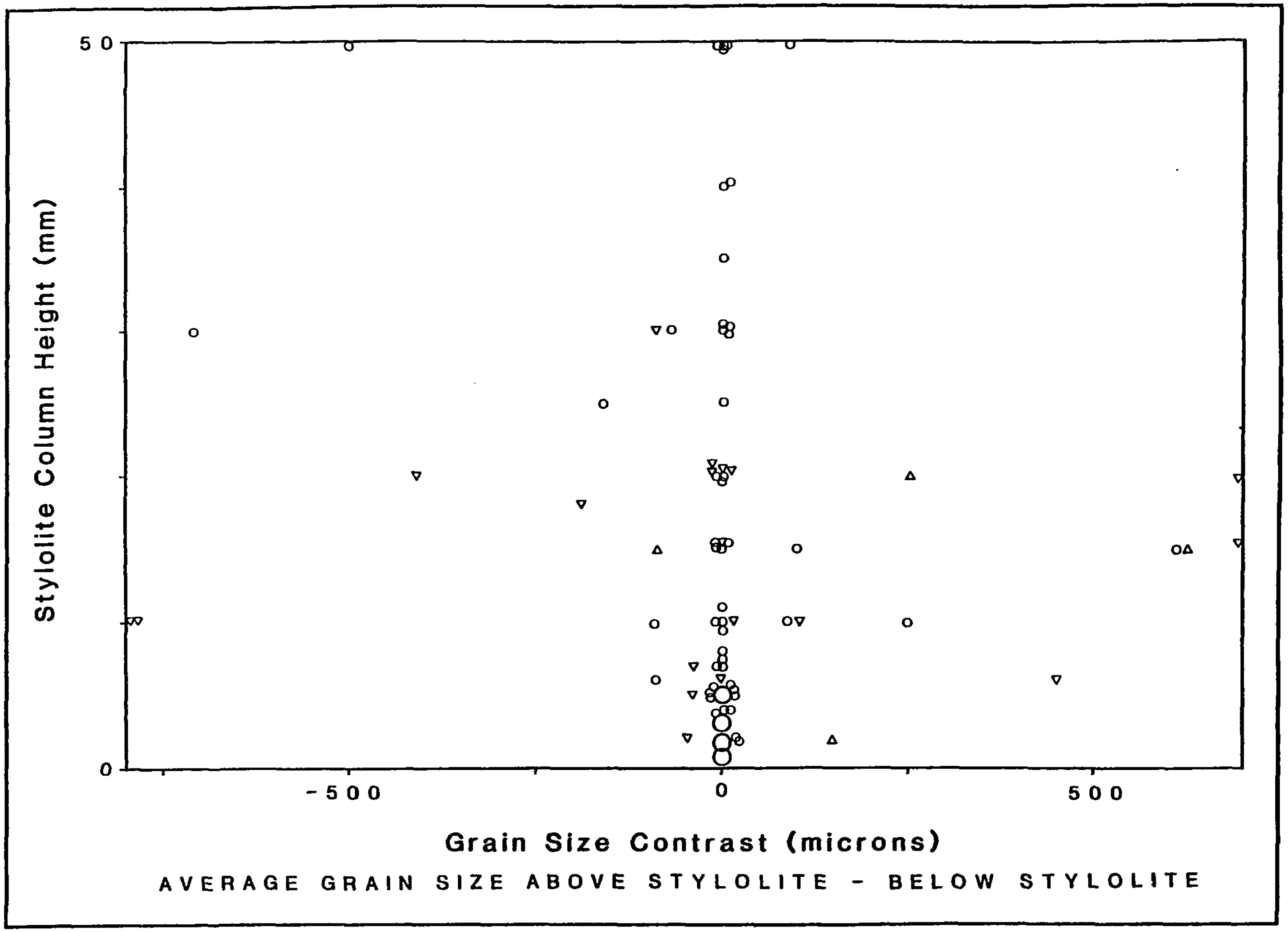
50
0
-500
0
500
Stylolite Column Height (mm)
Grain Size Contrast (microns)
AVERAGE GRAIN SIZE ABOVE STYLOLITE - BELOW STYLOLITE

height for any of the three symmetry categories. The fact that only symmetric stylolites are represented at the high end of the observed grain sizes may simply reflect the smaller dataset of asymmetric stylolites, compared to symmetric ones.

The vast majority of data points in the Figure 43 occur on or near a grain size contrast of 0 for all column heights. Most other points represent asymmetric stylolites. Although most data on the negative side represent negatively asymmetric stylolites, there are approximately as many points representing negatively asymmetric stylolites on the positive side of the grain-size-difference scale. Most data for positively asymmetric stylolites occur on the positive side of the scale. All asymmetric stylolites on or close to the vertical line at 0 represent negatively asymmetric stylolites.

Interpretations

Figure 42 indicates that regardless of mineralogy, there is no effect of grain size on stylolite column size. The wide scattering of data points representing asymmetric stylolites in Figure 42 is inconsistent with the hypothesis that negatively asymmetric stylolite development is associated with coarse grain size and driven by high permeability.

The clustering of data points representing symmetric stylolites marked by 0 grain contrast indicates that symmetric stylolites occur mainly where there is no vertical change in grain size. Column height appears to be unrelated to grain size contrast.

It was shown earlier (Plate 13) that grain size contrast does affect stylolite symmetry. Where there is significant vertical difference in grain size, an asymmetric stylolite develops. Shale breaks, clay seams, and organic laminations occurring between rocks with contrasting grain size develop into asymmetric stylolites. Organic-rich and clay-rich layers and laminations occurring within rock having a homogeneous grain-size distribution develop into symmetric or negatively asymmetric stylolites. The mechanism for development of the latter, though, is not understood. However, high permeability, or even high permeability contrasts associated with coarse grain size and large grain size contrast, do not appear to influence the development of negatively asymmetric stylolites.

Positively asymmetric stylolites, on the other hand, appear to require vertical grain size contrasts and, presumably, permeability contrast, in order to develop. Specifically, positively asymmetric stylolites develop where the grain size is greater above the developing stylolite than below. This relationship is consistant with the idea that greater permeability above the stylolite stimulates growth of stylolite columns in the upward direction. It is possible, however, that there is no good correlation between grain size and permeability, leaving mineralogy associated with grain size contrast as the probable cause for preferred column growth into coarse-grained rock.

E. Sorting in Stylolite Host Rock

Grain-size sorting in the host rock overlying and underlying symmetric and asymmetric stylolites is shown in Figure 44. The upper graphs display sorting in rock overlying stylolites, and the lower graphs display sorting in rock underlying stylolites. The left column represents the frequency of occurrence of poor sorting in rock adjacent to stylolites; the middle column indicates moderate sorting, and the right column indicates good sorting.

The vertical axes indicate percentages of occurrence for particular degrees of sorting (poor, moderate and good).

The dotted line in each graph in the upper row

Figure 44.

Matrix of bar graphs depicting grain sorting above and below stylolites occuring in various lithofacies environments. Positively assymetric stylolites are represented by a (+) pattern, negatively asymmetric stylolites by a (-) pattern, and symmetric stylolites by a blank pattern.

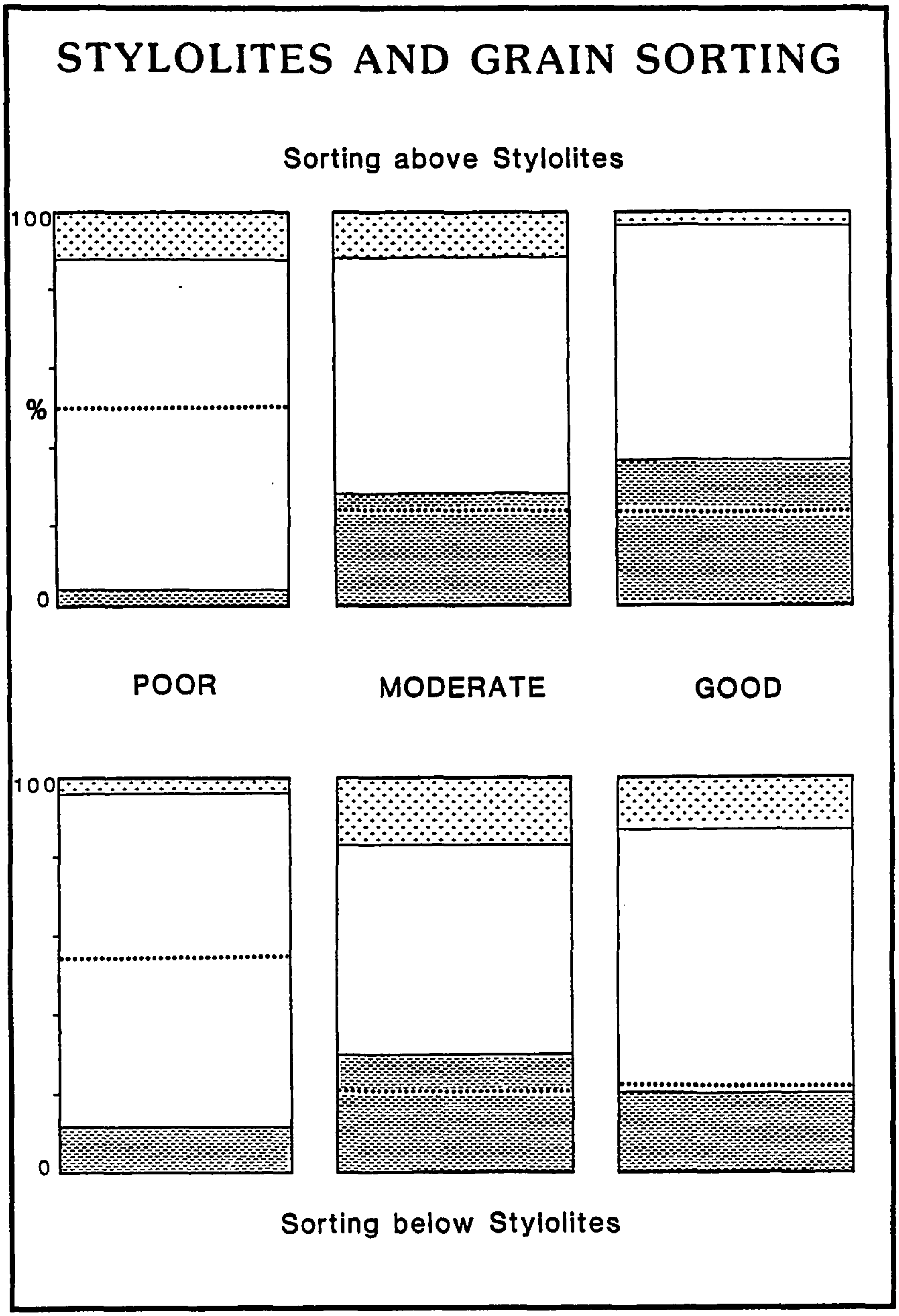
STYLOLITES AND GRAIN SORTING
Sorting above Stylolites
100
%
0
POOR
MODERATE
GOOD
100
0
Sorting below Stylolites

indicates the percentage of all stylolites surveyed that are overlain by rock with the degree of sorting represented by that graph. In the lower row, the dotted line indicates the percentage of all stylolites surveyed that are underlain by rock with the particular degree of sorting.

In each graph, the vertical heights of the three regions (two marked with patterns) indicate the percentage of stylolites having a particular symmetry. From bottom to top (within each graph), the three regions represent negatively asymmetric stylolites, symmetric stylolites, and positively asymmetric stylolites, respectively; the sum of the heights is 100%.

<u>**Results**</u>

The percentages of rocks with poor, moderate, and good sorting overlying stylolites are essentially equal to those for rocks underlying stylolites. Poor sorting characterizes 52% of rocks above stylolites, and 57% of rocks below stylolites. Moderate sorting characterizes 24% of rocks above stylolites, and 21% of rocks below. Good sorting characterizes 24% of rocks above, and 22% of rocks below stylolites. Thus, most rock adjacent to stylolites--both overlying and underlying the stylolites--is poorly sorted. The remaining rock is divided equally into moderately sorted, and well sorted rock.

Rock overlying positively asymmetric stylolites is more likely to have poor or moderate sorting than good sorting. Positive asymmetry characterizes 12% of stylolites overlain by poorly sorted rock, 11% of stylolites overlain by moderately sorted rock, and 3% of stylolites overlain by well sorted rock. Considering the percentages of all rock overlying stylolites that is poorly (52%), moderately (24%), or well (24%) sorted, this means that 65% of all positively asymmetric stylolites are overlain by poorly sorted rock, 27.5% by moderately sorted rock, and 7.5% by well sorted rock.

Rock underlying positively asymmetric stylolites is more likely to have moderate or good sorting than poor sorting. Positive asymmetry characterizes 13% of stylolites underlain by well sorted rock, 17% of stylolites underlain by moderately sorted rock, and 4% of stylolites underlain by poorly sorted rock. Considering the percentages of all rock underlying stylolites that is well (22%), moderately (21%), or poorly (57%) sorted, this means that 33% of all positively asymmetric stylolites are underlain by well sorted rock, 41% by moderately sorted rock, and 26% by poorly sorted rock.

Rock overlying negatively asymmetric stylolites is more likely to be well or moderately sorted than poorly sorted. Negative asymmetry characterizes 37% of stylolites overlain by well sorted rock, 29% of stylolites overlain by moderately sorted rock, and 4% of stylolites overlain by poorly sorted rock. Considering the percentages of all rock overlying stylolites that is well, moderately, or poorly sorted, this means that 49.5% of all negatively asymmetric stylolites are overlain by well sorted rock, 39% by moderately sorted rock, and 11.5% by poorly sorted rock.

Rock underlying negatively asymmetric stylolites is more likely to be poorly sorted than well sorted. Negative asymmetry characterizes 12% of stylolites underlain by poorly sorted rock, 30% of stylolites underlain by moderately sorted rock, and 20% of stylolites underlain by well sorted rock. Considering the percentages of all rock underlying stylolites that is poorly, moderately, or well sorted, this means that 39% of all negatively asymmetric stylolites are underlain by poorly sorted rock, 36% by moderately sorted rock, and 25% by well sorted rock.

Rock adjacent to symmetric stylolites, both underlying and overlying the stylolites, is more likely to be poorly sorted than moderately or well sorted. Symmetry characterizes 84% of stylolites overlain by poorly sorted rock, 60% of stylolites overlain by moderately sorted rock, and 60% of stylolites overlain by well sorted rock. This means that 60% of all symmetric stylolites are overlain by poorly sorted rock, 20% by moderately sorted rock, and 20% by well sorted rock.

Symmetry (zero asymmetry) characterizes 84% of stylolites underlain by poorly sorted rock, 53% of stylolites underlain by moderately sorted rock, and 67% of stylolites underlain by well sorted rock. This means that 65% of all symmetric stylolites are underlain by poorly sorted rock, 15% by moderately sorted rock, and 20% by well sorted rock. The frequency of poorly, moderately, and well sorted rock is almost the same above stylolites as below them.

Interpretations

Poorly sorted rock appears to be a more favorable host for stylolites than well sorted rock. Packstone is the most poorly sorted lithofacies in the Salem Limestone; it is also the most stylolite-rich facies (Section A, Plate 13). Therefore, the observations relating stylolites to sorting and lithofacies are consistent with each other.

Contrasts in sorting across a stylolite appear to affect stylolite symmetry. Results from the previous section (Section D) indicate that positively asymmetric stylolites occur where overlying rock is coarser than underlying rock. This section (Section E) indicates that grain sorting affects both positively and negatively asymmetric stylolites. Positively asymmetric stylolites develop where sorting is better in underlying rock than in overlying rock, whereas negatively asymmetric stylolites develop where sorting is better in overlying rock than underlying rock.

Physical parameters related to grain sorting and, in some cases, grain size, apparently affect stylolite symmetry, whereas chemical parameters related to dolomitization apparently affect stylolite column size, as shown in previous sections.

F. Fossils in Stylolite Host Rock

The analysis of fossil fauna adjacent to stylolites is based on six categories of fossils and related sedimentary features, listed below (Figure 45):

1. Foraminifera and ooids.
2. Bryozoans (branching, and fenestrate).
3. Brachiopods and pelecypods.
4. Crinoids and other echinoderms.

5. Corals (mainly rugose).

6. Organic laminations.

Foraminifera and ooids are grouped because they are intimately associated in many parts of the Salem Limestone, especially the lower parts of deposections. Many ooids have foraminifera as nuclei, and in many cases there are only a few layers of cortex. Consequently, the distinction between ooids and foraminifera is unclear in many parts of the Salem Limestone.

Both types of bryozoans are ubiquitous throughout the Salem Limestone and a separation into separate groups is unnecessary.

Many brachiopods and pelecypods occur as small fragments, making distinction between them difficult with a hand lens, the principal observational tool for the outcrop descriptions, and for many core descriptions. Separation of brachiopods and pelecypods into two groups seems unjustified under these circumstances.

Crinoids constitute the bulk of echinoderms in the Salem Limestone, and, like bryozoans, are ubiquitous throughout the Salem Limestone.

Figure 45.

Bar graph illustrating fossil fauna frequencies above and below stylolites belonging to various symmetry groups. Positively assymetric stylolites are represented by a (+) pattern, negatively asymmetric stylolites by a (-) pattern, and symmetric stylolites by a blank pattern.

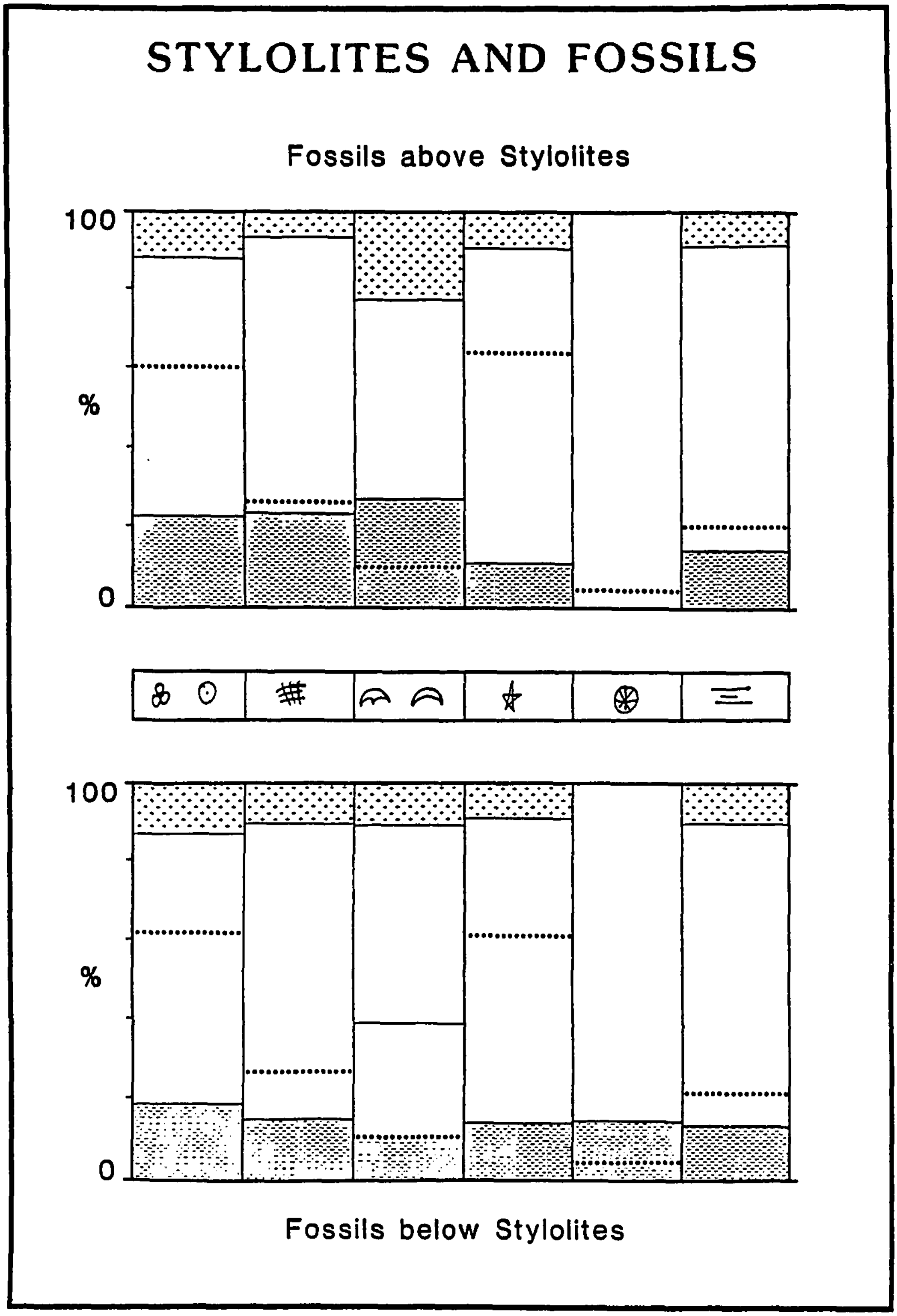
STYLOLITES AND FOSSILS
Fossils above Stylolites
100
%
0
100
%
0
Fossils below Stylolites

Corals are rare in the Salem Limestone. They occur mainly as fragments of individual colonies; most are rugose corals.

Organic laminations are an important, wide-spread biological product in the Salem Limestone. Their presence affects stylolite development. As in the previous section (Section E), two graphs represent rock overlying and underlying stylolites. The upper graph contains data from rock overlying stylolites, whereas the lower graph contains data from rock underlying stylolites.

Each graph consists of 6 columns, representing the 6 biological categories listed at the beginning of this section, 1 to 6 from left to right. The vertical axis represents percentage.

The dotted lines in the upper graph represent the percentage of all rock overlying stylolites containing the particular fossil of interest as one of the two most abundant fossils present. In the case of organic laminations, the dotted line represents the percentage of all rock overlying stylolites with organic laminations as a characteristic feature of the rock. Similarly, the solid lines in the lower graph represent data from rock underlying stylolites.

The sum of percentages represented by solid lines in the 6 columns of each graph may exceed 100% since each column represents a fossil category as one of the two most abundant fossils present.

The columns in each graph are separated into patterned sections. As in Sections E and A, the vertical height of each section indicates the percentage of stylolites belonging to a particular symmetry group which are overlain (upper graph) or underlain (lower graph) by rock dominated by the particular fossil of interest. In each column, the lowest section represents negativley asymmetric stylolites, the middle section represents symmetric stylolites, and the upper section represents positively asymmetric stylolites. The heights of the three patterned sections sum to 100%.

Results

Crinoids are the most common fossil in rock overlying stylolites, and 64% of all stylolites surveyed have crinoids as one of two most abundant fossils in rocks overlying the styloites. Foraminifers and ooids are the second most common category (60%), followed by bryozoans (26%), brachiopods and pelecypods (10%), and corals (4%). Organic laminations dominate 20% of all rock overlying stylolites.

The relative abundances of fossils and organic laminations in rock underlying stylolites are essentially the same as in rock overlying stylolites. The fact that Foraminifera and ooids (62%) lead over crinoids (61%) is statistically insignificant. The third most common fossil, again, are bryozoans (27%), followed by brachiopods and pelecypods (10%), and corals (4%). Organic laminations dominate 21% of all rock underlying stylolites.

For each fossil category, as well as for organic laminations, the difference between its abundance in rock overlying and underlying symmetric stylolites is statistically insignificant. Symmetric constitute at least 50% of all stylolites adjacent to any given category of fossils or biological products.

Symmetric stylolites constitute 100% of stylolites overlain by many corals, 79.5% of those overlain by crinoids, 77.1% of those overlain by organic laminations, 69.6% of those overlain by bryozoans, 65.1% of those overlain by foraminifers and ooids, and 50% of those overlain by brachiopods and pelecypods. Symmetric stylolites constitute 85.7% of stylolites overlain by many corals, 76.6% of those overlain by crinoids, 75.7% of those overlain by organic laminations, 74.5% of those overlain by bryozoans, 68.5% of those overlain by foraminifers and ooids, and 50% of those overlain by brachiopods and pelecypods.

Asymmetric stylolites are especially abundant adjacent to rock rich in brachiopods and pelecypods. Compared to the abundance of positively asymmetric stylolites with overlying rocks dominated by other fossil categories, it is clear that positively asymmetric stylolites are especially abundant beneath rock dominated by brachiopods and pelecypods. Analogously, negatively asymmetric stylolites are especially abundant above rock dominated by brachiopods and pelecypods. Negatively asymmetric stylolites generally constitute a larger portion of asymmetric stylolites for each of the 6 biological categories than positively asymmetric stylolites.

Positively asymmetric stylolites constitute 22.2% of stylolites overlain by many brachiopods and pelecypods, 12.3% of those overlain by foraminifers and crinoids, 9.8% of those overlain by crinoids, 8.6% of those overlain by organic laminations, 6.5% of those overlain by bryozoans, and none (0%) of those overlain by corals. Negatively asymmetric stylolites constitute 27.8% of stylolites overlain by many brachiopods and pelecypods, 23.9% of those overlain by bryozoans, 22.6% of those overlain by foraminifers and ooids, 14.3% of those overlain by organic laminations, 10.7% of those overlain by crinoids, and none of those overlain by corals.

Positively asymmetric stylolites constitute 13% of stylolites underlain by many foraminifers and ooids, 11.1% of those underlain by brachiopods and pelecypods, 10.8% of those underlain by organic laminations, 10.6% of those underlain by bryozoans, 9.2% of those underlain by crinoids, and none of those underlain by corals. Negatively asymmetric stylolites constitute 38.9% of stylolites underlain by many brachiopods and pelecypods, 18.5% of those underlain by foraminifers and ooids, 14.9% of those underlain by bryozoans, 14.3% of those underlain by corals, 14.2% of those underlain by crinoids, and 13.5% of those underlain by organic laminations.

Interpretations

The abundances of fossils adjacent to stylolites reflects the overall abundances of those fossils in the Salem Limestone. There is no difference between the relative abundances of particular fossils in rock overlying as opposed to underlying stylolites. Thus, there is no linkage between any particular fossil type and stylolite development.

Although organic laminations dominate only 20% of rock adjacent to stylolites, the importance of organic laminations should not be underestimated. Organic laminations appear to foster stylolite development in stylolite zones within packstone and wackestone of the upper parts of deposequences, as shown in Chapter 3. Organic material concentrated in "shale breaks" and "clay seams" is also important for the development of individual stylolites, in grainstone and packstone of the lower parts of deposections.

The low percentage (20%) of rock adjacent to stylolites that is dominated by organic laminations reflects the fact that the survey does not account for individual stylolites within stylolite zones. Another control on the number of organic laminae actually counted is the difficulty in identifying distinct organic laminae in some highly organic anc micritic wackestone to packstone. There, the organic material is almost homogeneously spread throughout the rock, rather than being concentrated along distinct laminations.

The fact that brachiopods and pelecypods are especially common above positively asymmetric stylolites, and below negatively asymmetric stylolites probably reflects the fact that rock dominated by brachiopods and pelecypods tends to be poorly sorted. The shell fragments are typically much larger than other fragments of other fossils, such as foraminifers and crinoids that commonly occur in the same rock.

The unusually low percentages of asymmetric stylolites adjacent to coral-rich rock probably reflect the low sample size for this fossil category.

The greater abundance of negatively asymmetric stylolites over positively asymmetric ones within each of the six biological categories analyzed in this section, reflects the same trend within lithological categories (lithologic contacts) analyzed in Section A. These data simply reflect the fact that negatively asymmetric stylolites are somewhat more common than positively asymmetric ones.

G. Fossils and Column Heights

Figure 46 illustrates the relationships between the abundance of fossils and organic laminations, and the heights of stylolites columns.

The six biological categories, represented by 6 columns in each of the two graphs, are the same as in Section F. The vertical axes of the graphs in this section represent the heights of stylolite columns, in mm.

Figure 46.

Bar graphs illustrating the relationships between fossil fauna and stylolite column heights for various stylolite symmetries. Positively asymmetric stylolites are represented by a dotted line, negatively asymmetric stylolites by a dashed line, and symmetric stylolites by a wavy line. A solid line represents the average column height of all stylolites.

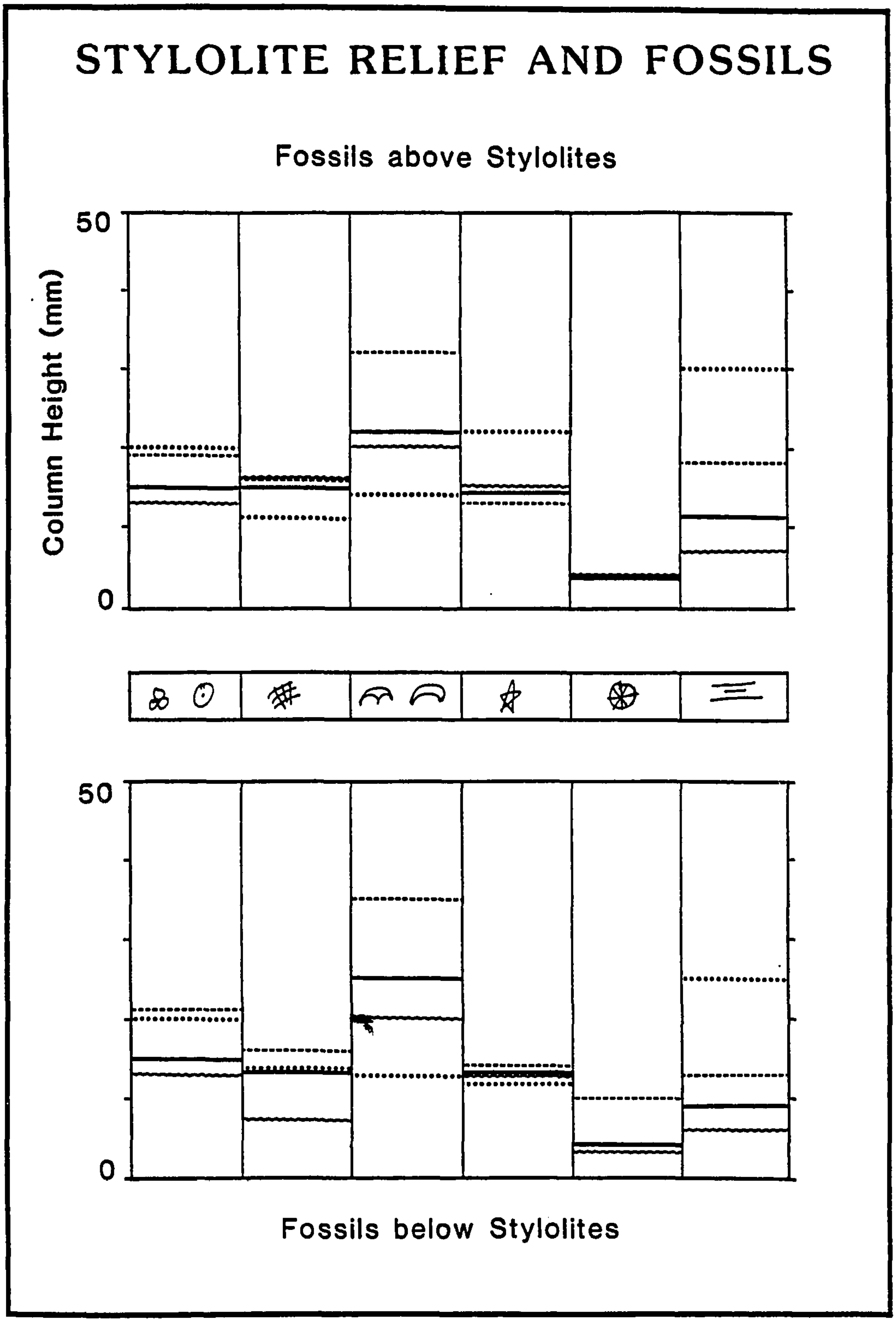
STYLOLITE RELIEF AND FOSSILS
Fossils above Stylolites
50
Column Height (mm)
0
50
0
Fossils below Stylolites

The solid lines in the upper graph represent the average column heights of all stylolites overlain by rock containing the particular fossil of interest as one of the two most abundant fossils present. In the case of organic laminations, the solid line represents the average column heights of all stylolites overlain by rock with organic laminations as a characteristic feature of the rock. Similarly, the solid lines in the lower graph represent data from rock underlying stylolites.

The wavy, dotted, and dashed lines in each graph indicate the average column heights of symmetric, positively asymmetric, and negatively asymmetric stylolites, respectively for each of the 6 biological categories analyzed in this section.

Results

The average column height of all stylolites overlain by rock belonging to a given biological category is roughly the same as the average column height of all stylolites underlain by rock belonging to that category.

The average column height is 22 mm in all stylolites overlain by many brachiopods and pelecypods, 16 mm in those overlain by bryozoans, just over 15 mm in those overlain by foraminifers and ooids, just under 15 mm in those overlain by crinoids, 11 mm in those overlain by organic laminations, and 4 mm in those overlain by corals. Average columns height is 26 mm in all stylolites underlain by many brachiopods and pelecypods, 16 mm in those underlain by foraminifers and ooids, 15 mm in those underlain by bryozoans, 13 mm in those underlain by crinoids, 10 mm in those underlain by organic laminations, and 4 mm in those underlain by corals.

Average column heights for stylolites adjacent to brachiopod- and pelecypod-rich rock are noticably greater (about 20 to 25 mm) than for stylolites adjacent to rocks dominated by other fossils (10 to 15 mm).

Stylolites adjacent to rocks rich in corals and organic laminations have noticably smaller average column heights (about 4 mm and 10 mm, respectively) than other stylolites. Positively asymmetric stylolites adjacent to (overlain or underlain by) rock rich in brachiopods and pelecypods have average column heights that are significantly smaller than average column heights of all stylolites adjacent to brachiopod- and pelecypod-rich rock. Positively asymmetric stylolites adjacent to (overlain or underlain by) rock rich in organic laminations have average column heights that are significantly larger than average column heights of all stylolites adjacent to organic-laminated rock.

Specifically, positively asymmetric stylolites overlain by rock rich in foraminifers and ooids, or bryozoans, have average column heights which deviate by only 5 mm or less from average column heights of all stylolites in those two biological categories. Positively asymmetric stylolites overlain by rock rich in brachiopods and pelecypods have average column heights that are 8 mm smaller than average column heights of all stylolites in that biological category. Positively asymmetric stylolites overlain by rock rich in crinoids or organic laminations have average column heights that are 8 mm and 19 mm greater, respectively, than average column heights of all stylolites in those two biological categories. No positively asymmetric stylolites overlain by corals were recorded.

Postively asymmetric stylolites underlain by rock rich in foraminifers and ooids, bryozoans, crinoids, or corals have average column heights that deviate by only 5 mm or less from average column heights of all stylolites in those four biological categories. Positively asymmetric stylolites underlain by rock rich in brachiopods and pelecypods have average column heights that are 12 mm smaller than average column heights of all stylolites in that biololgical category. Positively asymmetric stylolites underlain by rock rich in organic laminations have average column heights that are 16 mm greater than average column heights of all stylolites in that biological category.

Negatively asymmetric stylolites which are overlain by rock rich in foraminifers and ooids, bryozoans, or crinoids have average column heights that deviate by only 5 mm or less from average column heights of all stylolites in those three biological categories. Negatively asymmetric stylolites overlain by rock rich in brachiopods and pelecypods, or organic laminations, have average column heights that are 10 mm and 7 mm greater than average column heights of all stylolites in those two biological categories, respectively. No negatively asymmetric stylolites overlain by coral-rich rock were recorded.

Negatively asymmetric stylolites underlain by rock rich in crinoids or organic laminations have average column heights that deviate by less than 5 mm from average column heights of all stylolites in those two biological categories. Negatively asymmetric stylolites underlain by rock rich in bryozoans has average column heights that are 7 mm smaller than average column heights of all stylolites underlain by such rock. Negatively asymmetric stylolites underlain by brachiopods and pelecypods, foraminifers and ooids, or corals, have average column heights that are 10 mm, 6 mm, and, again, 6 mm larger than average column heights of all stylolites in those three biological categories, respectively.

Interpretations

Stylolite columns are relatively tall in lithofacies with brachiopods and pelecypods as major fossils because packstones and grainstones in lower parts of deposections are especially coarse-grained where these fossils predominate.

Stylolite columns are relatively short in lithofacies dominated by corals because corals occur mainly in wackestones to packstones, in the upper parts of deposequences, where most stylolites occur within stylolite zones. Organic laminations are associated with stylolites having relatively short columns for the same reason that corals are associated with such stylolites: organic-rich packstones in upper parts of deposections host stylolite zones with many closely-spaced stylolites having short columns.

Column heights of asymmetric stylolites display the greatest deviations from average column heights for all stylolites when the asymmetric stylolites are adjacent to rock with abundant brachiopods and pelecypods, or organic laminations. The stratigraphic position of such rock relative to the stylolites has no significant effect on the average column heights. This evidently reflects the fact that stylolites generally occur within rock rich in brachiopods and pelecypods, or organic laminations, rather than just above or below such rock.

Negatively asymmetric stylolites have columns that are taller than average when they are adjacent to brachiopod- and pelecypod- rich rock. Positively asymmetric stylolites have columns that are shorter than average when adjacent to such rock. Perhaps the high permeabilities expected in such coarse grained and poorly sorted rock are more amenable to the gravity-driven mechanisms that might be responsible for negative asymmetry in stylolites, than to the permeability-differential-driven mechanisms that might be responsible for positive asymmetry in stylolites.

Both negatively and positively asymmetric stylolites have columns that are taller than average when they occur adjacent to organic-laminated rock. This is probably because symmetric stylolites in organic-laminated rock typically occur within stylolite zones characterized by short columns(in upper parts of deposections), whereas asymmetric stylolites in organic-laminated rock typically occur outside such zones and are characterized by normal-sized columns (in lower parts of deposections).

Summary and Conclusions

Stylolites occur within single lithofacies more often than along contacts between lithofacies. Stylolites are most common in packstone, and least common in dolostone. The height and width of a stylolite column are linearly related. They are influenced by mineralogy (they tend to be small in dolostone), but not by physical features of host rock, such as grain size and sorting. The thickness of column caps is unrelated to column size.

Stylolite symmetry is influenced by grain sorting, and, at least in some cases, by grain size. Columns of asymmetric stylolites penetrate into poorly sorted, typically coarse-grained, rock, and away from well sorted rock.

Certain fossils--notably, brachiopods and pelecypods--are associated with poor sorting and coarse grain size. The abundance of such fossils fosters the development of asymmetric stylolites.

Organic content stimulates stylolite development. Stylolites develop along pre-existing, sedimentary layers or laminations that are rich in organic material, and clay minerals. These layers can be shale breaks, clay seams, or organic laminations. The distribution of such layers in the stratigraphic section strongly influences the distribution of stylolites in the section.

Stylolite density is higher in packstones in upper parts of deposequences than in lower parts of deposequences. This observation favors the hypothesis that stylolites form along preexisting organic laminations, because packstone in upper parts of deposequences is commonly rich in closely-spaced, organic laminations, whereas packstone in lower parts of deposequences has fewer laminations. Instead, packstone in lower parts of deposequences contains fewer, widely spaced but substantially thick (>2 mm), organic-rich and clay-rich seams (partings). This fact is reflected in the larger, more widely spaced stylolites in lower deposequence packstones compared to upper deposequence packstones.

These observations argue against the textural advantage of packstone as a reason for its higher stylolite density compared to other lithofacies.

Pressure solution alone is insufficient as a mechanism for stylolite development. The sizes and shapes of stylolite columns and column caps cannot be explained by the pressure solution hypothesis. Gravity-driven flow, or even local convective currents, in the vicinity of pre-existing layers associated with acidic, carbon-dioxide-rich pore fluids, is a viable, alternative explanation for the development of stylolites characterized by the asymmetry (and symmetry), the size and shape relationships, and the lithologic setting--textural, mineralogical, and biological--of many stylolites in the Salem Limestone.

CHAPTER 6

BASIN-WIDE TRENDS

A series of 22 contour maps illustrates basin-wide trends of parameters related to stylolites and their host rocks. A database of stylolite-related parameters calculated from 12 stratigraphic sections of the Salem Limestone distributed throughout the Illinois Basin provides the basis for the contour maps.

The 12 stratigraphic sections include 5 surface outcrops and 7 subsurface cores. Outcrops include 3 in the vicinity of St. Louis, Missouri, and 2 in the vicinity of Bedford, Illinois. Cores are distributed throughout the basin, as shown in Figure 47.

Nine variables represent data from the stratigraphic sections:

B = Depth to bottom of Salem Limestone (feet) (1)

T = Thickness of Salem Limestone (feet) (2)

G = Thickness of grainstone (feet) (3)

P = Thickness of packstone (feet) (4)

W = Thickness of wackestone-micstone (feet) (5)

D = Thickness of dolostone (feet) (6)

S = Number of stylolites (7)

Figure 47.

Location map of Salem Limestone outcrop and core locations in the Illinois Basin, indicating map area used in basin-wide analysis of stylolite-related parameters.

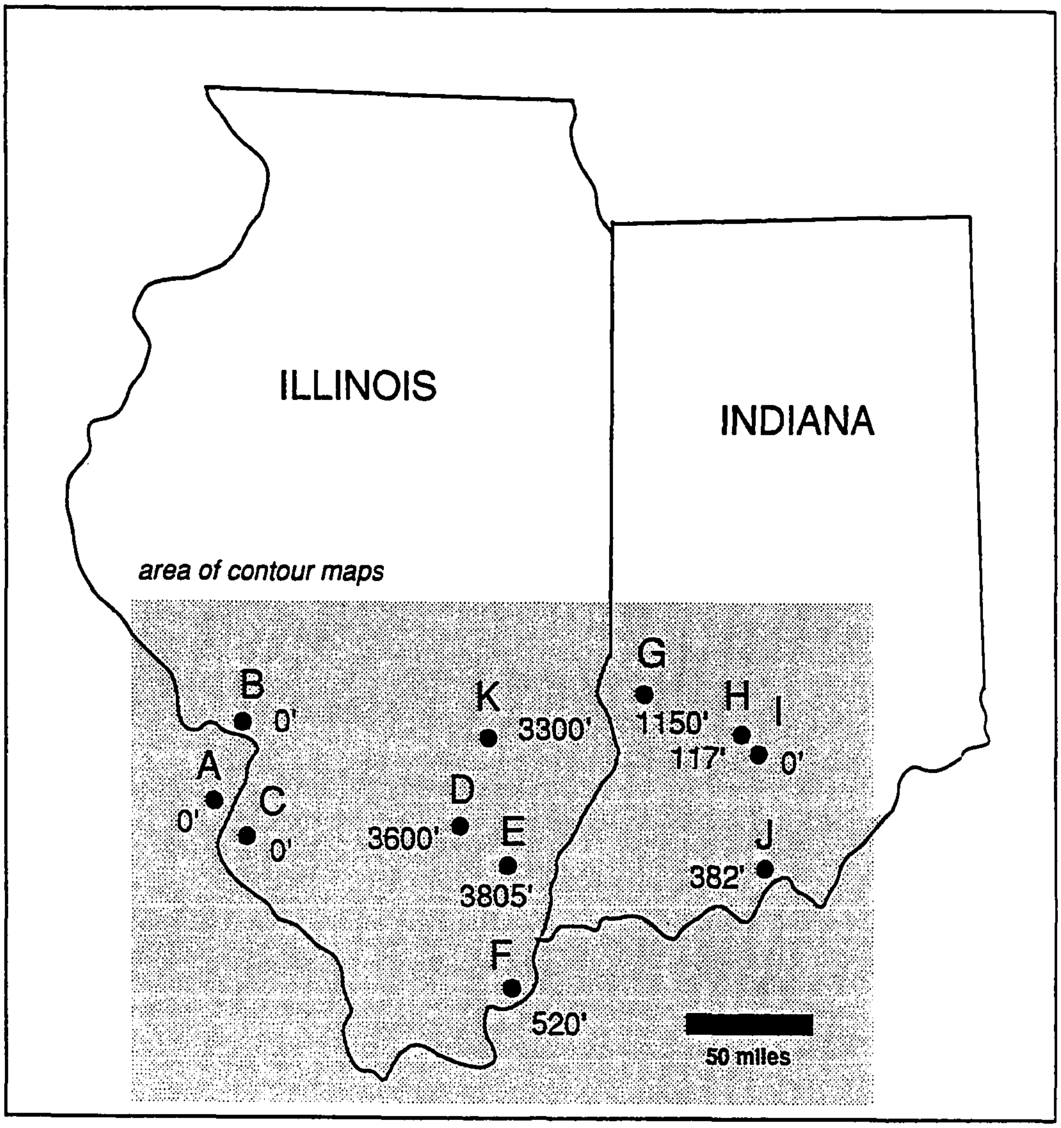

Outcrop and core locations of Salem LImestone in Illinois Basin, with depths to tops of sections, in feet.

H = Number of hummocky seams (8)

R = Relief (height) of stylolite columns (mm) (9)

These 9 variables define 22 parameters, each represented by a contour map covering the entire basin. The first two variables, B and T, stand alone and are represented by 2 contour maps. The remaining 7 variables are combined as ratios, constituting 20 different parameters. The parameters can be separated into 4 groups of 4 parameters each.

The first four parameters denote the fractional portion of stratigraphic section that consitutes one of the 4 major lithofacies (grainstone, packstone, wackestone-micstone, and dolostone):

1. G/T
2. P/T
3. W/T
4. D/T

To obtain percentages of individual lithofacies within the stratigraphic section, multiply each fraction by 100.

The second group of parameters represents the number of stylolites per foot of a particular lithofacies:

5. S/G
6. S/P
7. S/W
8. S/D

Only columnar stylolites, with clearly developed columns at least 1 mm tall, were included in the counts of stylolites represented by the previous 4 parameters. Hummocky seams, on the other hand, were counted in the third set of parameters, representing the number of hummocky seams per foot of a particular lithofacies:

9. H/G
10. H/P
11. H/W
12. H/D

The fourth set of parameters represents stylolite relief per foot of a particular lithofacies. Stylolite relief is the average height of columns in an individual stylolite. The ratios are in terms of mm of column height per foot of rock:

13. R/G
14. R/P
15. R/W

16. R/D

The fifth set of parameters represents the average heights of stylolite columns within each lithofacies. The height of stylolite columns is referred to as the "relief" of a stylolite. This is the ratio of total stylolite relief to the number of stylolites in a particular lithofacies:

17. $(R/S)_G$

18. $(R/S)_P$

19. $(R/S)_W$

20. $(R/S)_D$

Subscripts denote the lithofacies for which the average stylolite relief is measured.

The contour maps of the 22 parameters given above reveal 3 general classes of cross-basinal trends: radial (represented by C for "circular"); linear, north-south trend (represented by NS); and linear, northwest-southeast trend (represented by NWSE). The NS trend is marked by change occuring in the NS direction, so that the contours trend EW. The NWSE trend is marked by trend in the NW-SE direction, so that the contours trend NE-SW. In addition to these 3, well-defined trends, some contour maps exhibit an apparently random distribution of values, represented by R.

Radially distributed values include 2 subclasses. Radially distributed values that increase toward the center of the basin are represented by +C. Radially distributed values that decrease toward the center of the basin are represented by -C.

North-south trending values also include 2 subclasses. In each subclass, values are distributed roughly symmetrically about an east-west trending axis, cutting through the center of the basin. In the first subclass, values increase toward this axis, so the subclass is represented by +/-NS. In the second subclass, values decrease toward the east-west trending axis, and this subclass is represented by -/+NS.

The class of northwest-southeast trending values includes 4 subclasses. Values that increase southeastward are represented by +NWSE; values that decrease southeastward are represented by -NWSE. In the third and fourth subclasses, values are distributed about a roughly northeast-southwest trending axis. In the third subclass, values increase toward this axis, so the subclass is represented by +/-NWSE. Finally, in the fourth subclass, values decrease toward the northeast-soutwest trending axis, and this subclass is represented by -/+NWSE.

The distribution of values on each contour map can be approximated by an equation relating the location of each point in the basin to a particular value of the parameter of interest. The western edge of each map defines the ordinate, and the southern edge of each map defines the abscissa. Distances are measured in units of mm on the contour maps, and each mm represents approximately 1.5 miles.

The equations are linear in the case of the two classes of linear trends, NS and NWSE. In the case of NS trends, parameter values are defined in terms of only one geographic variable, N, representing the distance along the vertical axis. In the case of NWSE trends, parameter values are defined in terms of two variables: N and E, representing distances along the vertical and horizontal axes, respectively. In the case of radially arranged values, the form of the equation is linear with respect to the radial distance, R, away from the center of symmetry of contours, but it is nonlinear with respect to the variables N and S.

The general form of the equation for parameter values exhibiting a NS trend (with EW-trending contours), is:

$$P(N) = k + aN \qquad (10)$$

where P(N) is the parameter of interest, and k and a are empirical constants, different for each contour map. In the case of NS trends characterized by an axis of symmetry (+/- NS or -/+NS), Equation (10) becomes:

$$P(N) = k + a|N - N_o| \quad (11)$$

where $\underline{N_o}$ is the intersection of the axis of symmetry on the ordinate, and vertical brackets (||) denote the absolute value of the enclosed quantity.

To generate equations for parameter values exhibiting a NWSE trend (with NE-SW-trending contours), an equation is first written with respect to axes parallel and perpendicular to the NWSE trend, labelled N' and E', and this equation is then transformed by a rotation of axes toward N and E, using the formulas:

$$E' = E \cos(-q) - N \sin(-q) \quad (12a)$$

$$N' = E \sin(-q) + N \cos(-q) \quad (12b)$$

where $\underline{q}$ is the angle between the two sets of axes.

The general form of the equation for a parameter exhibiting a radial trend and circular contours (C), is:

$$P(R) = k + aR \quad (13)$$

where R is the radial distance from the center of the basin. With reference to the vertical (N) and horizontal (E) axes, Equation (13) becomes:

$$P(N,E) = k + a((N - N_o)^2 + (E - E_o)^2)^{0.5} \quad (14)$$

where (N_o, E_o) are the coordinates of the center of symmetry of the contours.

Combinations of radial and linear symmetry result in contours that define elongate, oval shapes. Although such shapes may be represented using the equation for an ellipse, such a representation does not reveal the combined influence of linear and radial trends. Superposition of these two trends in one equation is preferred. The general equation for a combination of radial (C) and NS trends is, hence:

$$P(N,E) = k + a|N - N_o| + b((N - N_o)^2 + (E - E_o)^2)^{0.5} \quad (15)$$

where k, a, and b are constants, N_o is the intercept of the major axis with the ordinate, and E_o is intercept of the minor axis of symmetry with the abscissa.

Similarly, the general equation for a combination of radial (C) and EW trends is:

$$P(N,E) = k + a|E - E_o| + b((N - N_o)^2 + (E - E_o)^2)^{0.5} \tag{16}$$

where the orientations of the major and minor axes are reversed, compared to Equation (15). The equation for an EW trend is analogous to that for a NS trend, as given in Equation (11).

Contour maps are grouped into 5 categories:

A. Single Variable Parameters
B. Lithofacies Fractions
C. Stylolite Densities
D. Hummocky Seam Densities
E. Cummulative Stylolite Relief
F. Average Stylolite Relief

Parameters included within each of these categories are outlined in the introduction to this chapter.

A. Single Variable Parameters

Depth to Bottom of Salem Limestone

A contour map of the depth to the bottom of the Salem Limestone throughout the Illinois Basin (Figure 48) reveals a circular basin, centered around the Fairfield Basin in southeastern Illinois. This configuration agrees generally with previously published maps of the depth of the Salem Limestone (Pryor and others, 1991).

The maximum depth exceeds 3500 feet at the center ofthe basin, also in agreement with previously published maps. The outcrop belt, defined by the 0-foot depth contour, includes the Mississippi Valley along the border between Illinois and Missouri, and the area of Bedford, in south central Indiana. The outcrop belt reaches far southward into Kentucky, beyond the region covered by this study. The depth of the Salem Limestone at the Kentucky state line is approximately 500 feet. The study area reaches northward into central Illinois, where the Salem Limestone is 2000 feet deep, at maximum.

The equation describing the approximate distribution of depths to the Salem Limestone is of the radial, +C form:

Figure 48.

Contour map of the depth to the base of the Salem Limestone in the Illinois Basin, in feet.

DEPTH TO BOTTOM OF SALEM LS (FT)

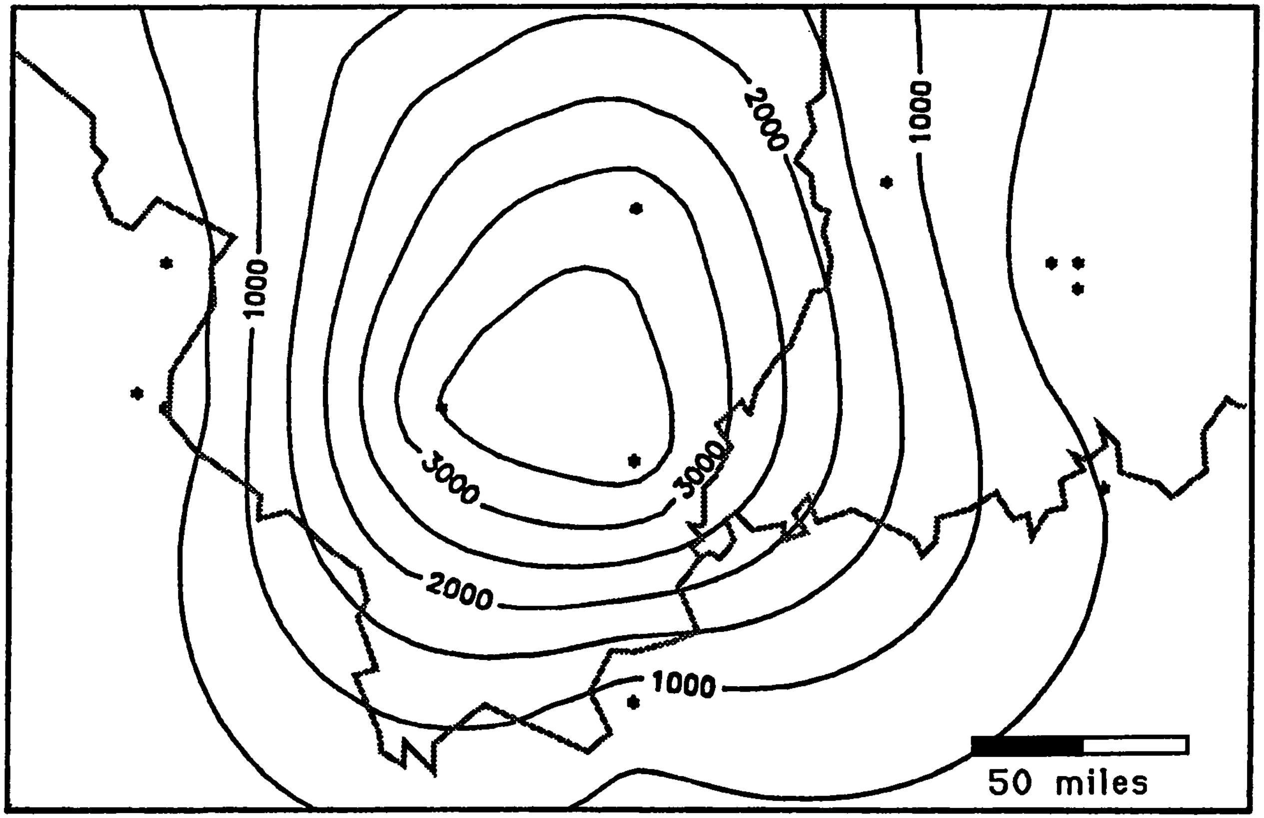

$$B = 4437.5 - 62.5((0.67N - 65)^2 + (0.67E - 80)^2)^{0.5} \quad (17)$$

where $\underline{B}$ is the depth in feet to the bottom of the Salem Limestone, and $\underline{N}$ and $\underline{E}$ are distances, in miles, north and east of the reference point at the southwest corner of the map. This point is located approximately 20 miles northwest of Alton, Missouri.

Equation (17) is only an approximation of the contours showing depth to the bottom of the Salem Limestone. The main purpose of the equation is to compare the depth to other parameters relevant to stylolites and their host rocks, analyzed below.

Thickness of Salem Limestone

Thickness contours of the Salem Limestone generally follow an EW trend, with minor deviations, especially at the center of the Illinois Basin (Figure 49). The thickness increases southward. At the latitude of St. Louis, Missouri, and Bedford, Indiana, along a line generally intersecting the center of the basin, the thickness is approximately 50 to 75 feet. At the southern margin of the study area, along the Ohio River, the thickness approaches 150 feet.

Figure 49.

Isopach map of the Salem Limestone in the Illinois Basin.

THICKNESS OF SALEM LS (FT)

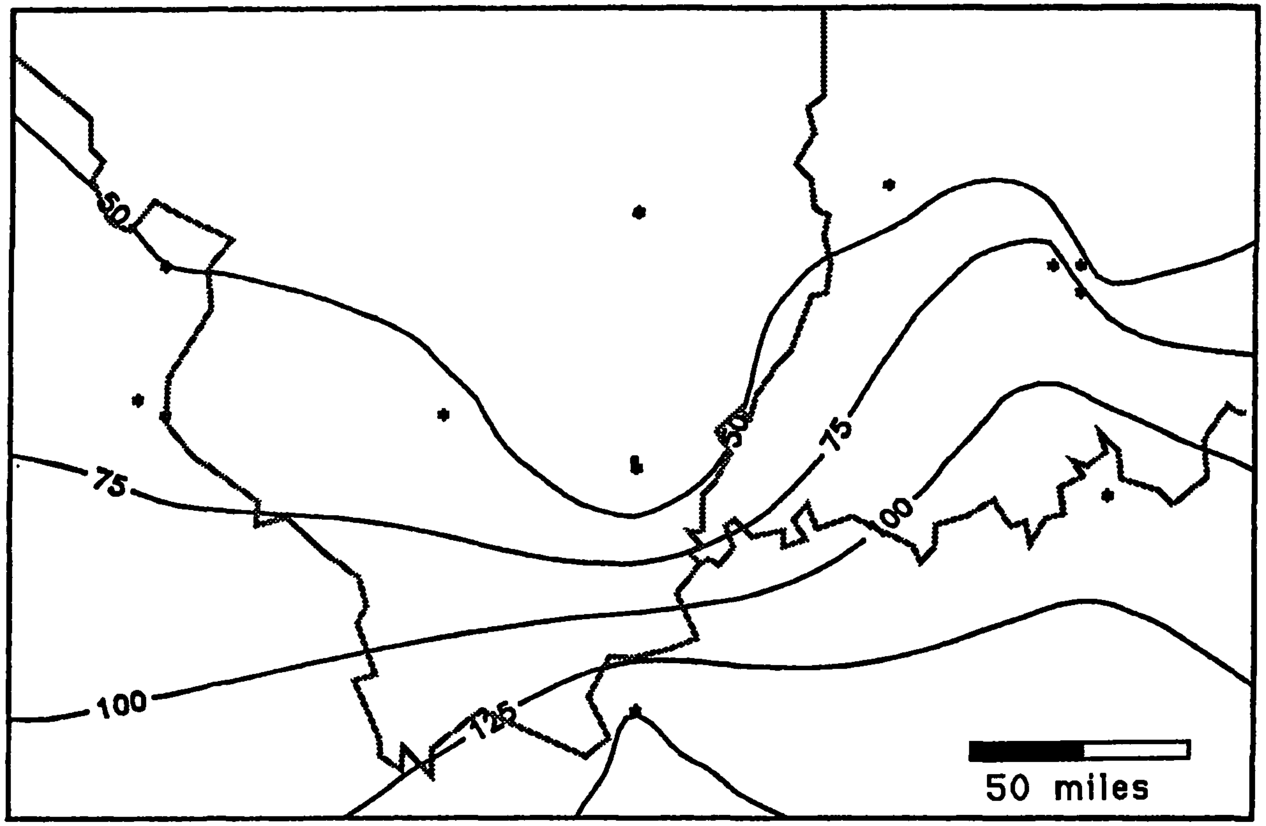

The equation approximating the thickness of the Salem Limestone across the study area is of the +NS form:

$$T = 152.38 - 0.793N \qquad (18)$$

in which $\underline{T}$ is the thickness of the Salem Limestone, in feet, and $\underline{N}$ is measured in mm on the contour map.

B. Lithofacies Fractions

Lithofacies fractions are expressed as percentages of grainstone, packstone, wackestone-micstone, and dolostone in the entire section of Salem Limestone at a given point in the basin.

Grainstone Fraction

Although the contours showing percentages of grainstone within the Salem Limestone across the Illinois Basin (Figure 50) exhibit significant convolution, the paucity of data across the basin precludes detailed accounting of such convolutions. Instead, it appears appropriate to generalize the configuration of contours as a NE-SW trending pattern, with the "slope," or inclination of the contours defined roughly by the orientations of the middle contours--representing 20% and 10%. The angle defined by the EW axis

Figure 50.

Contour map showing distribution of grainstone as a percentage of the total stratigraphic section of the Salem Limestone in the Illinois Basin. Dashed lines represent Equation 19.

PERCENT GRAINSTONE IN SALEM LS

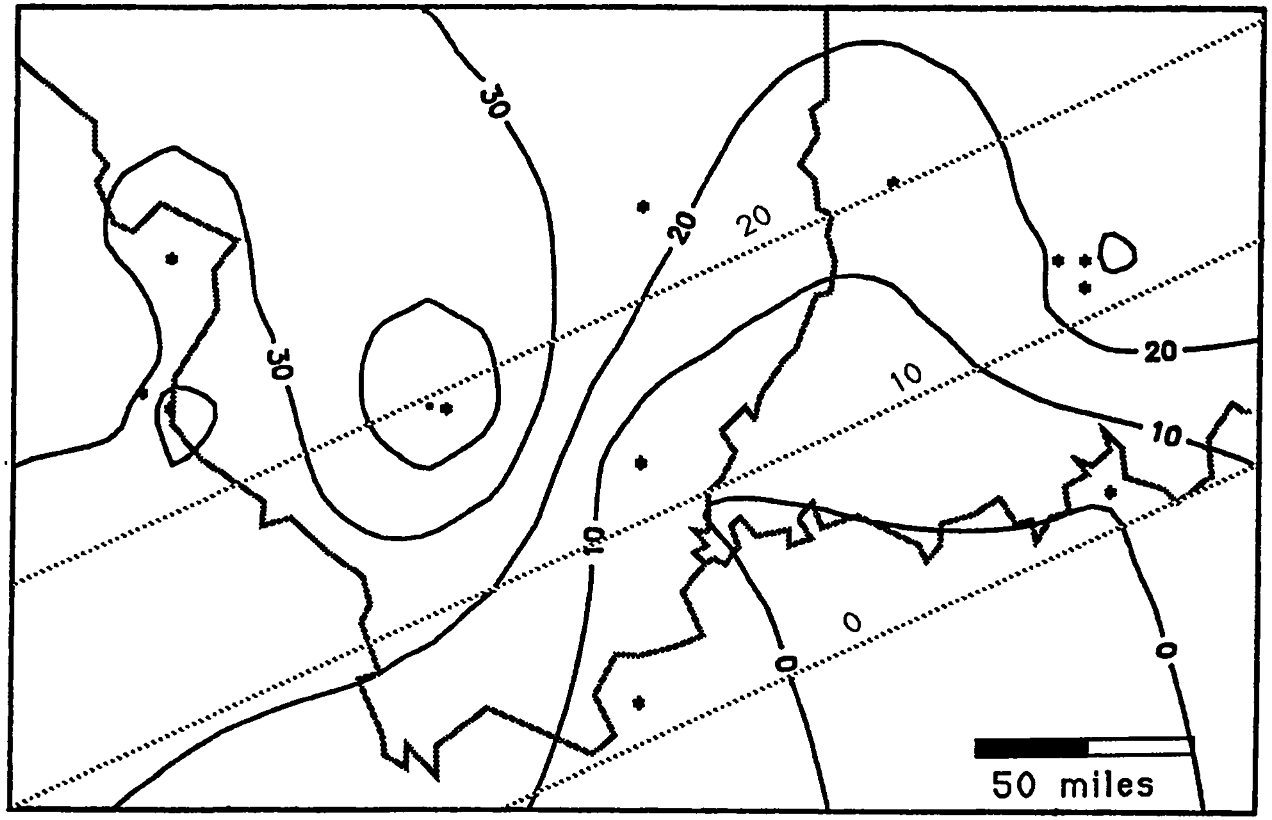

and the contour trend is 25 degrees.

With this simplification, it can be seen that the percentage of grainstone within the Salem Limestone diminishes southeastward, beginning at about 30% in the northwest corner of the map (including St. Louis and the northwestern edge of the Fairfield Basin) and approaching 0% toward the southeastern corner of the map (southern Indiana and southeastern Illinois). Salem Limestone at the center of the Illinois Basin contains approximately 10% to 20% grainstone. The equation approximating the general distribution of grainstone fractions (percentages divided by 100) is of the -NWSE form:

$$G/T = 0.1 + 0.002222(0.9063N - 0.4226E) \quad (19)$$

where G is the thickness of grainstone, and T is the total thickness of the Salem Limestone at a given point.

Packstone Fraction

As in the case of the grainstone fraction, contours of the packstone fraction in the Salem Limestone exhibit convolutions, and even localized peaks and troughs. These cannot be reasonably interpreted on the basis of the low density of data points (Figure 51) and a simplification of

Figure 51.

Contour map showing distribution of packstone as a percentage of the total stratigraphic section of the Salem Limestone in the Illinois Basin. Dashed lines represent Equation 20.

PERCENT PACKSTONE IN SALEM LS

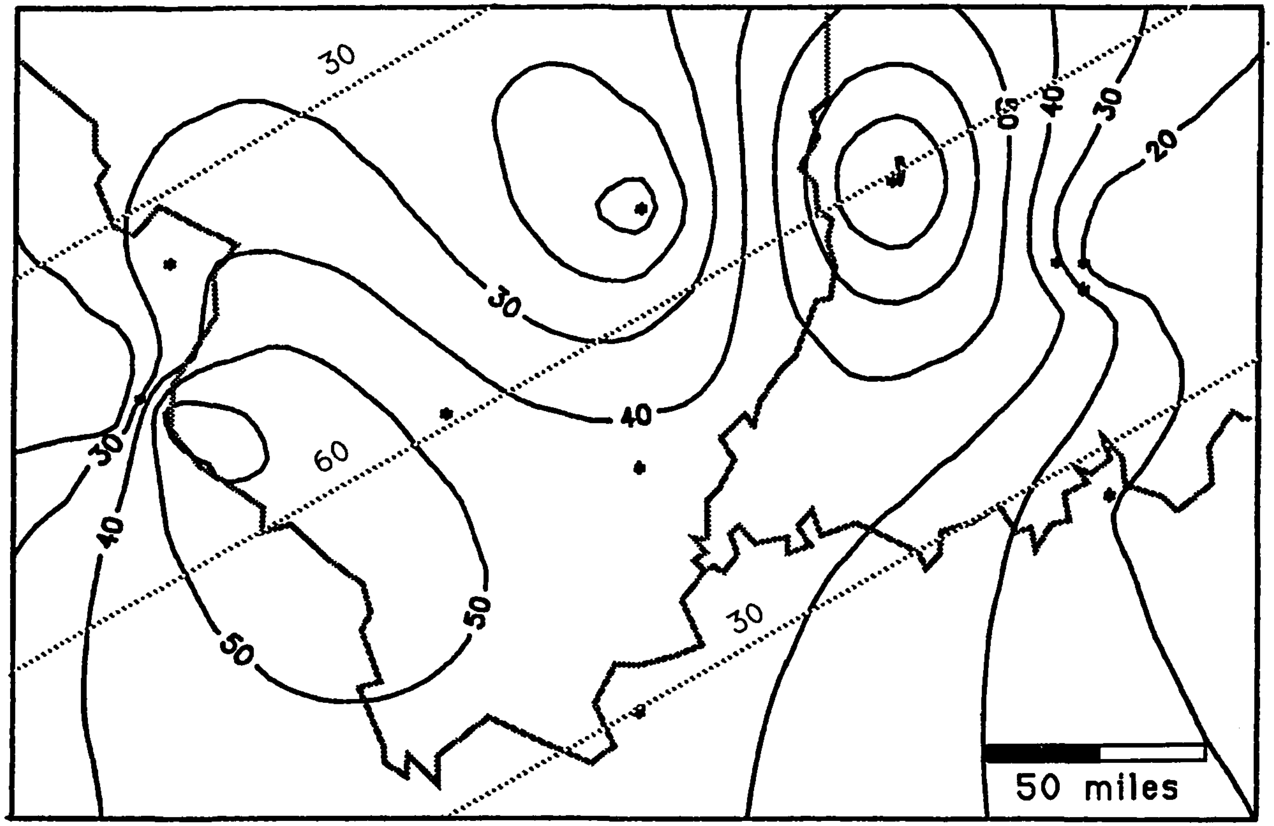

the contour pattern is assumed for comparison with other lithofacies fractions and other parameters. The contours are taken to represent a NE-SE trending pattern, with the inclination of the trend defined by the alignment of minor peaks. The angle described by the EW axis and the generalized contour trend is 30 degrees.

Since the trend is defined by an alignment of minor peaks and troughs, a line roughly connecting the peaks is an axis of symmetry, with values of packstone percentage increasing toward this axis. Along the axis, the percentage of packstone is roughly 60%, and it decreases to 20% or less toward the NW and SE corners of the study area.

The equation describing the generalized distribution of the packstone <u>fractions</u> (percentages divided by 100) has the +/-NWSE form:

$$P/T = 0.6 - 0.006|0.577N - 0.333E - 20.785| \quad (20)$$

in which $\underline{P}$ is the thickness of packstone, and $\underline{T}$ is the total thickness of the Salem Limestone, in feet.

<u>Wackestone-Micstone Fraction</u>

Contours of Wackestone-Micstone percentages within the

Salem Limestone across the Illinois Basin, too, are somewhat convolute, but they can be easily simplified as a NE-SE trending pattern (Figure 52). The inclination of this trend relative to the EW axis is 25 degrees.

The percentage of wackestone-micstone increases southeastward, reaching 80% near the southeast corner of the map, including southern Indiana, and diminishing to 10% toward the northwest, including St. Louis.

The equation approximating the wackestone-micstone fraction across the basin has a +NWSE form:

$$W/T = 0.4 - 0.00444(0.9063N - 0.4226E) \qquad (21)$$

where $\underline{W}$ and $\underline{T}$ are the thicknesses of wackestone-micstone, and the complete Salem Limestone, respectively.

Dolostone Fraction

Although the contours of dolostone percentage across the Illinois Basin exhibit a pronounced peak near Bedford, Indiana, the overall pattern conforms approximately to a NE-SW trend at an angle of 30 degrees with the EW axis (Figure 53).

Figure 52.

Contour map showing distribution of wackestone-micstone as a percentage of the total stratigraphic section of the Salem Limestone, Illinois Basin. Dashed lines represent Equation 21.

PERCENT WACKESTONE–MICSTONE IN SALEM LS

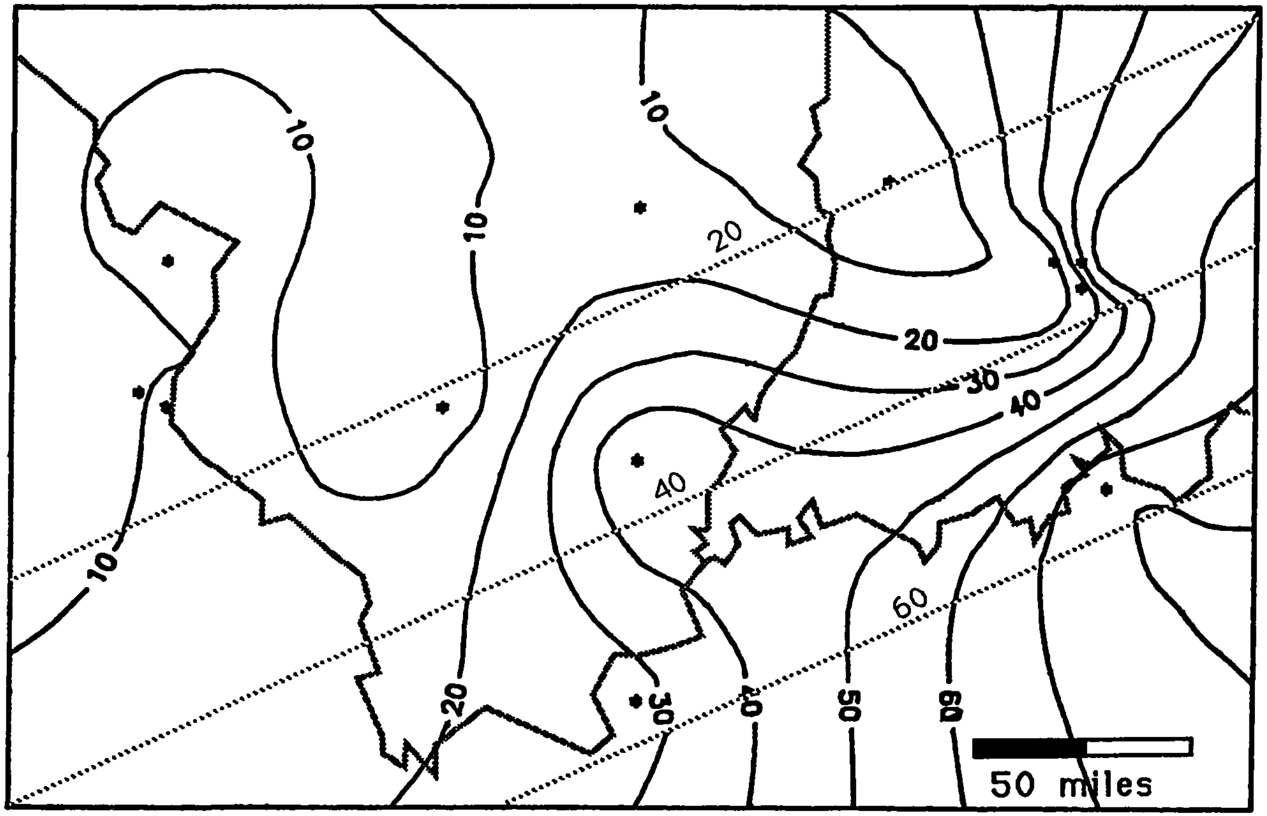

Figure 53.

Contour map of the distribution of dolostone as a percentage of the total stratigraphic section of the Salem Limestone in the Illinois Basin. Dashed lines represent Equation 22.

PERCENT DOLOSTONE IN SALEM LS

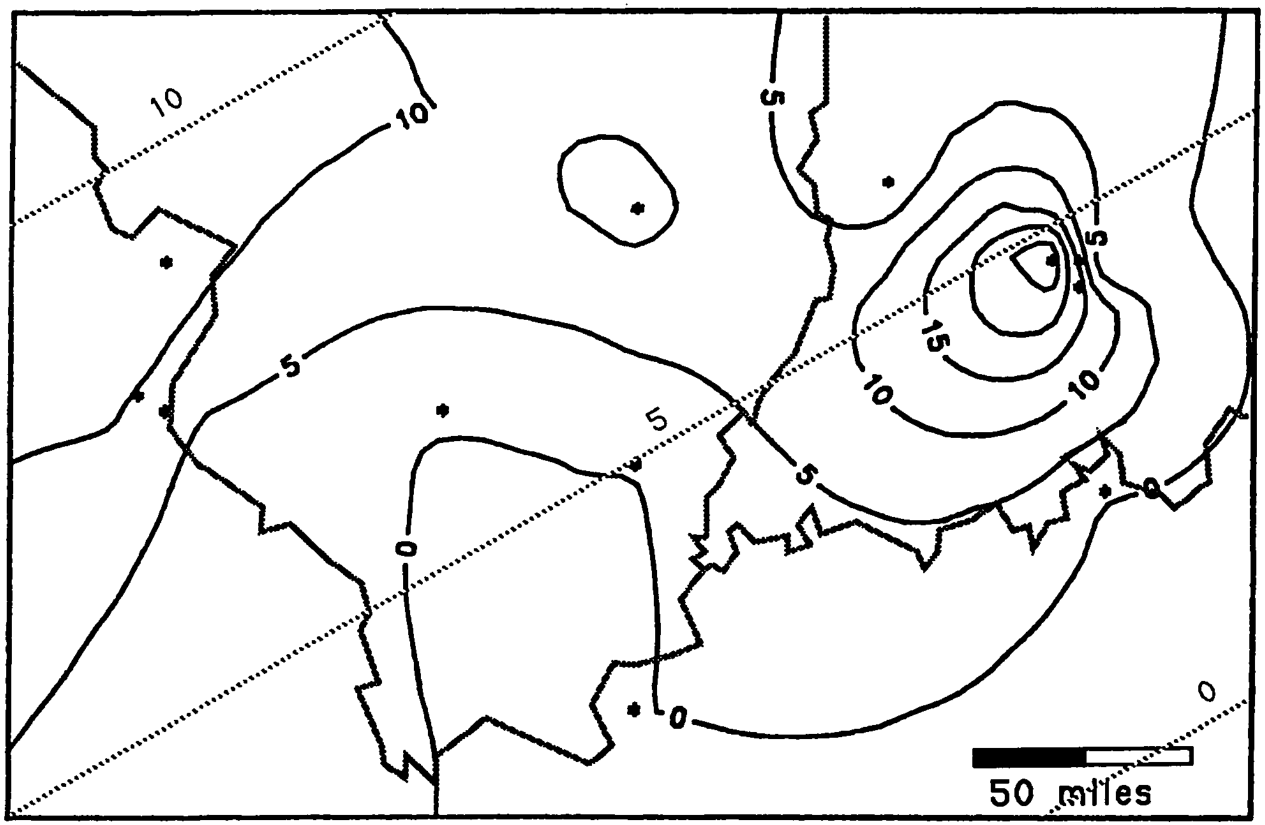

The percentage of dolostone approximately equals the percentage of wackestone-micstone in the northwest corner of the map (about 10%) but decreases toward the southeast, approaching 0% in southern Indiana and southeastern Illinois.

The equation representing the approximate distribution of the dolostone fraction across the Illinois Basin has the -NWSE form:

$$D/T = 0.05 + 0.000444(0.866N - 0.5E) \qquad (22)$$

where D and T are thicknesses of dolostone and total rock.

C. Stylolite Densities

Stylolite densities are measured in terms of the average number of stylolites per foot of the lithofacies of interest.

Stylolite Density in Grainstone

Except for a few minor variations, the contours of stylolite density in grainstone across the basin generally define an EW trend (Figure 54). There is an axis of symmetry lying just south of St. Louis, Missouri, in the west, and

Figure 54.

Contour map of stylolite densities (stylolite count per foot of rock) in grainstone in the Salem Limestone, Illinois Basin.

STYLOLITES PER FOOT OF GRAINSTONE

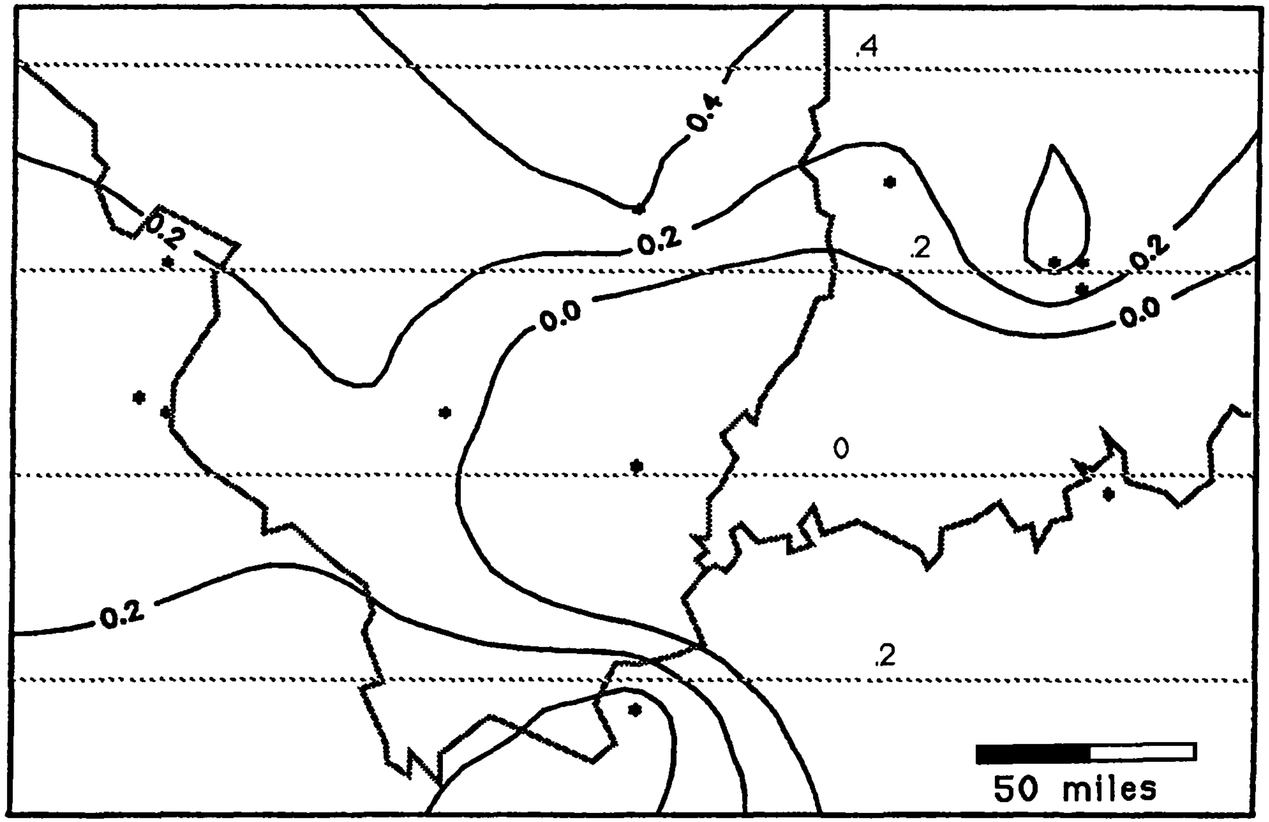

just north of the southern border of Indiana in the east. The axis roughly passes through the center of the Illinois Basin.

Stylolite densities are highest in the the northern and southern portions of the study area, where they attain values of 0.4 stylolites per foot of rock. In the basin center, along the axis of symmetry of the contour pattern, stylolite density approaches 0.0 (zero).

The equation approximating the distribution of stylolite densities within grainstone across the Illinois Basin has a -/+NS form:

$$S/G = 0.006667|0.67N-50| \qquad (23)$$

in which $\underline{S}$ is the number of stylolites, and $\underline{G}$ is the thickness of grainstone.

Stylolite Density in Packstone

Contours representing stylolite density in packstone across the Illinois Basin resemble an elongate trough with a NS-trending long axis (Figure 55). The center of the trough roughly coincides with the center of the Illinois Basin.

Stylolite density in packstone reaches maximum values

Figure 55.

Contour map of stylolite density (stylolite count per foot of rock) in packstone in the Salem Limestone, Illinois Basin.

STYLOLITES PER FOOT OF PACKSTONE

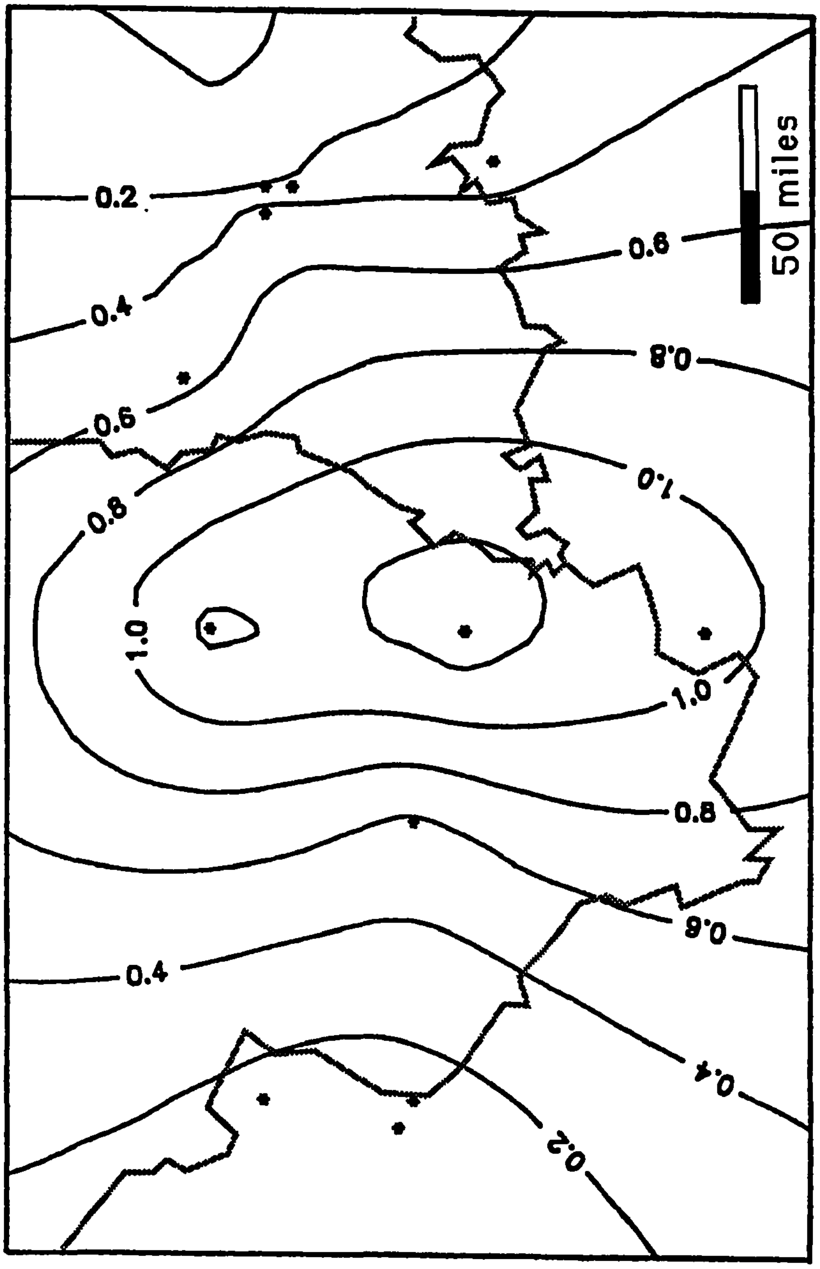

in the center of the basin, and in regions just north and south of the basin center. In those regions, there are up to 1.2 stylolites per foot of packstone. Toward the eastern and western margins of the Illinois Basin, stylolite densities in packstone diminish to values of 0.2 or less.

The equation approximately describing the approximate distribution of stylolite densities in packstone across the basin constitutes the sum of two trends: a radial (+C) trend, and a linear, +/-EW trend:

$$S/P = 1.2993 - 0.0029|0.67E - 90| - 0.0102((0.67N - 65)^2 + (0.67E - 90)^2)^{0.5} \quad (24)$$

where S is the stylolite count and P is packstone thickness, in feet.

Stylolite Density in Wackestone-Micstone

The contour map of stylolite densities within wackestones and micstone reveals a random scattering of values across the Illinois Basin (Figure 56). This may largely be due to the general lack of stylolite data in those lithofacies. Therefore no equation has been written to represent a systematic pattern.

Figure 56.

Contour map of stylolite density (stylolite count per foot of rock) in wackestone-micstone in the Salem Limestone, Illinois Basin.

STYLOLITES PER FOOT OF WACKESTONE–MICSTONE

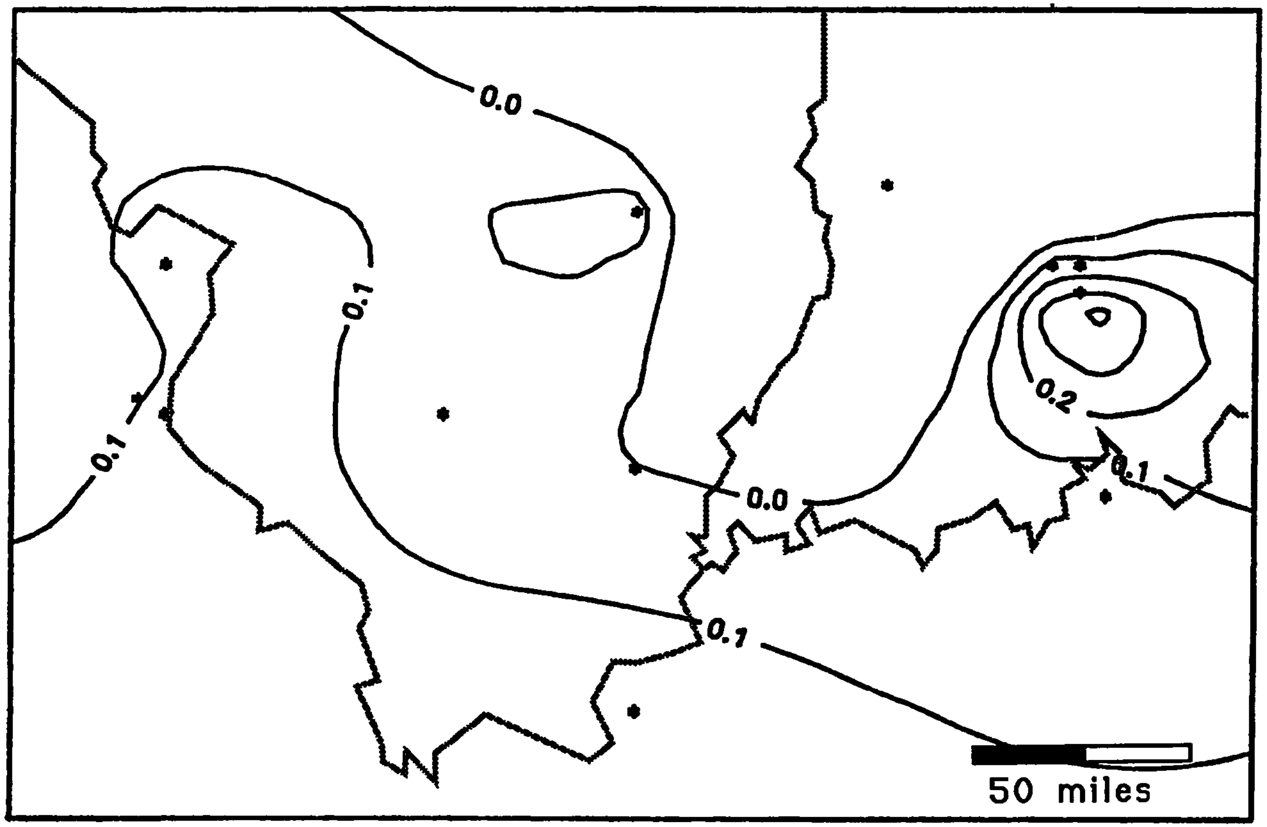

Stylolite Density in Dolostone

Stylolite densities in dolostone also exhibit a random distribution (Figure 57). As in the case of stylolite density distributions in wackestone-micstone, this nonsystematic pattern may reflect the paucity of data for dolostone.

D. Hummocky Seam Densities

Hummocky seam densities are analogous to stylolite densities. They are measured in terms of the average number of hummocky seams per foot of the lithofacies of interest.

Hummocky Seam Density in Grainstone

Density contours for hummocky seams in grainstone throughout the Illinois Basin trend NE-SW, defining an angle of 30 degrees with the EW axis (Figure 58). Hummocky seam densities are highest in the northwestern corner of the study area, including the region just north of St. Louis, Missouri. There, hummocky seam densities attain 0.4 hummocky seams per foot of grainstone. The zero contour runs across the middle of the map, intersecting the center of the basin, as well as Bedford, Indiana. Grainstones are rare in the southeastern part of the study area, and where they exist,

Figure 57.

Contour map of stylolite density (stylolite count per foot of rock) in dolostone in the Salem Limestone, Illinois Basin.

STYLOLITES PER FOOT OF DOLOSTONE

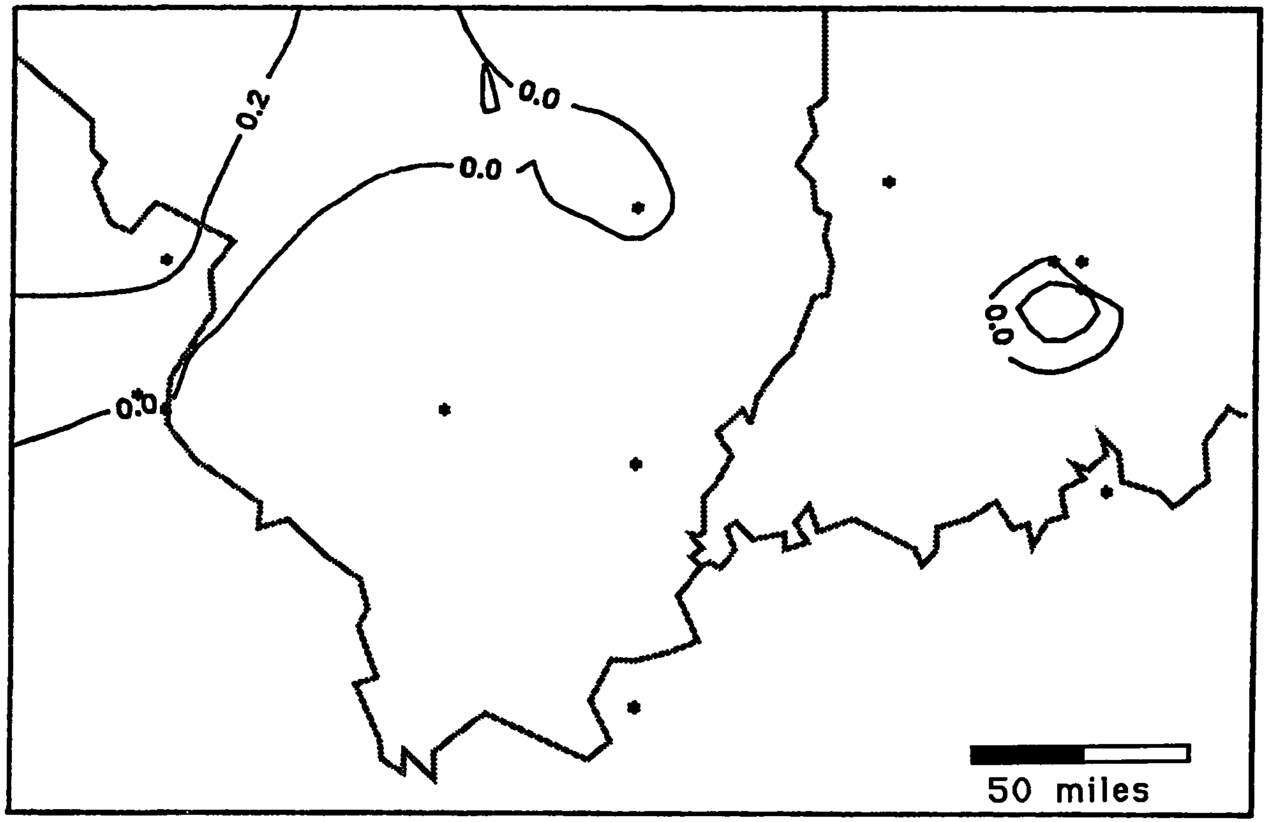

Figure 58.

Contour map of hummocky seam density (hummocky seam count per foot of rock) in grainstone in the Salem Limestone, Illinois Basin.

HUMMOCKY SEAMS PER FOOT OF GRAINSTONE

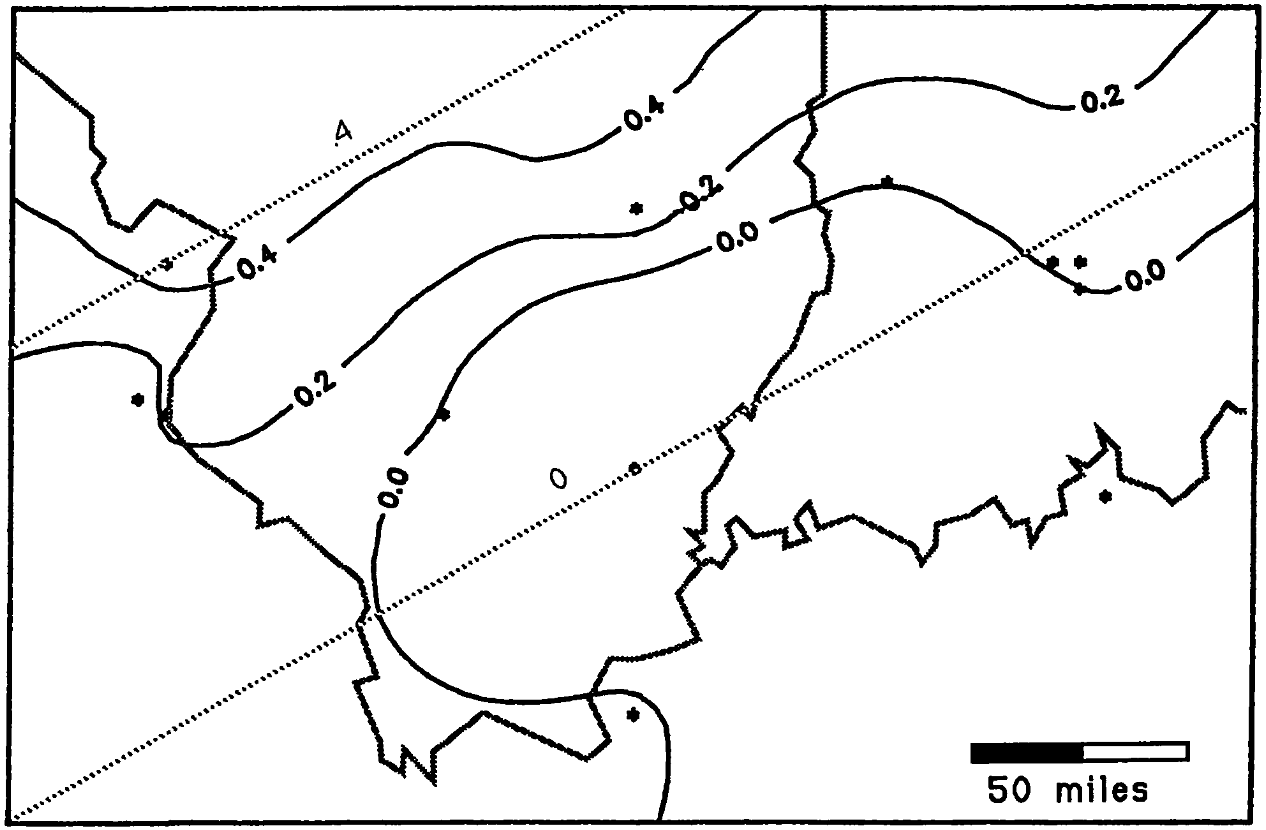

hummocky seams were not recognized.

The equation describing the general trend of hummocky seam densities in grainstone is of the -NWSE form:

$$H/G = 0.00444|0.866N - 0.5E| \quad (25)$$

in which H is the number of hummocky seams, and G is the number of feet of grainstone.

Hummocky Seam Density in Packstone

Contours of hummocky seams densities in packstone define a roughly elliptical trend across the Illinois Basin (Figure 59). The major axis of the ellipse trends EW, intersecting the center of the basin. The minor axis, trending NS, is offset slightly to the east, intersecting halfway between the center of the basin and the eastern rim, at Bedford, Indiana.

Hummocky seam densities are zero at the center of the ellipse, and they increase outward to 0.4 hummocky seams per foot, especially in the vicinity of St. Louis, Missouri.

The equation approximating the contour shapes reflects the combined influence of a radial trend, increasing

Figure 59.

Contour map of hummocky seam density (hummocky seam count per foot of rock) in packstone in the Salem Limestone, Illinois Basin.

HUMMOCKY SEAMS PER FOOT OF PACKSTONE

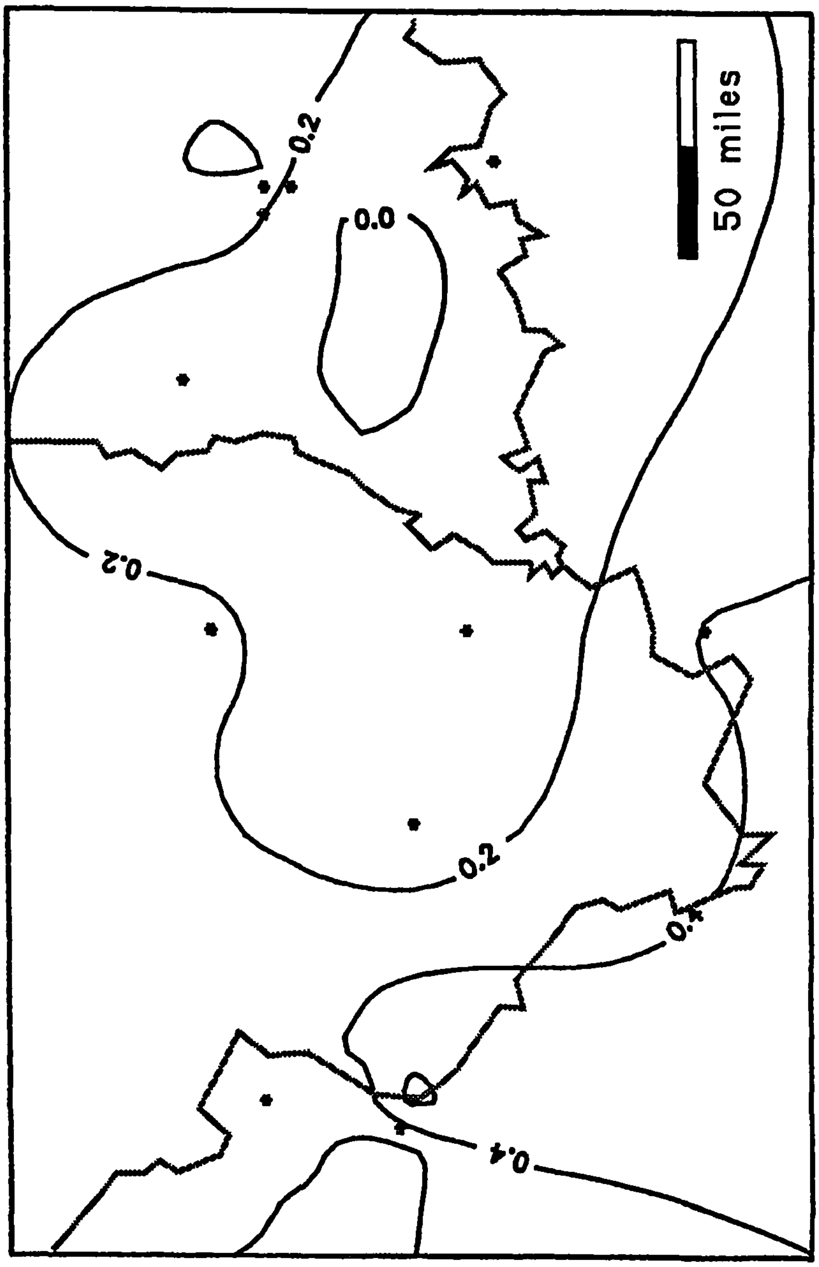

outwards (-C), and a linear, EW trend, increasing northward and southward of the axis of symmetry (-/+NS):

$$H/P = 0.0014|0.67N - 65| + 0.0026((0.67N - 65)^2 + (0.67E - 130)^2)^{0.5} \quad (26)$$

in which _H_ is the hummocky seam count, and _P_ is the thickness of packstone, in feet.

Hummocky Seam Density in Wackestone-Micstone

Although the contours representing hummocky seam density in wackestone-micstone lithofacies across the Illinois Basin (Figure 60) appear somewhat convolute at first glance, a general, NE-SW trend is reflected by the alignment of local maxima along an axis of symmetry, inclined 30 degrees to the EW axis. Hummocky seam densities are highest along this axis, attaining up to 1.0 hummocky seams per foot of wackestone-micstone. The axis of symmetry intersects St. Louis, Missouri, and it cuts northward of the center of the basin. Away from the axis, hummocky seam densities diminish to zero, in west central Illinois and in southern and even central Indiana.

The equation generalizing the contour trend for hummocky seam densities in packstone is of the +/-NWSE form:

Figure 60.

Contour map of hummocky seam density (hummocky seam count per foot of rock) in wackestone-micstone in the Salem Limestone, Illinois Basin.

HUMMOCKY SEAMS PER FOOT OF WACKESTONE—MICSTONE

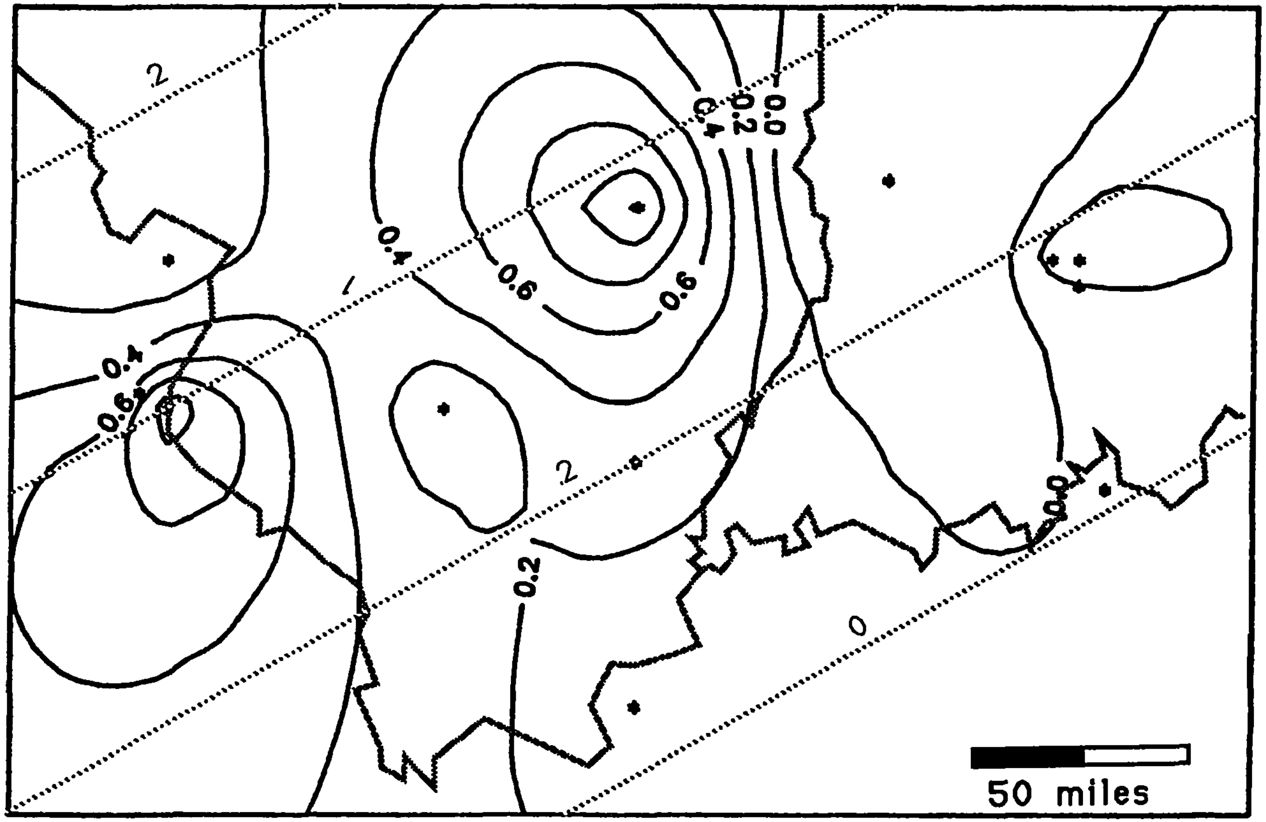

$$H/W = 1.0 + 0.025|0.577N - 0.333E - 45| \quad (27)$$

in which H is the hummocky seam count and W is the thickness of wackestone and micstone, in feet.

Hummocky Seam Density in Dolostone

The distribution of data points for hummocky seamdensities in dolostone across the Illinois Basin may be considered random, with no equation to describe it (Figure 61).

E. Cummulative Stylolite Relief

Cummulative stylolite relief is a measure of the average, cummulative height of stylolite columns per foot of a given lithotype. It is the sum of the average column heights of all stylolites in a lithotype, divided by the thickness of that lithotype, in feet.

Mixed units are used in measuring this parameter. Just as it is standard practice to measure mesoscopic and microscopic features such as stylolite column heights in mm, it is also standard practice to measure thicknesses and depths of rock formations in the Illinois Basin in feet,

Figure 61.

Contour map of hummocky seam densities (hummocky seam count per foot of rock) in dolostone in the Salem Limestone, Illinois Basin.

HUMMOCKY SEAMS PER FOOT OF DOLOSTONE

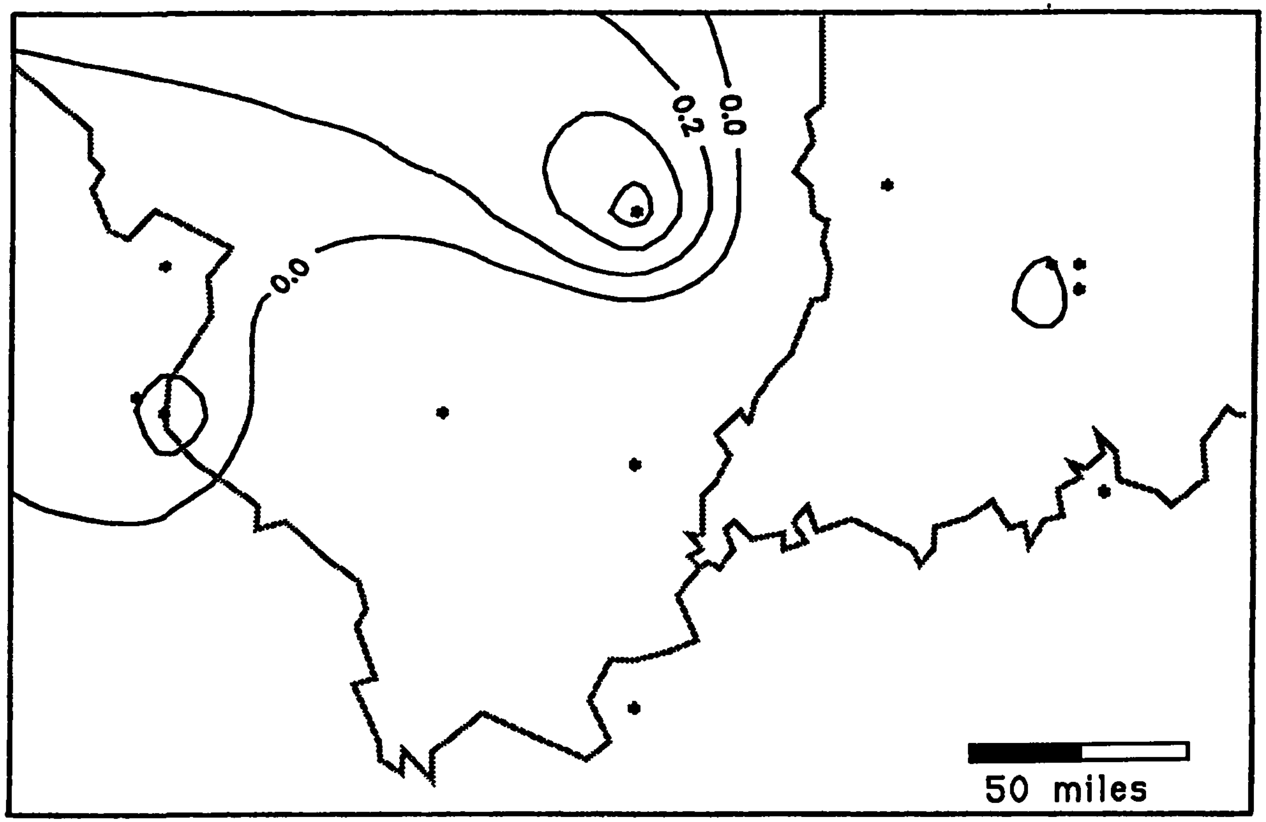

because all of the published data, including electric logs, contour maps, and the like, are measured in feet. Thus, the cummulative stylolite relief measured in terms of mm of stylolite column height, divided by feet of rock.

Stylolite Relief Per Foot Grainstone

Contours of cummulative stylolite relief in grainstone generally suggest an EW trend, with an axis of symmetry intersecting the center of the Illinois Basin (Figure 62). Along this axis, maximum values of cummulative stylolite relief of 4 mm per foot of grainstone are attained. North and south of the axis, cummulative stylolite relief diminishes to zero. There are minor deviations from this trend, notably in the northwest corner of the study area.

The equation generalizing the contour trends for cummulative stylolite relief across the basin has +/-NS form:

$$R/G = 4 - 0.08|0.67N - 75| \qquad (28)$$

in which R is the cummulative stylolite relief, or cummulative average column height, in mm, in grainstone, and G is the thickness of grainstone, in feet.

Figure 62.

Contour map of cummulative stylolite column height (stylolite relief) in grainstone in the Salem Limestone, Illinois Basin.

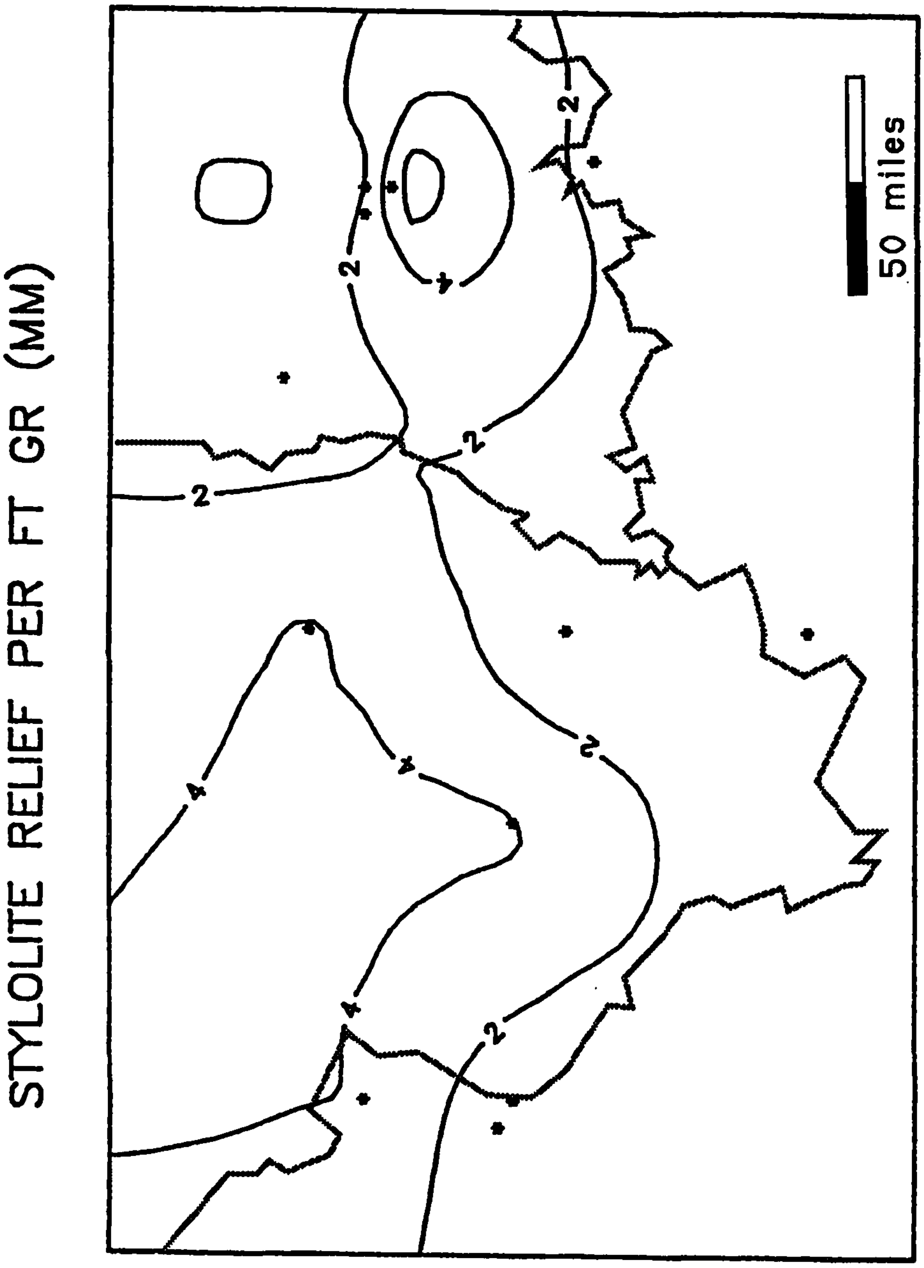
STYLOLITE RELIEF PER FT GR (MM)
2
4
50 miles

Stylolite Relief Per Foot Packstone

Contours of cummulative stylolite relief if packstone generally define an elliptical shape (Figure 63), with major axis oriented NS and intersecting the center of the Illinois Basin, and with minor axis, running EW, cutting north of the center of the basin, and north of both St. Louis, Missouri, and Bedford, Indiana. Maximum values of over 12 mm per foot of packstone occur just north of the center of the basin, and diminish outward from that point, down to values of 0 to 2 mm per foot along the eastern and western margins of the basin.

The equation describing the contour configuration for cummulative stylolite relief in packstone has the radial form (+C):

$$R/P = 12.9055 - 0.1022((0.67N - 85)^2 + (0.67E - 90)^2)^{0.5} \qquad (29)$$

in which $\underline{R}$ is the cummulative stylolite relief in packstone, in mm, and $\underline{P}$ is the thickness of packstone, in feet.

Stylolite Relief Per Foot Wackestone-Micstone

Despite the paucity of data, a general, NE-SW trend is

Figure 63.

Contour map of cummulative stylolite column height (stylolite relief) in packstone in Salem Limestone, Illinois Basin.

STYLOLITE RELIEF PER FT PK (MM)

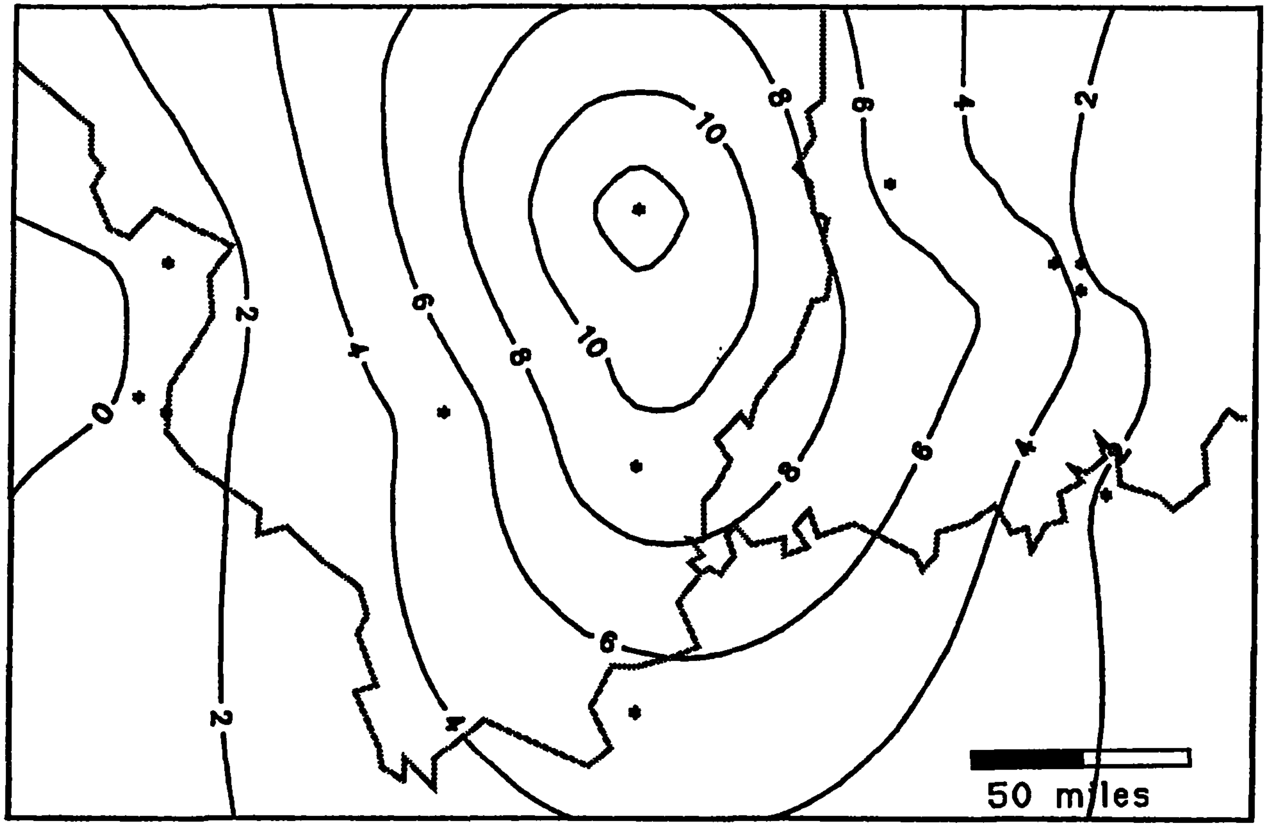

evident in the contours of cummulative stylolite relief in wackestone-micstone (Figure 64). The zero values dominate southeastward of an axis inclined 30 degrees to the EW direction, and intersecting St. Louis, Missouri. Northwestward of the zero axis, values increase until a maximum of 12 mm per foot is reached.

The region southeast of the zero axis, covering over half of the study area, is characterized by a random scattering of zero values and low, nonzero values. Equation (29) does not apply in that region.

Stylolite Relief Per Foot Dolostone

Although data for cummulative stylolite relief in dolostone are scarce, a basinwide, NE-SW contour trend is evident (Figure 65). An axis of symmetry, along which the value of cummulative stylolite relief per foot is zero, intersects the center of the Illinois Basin, and is inclined to the EW axis by 30 degrees. Away from this axis, values approach up to 2 mm per foot.

The equation generalizing the contour pattern across the basin has the -/+NWSE form:

$$R/D = 0.0222|0.766N - 0.6428E| \qquad (30)$$

Figure 64.

Contour map of cummulative stylolite column height (stylolite relief) in wackestone-micstone in the Salem Limestone, Illinois Basin.

STYLOLITE RELIEF PER FT WK–MC (MM)

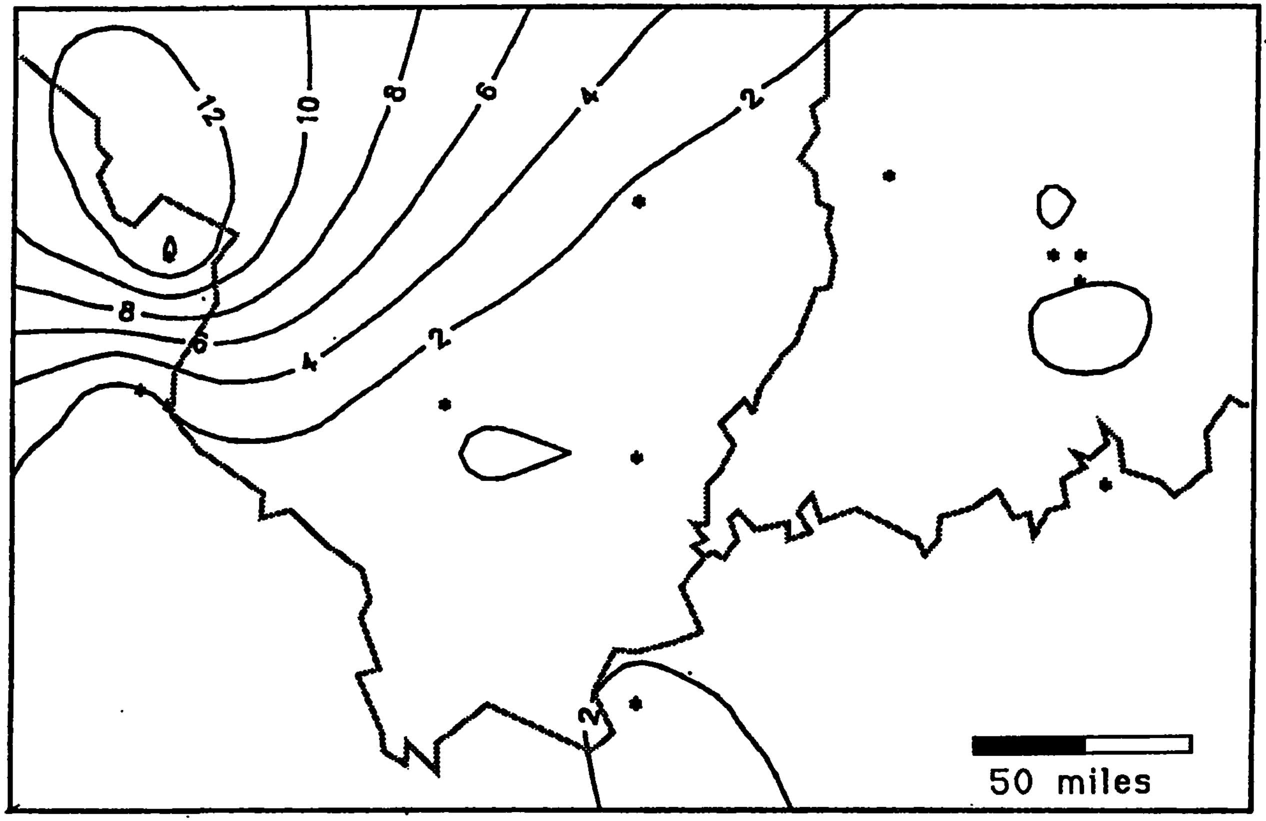

Figure 65.

Contour map of cummulative stylolite column height (stylolite relief) in dolostone in the Salem Limestone, Illinois Basin.

STYLOLITE RELIEF PER FT DOL (MM)

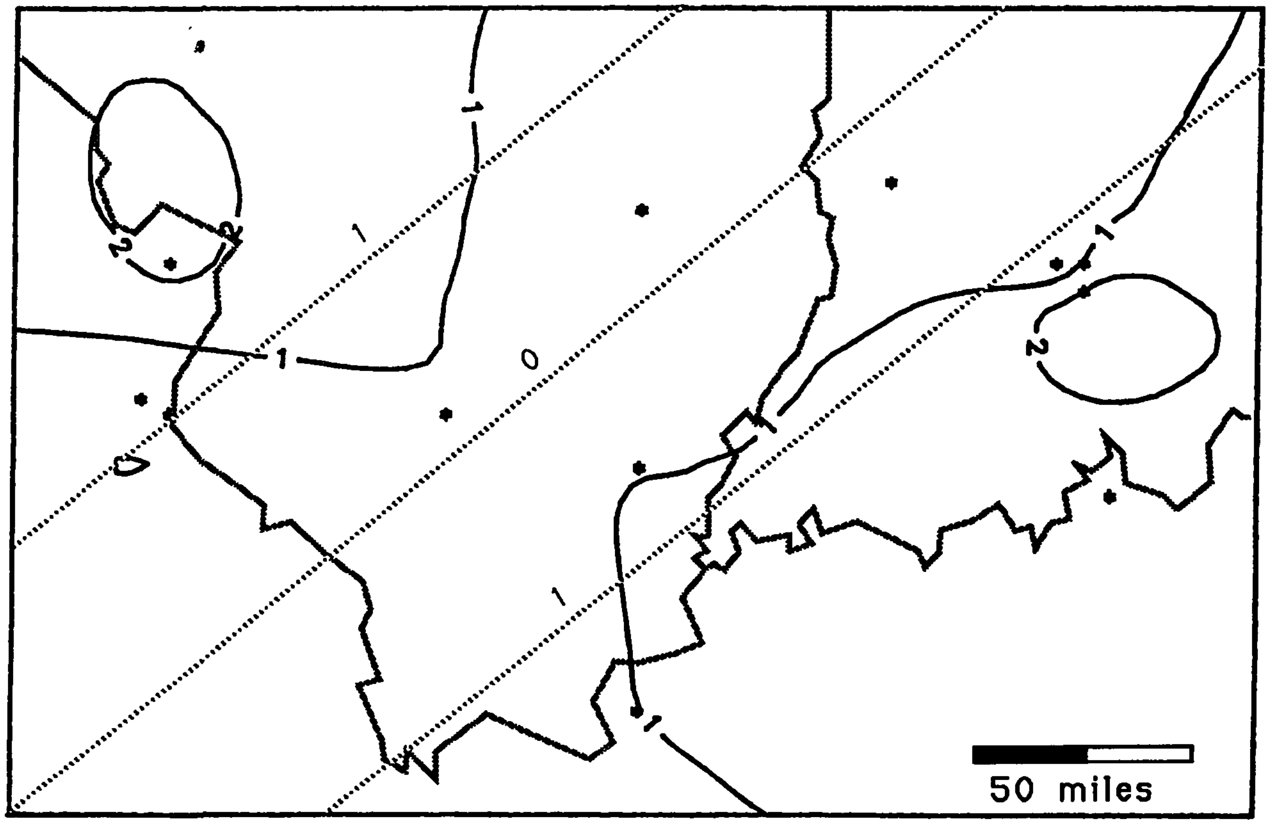

in which R is the cummulative stylolite relief, and D is the thickness of dolostone, in feet.

F. Average Stylolite Relief

Average stylolite relief is a measure of the average column height of stylolites in a particular lithofacies. As in the case of cummulative stylolite relief, column height is measured in mm. This number is divided by the total number of stylolites in the lithofacies in question.

Average Stylolite Relief in Grainstone

Contours of average stylolite relief in grainstone form several, local maxima and minima in various parts of the Illinois Basin, but the overall trend is NE-SW, inclined to the EW axis by 30 degrees (Figure 66). Average stylolite relief is zero in the southeastern corner of the study area, in southern Indiana, and it increases to 20 mm in the northwestern corner, north of St. Louis, Missouri. A local high of 20 mm occurs in Bedford, Indiana.

The equation generalizing the contour trend for average stylolite relief in grainstone across the Illinois Basin has the -NWSE form:

Figure 66.

Contour map of average stylolite column height (stylolite relief) in grainstone in the Salem Limestone, Illinois Basin.

AVE. STYLOLITE RELIEF IN GR (MM)

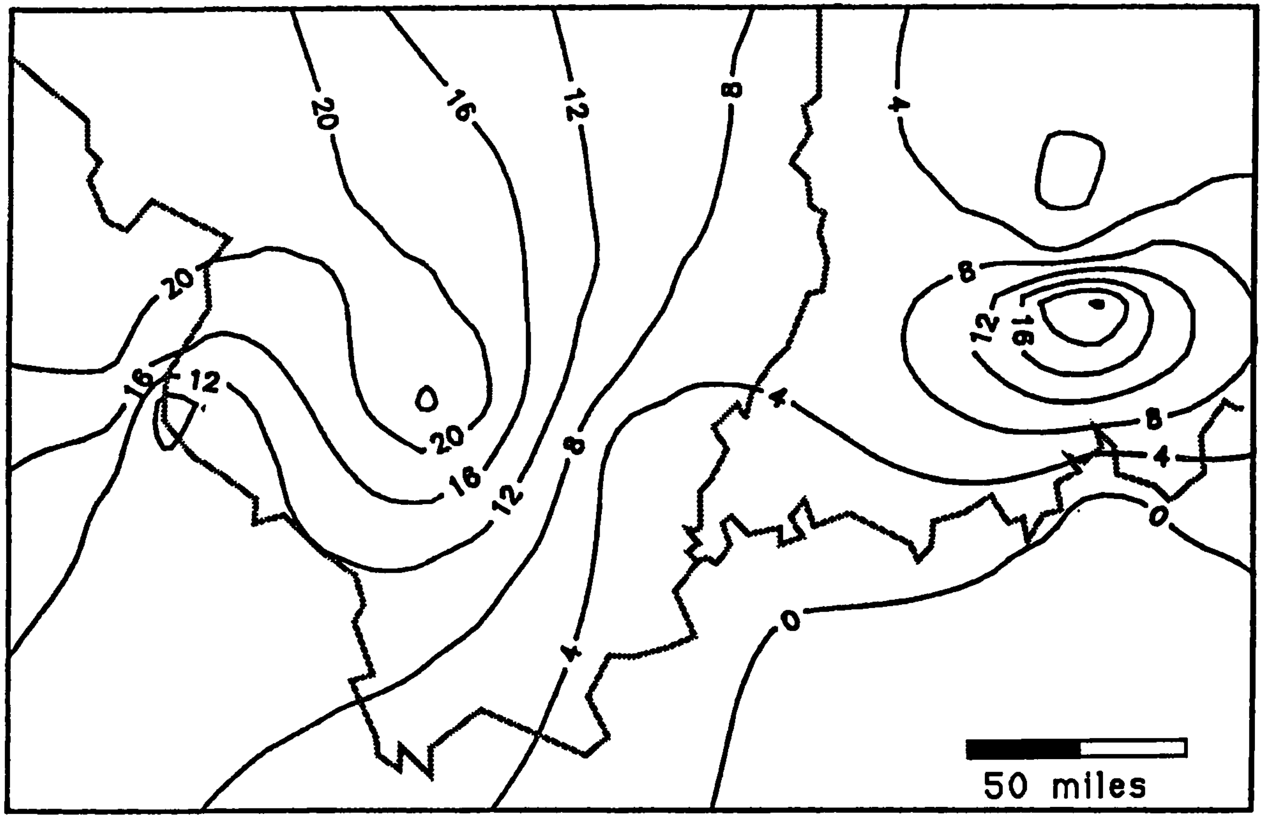

$$(R/S)_G = 8 + 0.267(0.866N - 0.5E) \qquad (31)$$

in which $(R/S)_G$ is the sum of average column heights of all stylolites in grainstone, divided by the total number of stylolites in grainstone.

Average Stylolite Relief in Packstone

Contours of average stylolite relief in packstone define an elliptical shape, with major and minor axes, trending NS and EW respectively, intersecting roughly at the center of the Illinois basin (Figure 67). Average stylolite relief is highest at the center of the basin, where it approaches 12 mm, and it diminishes to 4 mm, or even zero, at the eastern and western margins of the basin.

The equation describing the contours combines the radial form, +C, with the +/-NS form:

$$(R/S)_P = 11.0229 - 0.1870|0.67N - 65| - 0.0010((0.67N - 65)^2 + (0.67E - 90)^2)^{0.5} \qquad (32)$$

in which $(R/S)_P$ is the cummulative relief of stylolites divided by the total number of stylolites, in packstone.

Figure 67.

Contour map of average stylolite column height (stylolite relief) in packstone in the Salem Limestone, Illinois Basin.

AVE. STYLOLITE RELIEF IN PK (MM)

Average Stylolite Relief in Wackestone-Micstone

Contours of average stylolite relief in wackestone and micstone trend NE-SW across the Illinois Basin, defining an angle of 35 degrees with the EW axis (Figure 68). The symmetry axis, along which values are zero, cuts through the center of the Illinois Basin, and north of Bedford, Indiana. Average stylolite relief in packstone approaches 36 mm to 48 mm, in southern Indiana and west central Illinois, north of St. Louis.

The equation approximating the contour configuration has the -/+NWSE form:

$$(R/S)_W = 0.444|0.8192N - 0.5736E| \qquad (33)$$

in which $\underline{(R/S)_W}$ is the cummulative column height divided by the number of stylolites, in wackestone-micstone.

Average Stylolite Relief in Dolostone

Contours of average stylolite relief in dolostone indicate zero values across most of the basin, and values increasing northwestward of a NE-SW trending axis (the zero axis) intersecting St. Louis, Missouri, and inclined by 32 degrees to the EW axis (Figure 69). Average stylolite relief

Figure 68.

Contour map of average stylolite column height (stylolite relief) in wackestone-micstone in the Salem Limestone, Illinois Basin.

AVE. STYLOLITE RELIEF IN WK–MC (MM)

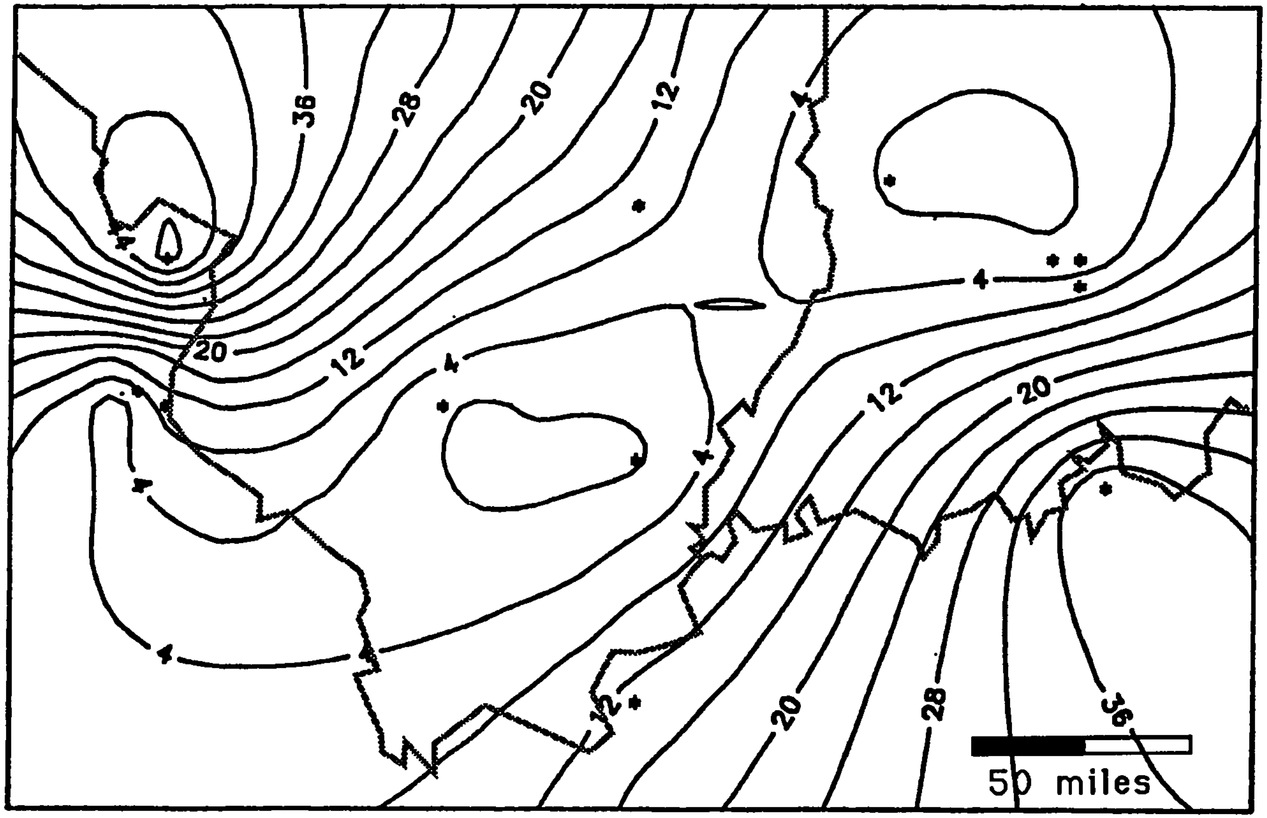

Figure 69.

Contour map of average stylolite column height (stylolite relief) in dolostone in the Salem Limestone, Illinois Basin.

AVE. STYLOLITE RELIEF IN DOL (MM)

in dolostone approaches a maximum of 8 mm, north of St. Louis.

An equation with the form of -NWSE is valid only in the region northwest of the zero axis, defined above:

$$(R/S)_D = -4.7236 + 0.1164(N - 0.6369E) \qquad (34)$$

in which $(R/S)_D$ is the cummulative column height divided by the number of stylolites in dolostone.

Alternatively, the distribution of data points for average stylolite relief in dolostone may be interpreted as being random, with no equation to describe it.

Summary

The general configuration of contours for various stylolite parameters follows one or two patterns within each lithofacies.

In grainstone, stylolite parameter contours trend either EW, or NE-SW. Hummocky seam density and average stylolite relief contours trend NE-SW, increasing northwestward. Stylolite density and cummulative relief contours trend EW, with an axis of symmetry cutting across the center of the Illinois Basin. Stylolite density increases away from the the axis ofsymmetry, whereas cummulative relief increases toward the axis.

In packstone, stylolite parameter contours follow a radial trend, generally centered around the center of the Illinois Basin, combined with a linear trend, which elongates the contours in either the NS or EW directions. Hummocky seam density and average stylolite relief both include an EW linear trend. Hummocky seam density contours define a trough elongated in the EW direction, whereas average stylolite relief contours define a dome elongated in the EW direction. Stylolite densities and cummulative relief contours define domes elongated in the NS direction.

In wackestone-micstone, stylolite parameter contours follow a NE-SW trend. Hummocky seam density and average stylolite relief contours include a NE-SW trending axis of symmetry, which roughly cuts across the center of the Illinois Basin. Hummocky seam densities increase toward the axis of symmetry, whereas average stylolite relief increases away from the axis of symmetry. Cummulative stylolite relief contours follow a NE-SW trend, but have no axis of symmetry, and values increase southeastward.

In dolostone, stylolite parameter contours define a NE-

SW trend, across all or part of the Illinois Basin. In parts of the basin, data distribution is random. Hummocky seam densities and average stylolite relief are zero throughout most of the study area, but increase northwestward of a NE-SW axis intersecting St. Louis, Missouri. Cummulative stylolite relief increases away from a NE-SW axis that roughly cuts across the center of the Illinois Basin.

The most important conclusion to be gleaned from these data is that only stylolites in packstone exhibit sensitivity to burial depth. Stylolite density, average relief, and cummulative relief all increase toward the basin center. Hummocky seam density, on the other hand, decreases toward the basin center, suggesting that the increase in stylolite density with depth occurs at the expense of hummocky seam density. This supports the hypothesis that stylolites form along preexisting hummocky seams. Increased horizontal permeability, increased acidity, and increased concentration of carbon dioxide along the clay-rich, organic-rich hummocky seam are three factors which would stimulate stylolite development.

The most surprising conclusion to be drawn from these data is the insensitivity of stylolites in grainstone to burial depth. Instead, stylolites appear to be responding to regionally, geographically controlled factors. Stylolite density is highest in the northern and southern parts of the study area. Thus, a NS profile of stylolite densities across the middle of the basin would convey a misleading image of sensitivity to depth. An EW profile, on the other hand, would show no change in stylolite density from basin rim through basin trough to basin rim. Cummulative stylolite relief, on the other hand, decreases northward and southward, inversely related to the stylolite density trend. This suggests that stylolite density in the northern and southern regions of the study area increases at the expense of cummulative stylolite relief in those regions. Such an interpretation supports the hypothesis that vertical strain, or loss of stratigraphic thickness, due to stylolites in grainstone is constant throughout the basin.

Both hummocky seam densities and average stylolite relief are insensitive to basin depth, and both increase northwestward. Influx of organic material from the north to northwest would help explain the combined increases of stylolite density, average stylolite relief, and hummocky seam density northward and northwestward.

CHAPTER 7

CONCLUSIONS

This study presents a detailed, megascopic and macroscopic view of the relationships between stylolite morphology and distribution on one hand, and various sedimentary aspects of the rocks containing them, on the other hand. These factors include grain size and distribution; carbonate mineral composition; concentration and textural distribution of calcite, micrite, organic matter and clays; paleontological attributes of the host rock; and the depth of burial.

This study has shown correlations between some morphological characteristics, such as stylolite column size and stylolite column symmetry, on one hand, and sedimentary aspects, such as grain sorting and lithfacies, on the other hand. Other morphological characteristics, such as seam thickness or column cap thickness, as well as other sedimentological features, such as grain size and fossil types, reveal only weak or no correlations between stylolite morphology and host lithology.

Several general patterns emerge from the observations presented in this thesis. Stylolites develop best in poorly-sorted, organic-rich rock environments. Packstone is thus an ideal host rock. Stylolite density generally increases with depth, but the depth-sensitivity depends highly upon lithofacies. It is strongest in packstones and weak in other lithofacies. Increased stylolite density with increasing depth in packstones seems to reflect the progressive stylolitization of preexisting, organic and clay-rich seams, or "shale breaks," with progressive depth of burial.

Hummocky seams appear to represent an intermediate stage between a smooth, purely depositional "shale break," and fully disjointed, segmented stylolite, with fissures (the walls of stylolite columns) separating formerly continuous segments of a clay seam.

Physical forces and dissolution undoubtably play a role in stylolite development. The precondition for stylolite development, though, is a thin sedimentary layer rich in materials such as organic matter and clay minerals that enhance the dissolution of calcite.

Further microscopic study of stylolites in the Salem Limestone focusing on mineral recrystallization within stylolite seams, shearing mechanisms along stylolite columns walls, and microstructure within the seams and in adjacent host rock, would help quantify the relative contributions of depositional and diagenetic processes to stylolite development. Such study would require utilization of techniques such as transmission electron microscopy and cathodoluminescence.

At the megascopic scale, the quantification of stylolite and host rock distribution throughout the Illinois Basin, presented in Chapter 6, leads to some interesting conclusions about the impact of stylolites on stratigraphic thinning and porosity reduction in the Salem Limestone. Integration of the equation for the thickness of the Salem Limestone (Equation 18, Chapter 6) over the area of the Illinois Basin yields a total volume of approximately 122 trillion cubic feet of rock.

The total thickness of each lithofacies equals the product of the function representing the lithofacies fraction (Equations 19-22, Chapter 6) and the function representing the thickness of the Salem Limestone. Integration of the total thickness of each lithofacies over the area of the Illinois Basin yields the volume of each lithofacies within the Salem Limestone. Thus, the calculated volume of grainstone is 10.1 trillion cubic feet; the volume of packstone is 16.9 trillion cubic feet; the volume of wackestone-micstone is 51.9 trillion cubic feet; and the volume of dolostone is 5.04 trillion cubic feet. The total of these four volumes is 83.9 trillion cubic feet. Appendix

C presents these calculations.

Compared to the volume of the Salem Limestone calculated from the equation of the total thickness of the Salem, 122 trillion cubic feet, the total of the four lithofacies volumes presents a difference of 31%. Since no other lithofacies were recognized in the Salem Limestone, 31% constitutes the magnitude of error in the preceding volume calculations.

Stylolite relief offers a measure of rock removal by dissolution along the stylolites, especially in grainstone and packstone, where stylolite caps are thin and hummocky seams are sparse. The volume of rock removed along stylolites in grainstone is calculated by integrating, over the area of the Illinois Basin, a function which is the product of the stylolite relief per unit thickness of grainstone, the grainstone fraction, and the thickness of the Salem Limestone (Equations 28, 19, and 18, Chapter 6). This integration yields a volume of 84 billion cubic feet of grainstone removed (Appendix C). Dissolution along stylolites in grainstone hence removed only 0.82% of the original grainstone volume.

A similar calculation for packstone, using Equations 29, 20, and 18 in Chapter 6, reveals a volume 882 billion cubic feet of packstone lost along stylolites (Appendix C). This represents 5.0% of the original packstone volume.

The original porosity of grainstone and packstone probably ranged from 20% to 50%. Current, post-diagenetic porosities are approximately 2% to 10% in the Salem Limestone (Lamborg, 1986), indicating porosity loss of about 20% to 40%. Rock dissolved along stylolites therefore constitutes only about 2% to 25% of the source of intergranular cement.

Although stylolites appear to have had a limited effect on the entire Salem Limestone, their influence on porosity within zones of high stylolite density may have been significant. Geochemical studies tracing the flow paths of cement material would help characterize the zone of stylolite-related cementation adjacent to an individual stylolite or stylolite zone.

Stylolites are part of the interactive set of lithologic and geochemical properties that define a sedimentary facies and determine its dynamic evolution, from deposition to deep burial, uplift and weathering. Their recognition and characterization is part of any thorough geological investigation.

ANNOTATED BIBLIOGRAPHY

1879

Nelson, E.T., 1879, On the origin of stylolites, American Journal of Science and Arts, 3rd Series, vol. 7, p. 68.

The author describes what he believes to have been the process of stylolite development in a 50' tall river bank composed of fine sand, 2 inches to 2 feet thick, and intercalated layers of clay. The surface was covered with stylolitic columns, reaching from one clay layer to the next. During rain, water falling over the edges of exposed clay layers washed the sand vertically from beneath, so that each sand bed "presented the same projections and criveces as its covering layer of clay," which helped preserve the stylolites. The author found well-preserved stylolites in the sand talus at the foot of the hill. "The inner face of the talus was...the exact obverse of the stylolites."

1897

Marsh, O.C., 1897, The Stylinodontia, a suborder of Eocene Edentates, American Journal of Science, 4th Series, vol. 3, p. 137-147.

The author describes what he believes to be the lower molar teeth of an extinct mammal. It appears that his description is of stylolites. The "teeth" are cylindrical, inserted in deep sockets, and grew from persistent pulps. They were covered on all sides with a thin enamel. The "teeth" have peculiar, longitudinal grooves, as well as transverse growth lines. The grooves, or enamel markings, are less distinct in tow molar "teeth" than in an anterior "tooth." The "teeth" are about 2 inches long.

1904

Irving, J.D., 1904, Microscopic structure and origin of certain stylolitic structures in limestone, The American Geologist, vol. 33, p. 266-267.

The author examined stylolites in limestones of Indiana and Wyoming. Stylolites initiated along thin clay seams, and formed by interpenetration of limestone. Stylolites are independent of the amount of fossils. They were not formed by metamorphism or by weight of overburden, or by other causes that would lead to distortion or crushing of rock. They were produced while the rock was unconsolidated, soon after deposition. They formed under great pressure, in sediments soft enough to allow bending of individual stylolite columns, yet rigid enough to allow shearing of fossils. These conditions might have been met under hydrostatic pressure of water at depths of 400 to 2500 fathoms.

The term "stylolite" refers to an individual stylolite column.

1906

Weller, S., 1906, Kinderhook faunal studies, IV; The fauna of the Glen Park limestone, St. Louis Academy of Sciences Transactions, vol. 16, p. 468.

Earliest recognition of Salem Limestone as an independent stratigraphic unit in western Illinois.

1916

Tarr, W.A., 1916, Stylolites in quartzite, Science, vol. 43, no. 1119, p. 819-820.

The author describes stylolites in quartzite boulders from the Dakota Quartzite formation of Colorado. Stylolite columns are up to 2 inches long, with average length of 0.25 to 0.5 inches. Ferruginous clay coatings adorn the stylolite columns.

1918

Gordon, C.H., 1918, On the nature and origin of the stylolitic structure in Tennessee Marble, Journal of Geology, vol. 26, p. 561-568.

Stylolites in the Ordovician aged, Holston Marble formation of the Tennessee Valley are slickensided, and the sutures are approximately parallel to bedding. In places they form an interwoven network. Stylolites normal to bedding are non-columnar; they are wavy or serrated. Such stylolites are called "pressure sutures." Stylolite columns are perpendicular to bedding, even in oblique stylolites. The stylolites are believed to have formed mainly along along preexisting fracture planes.

1920

Stockdale, P.B., 1923, Solutive genesis of stylolitic structures, Pan-American Geologist, vol. 39, p. 353-365.

This paper is a synopsis of a study published in the Indiana University Studies. The author studied Mississippian aged, Harrodsburg, Salem, and Mitchell Limestone formations. The Salem Limestone is especially well suited for the study of "abundant stylolite complexities." The author refers to individual stylolite columns as "stylolites," which are up to 13 inches tall in the Salem Limestone. Clay caps and striations ("flutings") are defining features of stylolites.

Stylolite development begins with a smooth crevice, which gradually becomes undulating, then serrated, and, finally, columnar. They are formed by dissolution of calcite by groundwater saturated with carbon dioxide, which reacts to form carbonic acid. Undulation is initiated by variable resistance to dissolution, and enhanced by the increase of pressure at the crests and troughs. Supersaturation of groundwater causes mineral precipitation along sides of columns. Clay caps are insoluble residue, and their thicknesses are proportional to the length of the columns, and hence, to the amount of dissolution. Limestone purity also affects clay cap thickness.

Evidence for stylolite formation in lithified sediments includes sharply cut laminae, fossils, and crystals; identical lithology within and around stylolite columns; striated mineral coatings alons sides of columns; stylolites are not intercemented; and vertical columns even in stylolite seams following inclined beds.

Evidence that clay caps are insoluble residue includes identical mineral proportions in cap and host rock; cap thickness proportional to column length; cap thickness proportional to limestone purity; and corroded fossil fragments within caps.

1933

Bastin, E.S., 1933, Relations of cherts to stylolites at Carthage, Missouri, Journal of Geology, vol. 41, p. 371-381.

Stylolites and chert nodules occur along bedding planes in Warsaw aged limestone of Missouri. Cherts formed by replacement. Chert nodules that formed prior to stylolites have striated sides, smooth tops, and they are flanked by stylolites. Chert nodules that formed later than stylolites have serrated tops and bottoms, which are laterally continuous with stylolites. The stylolites served as barriers to silica replacement. Certain bedding planes were particularly favorable channels for dissolution, leading to the formation of stylolites and chert nodules.

1934

Price, P.H., 1934, Stylolites in sandstone, Journal of Geology, vol. 42, p. 188-192.

Asymmetric, striated, columnar stylolites occur along bedding planes in Pennsylvanian aged sandstone, and along fractures in Silurian aged quartzite, in West Virginia. The stylolites gave very little residue, and rock within the columns is porous, containing oxide coatings in some places. the styloites are thought to have formed by "differential solution brought about by atmospheric waters," helped along by organic acids.

1936

Stockdale, P.B., 1936, Rare stylolites, American Journal of Science, 5th Series, vol. 32, p. 129-133.

Lower Pottsville aged quartzite of Tennessee contains stylolites with 1 inch long columns which are striated and contain clay-rich caps and clay coatings along their walls. The stylolites formed after metamorphism. Column caps are blunt or rounded.

Permian aged gypsum of Texas contains closely spaced, interlocking stylolites, with 0.25 to 0.5 inch long, striated columns and pointed, tapered caps. Column walls are coated with clay. Occasional columns with blunt caps have especially thick (> 1 mm) clay caps. Stylolites are rare in gypsum despite its solubility because its porosity allows free percolation of groundwater, thus avoiding channeled flow necessary for stylolite development.

Stylolites form best in soluble strata that are compact and fine-grained, compelling movement of groundwater along restricted channels such as bedding planes and crevices.

1937

Grim, R.E., Lamar, J.E., and Bradley, W.F., 1937, The clay minerals in Illinois limestones and dolomites, Journal of Geology, vol. 45, p. 829-843.

Represents an early look at the distribution of residual clay minerals in various carbonate facies of the Illinois Basin.

1938

Frye, J.C., and Scoby, E.H., 1938, Stylolites of Burlington Limestone, Near Kinderhook, Illinois, Pan-American Geologist, vol. 70, p. 155-156.

Stylolites occur in cherty limestone of the Burlington Formation. They are thought to have formed by pressure solution in lithified sediment ("indurated rock"). Evidence includes fluted crinoid stems along column walls; similarity of composition of clay caps and host rock residues; chert nodules fluted along their sides and pitted along their upper and lower boundaries (author believes this indicates chert formation precedes stylolite development, in contrast to Bastin, 1933); and smaller stylolites crosscutting columns of earlier, larger stylolites. Thickness of the clay cap is mostly unrelated to the amount of dissolution, but maximum column height approximates the thickness of strata removed.

1939

Shaub, B.M., 1939, The origin of stylolites, Journal of Sedimentary Petrology, vol. 9, p. 47-61.

Evidence against the formation of stylolites by dissolution in lithified sediment includes stylolites in extremely insoluble material, such as quartzite; limited lengths of columns; improbability of sedimentary juxtaposition of materials with highly contrasting solubilites; lack of association between stylolites and karst features; excessive volumes of water needed to dissolve relatively small amounts of calcite in seawater (20 miles seawater depth per 10 feet dissolved limestone thickness); lack of association between stylolites and joints; and similarity of striations to plastic extrusion features.

According to the contraction-pressure theory, stylolites develop by compaction of fine-grained, porous, unlithified sediment. The compaction is accompanied by upward movement of pore water, which accumulates beneath impermeable clay partings, while overlying sediment becomes dry and brittle. Dried out lime contracts laterally, causing horizontal stress to decrease. Unconsolidated, wet sediment flows into zone of low stress, and clay layer shears. Contraction and material transfer continues until pore water movement ceases, or sediment dries out.

Stockdale, P.B., 1939, Stylolites [abstract], Geological Society of America Bulletin, vol. 50, p. 1989.

The author presents a rebuttal to the paper by Shaub (1939), advocating the contraction-pressure theory. The pressure solution theory is supported by penetration of fossils; interpenetration of adjoining seams; occurrence of stylolites along sedimentary unconformities, in marble, along partings oblique to bedding, and along pebble contact surfaces. The author questions whether all features described as stylolites are "true stylolites," and suggests that more than one mode of development may exists.

1940

Bastin, E.S., 1940, Discussion: a note on pressure stylolites, Journal of Geology, vol. 48, p. 214-216.

The author presents a rebuttal to the paper by Shaub (1939), advocating the contraction-pressure theory. The author describes stylolitic contacts between impressed pebbles. He cites the example of the Potomac Marble formation, which is a conglomerate lens in the Upper Triassic aged Newark Group. The pebbles consist of dolomite or dolomitic marble, probably derived from the Shenandoah Limestone formation. They are embedded in red calcareous matrix, occasionally mixed with some sand. The conglomerate grades laterally into sandstone, and it exhibits no signs of metamorphism. The pebbles are smooth, round (not distorted), and 2 to 3 inches in diameter. Where pebbles are inset into each other, the contact is microstylolitic (serrated), with very little clay. The microstylolites are identical in shape to larger stylolites. Pressure due to overburden would have been sufficient to form the micorstylolites.

Goldman, M.I., 1940, Stylolites, Journal of Sedimentary Petrology, vol. 10, p. 146-147.

The author presents a rebuttal to the paper by Shaub (1939), advocating the contraction-pressure theory. The author argues that zones of differential solubility need not be arranged in a precise, alternating pattern, as Shaub claims the pressure solution theory demands. Differential solubility is easily achieved by differences in structure and compositon of shells of different organisms, and by differences in solubility of crystalline substances in different crystallographic directions. Spacing of columns is generally of the same scale as the grain size to the host rock. Fine, acicular projections are more likely to form in lithified than in unlithified sediment.

The author believes that, in addition to differential solution, some form of flow in the consolidated state is evidenced by diverging striations. The flow occurs to adjust to different rates of advancement of adjacent parts of rock along a stylolite.

1943

Stockdale, P.B., 1943, Stylolites: primary or secondary? Journal of Sedimentary Petrology, vol. 13, p. 3-12.

True stylolites are of secondary origin. The issue is fogged by pseudo-stylolites. Clay films are largely to entirely residual. Slickensides are due to slippage. Stylolites are most common in calcareous, soluble rocks.

Evidence for the secondary origin of stylolites includes stylolites in metamorphic rocks, including marble and quartzite; stylolites along unconformities (e.g., the Devonian aged Columbus Limestone formation of central Ohio, which is a well-defined unconformity, exposed for thousands to millions of years, and in which stylolite columns are several inches tall); stylolites oblique to bedding; stylolites along faults; stylolites formed later than chert nodules (from Bastin, 1933); the absence of stylolites in unconsolidated sediments.

Evidence for the removal of rock along stylolites includes impressed pebbles; undisturbed laminae above and beneath stylolites; penetration of small stylolite seams by larger stylolites; tilting and faulting of layers to adjust for nonuniform dissolution; and penetration of fossil shells by comparatively small stylolite columns.

Chemical analyses of clay caps indicate that the clays are insoluble residues. Thicknesses of clay caps vary in direct proportion to the purity of the limestone host. Dissolution is by groundwater, which can occur even in sandstone, given sufficient time.

1947

Andrews, D.A., 1947, Significance of stylolites in sandstone, Journal of the Washington Academy of Sciences, vol. 37, no. 10, p. 372-373.

Pennsylvanian aged sandstone in western Maryland and northeastern Alabama contain stylolites throughout the stratigraphic section. The stylolite columns are up to 2 inches tall, with slickensided walls. They formed after lithification. Some grains adjacent to stylolites are completely obliterated, and all show some degree of dissolution. Seams are coated with "residual clay" and carbonaceous material. Stylolites are abundant in quartzitic sandstones, but they are sparse in some other sandstones. Stylolites are associated with the mineral dickite, indicating a temperature of formation of 100 degrees Centigrade. Maximum burial depth was no greater than 3000 feet. Appalachian folding was accompanied by an increased thermal gradient.

Unanswered questions include, whether the quartz dissolution was accomplished by normal groundwaters, and whether there was more dissolution than the stylolite column heights suggest.

1949

Gilbert, C.M., 1949, Cementation of some California Tertiary reservoir sands, Journal of Geology, vol. 57, p. 1-17.

The Middle Eocene aged Gatchell and McAdams Sandstone formations, and the Upper Miocene Puente Sandstone formation, all of which are feldspathic, contain an interlocking grain texture with serrated grain contacts, mainly in layers where pore cement consists of quartz or quartz with some calcite, feldspar, or minor clay. Tight packing of grains without interlocking, sutured grain texture, on the other hand, occurs in rocks with significant amounts of clay in the matrix. The clay-cemented, non-interlocking sandstones have high permeability (about 200 millidarcy's), whereas quartz-cemented, interlocking sandstones have low permeability (about 10 millidarcy's). Porosities are about 10% to 15% in both rock types. Clay inhibited normal precipitation of secondary minerals within the pores.

Interlocking grains exhibit undulatory extinction, but not fracturing. Association of secondary quartz and feldspar with interlocking texture suggests an indigenous source, rather than groundwater.

Clay between sand grains prevents or diminishes pressure solution by reducing the heterogeneity of overburden stress. Compact clay transmits stress uniformly. In some cases, grains my be floating in the clay matrix.

Shaub, B.M., 1949, Do stylolites develop before or after the hardening of the enclosing rock? Journal of Sedimentary Petrology, vol. 19, p. 26-36.

The author presents a lengthy rebuttal of various arguments put forth by Stockdale (1943). Similarity of composition of clay cap with host rock is not proof that the cap is insoluble residue, because the similarity would be expected in a depositional clay seam, as well. Thicknesses of clay caps do not always vary proportionally with column lengths. Offset laminations across column walls may reflect contraction of plastically behaving sediments, since differential dewatering can cause changes in thicknesses of laminae. Bent laminae around columns are thinned along the arc of greatest bending, suggesting that material is displaced, and not removed. Offset color banding in limestones of Indiana need not be depositional. "Adhesion ridges" found along some column walls can form only in plastic material. Pulling apart of hard steel blocks with adhesive force of over 200 pounds yields flat, undeformed surfaces.

The Tennessee Marble formation contains keystone offsets (wedge-shaped displacements) along stylolites and differential displacement across faults that cross-cut stylolites over short distances (several cm or mm), suggesting that the stylolites formed prior to lithification. Cherty limestone of the Corniferous Formation near Port Dover, Canada, contains stylolite columns penetrating chert. The chert formed by limestone dissolution.

1950

Conybeare, C.E.B., 1950, Microstylolites in Pre-Cambrian quartzite: A reply, Journal of Geology, vol. 58, p. 652-654.

In his reply to Shaub's (1949) discussion, Conybeare points out that the foliation in the quartzite was produced by intense shearing or mylonitization, and that the stylolites are younger than the foliation. The amount of internal deformation in the rock would have destroyed any primary sedimentary features. Quartz-filled fractures which could only have developed after the rock became schistose are cross-cut by stylolites.

A quartzite from the pre-Cambrian rocks of the Kenora district, Ontario, Canada, shows stylolite seams cutting the foliation of a sheared quartzite at right angles. Stylolites in quartzite may cut the bedding at any angle.

Shaub, B.M., 1950, Microstylolites in Pre-Cambrian quartzite: A discussion, Journal of Geology, vol. 58, p. 650-652.

Displacement of specularite stringers across fractures associated with stylolites varies along the fractures, and diminishes to zero. This differential displacement suggests soft-sediemnt deformation. Some fractures cut stylolites, so the stylolites, too, are pre-consolidation. There are tow sets of cross-cutting stylolites. If pressure solution had been involved, the stylolites would have formed along the cross-fractures during the second episode of stylolite development. Elongated quartz grains are continuous across fractures, so they do not represent fracture fillings. These observations suggest pre-consolidation origin of stylolites.

1951

Bastin, E.S., 1951, A note on stylolites in oolitic limestone, Journal of Geology, vol. 59, p. 509-510.

A stylolite in Silurian aged, oolitic limestone of Oklahoma, cuts across the centers of ooids and appears not to have formed along ooid contacts. Instead, the stylolite formed either along an obscure bedding plane, or along fractures. There is no clayey residue accumulation. The stylolite formed after cementation (post-lithification).

1952

Prokopovich, N., 1952, The origin of stylolites, Journal of Sedimentary Petrology, vol. 22, p. 212-220.

It is probable that stylolites originated in several different ways. Weaknesses exist in both the pressure solution and contraction-pressure theories. The author proposes the theory that stylolites form by dissolution in soft sediments.

Weaknesses of the pressure solution theory include uniformity of pressure on small surfaces in rock; out-of-phase nature of neighboring stylolites; lack of stylolies in cavernous limestones; absence of stylolite horizons in lowest strata; abundance of stylolites in carbonate rocks, where groundwater circulation is restricted and volume of pore water is small; occurrence of styolites within beds and their absence between beds; uniform bed thickness between stylolite-bearing and stylolite-free parts; stylolites cross-cutting units with widely varying solubilities; curved and corroded columns; columns that are narrower at the base than near the cap; and the presence of fucoids on seams surfaces, indicating that they were ordinary sea-bottom surfaces.

Weaknesses of the contraction-pressure theory include the truncation of fossils; the penetration of seams and bedding surfaces; the general absence of fossils in column caps; the absence of involutions in sediments adjacent to columns; and the overall scarcity of stylolites.

The alternative hypothesis, that stylolites form by dissolution in soft sediments, combines elements of both previous hypotheses. Stylolites are similar to lapies, which are formed by surface solution of limestone. Soft-sediment dissolution is related to pH and carbon dioxide content. The carbon dioxide content of seawater controls the pH. Carbon dioxide content is low in shallow water, due to photosynthesis, but it increases with depth due to decomposition of planktonic remains, thus causing pH to decrease. Lowest pH is found in bottom water of a shallow sea. Periodic plankton enrichment could lower pH sufficiently to cause dissolution.

Stylolites occur in the Middle Triassic aged Muschelkalk Limestone formation, which is partially dolomitic. Both bedding planes and stylolite surfaces are covered with a thin film of black, fatty, colloidal and clayey material. Stylolites occur only in the thickest beds. Large columns are striated, and some striae are curved. Some columns are narrower at the base than at the cap. Stylolites cut fossils more often than they contain fossils in their caps.

In the Upper Jurassic aged Malm Limestone formation, stylolite seams are vertical, but the number of seams diminshes toward a fault. The stylolites appear to be independent of the tectonic framework.

Seams cut beds, which show small offsets. Many columns are curved.

Ramsden, R.M., 1952, Stylolites and oil migration, AAPG Bulletin, vol. 36, p. 2185-2186.

Stylolites in Jurassic aged limestone and dolomite oil reservoir rocks of the Middle East cause significant rock volume loss and expulsion of fluids. This leads to oil accumulation. Oil typically accumulates in fractured limestone or in stylolitic zones.

1953

Heald, M.T., 1953, Significance of stylolites in sandstones, Geological Society of America Bulletin, vol. 64, p. 1432.

Stylolites occur in nearly every quartzose or calcareous sandstone in the Appalachians. Most are bedding-parallel, and some formed along fractures and are inclined. Bedding-parallel seams are equally well developed in outcrop and in the subsurface. Interpenetration along seams occurs between quartz grains, as well as between quartz and calcite, feldspar, biotite, and muscovite. Stylolites form by pressure solution.

Permeability across stylolite seams along bedding planes is low due to residue accumulation. Interlocking columns lend competency to the rock. Most stylolitic dissolution occurred before folding, but some occurred after. Dissolved silica may be the source of much cement in sandstones, but no simple relationship betweeen amounts of pressure solution and cementation exists.

Seibold, E., 1953, Fiederspalten und Drucksuturen, Neues Jahrbuch fuer Geologie un Palaeontologie, Abhandlungen, vol. 96, p. 357-374.

Helvetic chalks of the Vorarlberg region, Austria, contain bedding-perpendicular stylolites (solution cleavages) that formed within shear zones, concurrently with en-echelon veins that are sub-normal to the cleavages. During formation of en-echelon veins, pre-existing solution surfaces become more closely spaced and bent. The released calcite commonly recrystallizes in adjacent pores, opening en-echelon cracks. The planar solution surfaces are considered to be precursors to columnar stylolites.

Shaub, B.M., 1953, Ruin-Marble: A stylolitic formation? American Journal of Science, vol. 251, p. 602-605.

Tabular fault blocks in ruin-marble formed due to differential pressures during dewatering while the material was in a plastic state. There are no signs of dissolution. This is an example of stylolite-like features forming without dissolution. In contrast to stylolites, ruin-marble contains faults that are continuous and quite long.

Young, R.S., 1953, Note on a microstylolite in oolitic limestone, Journal of Geology, vol. 61, p. 471-472.

Tectonic microstylolites in the Upper Cambrian aged, oolitic, Conococheague Limestone formation of Virginia, are coated with organic matter. Stylolites occur along chains of closely spaced ooids, cutting across the ooids. The stylolites have caused 8% to 10% shortening parallel to bedding. Their orientation is independent of local joints, suggesting that they after consolidation and before recrystallization, according to the author. Stylolite column heights are greatest within pore cement. Stylolites are best developed within oolitic rock. They are formed by dissolution in soft sediments, since macrostylolites are absent in the overlying limestone, according to the author.

1954

Dunnington, H.V., 1954, Stylolite development post-dates rock induration, Journal of Sedimentary Petrology, vol 24, p. 27-49.

A thorough petrographic study of stylolites in limestones of the Middle East has led the author to conclude that stylolites form late in rock history. They form after mechanical compaction. Dissolved material is redeposited locally, and pore fluids are expressed (squeezed) out of the rock, according to the author.

1955

Shaub, B.M., Notes on the origin of some agates and their bearing on a stylolite seam in petrified wood, American Journal of Science, vol. 253, p. 117-120.

Columnar stylolites occur along the periphery of a petrified tree trunk. the stylolites are bulbous, suggesting flow of silica gel into zones of reduced pressure, toward the core of the trunk. The pressure reduction is caused by shrinkage due to water loss.

1956

Heald, M.T., 1956a, Cementation of Simpson and St. Peter Sandstones in parts of Oklahoma, Arkansas, and Missouri, Journal of Geology, vol. 64, p. 16-30.

Greater amounts of dissolution occurred in argillaceous zones of the sandstones than in pure, clay-free zones, indicating that materials such as clay promote pressure solution.

Heald, M.T., 1956b, Cementation of Triassic arkoses in Connecticut and Massachusetts, Geologic Society of America Bulletin, vol. 67, p. 1133-1154.

The only example of megascopic stylolites in Triassic rocks of the eastern United States occurs in one zone in the sandstone at Raven Rock, New Jersey, where there are several very well developed, undulose stylolite seams. The stylolites contain pyrite instead of hematite, which is common in the sediments. This suggests that composition, not fluid circulation, controlled stylolite development.

1957

Herbert, P. Jr., and Young, R.S., 1957, Late stylolites, Journal of Geology, vol. 65, p. 107.

Tectonic stylolites in the tectonic breccia of the upper Beekmantown Formation of Virginia, formed after fracturing, brecciation, cementation, faulting, and hydrothermal sulfide mineralization, according to cross-cutting relationships described by the author.

1958

Kanes, W.H., 1958, A study of the Upper Middle Mississippian of southeastern West Virginia, M.S. Thesis, West Virginia University.

Microstylolites occur along carbonaceous bands entirely within individual oolites, suggesting the influence of foreign matter in promoting pressure solution.

Shaub, B.M., 1958, Some apparently misunderstood aspects concerning stylolites [note], Journal of Sedimentary Petrology, vol. 28, p. 376-377.

In Mississippian aged limestones of Bedford, Indiana, one finds numerous instances where stylolites columns are smaller than the sockets they "fit" into. There are cavities along stylolite seams, and open spaces between striated stylolite columns and adjacent walls. These cavities are filled with dolomite or calcite,a nd in some cases with coarse granular calcite. This is thought to indicate that the rock was in a plastic state during stylolite formation.

Weyl, P.K., 1958, Mechanism of stylolite formation [abstract], Geological Society of America Bulletin, vol. 69, p. 1660.

Stylolites form due to pressure solution along pre-existing, thin clay layers. Pressure solution is more rapid along clay partings than at clean grain contacts, because of rapid diffusion rates. Dissolved material may diffuse to unstressed grain surfaces and precipitate there, or it may be removed from the compacting rock by fluid flow. These fluids will not flow along the stylolitic seam, but rather, because of the relatively low permeability of the clay parting, they will tend to flow between the stylolites, and parallel to them.

1959

Brown, C.W., 1959, Diagenesis of late Cambrian oolitic limestone, Maurice Formation, Montana and Wyoming, Journal of Sedimentary Petrology, vol. 29, p. 260-266.

Stylolites occur within partially dolomitized, oolitic grainstone, and they occur as irregular, thin, linear zones of concentrated dolomite rhombs. The grainstone is mottled, containing zones of intense dolomitization (clusters of dolomite rhombs), but the dolomitization of those mottles is not related to the accumulation of dolomite along stylolites. Instead, the rhombs along stylolites are believed to have become concentrated by dissolution of the surrounding calcite matrix, prior to the collapse of the solution channel. The rock became lithified, at least in part, prior to dolomitization, implying that stylolites formed after lithification.

Heald, M.T., 1959, Significance of stylolites in permeable sandstones, Journal of Sedimentary Petrology, vol. 29, p. 251-253.

The occurrence of stylolites in permeable sandstone shows that dissolution is localized by the presence of clay and not by freer circulation along bedding planes. Well-developed stylolite seams with clay coatings occur in highly permeable sandstone of the Pottsville, Dakota, and Oriskany Sandstone formations of West Virginia, Wyoming, and West Virginia, respectively. Dissolution was promoted by clay or ash deposits (releasing alkalies) along partings. If circulation had been the controlling factor, dissolution would have occurred along grain contact surfaces throughout the permeable beds, and thick, porous beds would contain many stylolites instead of few, isolated seams. Also, few stylolites occur in porous Triassic rocks of the eastern United States, with many bedding planes.

Stylolite development begins along discontinuous clay partings in porous sandstone, and ends with truncation of quartz overgrowth by late stylolite growth. Lack of faults at stylolite seam margins indicates poorly lithified state of rock. Grain contact sutures develop where clay is evenly distributed throughout the rock.

Stress requirements are low, as evidenced by excellent preservation of fine textures in fossils, and of micas adjacent to dissolved quartz. Dissolution occurs along clay partings, where stresses are lower than at clean grain contacts, where dissolution does not occur.

Nitecki, M.H., 1959, Role of clay in stylolite formation [abstract], Geological Society of America Bulletin, vol. 70, p. 1651-1652.

Stylolites are most commonly found in "pure" limestone. Rocks with much disseminated clay develop sutured grain contacts, instead. Clay partings along stylolites are generally micaceous. The clay affects the rate of dissolution, and it acts as a catalyst for dissolution. Clay concentrates and orients water molecules along its surface. The oriented water has different solvent and ion exchange properties than bulk water. Dissolved calcium ions are in equilibrium with the calcium in the limestone. When the ions are adsorbed on clay surfaces, more calcium goes into solution in order to maintain equilibrium. Thus, stylolites may be related to differences in the solvent properties of pore water and water adsorbed onto clay layers.

Thomson, A.F., 1959, Pressure solution and porosity, SEPM Special Publication No. 7, p. 92-110.

According to a citation of this paper by Heald (1959), the author demonstrates that potassium derived from clay may promote dissolution along stylolites or sutured grain contacts.

1961

Pryor, W.A., and Glass, H.D., 1961, Cretaceous-Tertiary clay mineralogy of the Upper Mississippian Embayment, Journal of Sedimentary Petrology, vol. 31, p. 38-51.

Analyzes relationship between clay mineralogy and provenance of Mississippian limestones. No reference to stylolites.

1962

Hayes, J.B., 1962, Clay mineralogy of Mississippian strata of southeast Iowa, Proceedings of the 9th National Clay Conference, p. 413-425.

Helpful in relating clay mineralogy and provenance of Mississippian limestones. No reference to stylolites.

Nitecki, M.H., 1962, Observations on slickolites, Journal of Sedimentary Petrology, vol. 32, p. 435-439.

Slickolites are closely spaced grooves and ridges along subvertical planes in rock, commonly found along contacts between chert and limestone. They resemble striae along stylolite column walls, but they need not be associated with clay seams. Slickolites are coated with twinned calcite. The calcite fibers and the calcite twins are parallel to the slickolite surfaces. Slickolites are pressure solution features, and they develop along planes of movement (microfaults).

1964

Bosazza, V.L., 1964, A note on a stylolite in oolitic dolomitic limestone of the Transvaal system, South Africa [abstract], 22nd International Geologic Congress, Abstracts of Papers, Section 15, p. 219.

The stylolite referred to in the title of the abstract apparently formed both during and after lithification. The author notes that this is in agreement with interpretations put forth by Bastin (1951).

Amstutz, G.C., 1964, New mineralogic observations on stylolite seams [abstract], AAPG Bulletin, vol. 48, p. 515-516.

Galena and pyrite formed during stylolite development in Mississippian aged limestone of the fluorspar district of southern Illinois. Sphalerite formed prior to the stylolites. The time of stylolite development falls within the second and third periods of diagenetic compaction and crystallization, as defined by Dapples.

Schlanger, S.O., 1964, Petrology of the limestone of Guam, US Geological Survey Professional Paper 403-D, p. 1-52.

Petrographic analysis of limestones of Guam demonstrates the occurrence of microstylolites at a burial depth of less than 330 feet (100 m).

1965

Gibbs, R.J., 1965, Error due to segregation in quantitative clay mineral X-ray diffraction techniques, American Mineralogist.

Reference for interpreting X-ray diffraction data. No references to stylolites.

1967

Dunnington, H.V., 1967, Aspects of diagenesis and shape change in stylolitic limestone reservoirs, 7th World Petroleum Congress, Mexico, vol. 2, p. 339-352.

Stylolite development is a typical response to overburden pressure in carbonate rocks buried at depths greater than 600 to 900 m (2000 to 3000 feet). Stylolites complicate many oil reservoirs by reducing reservoir thickness, porosity and permeability. In cases where hydrocarbon accumulation originated before stylolite development, inhibition of dissolution by oil and gas may have caused stylolite distribution to become localized in zones of high water saturation levels. In cases where stylolite development preceded hydrocarbon migration, stylolite seams may have caused or influenced hydrocarbon accumulation. Stylolites may profoundly modify transmissivities and thicknesses of limestone aquifers connecting oil reservoirs. Stylolites cutting obliquely across bedding may constitute flow barriers capable of entrapping oil in large quantities. Such stylolites may produce anticlinal structures, either by movement along them (slickolites), or by removal of wedge-shaped portions of rock.

1968

Grim, R.E., 1968, Clay Mineralogy, McGraw-Hill, New York.

Standard refernece book on clay mineralogy. No references to stylolites.

Park, W.C., and Schot, E.H., 1968, Stylolites: Their nature and origin, Journal of Sedimentary Petrology, vol. 38, p. 175-191.

Stylolite morphology is classified into 6 types, including wavelike, sutured, up-peak (rectangular), down-peak (rectangular), sharp-peak, and seismogram types. In the Upper Mississippian aged St. Genevieve Limestone formation of Indiana, many stylolite seams grade laterally into shaley or clayey partings.

In the Upper Mississippian aged Downeys Bluff Limestone formation, multiple clay caps become thinner away from the stylolite seam, indicating that dissolution occurred at discrete time intervals. Clay caps contain dolomite and quartz. Quartz typically has crystallographic c-axes parallel to the stylolite seam, suggesting directional growth during stylolite development. Clay caps also contain fragments of early cements.

In the Lower Ordovician aged Jefferson City Dolomite formation, stylolites grade laterally into hummocky seams. Stylolites predominate in thickly bedded units, and hummocky seams in thinly bedded ones. Caps and seams contain clays, diagenetic quartz, pyrite, and bituminous material, oriented subparallel to the seams. Quartz and pyrite are finer grained in host rock than in caps and seams. Microfaults along seams do not continue into host rock. Geopetal structures along stylolites indicate rock was in plastic, incompletely lithified, highly porous state at time of stylolite formation. Stylolite rare or absent in dense carbonates.

1970

Fuechtbauer, H., and Mueller, G., 1970, Sedimente und Sedimentgesteine, Stuttgart, E. Schweitzerbart'sche Verlagsbuchhandlung, p. 364-365.

Evidence supporting post-lithification origin of stylolites includes the truncation of fracture-filling cement, and of late diagenetic crystals. Sutured dissolution surfaces form where adjacent units--grains or beds--have equivalent solubility, whereas smooth dissolution surfaces form where adjacent units have contrasting solubilities. Thus, stylolites develop only along thin clay seams, and not along thick ones. The ideal clay seam is just thin enough to restrict water movement within it, allowing flow only along the outer margins of the clay. Columns form when the water encounters an insoluble particle, such as a shell, and is diverted to the opposite side of the clay seam.

1971

Arthaud, F., and Mattauer, M., 1971, Sur l'origine tectonique de certains joints stylolitiques paralleles a la stratification; leur relation avec une phase de distension (exemple du Languedoc) [abstract], Societe Geologique de France, Compte Rendu Sommaire, p. 365.

Horizontal stylolitic joints with vertical columns in Mesozoic aged carbonate rocks in Languedoc, France, formed after late Eocene tectonic compression. This means the stylolites formed by tectonic processes. Evidence includes cross-cutting relationships between stylolites and other microstructures related to tectonic extension.

1972

Arthaud, F., and Mattauer, M., 1972, Sur l'origine tectonique de certains joints stylolitiques paralleles a la stratification; leur relation avec une phase de distension (exemple du Languedoc), Societe Geologique de France Bulletin (7), vol. 14, p. 12-17.

Mesozoic carbonate rocks containing bedding-parallel stylolites became lithified (indurated) during middle Cretaceous time (120 ma), and stylolitized during extension in Oligocene time (30 ma).

Vertical, calcite-filled veins both cut, and are cut by, horizontal stylolites, but the veins cut across all vertical stylolites. The vertical stylolites are older, having formed during Eocene compression, whereas the horizontal stylolites are contemporaneous with the veins, which are related to Oligocene, tectonic extension.

Bissell, H.J., 1972, Three-dimensional stylolites and migratory routes of oil and gas [abstract], AAPG Bulletin, vol. 56, p. 604.

Stylolites in Triassic aged limestones of Nevada are columnar, striated, bifurcating, and they follow along cross-beds. The stylolites served as channels for early hydrocarbon migration, especially to fill bioherms with oil. Stylolites form as a result of dissolutoin after deposition, and they represent early compaction.

Lawyer, G.F., and Larsen, N., 1972, Details of stylolite growth as shown by the electron microscope [abstract], GSA Abstracts with Programs, vol. 4, p. 386-387.

Scanning electron microscope (SEM) study of stylolitic limestones of the Virgin Member of the Moenkopi Formation, Nevada, suggests that styolite growth is controlled by dissolution, pressure solution, rock fabric, differential solubility, lithologic variations, crystal structures, and directed pressure. The direction of dissolution is controlled by the direction of pressure, differential solubility, and crystal structure. Stylolite development increases the permeability of a limestone, by creating permeability channels.

Mossop, G.D., 1972, Origin of the peripheral rim, Redwater Reef, Alberta, Bulletin of Canadian Petroleum Geol., vol. 20, p. 238-280.

The raised rim of a Devonian reef is due to late differential compaction caused by stylolite development. Overburden of 750 meters was required for stylolite development, which is a slow, drawn-out process. The secondary downwarp of the lagoon relative to the rim constitutes 50 meters. Compaction caused by stylolites is only 13% in the rim, but 24% in lagoonal carbonates. Stylolites are associated with anomalously high amounts of sparry, void-filling calcite. This controls the sealing of permeability in the caprock of the reef.\

Swarms of hummocky seams ("horsetails") converge into single seams. They occur mainly in fine-grained limestone containing large skeletal fragments, such as wackestone. Stylolites and hummocky seams do not occur in the same rock. Swarms of hummocky seams form where there is a high content of disseminated insoluble material. Both stylolites and hummocky seams occur preferentially in the lagoonal section, and not in the rim section.

1975

Bathurst, R.G.C., 1975, Carbonate Sediments and their Diagenesis, 2nd Edition, Developments in Sedimentology, vol. 12, Amsterdam, Elsevier, 658 p.

Stylolite development is promoted by the presence of micrite, carbonaceous matter, and clay minerals, especially along bedding planes. Diffusion is slow,a nd bulk transport of solvent and solute together by fluid flow could be important. Pressure solution at grain contacts cannot take place after pores are filled with second generation cement. After pore occlusion, pressure solution occurs along stylolites. Stylolites cut across laminations, grains, cement, and micrite. The initial dissolution surface is parallel to bedding. The serrate form of the surface is a consequence of lateral variations of solubility differences of the rock across the surface. The fact that stylolites tend to occur in part of rock with low porosity and permeability suggests that dissolved calcite moved parallel to the axis of prinicple stress and perpendicularly away from the stylolite surfaces. Stylolites development begins in lightly cemented rock, and drives the cementation process to completion. Stylolites form impermeable barriers.

The largest stylolite column is one meter tall, in Carboniferous aged limestone of Yorkshire, England. Stylolite column height ("amplitude") represents the minimum thickness of material lost due to pressure solution. The sides of stylolite columns act as piston faults.

Kaplan, M.Y., 1975, Origin of stylolites, Doklady Akademii Nauk SSSR, vol. 221, p. 205-207.

Stylolites develop during all stages of lithification, from late diagenesis to catagenesis and metamorphism. This supports the pressure solution hypothesis. Stylolite column height depends directly on the solubility of the limestone, and there is a close relationship between the height of columns and thicknesses of clay caps. Older stylolites tend to have taller columns than younger ones. Clay caps constitute insoluble residue, typically enriched in organic matter, microfossils, and other insoluble components.

Stylolite columns oriented parallel to bedding occur along joints. The density of stylolites in pure micritic limestone increases with that of joints. Bedding-oblique stylolites are subparallel to fold axes. Two stylolite sets, intersecting at acute angles (25 degrees) are common, suggesting that they formed along shear joint sets. Furthermore, stylolites grade into joints with smooth walls.

Pressure solution begins at a threshold solubility level, dependent upon temperature, pressure, and material properties. Pressure solution occurs along interfaces--bedding planes, joints, or grain contacts. The rock surfaces are rough due to differential solution rates, leading to nonuniform pressure. Microstylolites develop at asperities--tips of minute projections--and they contain insoluble residue films, as well as striations. The union of primary heterogeneity patches first produces serrated surfaces, then columnar stylolites, and finally, barrier-type forms. Dissolved material precipitates in zones of lower pressure along the sides of stylolite columns, and in pores, vugs, and tear joints.

Large columnar stylolites occur in Upper Cretaceous aged limestone of the Caucasus region in the USSR. The estimated decrease of sediment thickness due to stylolite development in that limestone is 7% to 8%.

Laubscher, H.P., 1975, Viscous components in Jura folding, Tectonophysics, vol. 27, p. 239-254.

Tectonically induced bedding-parallel stylolites occur in steeply dipping limbs of box folds. The creation of secondary tectonic pore space, such as macroscopic shear and tension joints in limestones, and microscopic dilatancy cracks in anhydrite, are essential to pressure solution. Pore space may be the rate-determining factor. Although stylolites are ubiquitous in limestone, their contribution to mass transport is small, because most of it occurred along discrete failure surfaces.

Ostapenko, G.T., 1975, The physicochemical mechanism of stylolite formation [abstract], Geochemistry International, vol. 12, p. 201-202.

Stylolites develop from microcrushed zones at contacts between brittle solids, during rock consolidation or under tectonic stress. The wavy shape of stylolites can arise from transport away from the microcrushed zone, out of the rock, which occurs when ore solutions infiltrate, or when there is rapic removal by diffusion. Transport away from the microcrushed zone to adjacent, undamaged parts of contacting grains, occurs when there is little removal and rapid crystallization from solution. This may occur during epigenesis, or metamorphism accompanied by tectonic stress.

1977

Garrison, R.E., and Kennedy, W.J., 1977, Origin of solution seams and flaser structure in Upper Cretaceous Chalks of southern England, Sedimentary Geology, vol. 19, p. 107-137.

Flaser structure consists of lenses of pure chalk surrounded by clay-rich dissolution seams. They formed during late burial diagenesis. Dissolution preferentially affected coccolith-rich, fine-grained matrix, leaving coarser skeletal particles undissolved. Dissolution was most intense in the most argillaceous parts of the chalks. True stylolites are present only in chalks that were lithified during early diagenesis. Burial depths range from 300 2000 meters.

Shinn, E.A., Halley, R.B., Hudson, J.H., and Lidz, B.H., 1977, Limestone compaction: An enigma, Geology, vol. 5, p. 21-24.

Seams consisting of insoluble organic matter form by physical compaction of unlithified, muddy carbonate sediment, instead of dissolution, as is commonly assumed.

1978

Delair, J., and Leroux, C., 1978, Methodes de quantification de la disparition de matiere au niveau de stylolites tectoniques et mecanismes de la deformation cassante des calcaires, Bulletin Societe Geologique de France, Ser. 7, vol. 20, p. 137-144.

In order to estimate the amount of rock lost by pressure solution during stylolitization, examples of tectonic stylolites associated with en echelon tension gashes in a shear zone, in micritic mudstone, were studied. Comparison of three methods to quantify deformation--offset of markers, amplitude of serrations, and composition of residue--for a single stylolite reveals that the results are comparable for the methods of offset of veins and composition of aluminum within residue. However, apparent shortening as measured from heights (amplitudes) of serrations is less than that measured with other methods, and it does not follow the same trend of decrease toward the stylolite tip that is exhibited by the other methods. Instead, shortening appears to be irregularly distributed along a stylolite, according to heights of serrations.

Greggs, R.G., and Helmstedt, H., 1978, Stylolitic axial-plane cleavage in Lower Paleozoic carbonate rocks of the great valley, Maryland [abstract], GSA Abstracts with Programs, vol. 10, p. 412.

Toothed structure is well-preserved in closely spaced, vertical stylolites within fold closures. In vertical fold limbs, it is difficult to distinguish among tectonic, penecontemporaneous, and diagenetic stylolites. Many widely spaced, bedding-parallel stylolites with tall columns in vertical fold limbs are of tectonic origin, as suggested by cross-cutting relationships among stylolites, shear fractures, and kink folds. Penetrative flow also occurred during stylolite development.

Purser, B.H., 1978, Early diagenesis and the preservation of porosity in Jurassic limestones, Journal of Petroleum Geology, vol. 1, p. 83-94.

In the Paris Basin of France, limestones that were cemented very early generally lack stylolites, whereas those that were cemented during burial abound with stylolites.

Wanless, H.R., 1978, Three types of pressure solution in limestones [abstract], AAPG Bulletin, vol. 62, p. 569-570.

Weight of overburden or tectonic stress cause limestone deformation by plastic or brittle deformation, neomorphism, and dissolution. The responsiveness of individual limestone beds, structures, or grains--called "units"--to change is influenced by impurities such as magnesium cations and clay particles. Sutured seams occur in limestone with little clay, whereas non-sutured seams occur in clay-rich limestone. Pervasive, non-seam dissolution occurs in non-resistant limestone, which develops nodules if it is silty or clayey. Limestone pressure solution produces finely crystalline, stratigraphic dolomite. It also causes pore cementation, and severly distorts primary sedimentary structures, or creates secondary structures.

1979

Collinson, C., Norby, R.D., and Baxter, J.W., 1979, Stratigraphy of the Mississippian stratotype: Upper Mississippian valley U.S.A., Illinois State Geological Survey, Ninth International Congress of Carboniferous Stratigraphy and Geology, Field Trip 8, 109 pp.

Provides stratigraphic columns for Salem Limestone outcrops in western Illinois.

Treworgy, J.D., McKay, D.E., and Wickham, J.T., 1979, Geology of Western Illinois, 43rd Annual Tri-State Geological Field Conference, Illinois State Geological Survey Guidebook 14, 90 pp.

Provides general stratigraphic overview of the Mississippian System in western Illinois.

Trurnit, P., and Amstutz, G.C., 1979, Die Bedeutung des Rueckstandes von Druck-Loesungsvorgaengen fuer stratigraphische Abfolgen, Wechsellagerung und Lagerstaetten-bildung, Geologische Rundschau, vol. 68, p. 1107-1124.

Stylolitic pressure solution surfaces form only when the adjacent rocks are equally soluble under pressure. Where residue accumulation is significantly thick, the residue behaves as an insoluble layer, and stylolites become planar. Specifically, stylolites become planar with age. Molasse deposits of Oligocene age contain grains or pebbles of calcite, dolomite, and shale. Stylolitic, sutured contacts occur between adjacent calcite grains and adjacent dolomite grains, but dolomite-calcite contacts are smooth, with dolomite penetrating the calcite. Similarly, shale penetrates dolomite along smooth contact surfaces. Stylolites form within basin centers, and dissolved material precipitates along basin margins, or ridges. Pure, monomineralic beds tend to resist pressure solution, whereas impure beds, especially those containing clay minerals, may shrink to their dissolution residue.

Minerals in order of decreasing pressure solubility are: halite; calcite; dolomite; anhydrite; gypsum; amphibole and pyroxene; chert; quartzite; quartz, glauconite, rutile, and hematite; tin and feldspar; mica and clay minerals; tourmaline and titanite; pyrite; zircon; and chromite.

Wanless, H.R., 1979, Limestone response to stress: Pressure solution and dolomitization, Journal of Sedimentary Petrology, vol. 49, p. 437-462.

Three styles of pressure solution are recognized in Paleozoic limestones of Arizona, western Maryland, and southeastern Kansas. Sutured-seam dissolution, including stylolites and grain-contact sutures, occurs in limestones that have structural resistance to stress and very little clay or platy silt content. Such limestones contain skeletal and non-skeletal grains and crystals, grain-supported beds, and units strengthened by large biogenic structures, early cementation, or precursor neomorphism. Non-sutured seam dissolution, including microstylolites and clay seams, occurs in limestones that contain significant amounts of clay or platy silt. The limestone may be structurally resistant or responsive. Stress is accommodated both by dissolution and by lateral movement along microstylolites. Dolomite rhomb growth may occur along microstylolites. Non-seam solution occurs in clean limestones that have little or no structural resistance to stress. Dolomite growth is generally associated with non-seam dissolution.

Where clean, structurally resistant limestone units interface with responsive limestone or silty, clayey limestone, solution surfaces are non-sutured. Nodular limestones are a typical product of non-sutured seam solution in silty, clayey limestone. Finely crystalline, stratigraphic dolomite may be the result of pressure solution, which provides local sources of magnesium for dolomitization and calcite for pore-filling cement. Pressure solution can severely distort primary sedimentary structures or create secondary structures.

1980

Meyers, W.J., 1980, Compaction in Mississippian skeletal limestones, southwestern New Mexico, Journal of Sedimentary Petrology, vol. 50, p. 457-474.

Stylolites in the Lake Valley Formation cut the latest generation of cement, which is a ferroan calcite cement. Compaction approaches 50% in packstones and grainstones. Chemical compaction occurred during cementation, and may have been the source of calcite for cements. Mechanical compaction includes breakage and plastic deformation. Breakage begins under low overburden, whereas plastic deformation and chemical compaction begin under moderate overburden.

Chemical compaction begins as intergranular pressure solution, and is promoted by undersaturated ground water in recharge regions of large meteoric phreatic lenses. Tops of echinoderm grains are preferentially pressure-solved, compared to bottoms. This is due to differential growth of early cements. Syntaxial cement formed at the bottom, but mud and fine debris accummulated on top.

Stylolites occur in grainstones, and they indiscriminately cut all grains and cement. Stylolites are not important in porosity reduction, since they occurred after most intergranular compaction and after essentially complete cementation.

Ortoleva, P., and Merino, E., 1980, A pressure-solution kinetic theory of stylolites and metamorphic banding, GSA Abstracts with Programs, vol. 12, p. 494-495.

Stylolites form by a feedback process involving concentration of pressure-solved solute, and rock texture. Equilibrium concentration of solute depends on local stress, which is controlled by local rock texture. Texture is modified by diffusion, induced by concentration gradients. The initial texture is unstable due to small textural fluctuations. A secondary instability sets in at right angles to the major one, giving rise to columnar projections.

Playford, P.E., 1980, Devonian "Great Barrier Reef" of Canning Basin, western Australia, AAPG Bulletin, vol. 64, p. 814-840.

Stylolites are most abundant in limestones whose primary porosity was not destroyed by early submarine cementation. Therefore, stylolitization is most intense in the platform interior of the reef, producing the concave shape of the platform. Cementation concomitant to stylolite development destroyed most of the porosity. The most porous rocks are dolomites with secondary moldic porosity. Stylolitization is more intense in back-reef subfacies than in reef margin and reef flat subfacies.

Stylolites follow depositionally inclined bedding planes. Overburden thickness is greater than 1000 meters. Stylolites are widely spaced and have short columns ("low amplitudes") where there was strong early cementation, whereas they are closely spaced with tall columns ("high amplitudes") where little or no cementation occurred.

1981

Buxton, T.M., and Sibley, D.F., 1981, Pressure solution features in a shallow buried limestone, Journal of Sedimentary Petrology, vol. 51, p. 19-26.

In the Devonian aged Alpena Limestone formation of Michigan, a distinct style of pressure solution characterizes each lithology. Columnar ("high-amplitude") stylolites occur in well-lithified grainstone without sutured grain contacts ("non-fitted fabric"). Non-sutured dissolution seams occur in uncemented or poorly cemented packstone and wackestone with intergranular pressure solution ("fitted fabric"). Stylolites and non-sutured seams occur preferentially along lithologic contact surfaces. Dissolved material does not precipitate nearby. Instead, it is carried out by fluid flow.

Janssen, C., and Mueller, H.J., 1981, Analyse palaeotektonischer Spannungen auf der Grundlage von Ultraschallmessungen an Horizontalstylolithen, Zeitschrift fuer angewandte Geologie, vol. 27, p. 607-610.

Ultrasound measurements of stylolites were performed to evaluate paleostress directions in stylolitic rocks of the Muschelkalk Formation in Germany. The maximum ultrasound velocity is directed normally to the principal stress direction. Paleocompression is normal to two sets of stylolites, and ultrasound measurements indicate the relative ages of the two stylolite sets.

Mazullo, S.J., 1981, Facies and burial diagenesis of a carbonate reservoir: Chapman Deep (Atoka) field, Delaware Basin, Texas, AAPG Bulletin, vol. 65, p. 850-865.

Oomoldic porosity and gash fractures form in rock adjacent to stylolites. Both features decrease in abundance away from the stylolites. They represent the most dramatic effect of burial diagenesis on reservoir evolution. The rejuvenation of porosity helps counterbalance physical and chemical compaction.

Moore, C.H., and Druckman, Y., 1981, Burial diagenesis and porosity evolution, Upper Jurassic Smackover, Alkansas and Louisiana, AAPG Bulletin, vol. 65, p. 597-628.

Stylolitization occurs after mechanical compaction (grain breakage) and after intergranular pressure solution. The stratigraphic section has been reduced by at least 3% under 8000 feet (2438 meters) of burial. Rocks that were cemented with intergranular calcite spar early, under meteoric conditions, had their overall physical integrity established, and compaction by stylolitization is minor. Rocks that experienced only fibrous marine cement, and no early meteoric cement, prior to burial, were later subjected to compaction by grain adjustment and intergranular pressure solution, followed by stylolite development.

Nelson, R.A., 1981, Significance of fracture sets associated with stylolite zones, AAPG Bulletin, vol. 65, p. 2417-2425.

Stylolites are most common in zones of low porosity. They are filled with poorly sorted, fine-grained material, so they have low permeability compared to adjacent rock. Laboratory measurements of permeability associated with stylolite zones can be misleadingly large, owing to the presence of unloading fractures and tension gashes.

Stylolites develop during slow tectonic deformation, whereas tectonic fracture sets form during rapid deformation. Tension gashes are intimately associated with some tectonic stylolites, formed under triaxial compression. Stylolites related to overburden pressure generally develop under uniaxial compression, and hence lack tension gashes.

Stylolites develop at or in zones of low porosity, which have a high modulus of elasticity. They further reduce porosity by dissolution and precipitation. In a hydrocarbon reservoir, stylolites create zones of highly directional, reduced permeability and porosity. Permeability reduction is greater perpendicular to stylolites than parallel to them.

Webb, F.Jr., and Moore, T.D., 1981, Stylolitic cleavage as a mechanism for fold development in thrust belts exemplified by Mississippian limestones, Valley and Ridge Province, southwestern Virginia [abstract], GSA Abstracts with Programs, vol. 13, p. 577.

Stylolites are normal to bedding in grainstone, where they are responsible for dissolution of 16% to 30% of the rock. Dissolved material migrates into pores in adjacent, silty and sandy rock units. Stylolites developed during the initial phase of horizontal compression and preceded the major phase of folding. There are no horizontal stylolites, so overburden was not too heavy. Stylolites in synclinal troughs helped the rocks adjust to the shorter radius of curvature due to folding.

Wong, P.K., and Oldershaw, A., 1981, Burial cementation in the Devonian Kaybob Reef Complex, Alberta, Canada, Journal of Sedimentary Petrology, vol. 51, p. 507-520.

Porosity occlusion occurs mainly at depths in excess of four kilometers. Stylolites are the source of cement, based on correlation of compositional zones. Stylolites are associated with an increase in zoned cementation, and with a decrease in porosity and permeability of adjacent sediments. Porosity increases away from stylolites. Zoned calcite cements are

symmetrically disposed with respect to stylolites. Dolomite cements are not derived from pressure solution.

1982

Ague, J.J., and Birnbaum, S.J., 1982, Insoluble residue accumulations at pressure solution boundaries: Control on stylolite development and morphology [abstract], GSA Abstracts with Programs, vol. 14, p. 430.

Observations of the Silurian aged Lockport Formation indicate that sutured stylolites form where there is solubility contrast above and below stylolites, and relatively large, insoluble fragments. Planar seams form where solubility contrast is low above and below the seam. The authors derive a formula for stress dissipation due to pressure solution. After accumulation of residue reaches a critical thickness, it is capable of dissipating stress in such way that grain size becomes unimportant. Thus, stylolites become locked into position and their morphology remains unchanged after a sufficient amount of residue has accumulated.

Moore, C.H., and Brock, F.C.Jr., 1982, Porosity preservation in the Upper Smackover (Jurassic) carbonate grainstone, Walker Creek field, Arkansas: Response of paleophreatic lenses to burial burial processes--Discussion, Journal of Sedimentary Petrology, vol. 52, p. 12-23.

Porosity is controlled by a combination of grain size, sorting, and grain types associated with late cementation. Rock dominated by resistant grains, such as ooids and intraclasts, preserve porosity. Rocks with a mixture of hard and soft grains, such as oncolites and pellets, have occluded porosity because of preferential compaction of soft grains. Bimodal grain size distribution favors porosity preservation if the larger grains are resistant. Fine-grained, well-sorted rocks are susceptible to effective porosity loss through compaction. In rocks with small pores, small amounts of compaction cause comparatively large losses in effective porosity and permeability.

Pratt, B.R., 1982, Limestone response to stress: Pressure solution and dolomitization--Discussion and examples of compaction in carbonate sediments, Journal of Sedimentary Petrology, vol. 52, p. 323-334.

Many of H. R. Wanless's (1979) examples of non-seam and non-sutured-seam "pressure solution" may have been caused by mechanical compaction prior to lithification. Such clay seams wrap around uncompressed burrows, which become preserved in chert nodules.

Read, J.F., 1982, Geometry, facies, and development of Middle Ordovician carbonate buildups, Virginia Appalachians, AAPG Bulletin, vol. 66, p. 189-209.

Large skeletal buildups in lower Middle Ordovician rocks of the Valley and Ridge Province, Virginia, are similar to Waulsortian type buildups. Shallow ramp buildups, with wackestone and mudstone at the core, and skeletal grainstone and packstone at the base, top and flanks, lacks stylolites. Downslope buildups, with wackestone and mudstone at the core, mudstone and bafflestone along the periphery, and skeletal grainstone and packstone with shale stringers at the base, contains thin stylolites, parallel to stromatactoid cavities, in wackestone and mudstone, and well developed stylolites in grainstone and packstone. Sutured grain contacts and stylolite swarms occur in thin-bedded to nodular, skeletal grainstone along the deep flanks of downslope buildups.

Ruzyla, K., and Friedman, G.M., 1982, Geological heterogeneities important to future enhanced recovery in carbonate reservoirs of Upper Ordovician Red River Formation at Cabin Creek Field, Montana, Society of Petroleum Engineers Journal, vol. 1982, p. 429.

Stylolites occur in subtidal, dolomitic micstones, wackestones and packstones that tend to have small pore throats and poor reservoir quality. Non-stylolitic, intertidal to supratidal dolomicstones with idiotopic to hypidiotopic dolomite tend to have large pore throats and excellent reservoir quality.

Salameh, E., and Zacher, W., 1982, Horizontal stylolites and paleostress in Jordan, Neues Jahrbuch fuer Geologie und Palaeontologie, Monatshefte, vol. 1982, p. 509-512.

Tectonic stylolites, with horizontal columns, occur in Upper Cretaceous limestone, especially in a nodular unit. There are two sets of vertical stylolites, and columns within each set are perpendicular to known compressive structures. The orientations of the stylolites do not change over an

area of approximately 22,000 square kilometers. The stylolites occur along vertical joints and fractures.

Wagner, P.D., and Matthews, R.K., 1982, Porosity preservation in the Upper Smackover (Jurassic) carbonate grainstone, Walker Creek field, Arkansas: Response of paleophreatic lenses to burial processes, Journal of Sedimentary Petrology, vol. 52, p. 3-18.

Rocks that stabilized under fresh water phreatic conditions resisted later compaction by pressure solution, and thus remain porous during burial. Rocks that represent relict vadose and subphreatic environments where metastable at the onset of burial, and were stabilized in a burial diagenetic environment by solution compaction, so their porosity is low. Thus, carbonate rocks altered under fresh water conditions are physically and chemically set into a stable framework, which resists dissolution under loading. Metastable sequences undergo solution-compaction. Alternating sequences of porous and nonporous rock can develop under the influence of sea level changes. Well developed stylolites occur only in nonporous rocks located between porous intervals.

Yonkee, W.A., and Mitra, G., 1982, Solution cleavage in the Wyoming-Idaho thrust belt, GSA Abstracts with Programs, vol. 14, p. 355.

Evenly spaced, stylolitic cleavage occurs in micstones of the Twin Creek Formation. The stylolites fan around fold hinges. Calcite filled fractures formed sub-perpendicular to and concurrently with stylolites. Styloites developed before and during folding, as indicated by sigmoidal calcite fibers and local shear along stylolites. Illite and chlorite are concentrated within the stylolites as residue. Illite crystallinity increases along stylolites, suggesting structural ordering and loss of expandable layers, which is consistent with temperatures near 200° C. Illite transformation provided water as a flux, and clay minerals provided easy diffusion paths.

1983

Bathurst, R.G., 1983, The integration of pressure solution with mechanical compaction and cementation, In: Stylolites and Associated Phenomena, Special

Publication by Abu Dhabi National Research Foundation, p. 41-55.

Burial diagenesis involves four interrelated processes: mechanical compaction; groundwater flow; cementation; and pressure solution. Mechanical compaction, which may occur with or without particle breakage, is followed by pressure solution at grain contacts. This is followed by stylolite development along preexisting joints or lithologic contacts, which retain water during compaction, or around rigid bodies, such as large fossils, concretions, chert nodules or masses of dolomite crystals. Mechanical compaction reduces porosity from 70% to 35%, whereas chemical compaction reduces it further, from 35% to as little as 5%.

Applied stress is divided among fewer contact points in grainstone than in mudstone, so the threshold stress is higher in mudstone. However, there is no simple way of identifying interpenetrant contacts with certainty in mudstone. Transmission electron microscopy would help identify pressure solution contacts in mudstone.

Burrus, R.C., and Cercone, K.R., 1983, Fluid inclusion petrography and tectonic-burial history of the Al Ali No. 2 well: Evidence for the timing of diagenesis and oil migration, northern Oman Foredeep, Geology, vol. 11, p. 567-570.

Stylolites developed during rapid burial--flysch deposition--and tectonism in Cretaceous wackestones and packstones buried up to 4000 meters deep, in the United Arab Emirates. The stylolites cut across two sets of fractures containing hydrocarbon inclusions, so oil migration is thought to have stopped when the styloites formed. A later, non-oily fracture set offsets the stylolites.

Eller, M.C., 1983, Early diagenetic formation of clay microseams (microstylolites) without pressure solution, In: Stylolites and Associated Phenomena, Special Publication by Abu Dhabi National Research Foundation, p. 137-148.

Clay microseams may form during early diagenesis by dissolution of carbonate in unsaturated pore waters, and subsequent compaction. Albin red chalks of eastern England are thoroughly bioturbated, and dissolution of carbonate around burrows and their subsequent

compaction resulted in the formation of clay microseams around the burrows. Distinction between these clay seams and stylolitic seams is difficult, and early-formed clay seams may affect later stylolite development.

Gillet, S.L., 1983, Major, through-going stylolites in the lower Ordovician Goodwin Limestone, southern Nevada: Petrography with dating from paleomagnetism, Journal of Sedimentary Petrology, vol. 53, p. 209-219.

Stylolites develop preferentially along boundaries between contrasting lithologic units, such as between wackestone and packstone. Stylolites cut across late spar cement. Differential compaction occurs where stylolites wrap around chert nodules. Stylolites--especially large ones--are the latest major diagenetic feature. Stylolites formed last post-date most cementation. Cement formed during earlier stylolite development became consumed later by coalescing stylolites and advancing stylolite fronts.

Gratier, J.P., 1983, Quantitative studies of pressure solution-deposition in rocks: Natural and experimental aspects, In: Stylolites and Associated Phenomena, Special Publication by Abu Dhabi National Research Foundation, p. 67-80.

In experimental compression of aggregates of angular quartz and calcite grains, it was found that no dissolution-deposition occurs in dry aggregates, whereas dissolution-deposition, accompanied by porosity reduction, occur in wet aggregates of sodium hydroxide. Stylolites forma long preexisting inhomogeneities or discontinuities. In an open system, the spacing between stylolites equals the size of inhomogeneites, whereas in a closed system, the spacing equals the size of rigid zones, which are formed by precipitation.

Halley, R.B., and Schmoker, J.W., 1983, High-porosity carbonate rocks of South Florida: Progressive loss of porosity with depth, AAPG Bulletin, vol. 67, p. 191-200.

Porosity of carbonate rocks in southern Florida ranges from 45% near the surface to 25% at 2600 ft (800 m) of burial. At shallow depths, dolomite and limestone are equally porous. Neither mechanical compaction nor externally derived cement are major contributing

factors to porosity reduction. Mechanical compaction over pressure ranges equivalent to equivalent to depths of up to 2950 ft (900 m) reduces porosity to only 35%. Externally derived cement should predominate in the most permeable units, but data indicate little difference in porosity loss between permeable, aquifer lithologies and impermeable (aquiclude) lithologies.

Pressure solution is a significant cement-producing process, and it occurs at depths as shallow as 390 ft (120 m) along grain contacts in the Avon Park Limestone. This may be attributed to the presence of freshwater, with low magnesium content, within the formation. Stylolite seams also occur in mudstones. In highly porous rock, dissolution at grain contacts is by itself sufficient to reduce porosity significantly. Redeposition of cement derived from pressure solution is a relatively unimportant porosity-reducing mechanism.

Koepnick, R.B., 1983, Distribution and vertical permeability of stylolites within a Lower Cretaceous carbonate reservoir, Abu Dhabi, United Arab Emirates, In: Stylolites and Associated Phenomena, Special Publication by Abu Dhabi National Research Foundation, p. 261-278.

Bedding-parallel stylolites produce barriers to fluid flow, except if they developed after hydrocarbon entrapment. Where stylolites developed prior to hydrocarbon entrapment, abundant crystal nucleation sites were present immediately adjacent to the stylolite, allowing local precipitation of calcium carbonate derived from dissolution along the stylolites. Where stylolites developed after hydrocarbon entrapment, hydrocarbons inhibited precipitation of calcium carbonate by coating many of the nucleation sites within the reservoir, so that most of the calcite dissolved along stylolites was transported away fromt the stylolite zone prior to precipitation.

Lent, M.C., and Houseknecht, D.W., 1983, Stylolites in the Muddy Sandstone, Wyoming [abstract], GSA Abstracts with Programs, vol. 15, p. 626-627.

Stylolites are a common feature in barrier island facies of the Muddy Sandstone, Powder River Basin. Insoluble residue includes detrital, whole, and partially dissolved feldspar, along with carbonate rock fragments, and heavy minerals. Authigenic minerals

include heavy minerals (pyrite), kaolinite, and illite. Authigenic illite is principally indigeneous to stylolites. The ratio of rock dissolved to insoluble material accumulated is approximately 20 to 1.

Primary intergranular porosity is preserved in contact with stylolites, and in adjacent sandstone. Authigenic kaolinite is mechanically compacted along stylolites but not in host rock. These observations suggest that stylolite development is primarily a chemical dissolution process, not a pressure solution process, because pressure solution would have resulted in precipitation of quartz cement in the contact pores. Alternatively, pressure solution may have been involved, but hydrocarbons within pores may have prevented quartz precipitation.

Losonsky, G., 1983a, The structural and lithologic setting of tectonic stylolites in the northern end of the Abbs Valley Anticline, Monroe County, West Virginia, M.S. Thesis, University of Cincinnati.

Describes correlations between vertical stylolite morphology and lithologic facies in the Mississippian Greenbrier Limestone, southeastern West Virginia. Analyzes the structural relationships among stylolites, regional joint sets, and folds in the Allegheny Plateau.

Losonsky, G., 1983b, The structural setting of tectonic stylolites in the Allegheny Plateau, southeastern West Virginia [abstract], GSA Abstracts with Programs, vol. 15, p. 631

Summarizes M.S. thesis of same year on relationships among vertical stylolites, regional joint sets, and folds in the Mississippian Greenbrier limestone of the Appalachian Basin.

Meike, A., 1983, Microstructures of stylolites in limestone [abstract], GSA Abstracts with Programs, vol 15, p. 642.

Transmission electron microscopy indicates that plastic deformation in grains is localized at dislocations concentrated on the r-plane (10.4) of the calcite unit cell. Microfracturing or preferential dissolution along unstable planes can produce suture-like morphology in single grains, parallel to the r-plane. Strain-induced dissolution can occur after stress is released. Deformation conditions and grain characteristics differ between calcite-filling in stylolites and limestone host. The filling is characterized by e-twinning, whereas the host rock contains r-plane dislocations. The morphology of phyllosilicates within single calcite grains shows that some clay nucleated within preexisting calcite grains, indicating that the calcite is not a secondary crystallization product around the phyllosilicate. Hence, the clay is authigenic. Clay also nucleates at sites of local deformation along calcite slip planes.

Meyers, W.J., and Hill, B.E., 1983, Quantitative studies of compaction in Mississippian skeletal limestones, New Mexico, Journal of Sedimentary Petrology, vol. 53, p. 231-242.

Intergranular pressure solution increases with compaction intensity, whereas mechanical breakage is relatively insignificant. Primary control over intergranular pressure solution intensity rested in the degree of saturation of pore fluids with respect to calcite. Pre-Pennsylvanian aged ground water constituted the pore fluid. Where ground water was undersaturated with respect to calcite, pressure solution was greatest.

Overburden was tens to hundreds of meters thick, but less than 1000 meters. Stylolites cut across the youngest cement zone, indicating that they developed after intergranular porosity had been largely destroyed. Stylolites were of minor importance in decreasing intergranular porosity in Mississippian aged packstone and grainstone.

Nelson, R.A., 1983, Localization of aggregate stylolites by rock properties, AAPG Bulletin, vol. 67, p. 313-322.

Inhomogeneities in fabric and composition are prerequisite to stylolite development. Stylolites typically develop along lithologic boundaries, such as beween dolomite and limestone. There are two possible reasons for this: (1) stylolite development began within the limestone, and stopped when the less soluble dolomite was encountered, or (2) stylolite development was initiated along the contact owing to stress concentration arising from the contrasting mechanical properties.

Stylolites are generally found in zones of low porosity in well cores. Low porosity zones may have formed during early diagenesis, and served to localize

stylolites, or the zones may have formed late in diagenesis, as a result of reprecipitation of pressure-dissolved matter. Stylolites may be localized by porosity variations in otherwise homogeneous sections. Stylolites commonly occur on planes of discontinuity, such as bedding planes, fractures, shale, or clay beds. Bedding planes and fractures may perturb the stress state, whereas clay or shale beds may act as catalysts to the dissolution process.

The location of stylolites in a hydrocarbon reservoir is due to interaction between stress conditions and lithology. Point load hardness mapping may be useful in making reservoir descriptions. Variations in hardness reflect cementation, which is related to stylolites. In some cases, there is a decrease in rock hardness away from the stylolite, whereas in other cases, no such decrease is detected, probably because of overall low porosity (< 1%).

Purser, B.H., 1983, Stratiform stylolites and the distribution of porosity: Examples from the Middle Jurassic limestones of the Paris Basin, In: Stylolites and Associated Phenomena, Special Publication by Abu Dhabi National Research Foundation, p. 203-217.

Stylolites constitute a stratiform barrier to fluid migration. Stylolites are sources of pore-destroying calcite during late diagenesis. Early diagenetic, pre-burial cements, precipitated from near-surface meteoric waters, do not normally result in total destruction of primary porosity. Early, pre-burial lithification, or partial cementation, of carbonate sediment tends to retard or prevent stylolite development and other compacational phenomena related to burial. Carbonate material liberated by stylolite development during burial may constitute part of the pore occluding, late sparitic cement. Carbon isotopes of sparitic cement and enclosing sediments are comparable. Stylolites also post-date late sparry cement.

Ricketts, B.D., 1983, The evolution of a Middle Precambrian dolostone sequence--a spectrum of dolomitization regimes, Journal of Sedimentary Petrology, vol. 53, p. 565-586.

Stylolites are most prominent in stromatolitic lithologies. Stylolites postdate pervasive dolomitization. Coarse dolomite crystals do not obliterate stylolites. The dolostones occur in a Middle

Precambrian carbonate-clastic platform succession in the Belcher Islands, Hudson Bay.

Schofield, K., 1983, Are pressure solution, neomorphism and dolomitization genetically related? In: Stylolites and Associated Phenomena, Special Publication by Abu Dhabi National Research Foundation, p. 183-202.

The mechanical contrast between dolomite and calcite is such that any dolomite within a limestone sequence would constitute an anisotropy. Increasing strain around growing dolomite crystal clusters causes calcite to go into solution. Migration of dissolution fronts results in neomorphic recrystallization. Eventually, as the dolomite crystals amalgamate to form a framework, the increase in differential stress causes ions to migrate out of the immediate area of dissolution, and neomorphism is succeeded by pressure solution. Stylolites may develop by a similar mechanism of dissolution and removal of material along a migrating fluid film. A stylolite may represent the coalescence of a number of much smaller films, or the propagation of a single widespread inhomogeneity such as a change in lithology.

Diffusion of significant amounts of carbonate in solution is not viable except over small distances, even with the considerable improvement in the efficiency of diffusion mechanisms with depth. In an open pore system, ionic transfer would be by fluid flow, which is more efficient. A stylolite may continue to grow despite significant buildup of insoluble material, by fluid flow through the center of the seam, while a thin film would be maintained along the stylolite-host interface.

Sellier, E., 1983, The mechanical approach as an hypothesis for stylolite genesis, In: Stylolites and Associated Phenomena, Special Publication by Abu Dhabi National Research Foundation, p. 57-65.

Stylolites are numerous where porosity is low (1-7%), but rare where porosity is high (10-35%). Stylolites form at discontinuities between rock units. These may be lithologic contacts or grain contacts. Mechanical deformation occurs along stylolites prior to dissolution, and it leads to the creation of an irregular discontinuity. Planar stylolites remain planar, V-shaped ones become flat with further dissolution, and U-shaped, columnar stylolites grow in amplitude with continuing dissolution.

Stylolites act as barriers to fluid migration if residue is present, or they may act as drains, or zones of circulation and deposition. Two feedback mechanisms involving stylolite development are possible. In the first mechanism, stylolites cause reduction of porosity, but they also require porosity reduction for continued growth. In the second mechanism, stylolites create directional flow, but they also require directional flow for continued growth.

Wanless, H.R., 1983, Styles of pressure dissolution, In: Stylolites and Associated Phenomena, Special Publication by Abu Dhabi National Research Foundation, p. 81-105.

Pressure solution requires stressed crystal surfaces, and fluid paths for material transfer. This can occur beginning at burial depths of 300 meters. Jagged stylolites and grain contact sutures occur in clean limestone, with low clay and organic matter content, and with minor coarse solubles. Columnar stylolites occur in clean, silty limestones. If the resistance contrast is high, the stylolites will have low relief. Non-sutured seams , or microstylolite seams and swarms, occur in limestone with much clay, platy silt, or organic matter. Shearing occurs along such stylolites. Pervasive, non-seam dissolution occurs in clean limestones with many, finely crystalline, responsive units. Nodular limestones are the result of pressure dissolution in clayey, responsive limestone.

Pressure solution involved precipitation of new minerals, and it is affected by fluid pressure and impurities. It can lead to enhanced porosity and permeability by creating new rock fabric. Resistant units have no response to stress, whereas responsive units undergo pervasive deformation--either elastic, or dissolution. Impurities affecting responsiveness of limestone to stress include fine, platy insolubles, such as clay and organic matter; and magnesium cations.

A feedback mechanism occurs where a styloltie is adjacent to dissolving rock on one side, and non-dissolving rock on the other side, which hardens by cementation. Dissolution of impurities, such as magnesium, leads to the formation of new minerals, such as dolomite. Dissolved ions are locally precipitated.

Wong, P.K., 1983, Origin of low permeability zones in the Upper Devonian Kaybob Reef, Alberta, Canada, In: Stylolites and Associated Phenomena, Special

Publication by Abu Dhabi National Research Foundation, p. 247-260.

Stylolites occur most commonly in carbonaceous and micritic facies, representing deepest, lowest-energy environments. These environments are found in the basal portions of lagoonal cycles, which have low depositional permeabilities that are further reduced by stylolite development and concomitant calcite cementation. Similar lithologies and stylolite morphologies also occur in parts of the reef foreslope. Grainy, micrite-poor deposits in the middle and upper portions of the reef interior cycles are generally porous and lack stylolites. Both non-sutured dissolution seams and stylolites occur in the lower and middle foreslope deposits, which are carbonaceous and micritic.

Zenger, D.H., 1983, Burial dolomitization in the Lost Burro Formation (Devonian), east-central California, and the significance of late diagenetic dolomitization, Geology, vol. 11, p. 519-522.

Dolomitization occurs subsequently to the onset of stylolite development. Some pressure solution occurs after dolomitization. Dolomite also forms along stylolites. Dolomite crystals truncate stylolites, indicating that they do not constitute insoluble residue.

1984

Bhattacharyya, A., and Friedman, G.M., 1984, Experimental compaction of ooids under deep-burial diagenetic temperatures and pressures, Journal of Sedimentary Petrology, vol. 54, p. 362-372.

Ooids from the Persian Gulf were stressed to a maximum of 1565 kg/cm^2 (1.5 kilobars), equivalent to 6.5 km of burial depth. Temperatures ranged from 150° C to 200° C, simulating a burial diagenetic environment. Pore fluid consisted of marine water or distilled water, and water was not allowed to escape the test sample. Bulk volume reduction was 21% for distilled water samples, regardless of pressure. The volume reduction occurred at pressures below 927 kg/cm^2 (0.9 kilobars), representing 3.88 km burial depth. Porosity reduction was 40% for distilled water, regardless of pressure or temperature. Bulk volume reduction for marine water was identical to that for distilled water at intermediate pressures of 1318 kg/cm^2 (1.3 kilobars), representing 5.25 km burial depth. Bulk volume reduction for marine water was higher than that for distilled water at pressures both higher and lower than intermediate pressure; it was highest at the maximum pressure.

Types of grain contacts include longitudinal and concavo-convex shapes, representing plastic deformation; sutured contacts, representing pressure solution; and point contacts, representing no deformation. The ratio of concavo-convex contacts over sutured contacts is greater in marine water than in distilled water. Pressure solution is enhanced by water purity, slow pressure increase, and high temperature. Sutured and concavo-convex conctacts do not grade into each other. Instead, they appear to be responses to independent processes.

Budai, J.M., 1984, Dedolomitization in tectonic veins and stylolites: Evidence for rapid fluid migration during deformation, AAPG Bulletin, vol. 68, p. 458-459.

In Mississippian aged dolostones of the Madison Group, oxygen and carbon isotope values (^{18}O and ^{13}C) indicate that mineralization along stylolites and veins occurred during Jurassic and Tertiary thrust-belt deformation, in the presence of allochthonous pore fluids.

Cluff, R.M., 1984, Carbonate sand shoals in the Middle Mississippian (Valmeyeran) Salem-St. Louis-St. Genevieve Limestone, Illinois Basin, In: Carbonate Sands--A Core Workshop, SEPM Core Workshop No. 5, p. 94-135.

Illustrates and describes sedimentary facies in Missippian Limestones of the Illinois Basin, and explains the depositional environment of each facies.

Henderson, R.A., 1984, Diagenetic growth of euhedral megaquartz in the skeleton of a stromatoporoid, Journal of Sedimentary Petrology, vol. 54, p. 1138-1146.

Microstylolite seams occur in Middle Devonian Burdekin Formation, a well-cemented, biostromal limestone. The seams follow laminae, and they are associated with organic debris, goethite and megaquartz crystallites. The quartz crystals predate the stylolites, because they exhibit strain across the stylolites. The stylolites are associated with galley enlargement in stromatoporoids by growth of neomorphic calcite spar, suggesting local precipitation of stylolite-derived calcite.

Calcite dissolved by stylolite was replaced by silica derived from adjacent sandstone beds. Two-way diffusion occurred along micropore network connecting intergranular films with films along stylolites. Stylolite-related strain field extended into adjacent sediment, evidenced by curved cleavage traces, rendering the sediment susceptible to dissolution.

Houseknecht, D.W., 1984, Influence of grain size and temperature on intergranular pressure solution, quartz cementation, and porosity in a quartzose sandstone, Journal of Sedimentary Petrology, vol. 54, p. 348-361.

Cathodoluminescence petrography and scanning electron microscopy of Middle Pennsylvanian quartzose Hartshorne Sandstone, Arkoma Basin, reveals that pressure solution decreases linearly with increasing mean grain size, while the volume of quartz cement and porosity both increase with increasing grain size. Thermal maturity increases the amount of pressure solution. In areas of low thermal maturity, the volume of intergranular cement is greater than the volume of pressure-dissolved quartz, whereas in areas of high thermal maturity, more quartz has been dissolved by intergranular pressure solution than is present as cement.

Meike, A., 1984, A model of incipient solution cleavage formation [abstract], Geological Society of America Abstracts with Programs, vol. 16, p. 592.

Transmission electron microscopy of the Scaglia Rossa Formation of Italy suggests that solution cleavage is similar to stress corrosion cracking in metal (ASTM STP #610). The aggregate loses cohesion below the expected yield point by selective corrosion. Dissolution occurs preferentially in the slip-plane direction (10.4 in calcite), and preferentially in crystals where the slip plane is parallel to the direction of maximum shear stress. Dissolution occurs where there is a high concentration of dislocations. Solution cleavages are therefore inclined to the principle stress direction. Solution cleavage dominates at temperatures, pressures and strain rates where corrosion keeps pace with deformation. At higher strain rates and in the absence of water, brittle deformation is favored, while higher temperatures and pressures favor ductile deformation.

1985

Alsharhan, A.S., 1985, Depositional environment, reservoir units evaluation and hydrocarbon habitat of Shuaiba Formation, Lower Cretaceous, Abu Dhabi, United Arab Emirates, AAPG Bulletin, vol. 69, p. 899-912.

Where stylolites are numerous, they cause a decrease in permeability, resulting in moderate to poor reservoir quality. Stylolites are numerous in a chalky lime mudstone (open to restricted marine setting); in a unit consisting of alternating argillaceous lime mudstones and packstones to wackestones (deep open-marine conditions with low energy); in dense and argillaceous lime mudstones and wackestones (lagoon margin); and in lime mudstones to wackestones (protected shallow-marine shelf or lagoon). Where stylolites are sparse, they do not significantly affect permeability, and reservoir quality is moderate to good. Stylolites are sparse, but present, in units consisting of lime mudstones to wackestones or packstones (shallow protected-marine to shallow open-marine shelf); and in algal lime mudstones (moderate to high-energy shelf or lagoon deposits). Stylolites are absent in a unit consisting of chalky and dolomitic wackestones to packstones, alternating with dense, argillaceous lime mudstones to wackestones with sparry calcite and dolomite (low-energy, shallow, open-marine deposit), which has low permeability and poor reservoir quality.

Ekdale, A.A., and Bromley, R.G., 1985, Multiple parallel microstylolites and early diagenetic pressure solution in chalk, AAPG Bulletin, vol. 69, p. 252.

Virtually uncemented chalk commonly exhibits extensive microstylolitization. Multiple parallel microstylolites occur in homogeneous, white chalks of Denmark. The stylolites are planar to slightly wavy. They are evenly spaced, so the chalk looks laminated. The stylolitic laminae are diagenetic, because they are imprinted on top of a totally bioturbated ichnofabric. Seams cut through burrows or are diverted around them. Relationships of microstylolites with microfractures and trace fossils, especially Zoophycos, suggest that the microstylolites are very early diagenetic in

origin, postdating the burrows but predating or coinciding with microfractures.

Losonsky, G., 1985, Localized pressure solution and stylolite growth in the Allegheny Plateau [abstract], Symposium on Deformation of the Middle Appalachian Foreland, GSA Abstracts with Programs, vol. 17, p. 32.

Presents the hypothesis that tectonic stylolites develop as either rigid or insoluble inclusions within host limestone.

Ruzyla, K., and Friedman, G.M., 1975, Factors controlling porosity in dolomite reservoirs of the Ordovician Red River Formation, Cabin Creek Field, Montana, In: Carbonate Petroleum Reservoirs, P.O. Roehl and P.W. Choquette, Eds., Springer-Verlag, New York, p. 39-58.

Stylolites are most abundant in subtidal biomicrite-wackestones and least abundant in supratidal dolomites. The lower abundance in fine-grained dolomites may reflect relative resistance of dolomite to pressure solution. The stylolites are mostly irregular, low-amplitude, and sub-horizontal. They commonly form groups, especially if they have short columns (low amplitude). Porosity is restricted to the dolomite units, which are non-stylolitized. Subtidal zones represent the lower portions of shoaling-upwards cycles.

Scholle, P.A., and Halley, R.B., 1985, Burial diagenesis: out of sight, out of mind, In: Carbonate Cements, N. Schneidermann and P.M. Harris, Eds., SEPM Special Publication No. 36, p. 309-334.

Porous carbonate sediments become well-cemented, low-porosity carbonate rocks in the subsurface. Near-surface, porosity is reduced to 30% by dewatering, grain reorientation, and grain breakage. Beyond 30%, pressure solution at grain contacts and along stylolites or solution seams, along with reprecipitation of calcite as cement, is responsible for porosity loss. Carbonate rock porosity may be reduced to almost zero without significant introduction of allochthonous cementing material.

To fill pores with externally derived cement, 10,000 to 50,000 pore volumes of water are needed, because calcite is only slightly soluble in subsurface waters. This suggests that much of the cement is

derived locally, mostly by pressure solution. Transport is by diffusion and fluid flow.

Early diagenesis may retard later mechanical or chemical compaction. Fresh-water alteration causes mineralogical stabilization, lithification, decreased permeability, and preserved porosity.

Near-surface meteoric diagenesis results in enrichment of ^{12}C in limestones, but most Phanerozoic marine limestones have the same range of carbon isotope values as modern marine shells and carbonate sediments, and are not enriched in ^{12}C, so the vast majority of ancient limestones were cemented mainly during the compactional phase of burial diagenesis. The cement material was released by pressure solution. Since isotopic signatures vary over distances of meters, it appears that the source of cement is local.

Simpson, J., 1985, Stylolite-controlled layering in an homogeneous limestone: pseudo-bedding produced by burial diagenesis, Sedimentology, vol. 32, p. 495-505.

Stylolites are evenly spaced in lower Carboniferous age, High Tor Limestone formation of the Gower, South Wales. The creation of layering supports the hypothesis of self-patterning in limestones by pressure solution.

1986

Braithwaite, C.J.R., 1986, Mechanically induced stylolites and loss of porosity in dolomites, Journal of Petroleum Geology, vol. 9, p. 343-348.

Devonian age dolomites from wells in the northwestern United States and southern Canada, at depths of 975 to 1700 meters (3200-5600 ft), contain clusters of stylolites, which are associated with areas in which irregular dolomite crystals are separated by consertal tesselated boundaries, creating a network of interweaving sutured seams (fitted fabric). Stylolites are associated with broken zones, which are packed with fragments of collapsed, mechanically broken dolomite crystals. Stylolite development is accompanied by localized mechanical collapse, which leads to stress concentrations, and hence, to further dissolution. Fractures and collapsing vugs provide pathways for escaping fluids.

Devaney, K.A., Wilkinson, B.H., and Van der Voo, R., 1986, Deposition and compaction of carbonate clinothems: the Silurian Pipe Creek Junior complex of east-central Indiana, GSA Bulletin, vol 97, p. 1367-1381.

Compaction mechanisms vary in different lithofacies. Dewatering causes 50% compaction of mudstone and 13% compaction of grainstone-mudstone units. Pressure solution is most intense in grainstone-mudstone facies. Dissolution thinned mudstone units by 8%, grainstone units by 3%, and combined grainstone-mudstone units by 17%. Stylolites occur in facies consisting of grainstone-mudstone graded couplets. On average, 34% of bedding planes in grainstone-mudstone units are stylolitic. Stylolite columns are up to 5 cm tall. Stylolites occur preferentially along inclined, mudstone-grainstone contact surfaces.

Hicks, B.D., Applin, K.R., and Houseknecht, D.W., 1986, Crystallographic influences on intergranular pressure solution in a quartzose sandstone, Journal of Sedimentary Petrology, vol. 56, p. 784-787.

Petrofabric study of Bromide Sandstone, Simpson Group, Oklahoma, reveals that the orientations of optic axes in opposing grains have no significant influence on the type (geometry) of grain contact resulting from pressure solution. Geometries include planar, concavo-convex, and sutured. The only crystallographic influence was that in grains with concavo-convex contacts, the optic axis of the concave grain tends to define a lower angle with the pole of the contact plane than does the optic axis of the convex grain. This reflects the greater solution rate of quartz along its optic axis.

Lamborg, A.D., 1986, Subsurface geology and petrography of the Salem Limestone in portions of Hamilton, White, and Wayne counties, Illinois, M.S. Thesis, University of Cincinnati.

Provides detailed petrographic examination of each sedimentary facies within the Salem Limestone, and discusses their depositional environments. Includes photomicrographs of stylolites.

Schmoker, J.W., and Hester, T.C., 1986, Porosity of the Miami Limestone (Late Pleistocene), lower Florida Keys, Journal of Sedimentary Petrology, vol. 56, p. 629-634.

Study of the amount and variability of porosity in late Pleistocene oolitic grainstones shows that porosity variability is low (5-10%), mostly due to small-scale, primary sedimentary fabric. This implies that significant porosity loss and porosity diversity in ancient oolites develop during burial diagenesis. The rocks were subjected to fresh-water diagenesis, above sea level. The aragonite content is 40%, so it is no yet approaching mineralogical stabilization. The matrix porosity is 36%; initial porosity was 40-45%. Pore volume is enhanced by moldic porosity; it is occluded by micritic envelopes, drusy calcite mosaic, and sparry caocite. Dissolution of aragonite and its precipitation as calcite results in reduction of pore volume. Complete inversion of aragonite to calcite in fresh-water environments would reduce porosity further to 20-30%. This is much higher than typical North American carbonate reservoirs, suggesting that considerable loss of porosity occurs during burial.

1987

Cercone, K.R., and Lohmann, K.C., 1987, Late burial diagenesis of Niagaran (Middle Silurian) Pinnacle Reefs in Michigan Basin, AAPG Bulletin, vol. 71, p. 156-166.

Long residence time in the deep subsurface, where temperature and pressure are high, promotes diagenetic alteration, but high salinity and slow rates of groundwater flow typical in deep subsurface environments inhibit diagenesis. In rapidly buried, up to 2,200 m deep reef rock, fluid flow was driven by gravity or compaction. Diagenetic phases occur in stylolite-related fractures and solution voids, and they include geopetal diagenetic sediment, disseminated pyrite, pyrobitumen and liquid hydrocarbons, rhombic dolomite, and late equant calcite spar. The calcite spar postdates the dolomite cement, and fluid inclusions indicate temperatures ranging from 80 to 120 degrees C.

Oxygen isotope data suggest that parent fluids of late calcite and dolomite cements were brines that equilibrated in regional aquifers or marine carbonates before entering the reefs. Connate reef fluids did not precipitate the cements. The cements are insufficiently depleted in ^{18}O to have precipitated from modern brines or Silurian ocean water.

1990

Finkel, E.A., and Wilkinson, B.H., 1990, Stylolitization as source of cement in Mississippian Salem Limestone, west-central Indiana, AAPG Bulletin, vol. 74, p. 174-186.

Vertical textural profiles in stylolite-bounded units are inconclusive concerning controlling factors of stylolite development. Trace element trends for whole-rock analysis in the same units are also inconclusive. Increases in Fe and Mg near stylolites may be related to weathering, since seams are conduits for meteoric water. Increase in Fe away from stylolites is not observed. Stylolites do not appear to affect the trace element distribution; other textural inhomogeneities control it, instead.

1991

Pryor, W.A., Lamborg, A.D., Roberts, M.J., Tharp, T.C., and Wilsey, W.M.L., 1991, Geologic controls on porosity in Mississippian limestone and sandstone reservoirs in the Illinois Basin, In: Interior Cratonic Basin, by Leighton, M.W., Kolata, D.R., Oltz, D.F., and Eidel, J.J., AAPG Memoir 51, pp. 329-359.

Summarizes depositional facies of Mississippian age formations in Illinois Basin. Analyzes eogenetic, mesogenetic and diagenetic history of the basin. Includes Valmeyeran and Chesterian Series isopach map, burial history chart, petrographic information, and detailed discussions of porosity distribution in various Mississippian formations in the Illinois Basin. The role of stylolites in Valmeyeran limestones is mentioned.

APPENDIX A

X-Ray Diffraction Results

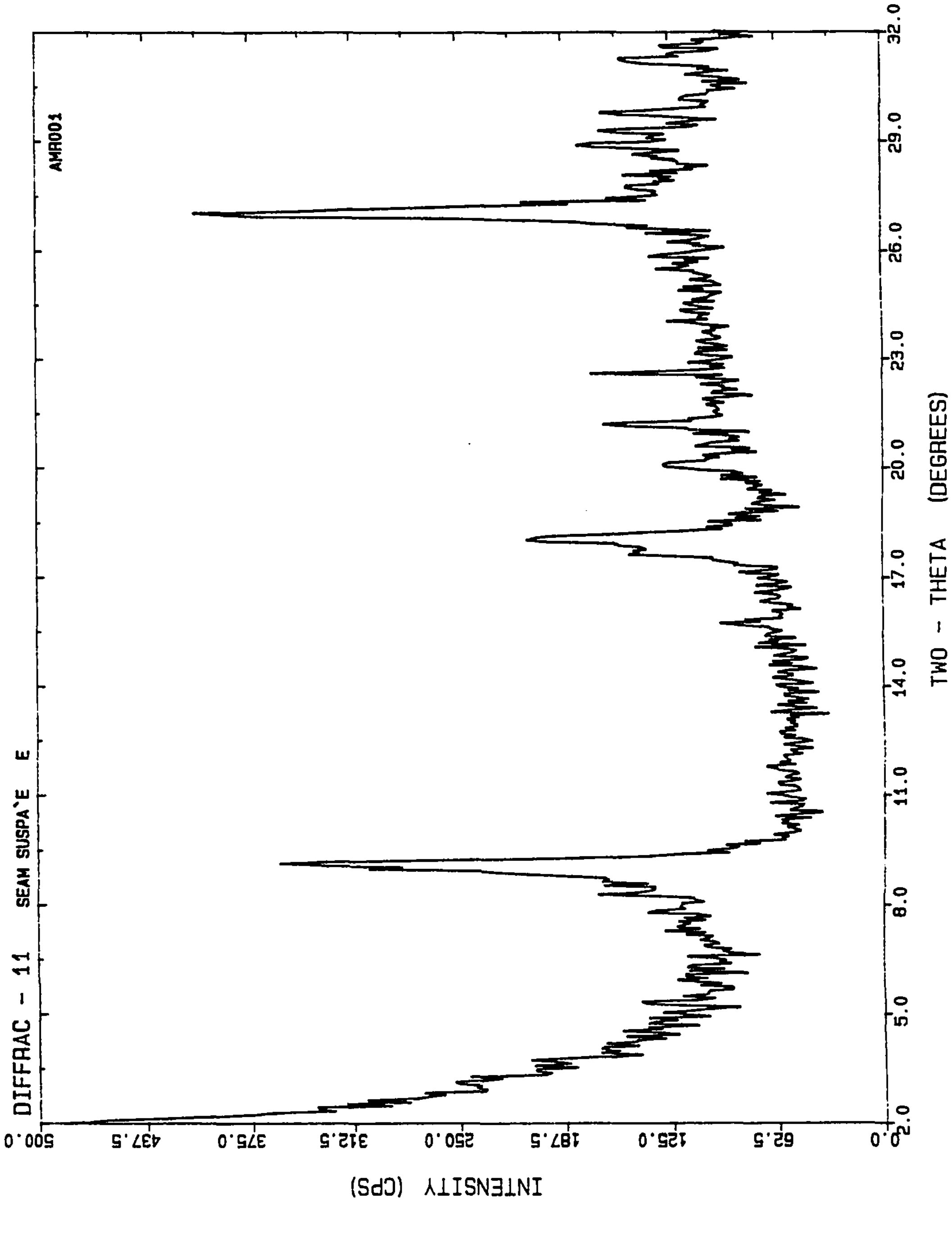
DIFFRAC - 11
SEAM SUSPA`E E
AMR001
TWO - THETA (DEGREES)
INTENSITY (CPS)
2.0
5.0
8.0
11.0
14.0
17.0
20.0
23.0
26.0
29.0
32.0
0.0
62.5
125.0
187.5
250.0
312.5
375.0
437.5
500.0

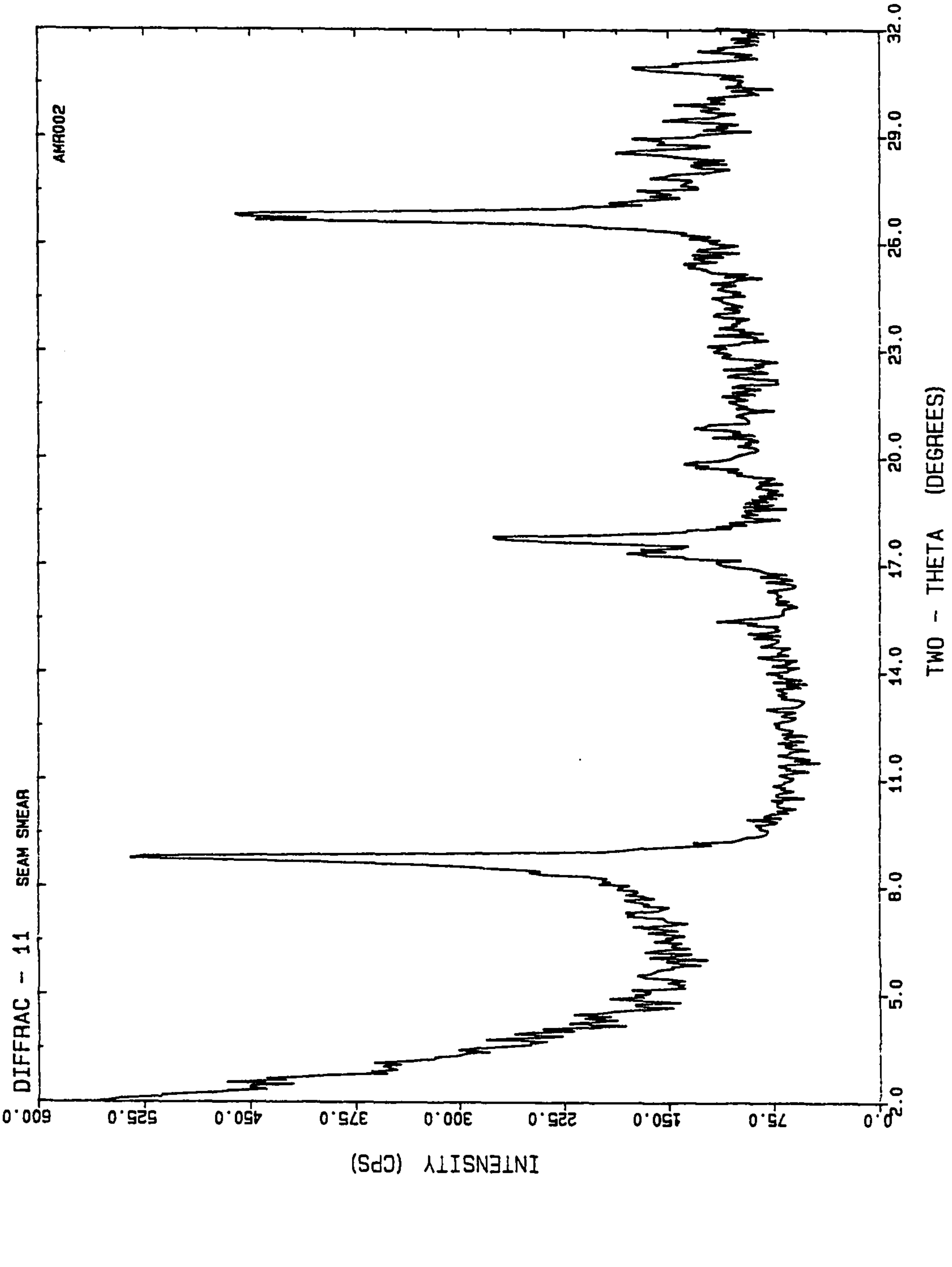
DIFFRAC - 11
SEAM SMEAR
AMR002
INTENSITY (CPS)
600.0
525.0
450.0
375.0
300.0
225.0
150.0
75.0
0.0
2.0
5.0
8.0
11.0
14.0
17.0
20.0
23.0
26.0
29.0
32.0
TWO - THETA (DEGREES)

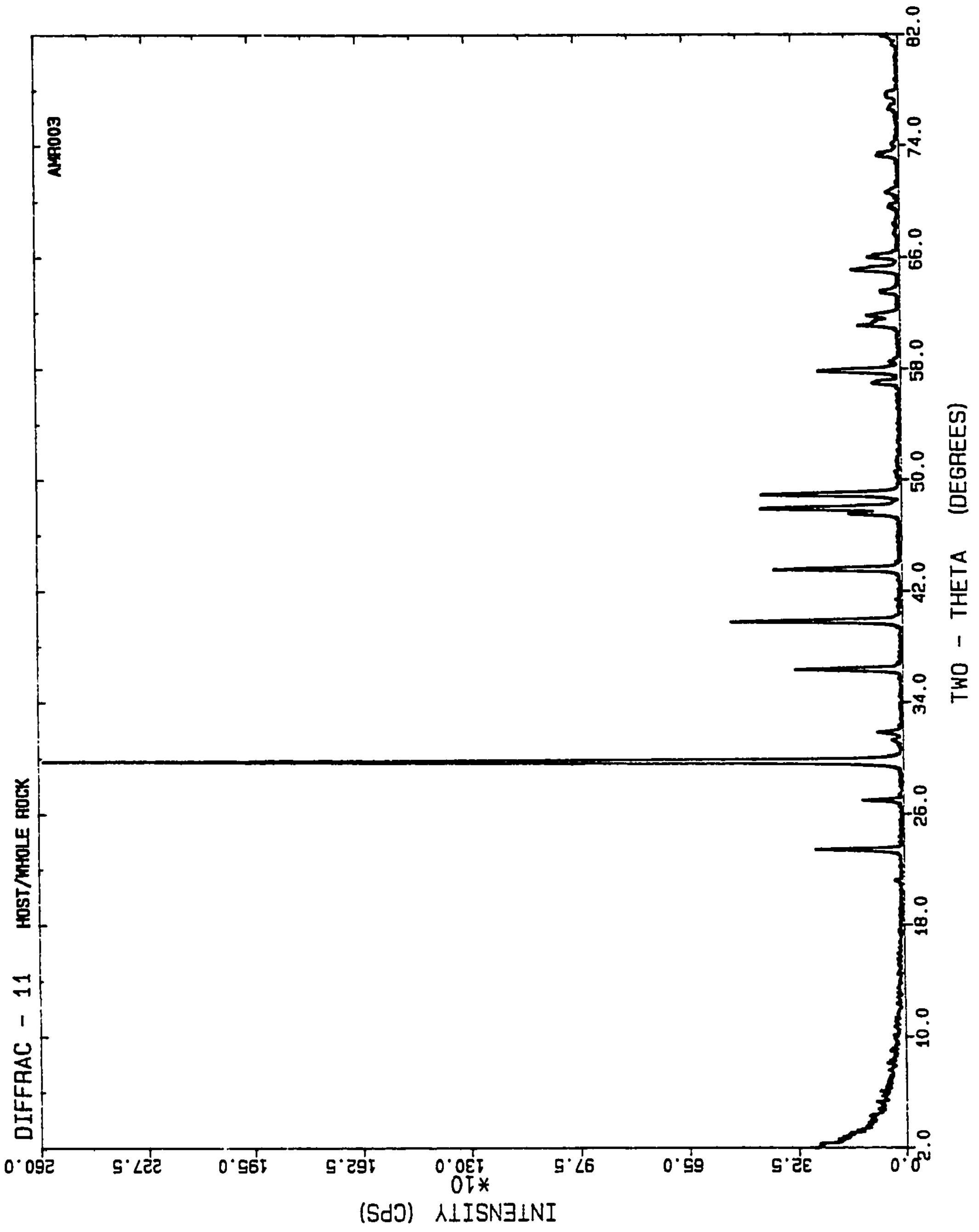

DIFFRAC - 11
HOST/WHOLE ROCK
AMR003
TWO - THETA (DEGREES)
2.0
10.0
18.0
26.0
34.0
42.0
50.0
58.0
66.0
74.0
82.0
INTENSITY (CPS)
*10
0.0
32.5
65.0
97.5
130.0
162.5
195.0
227.5
260.0

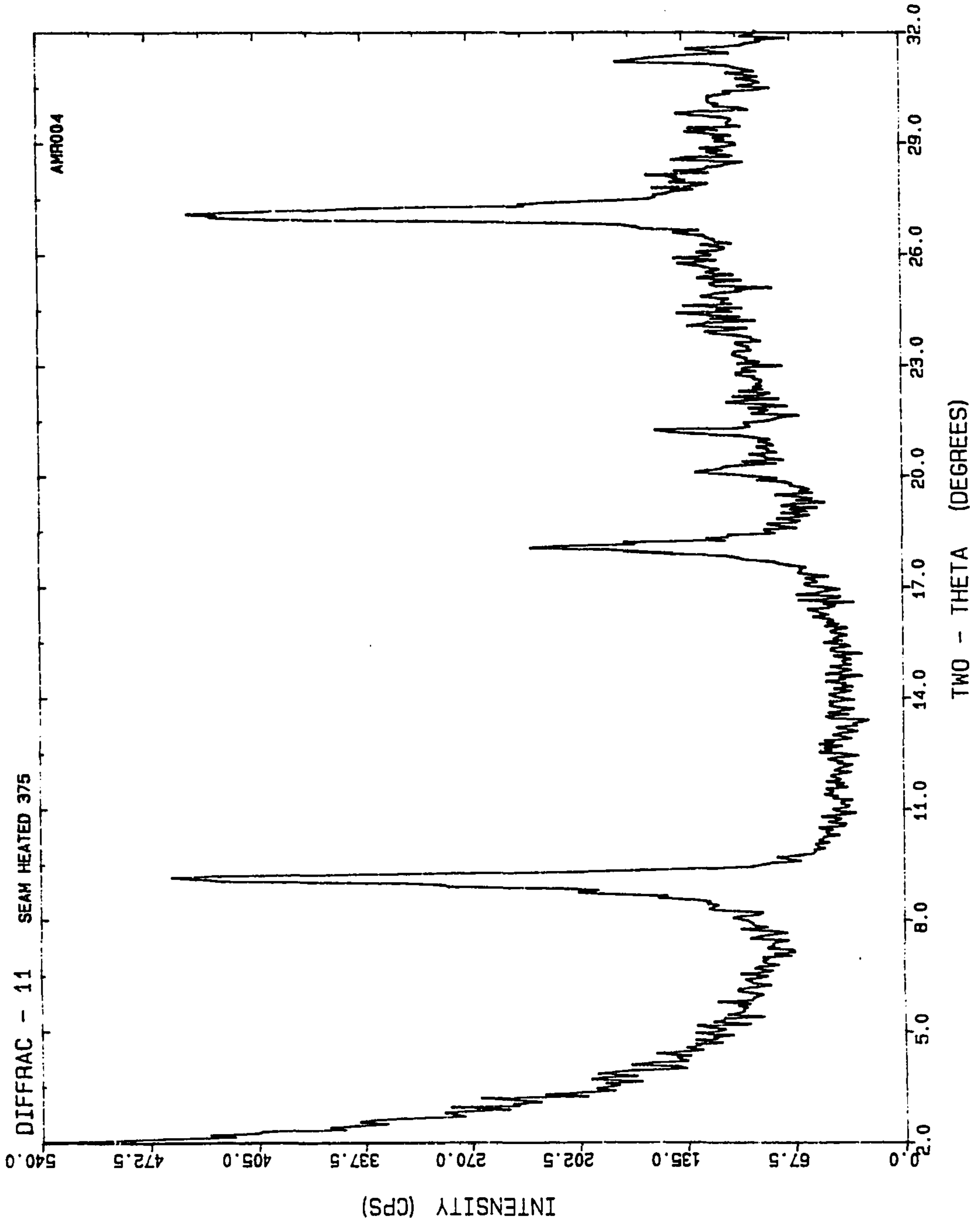

DIFFRAC - 11
SEAM HEATED 375
AMR004
TWO - THETA (DEGREES)
INTENSITY (CPS)
2.0
5.0
8.0
11.0
14.0
17.0
20.0
23.0
26.0
29.0
32.0
0.0
67.5
135.0
202.5
270.0
337.5
405.0
472.5
540.0

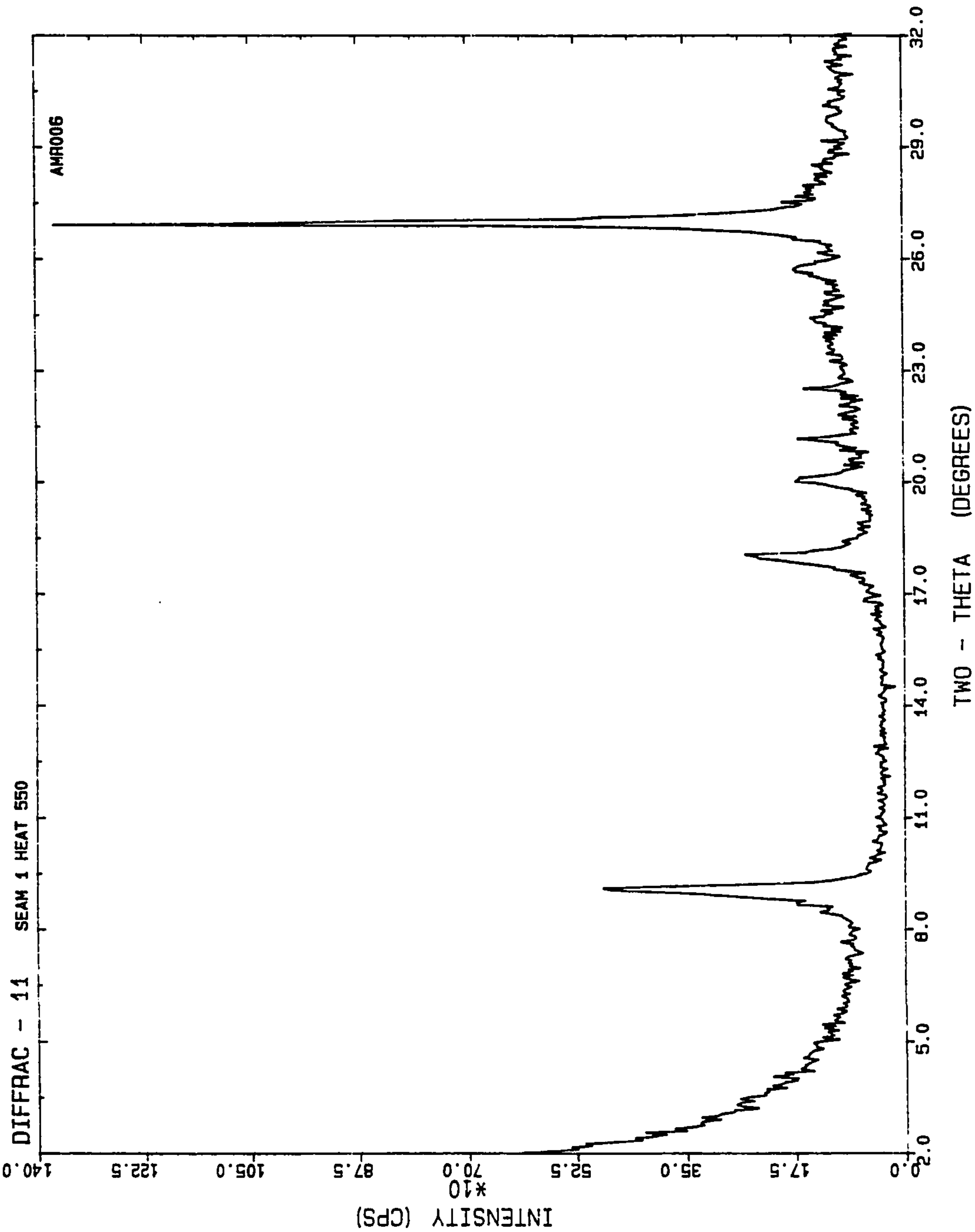
DIFFRAC - 11
SEAM 1 HEAT 550
AMR006
TWO - THETA (DEGREES)
INTENSITY (CPS)
*10
2.0
5.0
8.0
11.0
14.0
17.0
20.0
23.0
26.0
29.0
32.0
0.0
17.5
35.0
52.5
70.0
87.5
105.0
122.5
140.0

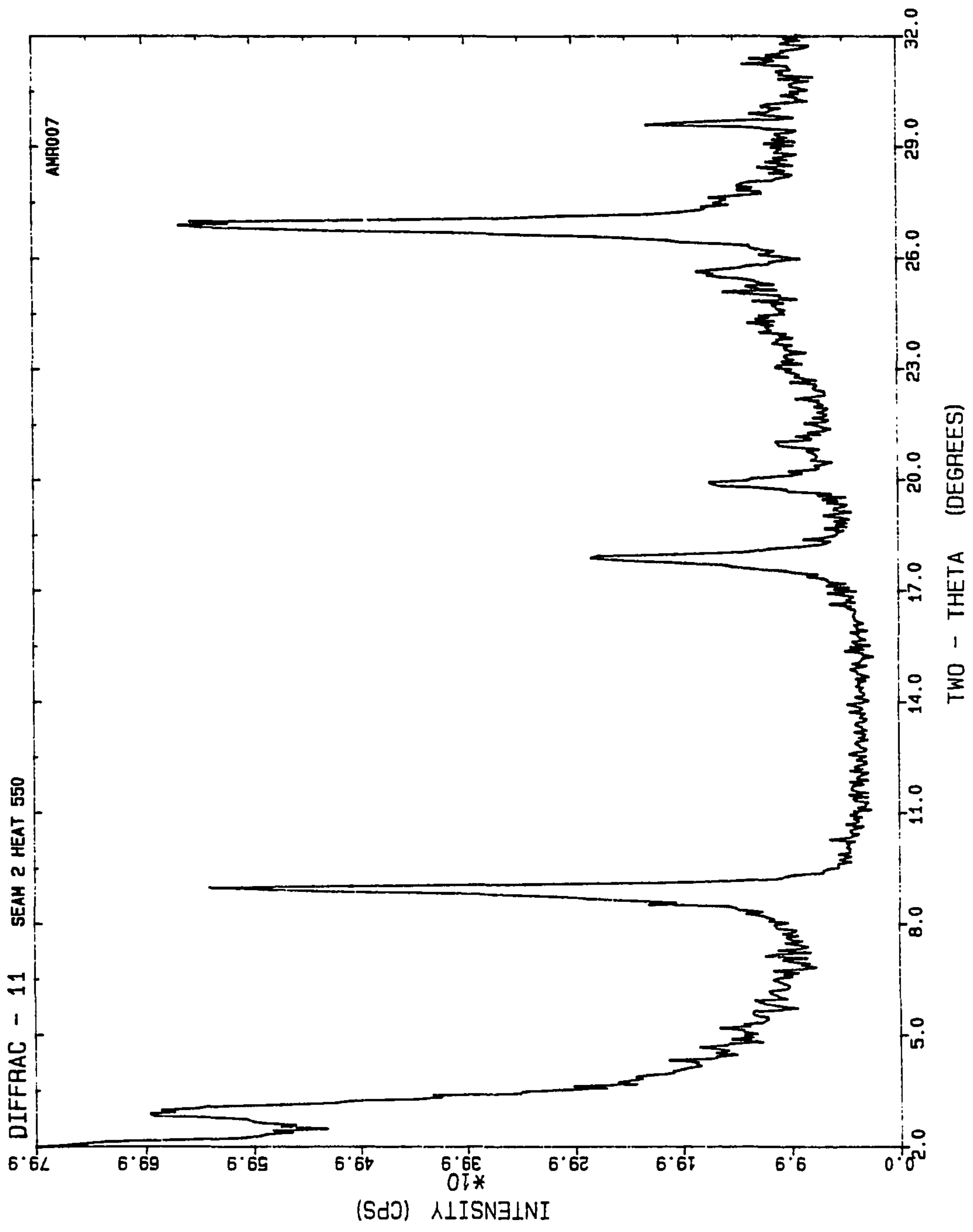
DIFFRAC - 11
SEAM 2 HEAT 550
AMR007
INTENSITY (CPS)
*10
79.9
69.9
59.9
49.9
39.9
29.9
19.9
9.9
0.0
2.0
5.0
8.0
11.0
14.0
17.0
20.0
23.0
26.0
29.0
32.0
TWO - THETA (DEGREES)

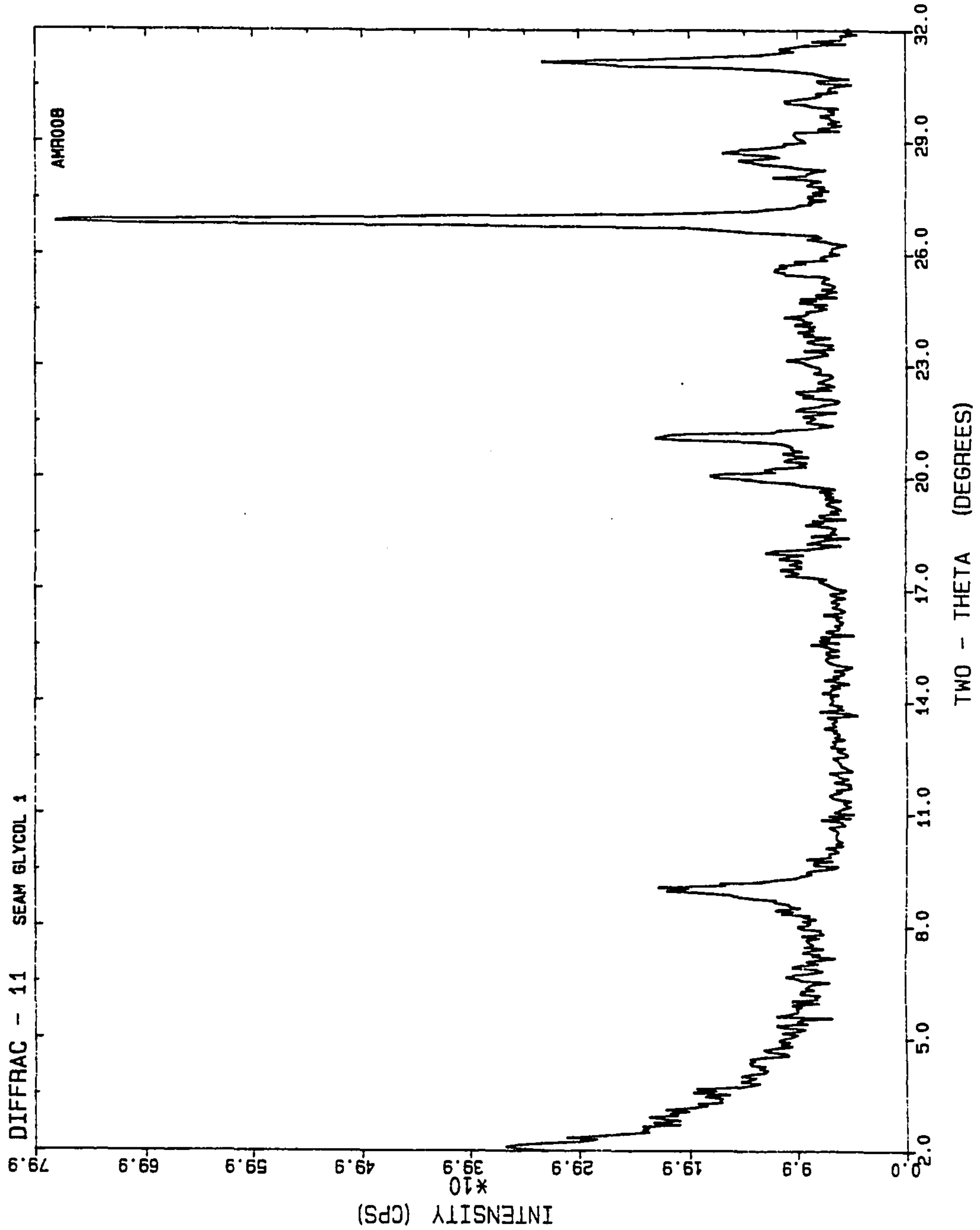

DIFFRAC - 11
SEAM GLYCOL 1
AMR008
INTENSITY (CPS)
*10
0.0
9.9
19.9
29.9
39.9
49.9
59.9
69.9
79.9
TWO - THETA (DEGREES)
2.0
5.0
8.0
11.0
14.0
17.0
20.0
23.0
26.0
29.0
32.0

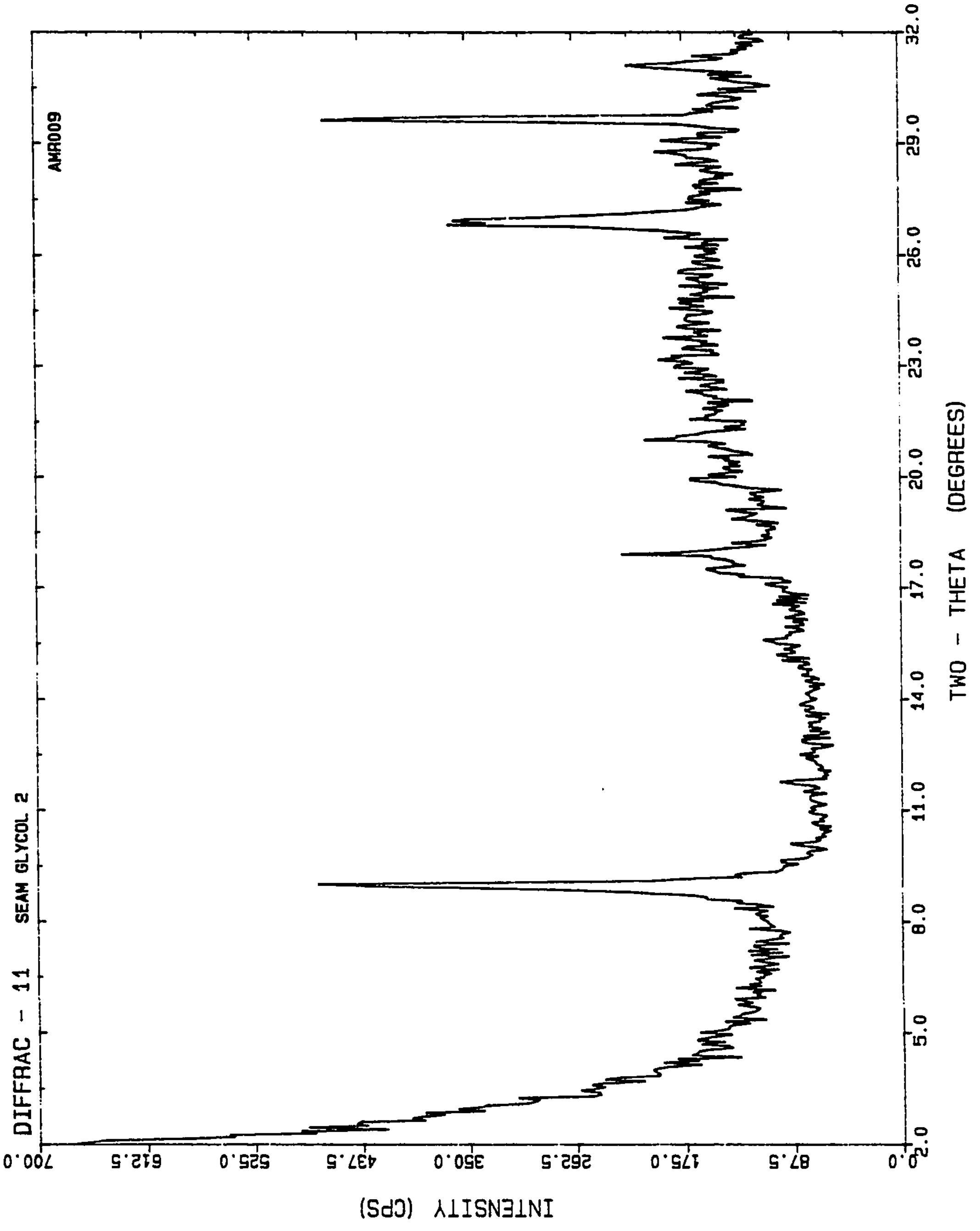
DIFFRAC - 11
SEAM GLYCOL 2
AMR009
TWO - THETA (DEGREES)
INTENSITY (CPS)
0.0
87.5
175.0
262.5
350.0
437.5
525.0
612.5
700.0
2.0
5.0
8.0
11.0
14.0
17.0
20.0
23.0
26.0
29.0
32.0

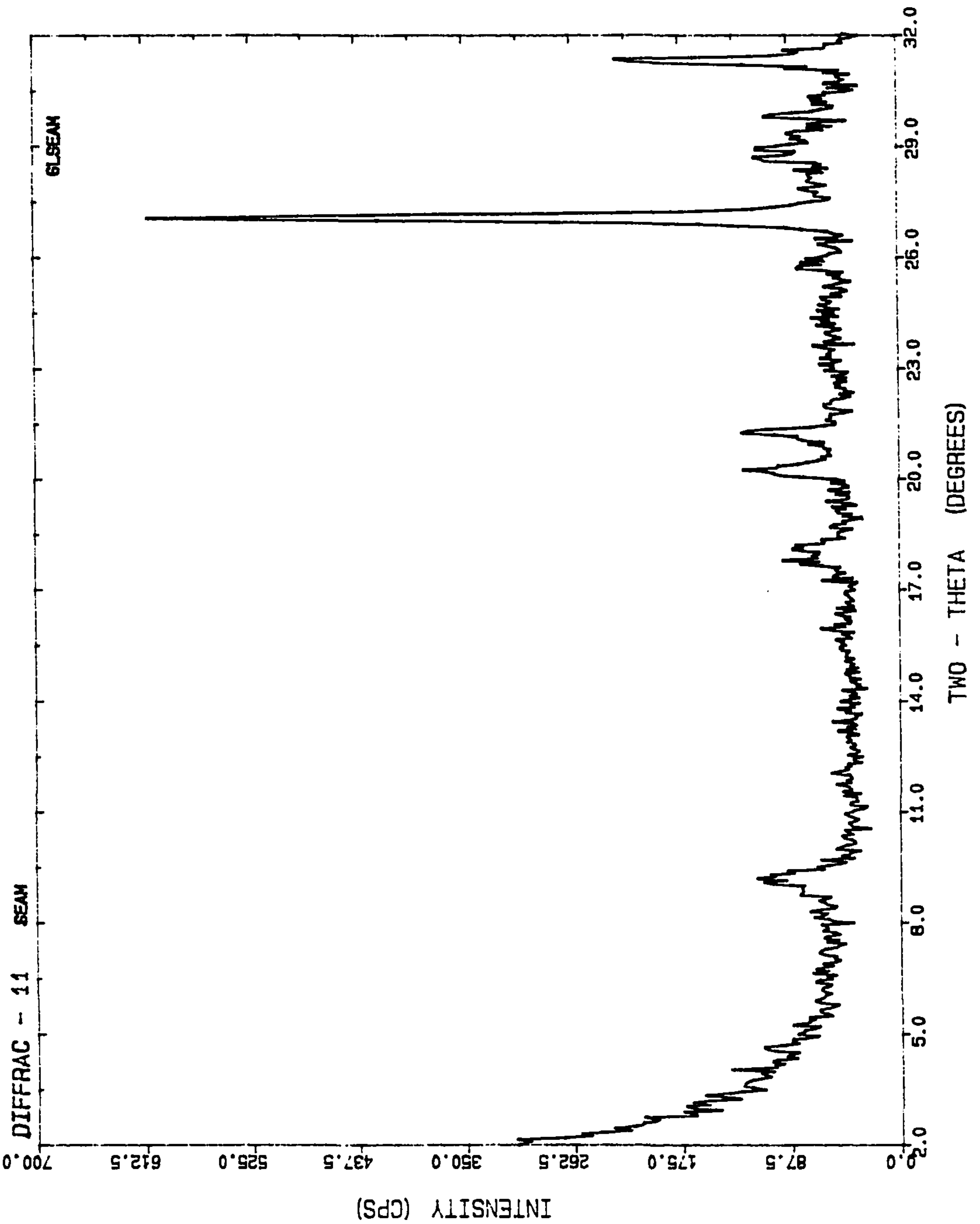
DIFFRAC - 11
SEAM
GLSEAM
INTENSITY (CPS)
0.0
87.5
175.0
262.5
350.0
437.5
525.0
612.5
700.0
TWO - THETA (DEGREES)
2.0
5.0
8.0
11.0
14.0
17.0
20.0
23.0
26.0
29.0
32.0

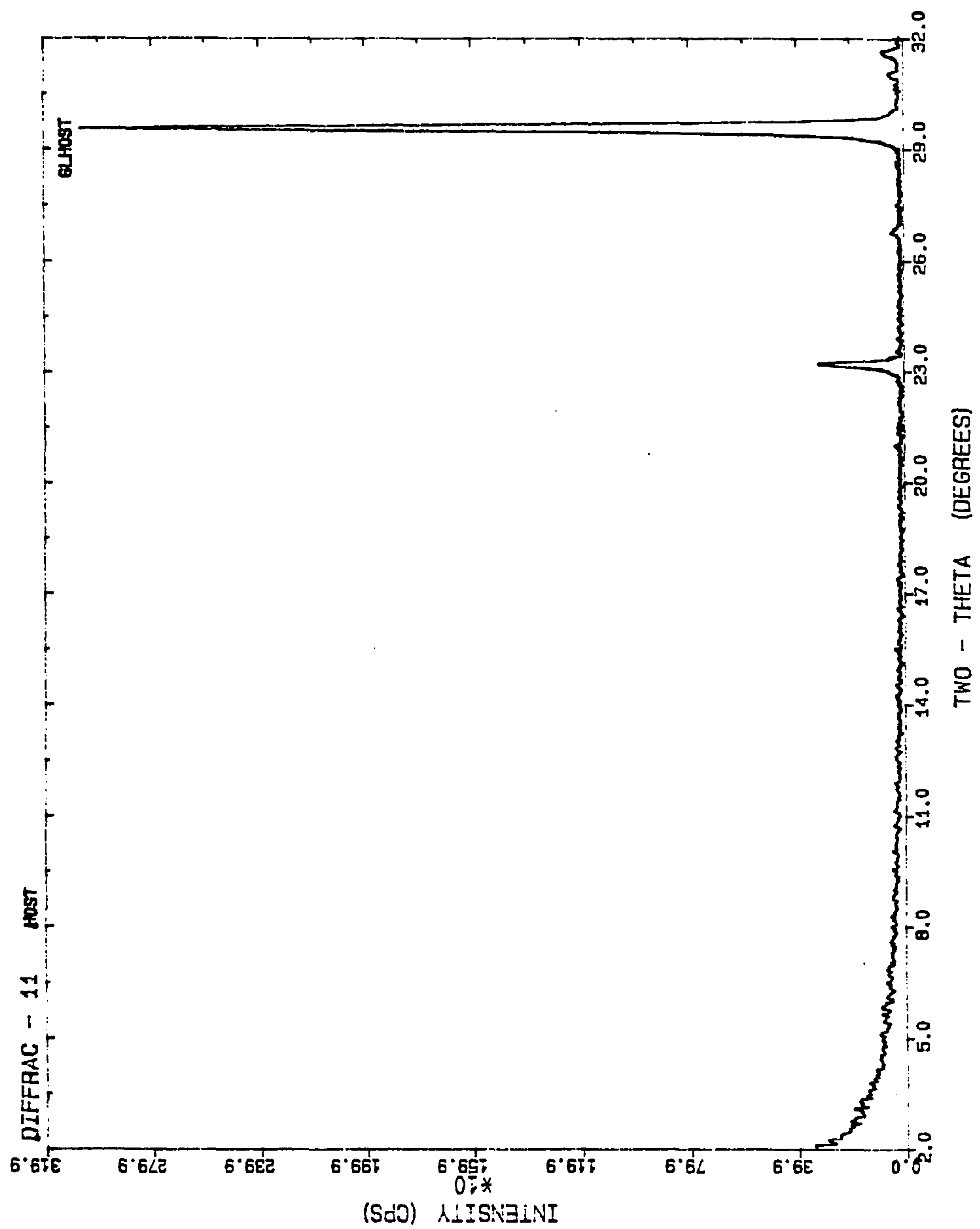
DIFFRAC - 11
HOST
GLHOST
INTENSITY (CPS)
*10
0.0
39.9
79.9
119.9
159.9
199.9
239.9
279.9
319.9
TWO - THETA (DEGREES)
2.0
5.0
8.0
11.0
14.0
17.0
20.0
23.0
26.0
29.0
32.0

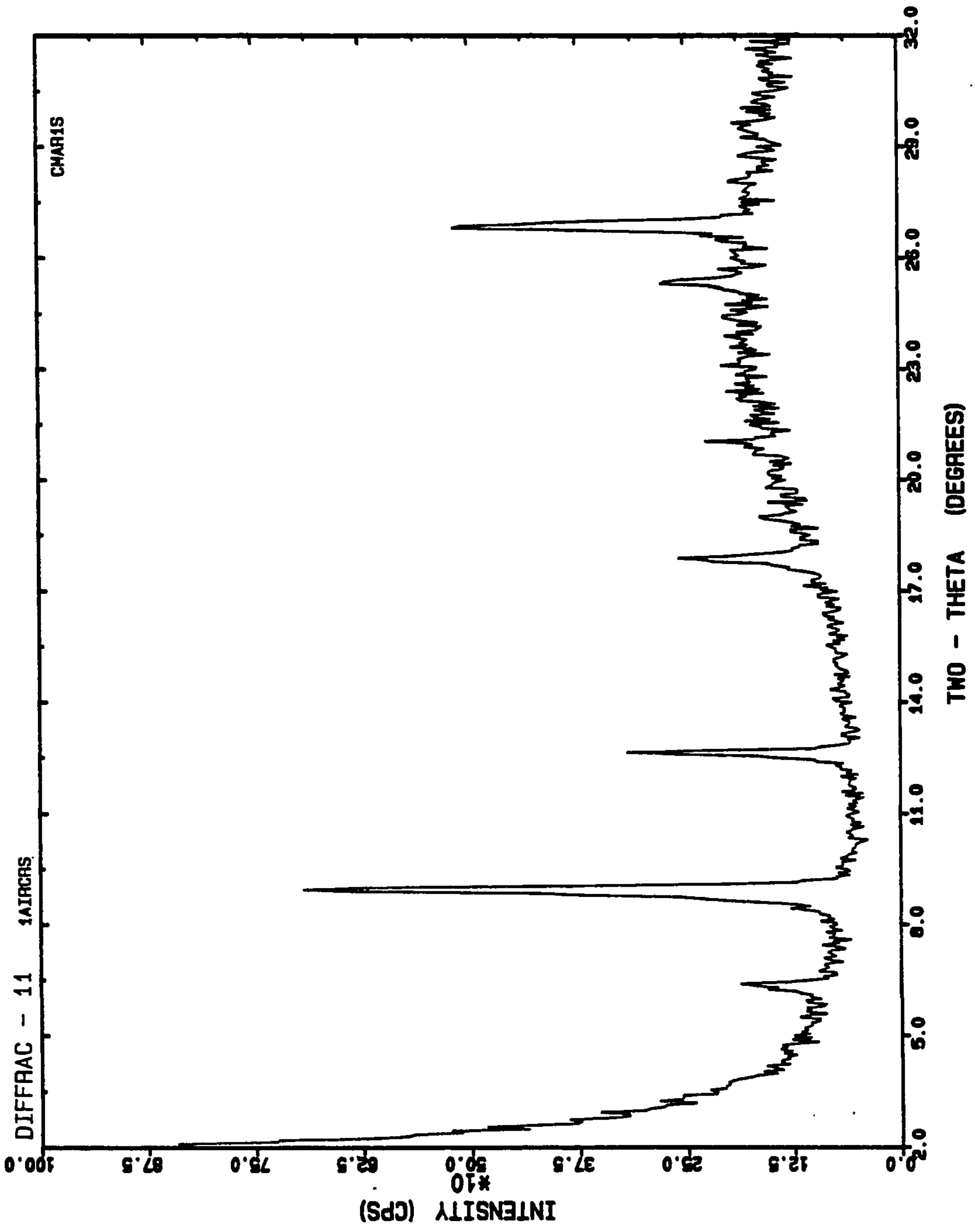
DIFFRAC - 11
1AIRCRS
CHAR1S
TWO - THETA (DEGREES)
2.0
5.0
8.0
11.0
14.0
17.0
20.0
23.0
26.0
29.0
32.0
INTENSITY (CPS)
*10
0.0
12.5
25.0
37.5
50.0
62.5
75.0
87.5
100.0

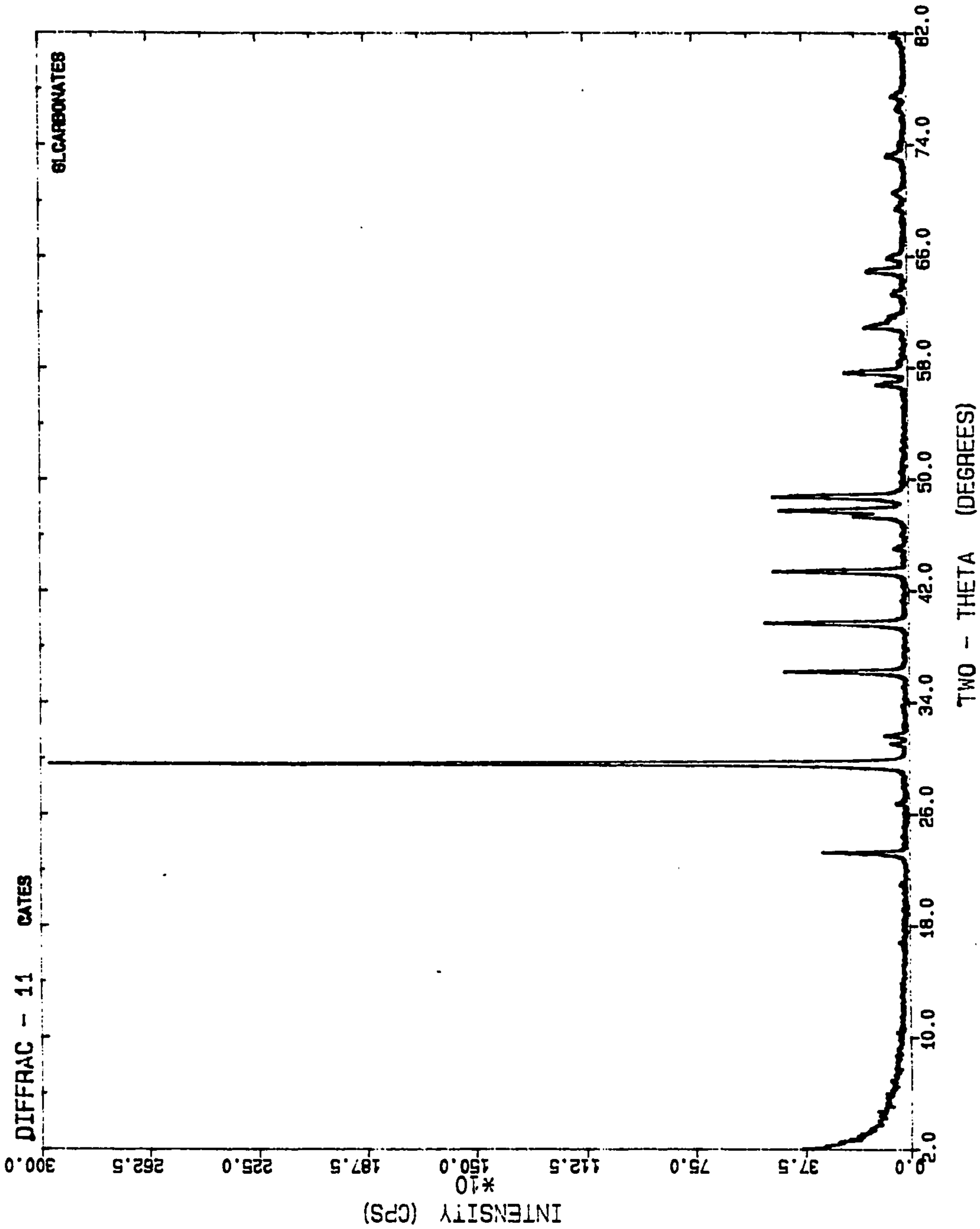
DIFFRAC - 11
CATES
BICARBONATES
TWO - THETA (DEGREES)
2.0
10.0
18.0
26.0
34.0
42.0
50.0
58.0
66.0
74.0
82.0
INTENSITY (CPS)
*10
0.0
37.5
75.0
112.5
150.0
187.5
225.0
262.5
300.0

APPENDIX B

Plates 1-13 (back cover jacket)

APPENDIX C

Basin-Wide Integrations

BASIN-WIDE VOLUMETRIC CALCULATIONS

Chapter 6 presented functions representing approximations of the thicknesses of the Salem Limestone and its four lithofacies, and stylolite relief (column height) within each lithofacies, throughout the Illinois Basin. These functions are integrated over the area of the basin to yield rock and stylolite volumes. Stylolite volume includes the rock within stylolite columns. This volume represents an estimate of the amount of material removed along the stylolite. Comparison of rock and stylolite volumes, along with estimates of original porosity, reveals the contribution made by stylolites to porosity occlusion in the Salem Limestone.

A. Volume of Salem Limestone

Integrating the function T given in Equation 18 of Chapter 6 over the area of the Illinois Basin as defined by Figure 47, we derive the volume of the Salem Limestone, V_S:

$$V_S = \int_0^{300} \int_0^{192} 152.38 - 0.793N \, dN \, dE$$

$$= \int_0^{300} 152.38(192-0) - (0.793/2)(192^2-0^2) \, dE$$

$$= 29256.96(300-0) - 14616.576(300-0)$$

$$= 4392115.2 \text{ mi}^2\text{-ft}$$

$$= 122,445,144,400,000 \text{ ft}^3$$

The northern limit of integration, 192 miles, is defined to avoid negative thickness values (compare Equation 18, Chapter

6, with Figure 49). Integrating in the N direction from 0 to 200 yields a value for VS that is only 0.17% smaller than the result given above. This error is insignificant.

B. Volume of Grainstone in Salem Limestone

Integrating the product of the functions T and G/T, given in Equations 18 and 19 (Chapter 6), over the area of the Illinois Basin, we derive the volume of grainstone within the Salem Limestone, V_G:

$$V_G = \int_0^{300} \int_0^{200} ac+adeN-adfE-bcN-bdeN^2+bdfEN \, dN \, dE$$

$$= \int_0^{300} 200ac+20{,}000ade-200adfE-20{,}000bc$$

$$-2{,}666{,}667bde+20{,}000bdfE \, dE$$

$$= 200(300)ac+20{,}000(300)ade-100(300^2)adf$$

$$-20{,}000(300)bc-2{,}666{,}667(300)bde$$

$$+10{,}000(300^2)bdf$$

$$= 384{,}540 \text{ mi}^2\text{-ft}$$

$$= 10{,}720{,}364{,}220{,}000 \text{ ft}^3$$

where a=152,38; b=0.793; c=0.1; d=0.00222; e=0.9063; and f=0.4226. This indicates that grainstone represents approximately 10% of the total thickness of the Salem Limestone. This percentage is surprisingly low. Significant error is generated by using planar approximations for the thickness functions.

C. Volume of Packstone in Salem Limestone

Integration of the thickness of packstone over the area of the Illinois Basin is performed in a coordinate system rotated 30° counterclockwise, to accommodate the discontinuity in the function P/T (Equation 20 and Figure 51, Chapter 6). The axes of the rotated coordinate system are represented by N' and E'. Integrating the product of rotated versions of functions T and G/T, given in Equations 18 and 20 (Chapter 6) over the area of the basin, we derive the volume of packstone within the Salem Limestone, V_P:

$$
\begin{aligned}
V_P &= \int_0^{300} \int_0^{31.2} [a-b(cE'+dN')][f+g(hN'-j)]\, dN'\, dE' \\
&\quad + \int_0^{300} \int_{31.2}^{48.7} [a-b(cE'+dN')][f-g(hN'-j)]\, dN'\, dE' \\
&= 31.2(300)af-15.6(3002)cbf-486.72(300)bdf \\
&\qquad +486.72(300)agh-31.2(300)agj-243.36(300^2)bcgh \\
&\qquad +15.6(300^2)bcgj-10{,}123.8(300)bdgh \\
&\qquad +486.72(300)bdgj+17.5(300)af-8.75(300^2)bcf \\
&\qquad -699(300)bdf-699(300)agh+17.5(300)agj \\
&\qquad +349.5(300^2)bcgh-8.75(300^2)bcgj \\
&\qquad +28{,}377(300)bdgh-699(300)bdgj \\
&= 606146.3031 \text{ mi}^2\text{-ft} \\
&=16{,}898{,}389{,}101{,}000 \text{ ft}^3
\end{aligned}
$$

where a=152.38; b=0.793; c=0.5; d=866; f=0.6; g=0.006; h=0.67; and j=20.785. The upper limit of N' is chosen at 48.7 miles to avoid negative thickness values. The value of V_P indicates that packstone constitutes approximately 15% of the Salem Limestone in the Illinois Basin. As in the grainstone case, the percentage appears low, probably reflecting error introduced by the planar approximations used in the integration.

D. Volume of Wackestone-Micstone in Salem Limestone

Integrating the product of the functions T and W/T, given in Equations 18 and 21 (Chapter 6), over the area of the Illinois Basin, we derive the volume of wackestone-micstone within the Salem Limestone, V_W:

$$V_W = \int_0^{300} \int_0^{200} (a-bN)[c-d(fN-gE)]\ dN\ dE$$

$$= 200(300)ac-20,000(300)adf+100(300^2)adg$$

$$-20,000(300)bc+2,666,667(300)bdf$$

$$-10,000(300^2)bdg$$

$$= 1,861,800\ mi^2\text{-}ft$$

$$= 51,904,005,430,000\ ft^3$$

where a=152.38; b=0.793; c=0.4; d=0.00444; f=0.9063; and g=0.4226. This calculation indicates that wackestone-micstone constitutes approximately 43% of the Salem Limestone in the Illinois Basin. This percentage appears reasonable, based on field observations and review of Plates 1-10 (Appendix B).

E. Volume of Dolostone in Salem Limestone

Integrating the product of the functions T and D/T, given in Equations 18 and 22 (Chapter 6), over the area of the Illinois Basin, we derive the volume of dolostone within the Salem Limestone, V_D:

$$V_D = \int_0^{300} \int_0^{200} c+d(fN-gE)\ dN\ dE$$

$$= 200(300)ac+20,000(300)adf-100(300^2)adg$$

$$-20,000(300)bc-2,666,667(300)bdf$$

$$+10,000(300^2)bdg$$

$$= 180,841\ mi^2\text{-}ft$$

$$= 5,041,560,773,000\ ft^3$$

where a=152,38; b=0.793; c=0.05; d=0.000444; f=0.866; and g=0.5. This calculation indicates that dolostone constitutes approximately 4% of the total volume of the Salem Limestone. Compared to the calculated volumes of grainstone and packstone, this means that the volume of grainstone is only 2-1/2 times that of dolostone, and that the volume of packstone is slightly less than 4 times that of dolostone.

F. Stylolite Volume in Grainstone in Salem Limestone

Integration of stylolite relief, or column height, over the area of the Illinois Basin yields the volume of rock contained within stylolite columns, or the volume of rock enveloped by the upper and lower boundaries of individual stylolites. This volume is an *estimate* of the volume of rock dissolved along the stylolites. The stylolite volume in grainstone, V_{SG}, is derived by integrating the product of the functions T, G/T, and R/G in Equations 18, 19 and 28 in Chapter 6 over the area of the Illinois Basin:

$$V_{SG} = \int_0^{300} \int_{38}^{112} (a-bN)[c+d(eN-fE)][g+h(iN-j)]\ dN\ dE$$
$$+ \int_0^{300} \int_{112}^{200} (a-bN)[c+d(eN-fE)][g-h(iN-j)]\ dN\ dE$$
$$= 74(300)acg+5550(300)achi-74(300)achj$$
$$+5550(300)adeg+450,019(300)adehi$$
$$-5550(300)adehj-37(300^2)adfg-2775(300^2)adfhi$$
$$+37(300^2)adfhj-5550(300)bcg-450,019(300)bchi$$
$$+5550(300)bchj-450,019(300)bdeg$$
$$-38,816,700(300)bdehi+450,019(300)gdehj$$
$$+2775(300^2)bdfg+225,010(300^2)bdfhi$$
$$-2775(300^2)bdfhj+88(300)acg-13,728(300)achi$$
$$+88(300)achj+13,728(300)adeg$$
$$-2,198,357(300)adegi+13,728(300)adehj$$
$$-44(300^2)adfg+6864(300^2)adfhi-44(300^2)adfhj$$
$$-13,728(300)bcg+2,198,357(300)bchi$$
$$-13,728(300)bchj-2,198,357(300)bdeg$$
$$+360,662,016(300)bdehi-2,198,357(300)bdehj$$
$$+6864(300^2)bdfg-1,099,179(300^2)bdfhi$$
$$+6864(300^2)bdfhj$$
$$= 922,106\ mi^2\text{-}ft$$
$$= 84,339,988,600\ ft^3$$

where a=152.38; b=0.793; c=0.1; d=0.00222; e=0.9063; f=0.4226; g=4; h=0.08; i=0.667; and j=75. Comparson of V_{SG} and V_G reveals that the stylolite volume consitutes approximately 0.8% of grainstone in the Salem Limestone. This percentage appears to be reasonable, based on field observations summarized in Chapter 3 and Plates 1-10 (Appendix B).

G. Stylolite Volume in Packstone in Salem Limestone

The calculation of the stylolite volume in packstone, V_{SP}, requires the rotation of coordinates by 30° counterclockwise, as with the calculation of V_P. The rotated coordinate axes are represented by E' and N'. The value of V_{SP} is derived by integrating the product of the rotated versions of the functions T, P/T, and R/P in Equations 18, 20 and 29 in Chapter 6 over the area of the Illinois Basin:

$$V_{SP} = \int_0^{31} \int_0^{300} [a-b(cE'+dN')][f+g(hN'-j)]$$

$$[1-m\{[h(cE'+dN')-n]^2+[h(dE'-cN')-o]^2\}^{0.5}\, dE\, dN$$

$$+ \int_{31}^{49} \int_0^{300} [a-b(cE'+dN')][f-g(hN'-j)]$$

$$[1-m\{[h(cE'+dN')-n]^2+[h(dE'-cN')-o]^2]^{0.5}\, dE\, dN$$

$$= \int_0^{31} 300afl-45{,}000bcfl-300fbdlN'+300aghlN'-300agjl$$

$$-45{,}000bcghlN'+45{,}000bcgjl-300bdghlN'^2$$

$$+300bdgjlN'-300afmR+45{,}000bcfmR +300bdfmRN'$$

$$-300aghmRN'+300agjmR+45{,}000bcghmRN'$$

$$-45{,}000bcgjmR +300bdghmRN'^2-300bdgjmRN'\, dN$$

$$+ \int_{31}^{49} 300afl-45{,}000bcfl-300fbdlN'+300aghlN'-$$

$$300agjl-45{,}000bcghlN'+45{,}000bcgjl-300bdghlN'^2$$

$$+300bdgjlN'-300afmR+45{,}000bcfmR+300bdfmRN'$$

$$-300aghmRN'+300agjmR+45{,}000bcghmRN'$$

$$-45{,}000bcgjmR+300bdghmRN'^2-300bdgjmRN'\, dN$$

in which

$$R = [600r-s(90{,}000r-300s+rN'^2-tN'+n^2+o^2)^{0.5}]/4r$$

$$+[(4r(rN'^2-tN'+n^2+o^2)-s^2)/(8r\sqrt{(r)})]$$

$$\log_e\{2\sqrt{[r(90{,}000r-300s+rN'^2-tN'+n^2+o^2)]}+600r-s\}$$

where

$r = (hc)2+(hd)2$

$s = 2hcn+2hdo$

$t = 2hdn-2hco$

and, finally, a=152.4; b=0.793; c=0.5; d=0.866; f=0.6; g=0.006; h=0.67; j=20.8; l=12.9; m=0.1099; n=85; and o=90. This integral is solved numerically using the basic language program attached to the end of this Appendix. This calculation yields a value of 881,520,700,000 ft^3 for V_{SP}. Comparson of V_{SP} and V_P reveals that the stylolite volume consitutes approximately 5.2% of packstone in the Salem Limestone. This percentage appears to be reasonable, based on field observations summarized in Chapter 3 and Plates 1-10 (Appendix B). Stylolite volumes within stylolite zones, common in packstone, are probably underrepresented, so the actual stylolite volume in packstone may be greater than the calculated value.

PLATE 1

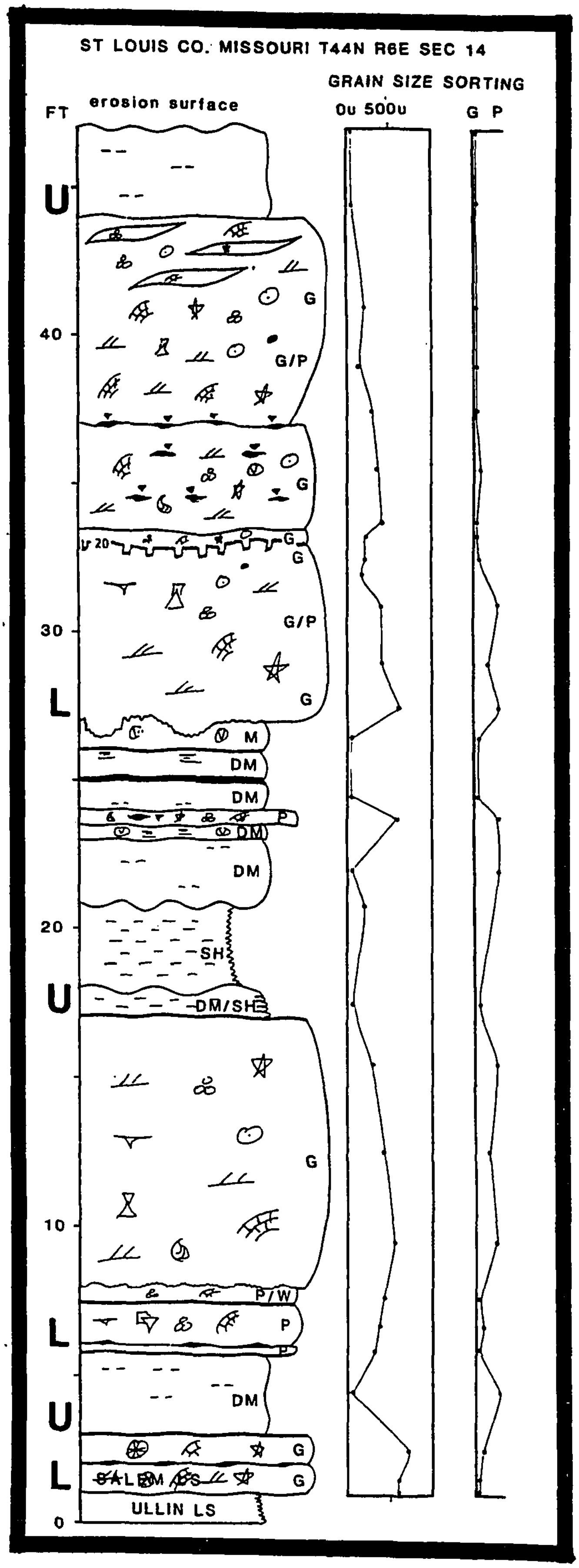
ST LOUIS CO. MISSOURI T44N R6E SEC 14
GRAIN SIZE SORTING
FT
erosion surface
0u 500u
G P
U
G
40
G/P
G
G
G
30
G/P
L
G
M
DM
DM
P
DM
DM
20
SH
U
DM/SH
G
10
P/W
L
P
P
U
DM
L
G
SALEM LS
G
ULLIN LS
0

PLATE 2

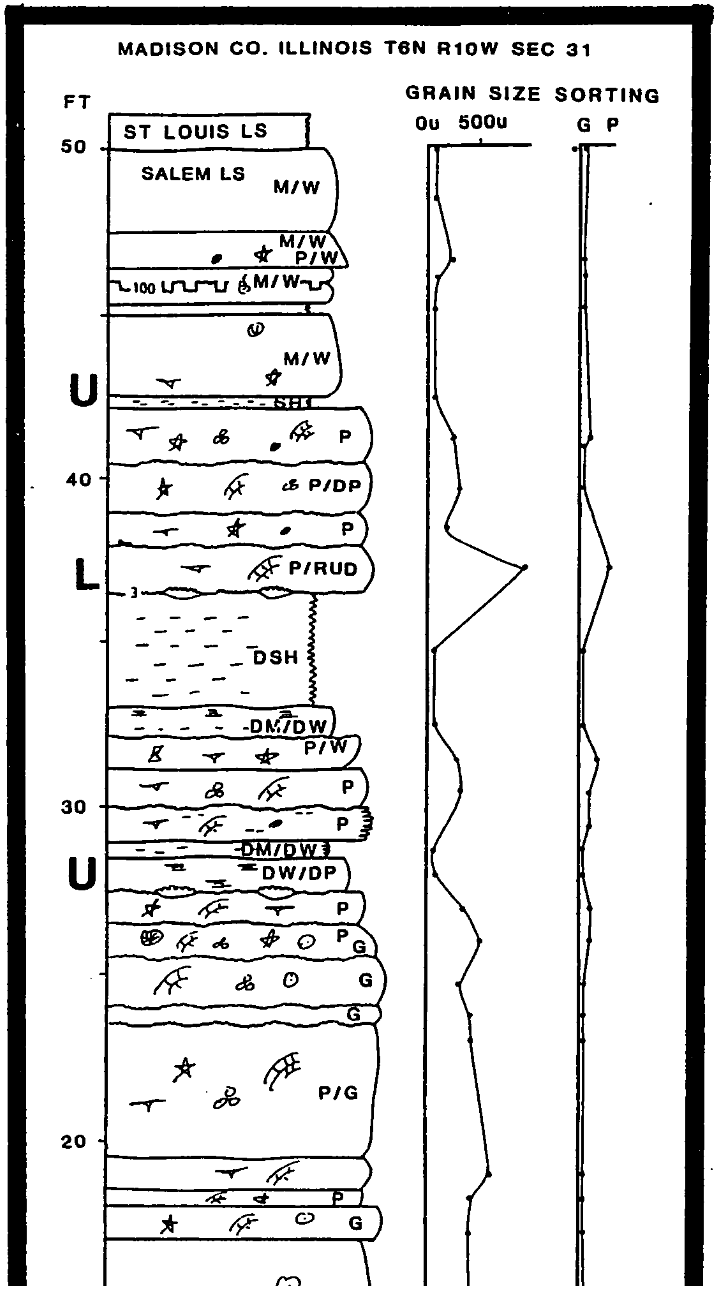

MADISON CO. ILLINOIS T6N R10W SEC 31
FT
GRAIN SIZE SORTING
0u 500u
G P
ST LOUIS LS
SALEM LS
M/W
M/W
P/W
100
M/W
M/W
SH
P
P/DP
P
P/RUD
DSH
DM/DW
P/W
P
P
DM/DW
DW/DP
P
P
G
G
G
P/G
P
G
U
L
U
50
40
30
20

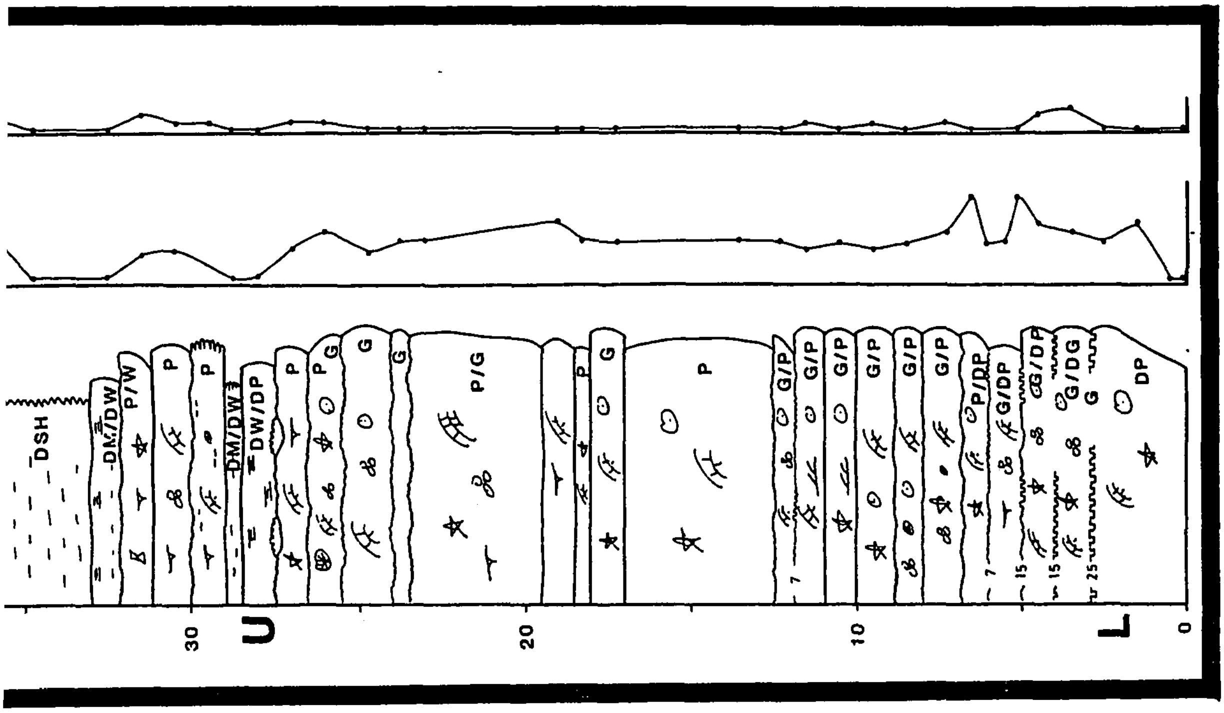
DSH
DM/DW
P/W
DW/DP
P/G
G/P
P/DP
G/DP
G/DG
DP
U
L
30
20
10
0

PLATE 3

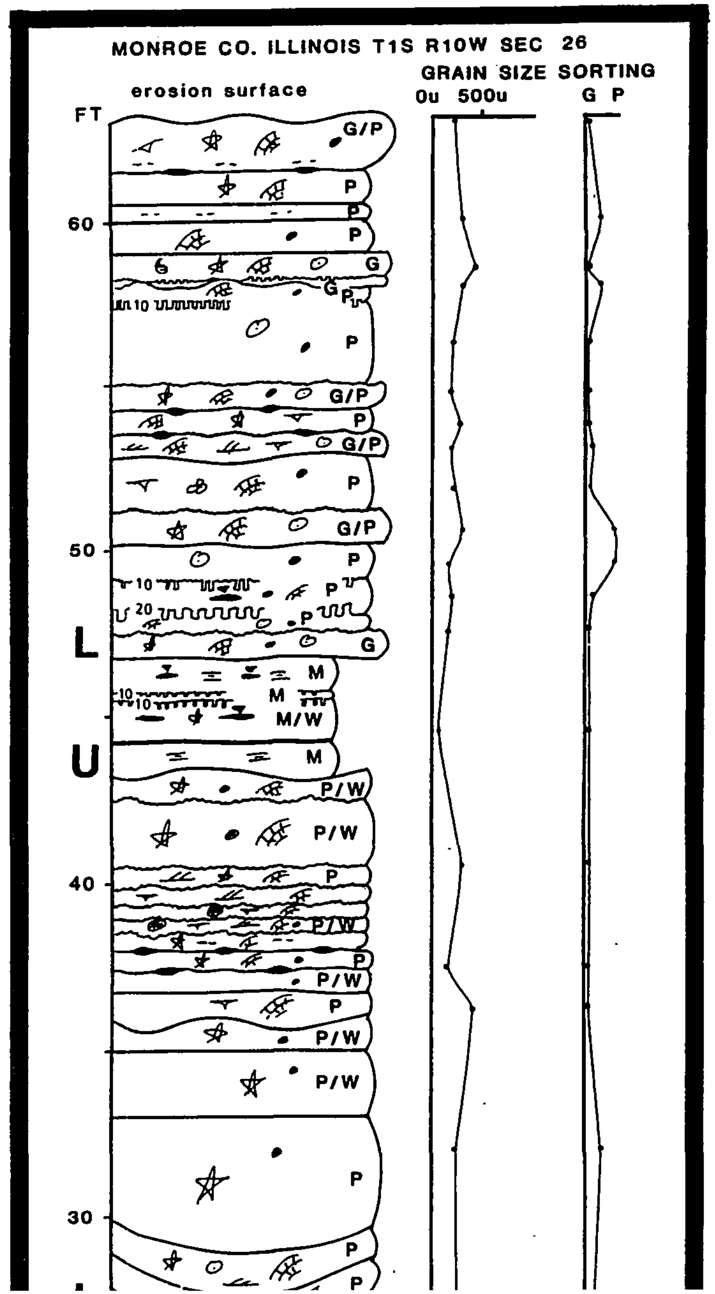
MONROE CO. ILLINOIS T1S R10W SEC 26
erosion surface
GRAIN SIZE SORTING
0u 500u
G P
FT
60
50
40
30
L
U
G/P
P
G
M
M/W
P/W
10
20

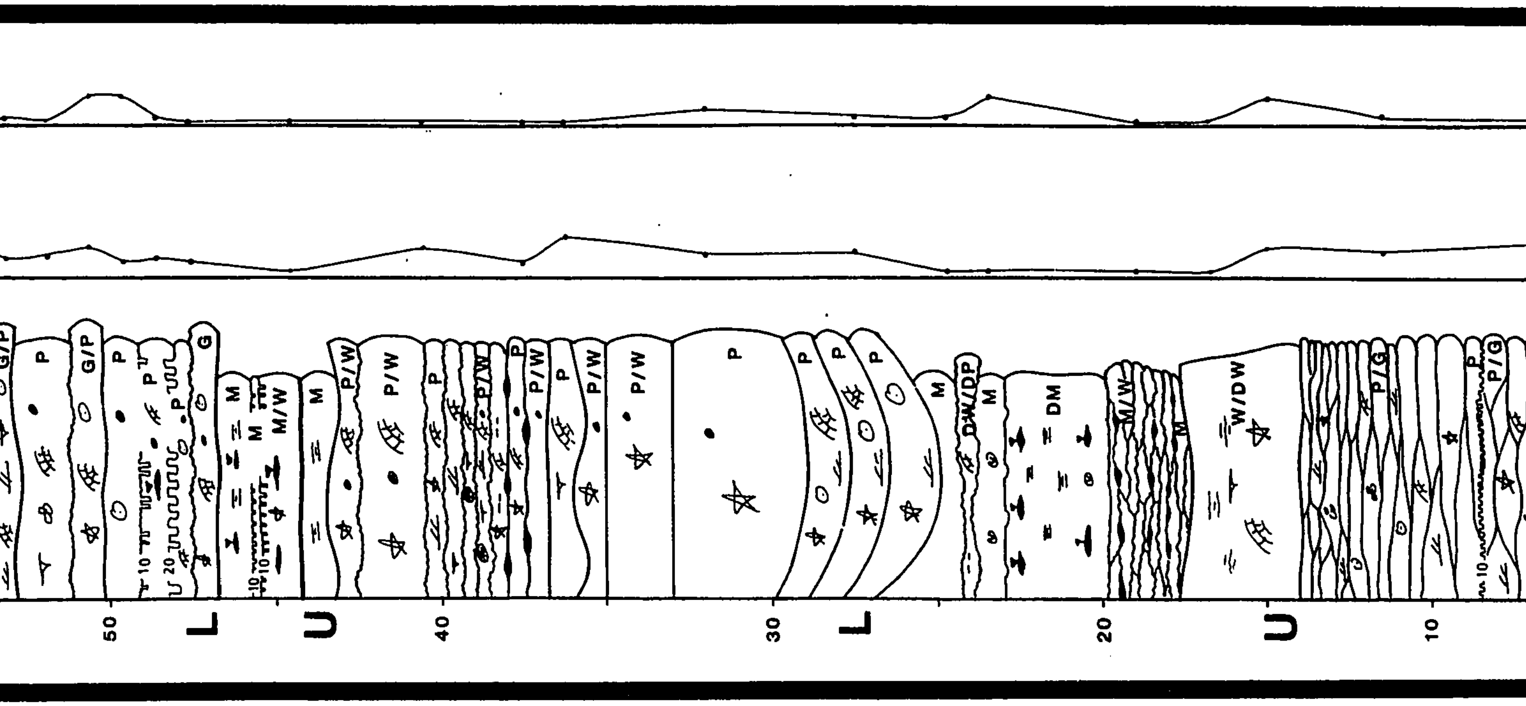

50
40
30
20
10

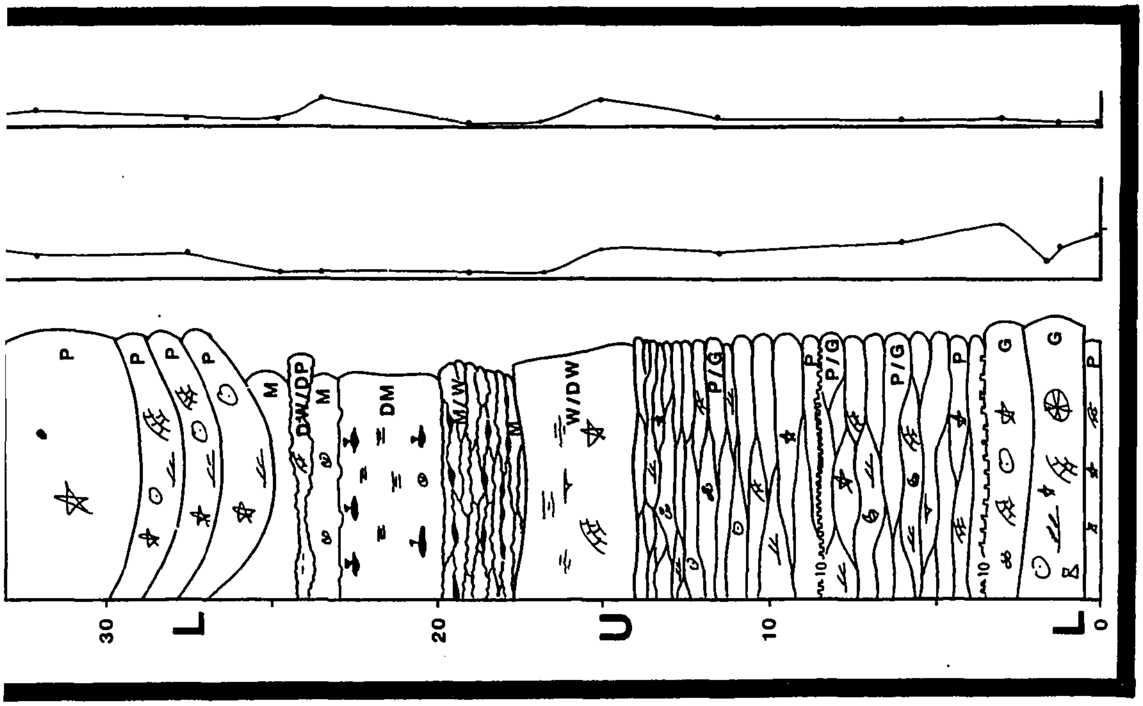

P
M
DM
M/W
W/DW
P/G
G
30
20
10
0
L
U

PLATE 4

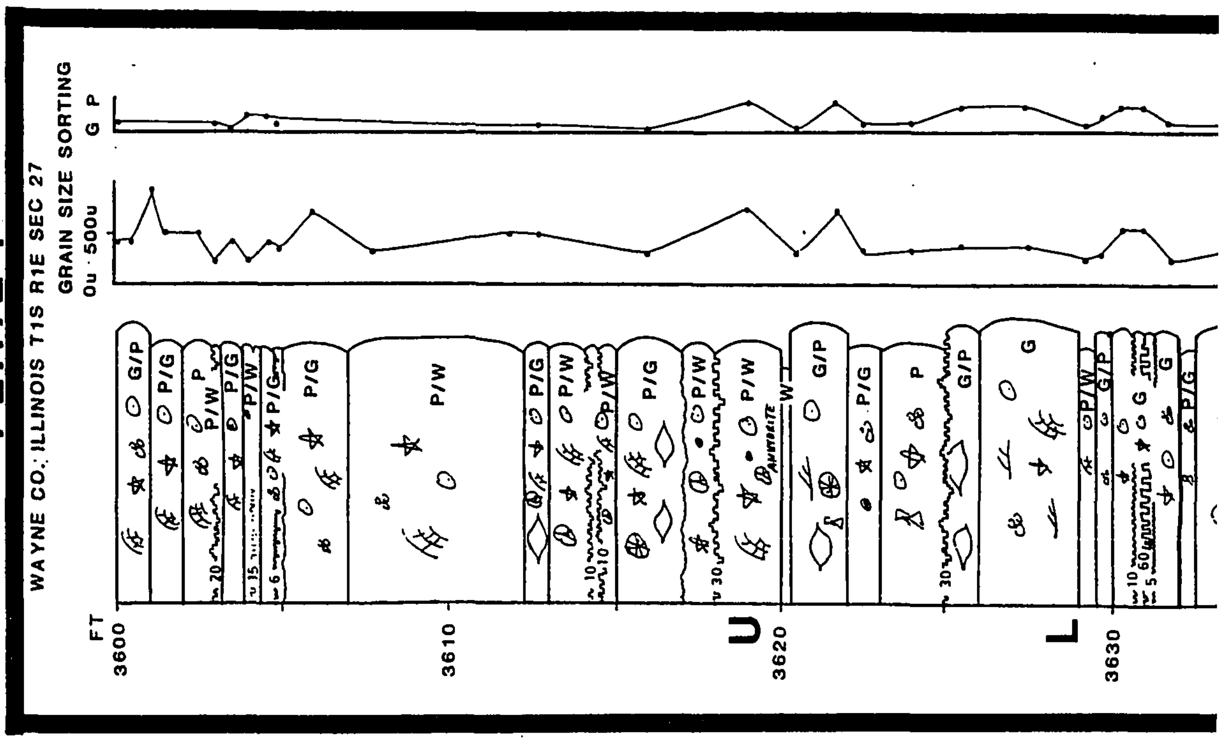
WAYNE CO.; ILLINOIS T1S R1E SEC 27
GRAIN SIZE SORTING
G P
0u 500u
FT
3600
3610
3620
3630
U
L
ANHYDRITE

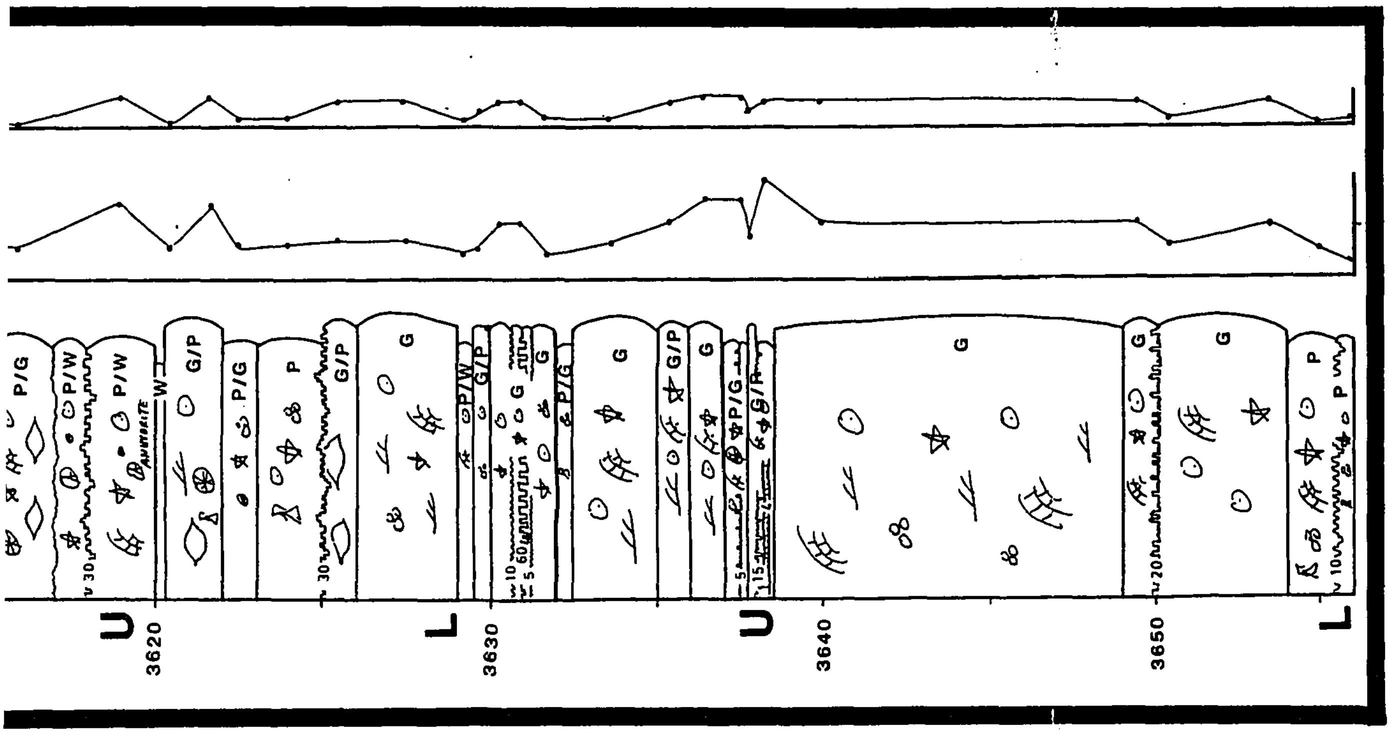

3620
3630
3640
3650
U
L
U
L
P/G
P/W
P/W
W
G/P
P/G
P
G/P
G
P/W
G/P
G
P/G
G
G/P
G
P/G
G/P
G
G
G
P

PLATE 5

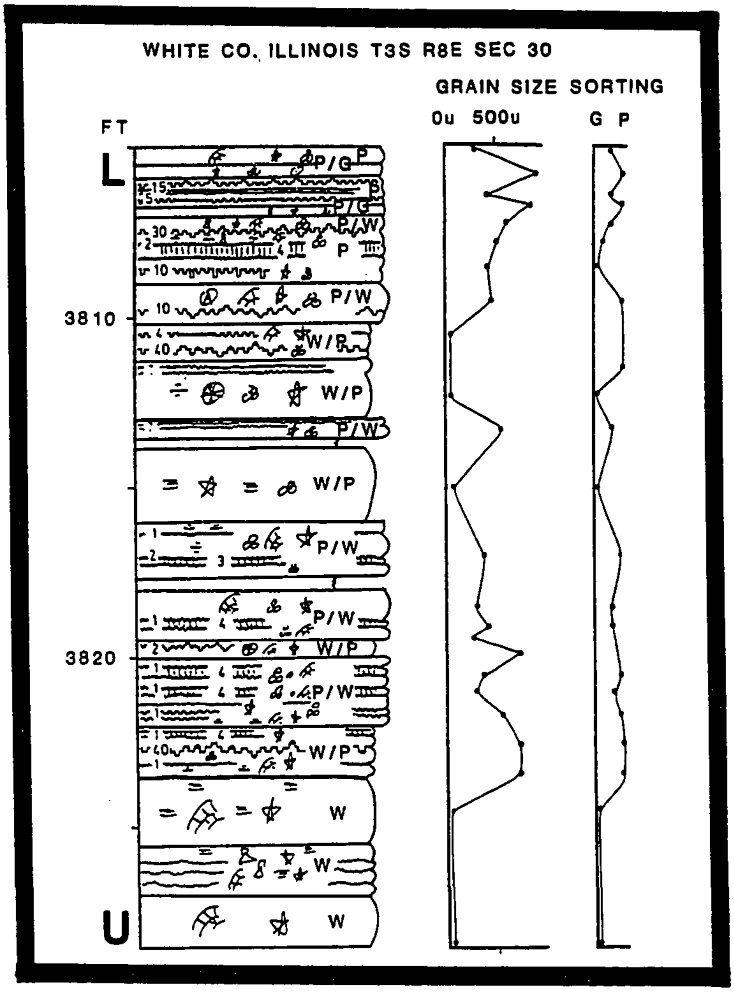
WHITE CO. ILLINOIS T3S R8E SEC 30
GRAIN SIZE SORTING
0u 500u
G P
FT
L
3810
3820
U
P/G
P/W
P
W/P
W

PLATE 6

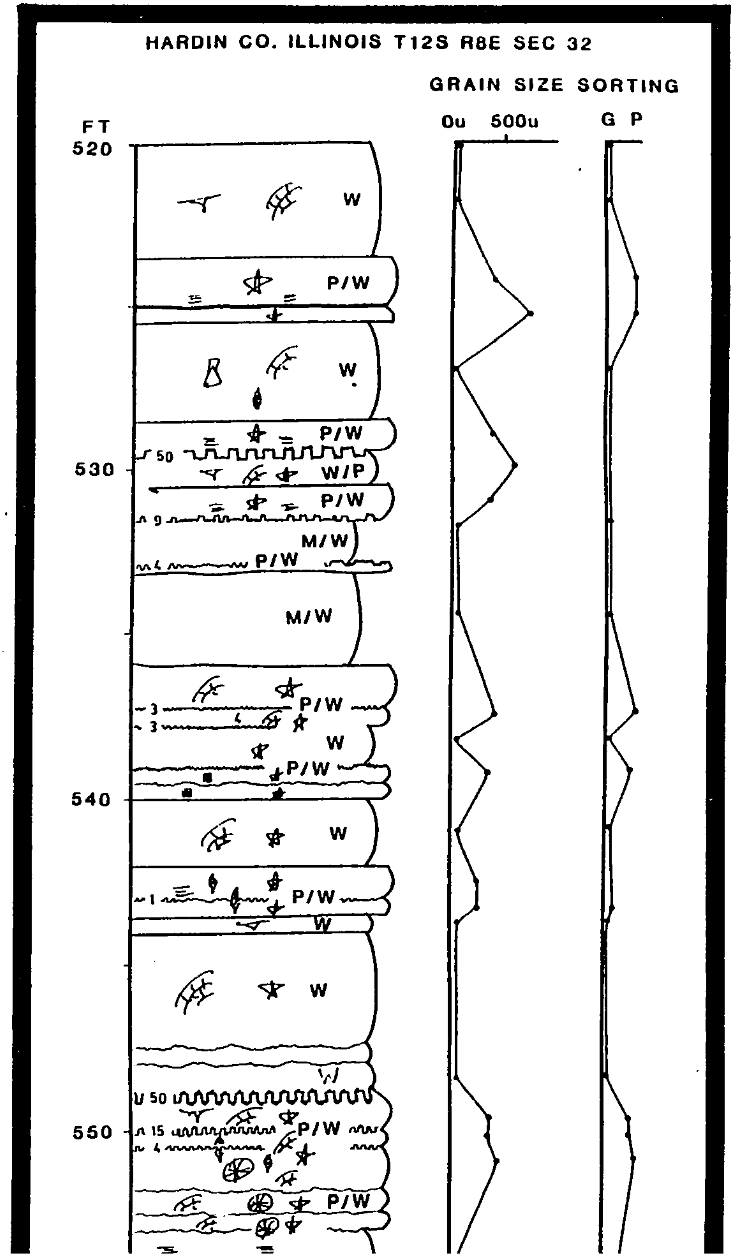

HARDIN CO. ILLINOIS T12S R8E SEC 32
GRAIN SIZE
SORTING
0u 500u
G P
FT
520
530
540
550
W
P/W
W
P/W
W/P
P/W
M/W
P/W
M/W
P/W
W
P/W
W
P/W
W
W
P/W
P/W
50
9
3
3
1
50
15
4

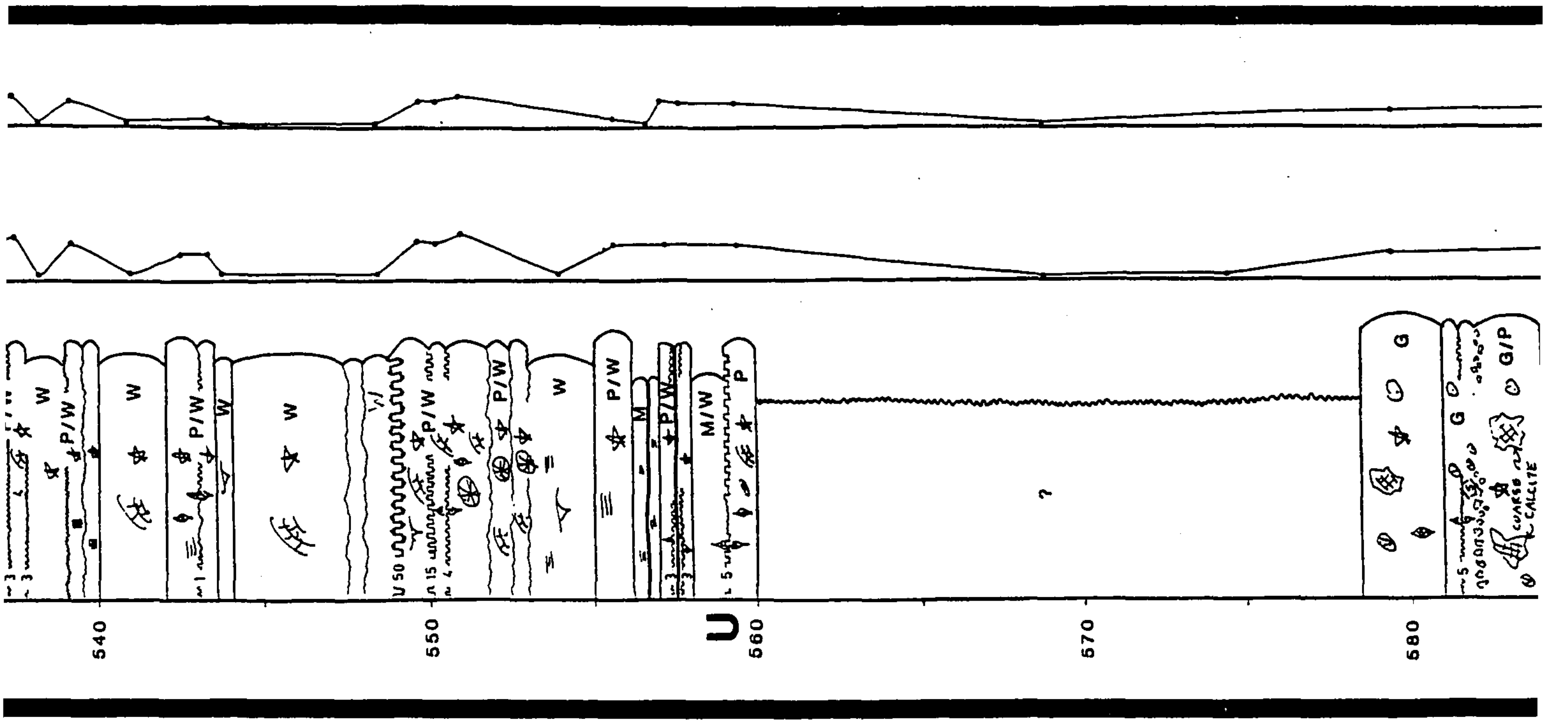
540
550
U
560
570
580
W
P/W
M/W
P
M
G
G/P
COARSE CALCITE
?

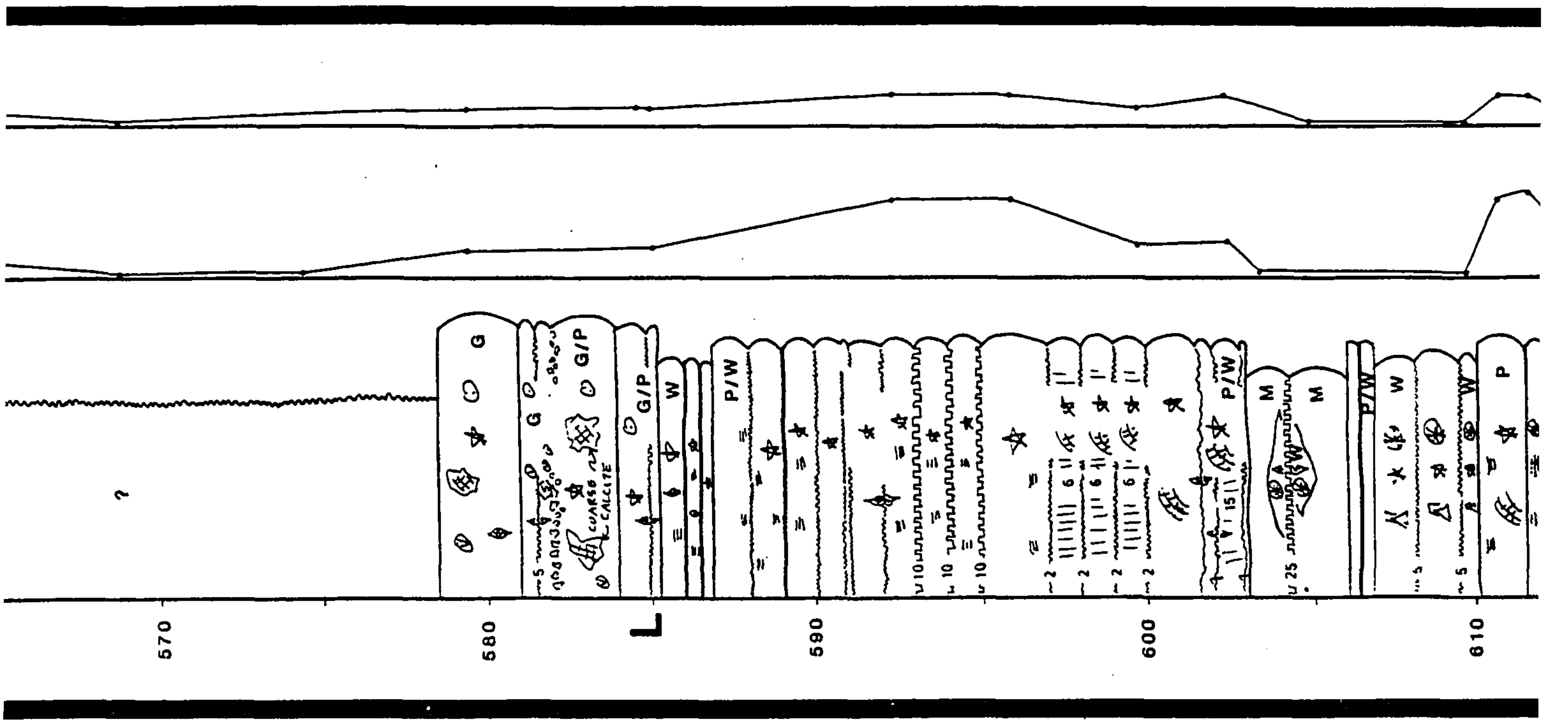
570
580
590
600
610

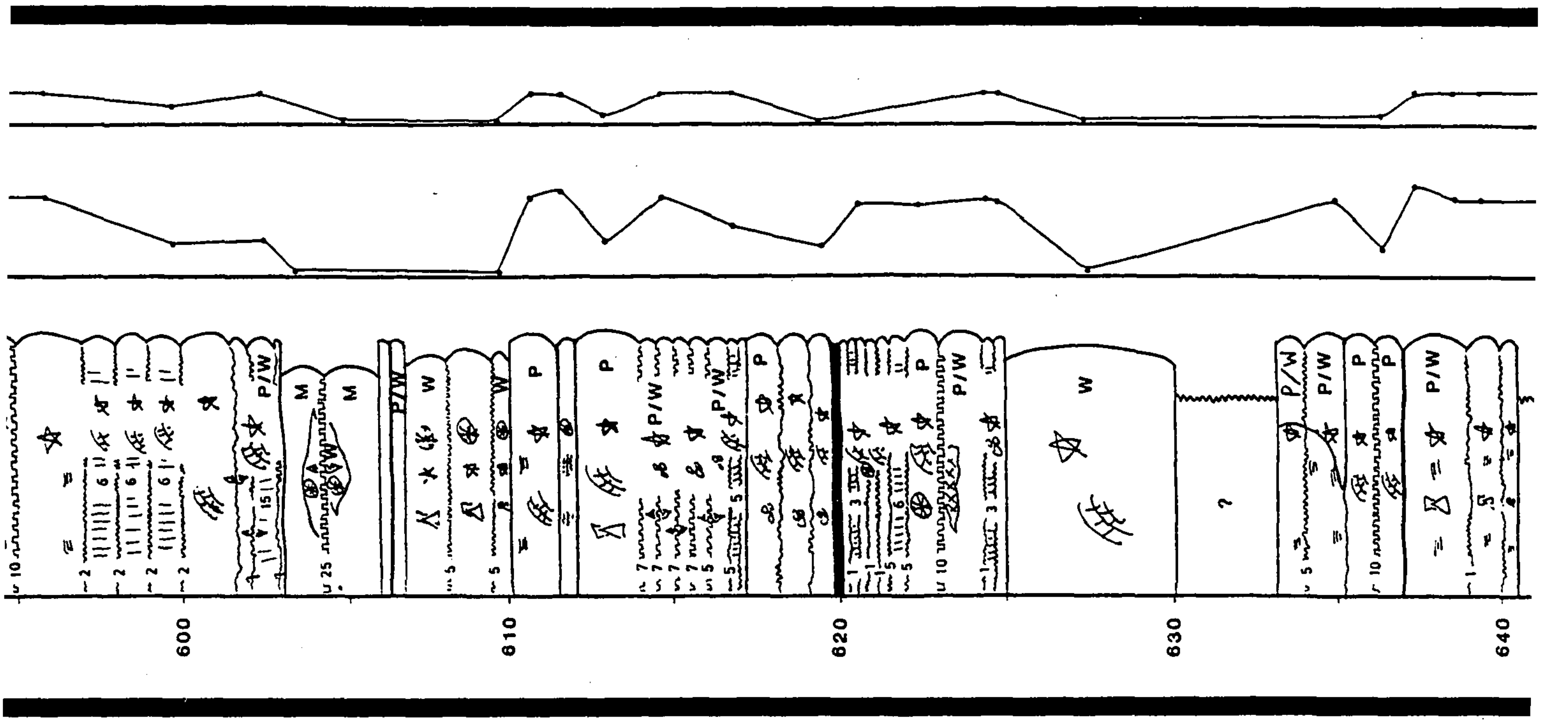
600
610
620
630
640
P/W
M
W
P

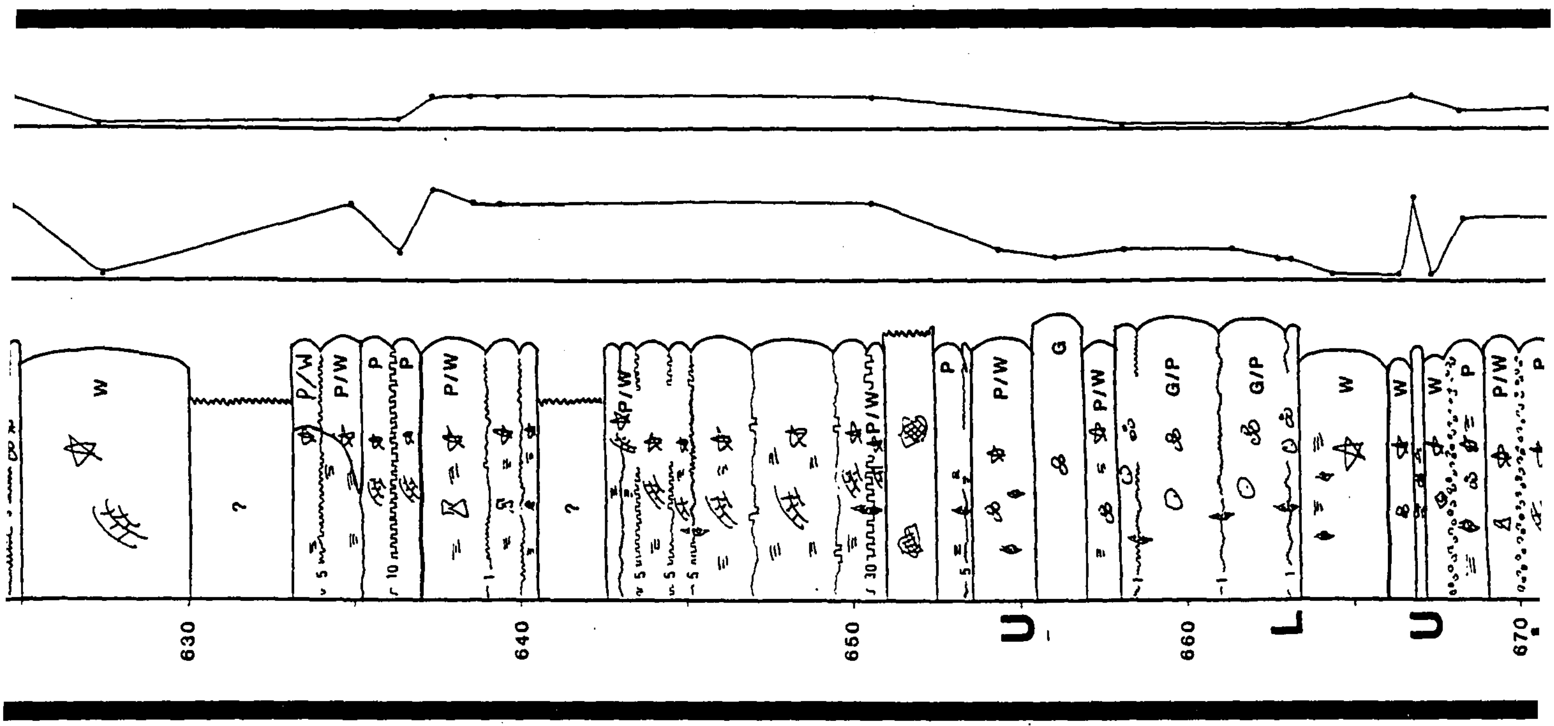
630
640
650
660
670
W
P/W
P
G
G/P
U
L

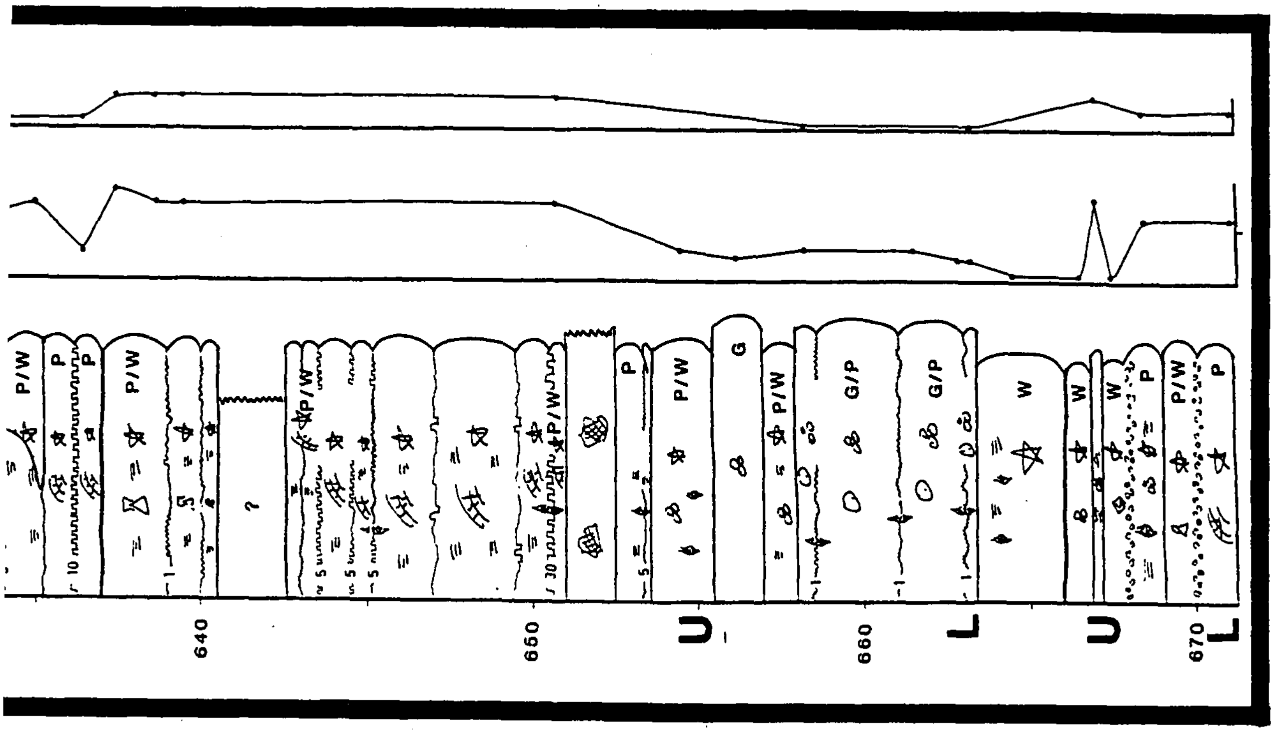

640
650
660
670
P/W
P
G
G/P
W
U
L

PLATE 7

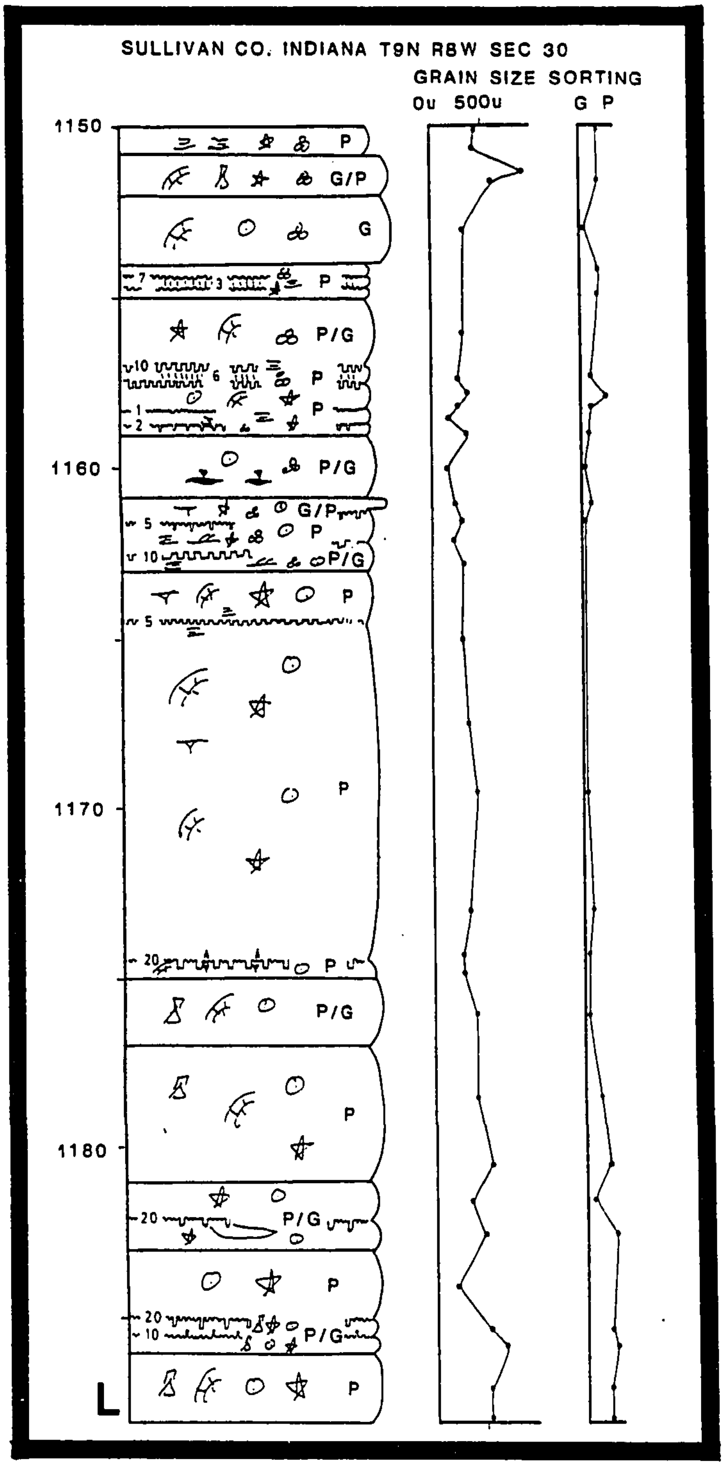
SULLIVAN CO. INDIANA T9N R8W SEC 30
GRAIN SIZE SORTING
0u 500u
G P
1150
1160
1170
1180
L

PLATE 8

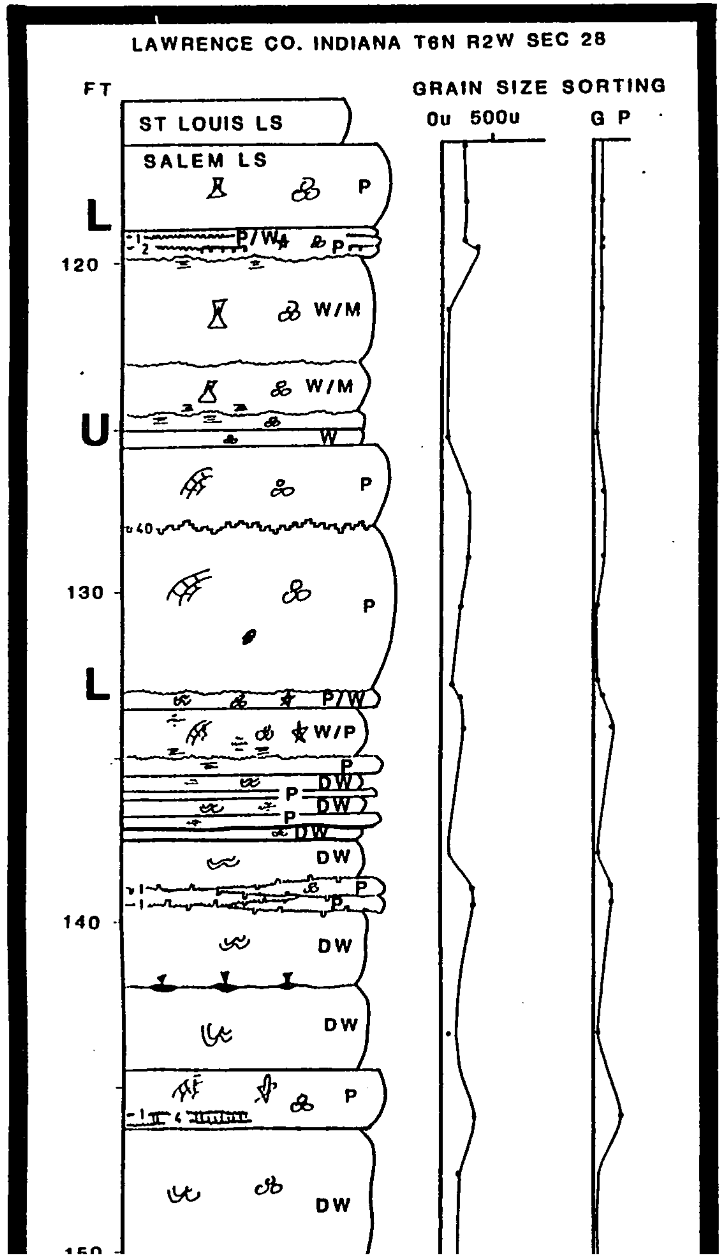
LAWRENCE CO. INDIANA T6N R2W SEC 28
FT
GRAIN SIZE SORTING
0u 500u
G P
ST LOUIS LS
SALEM LS
P
L
P/W
P
120
W/M
W/M
U
W
P
130
P
L
P/W
W/P
P
DW
P
DW
P
DW
DW
P
P
140
DW
DW
P
DW
150

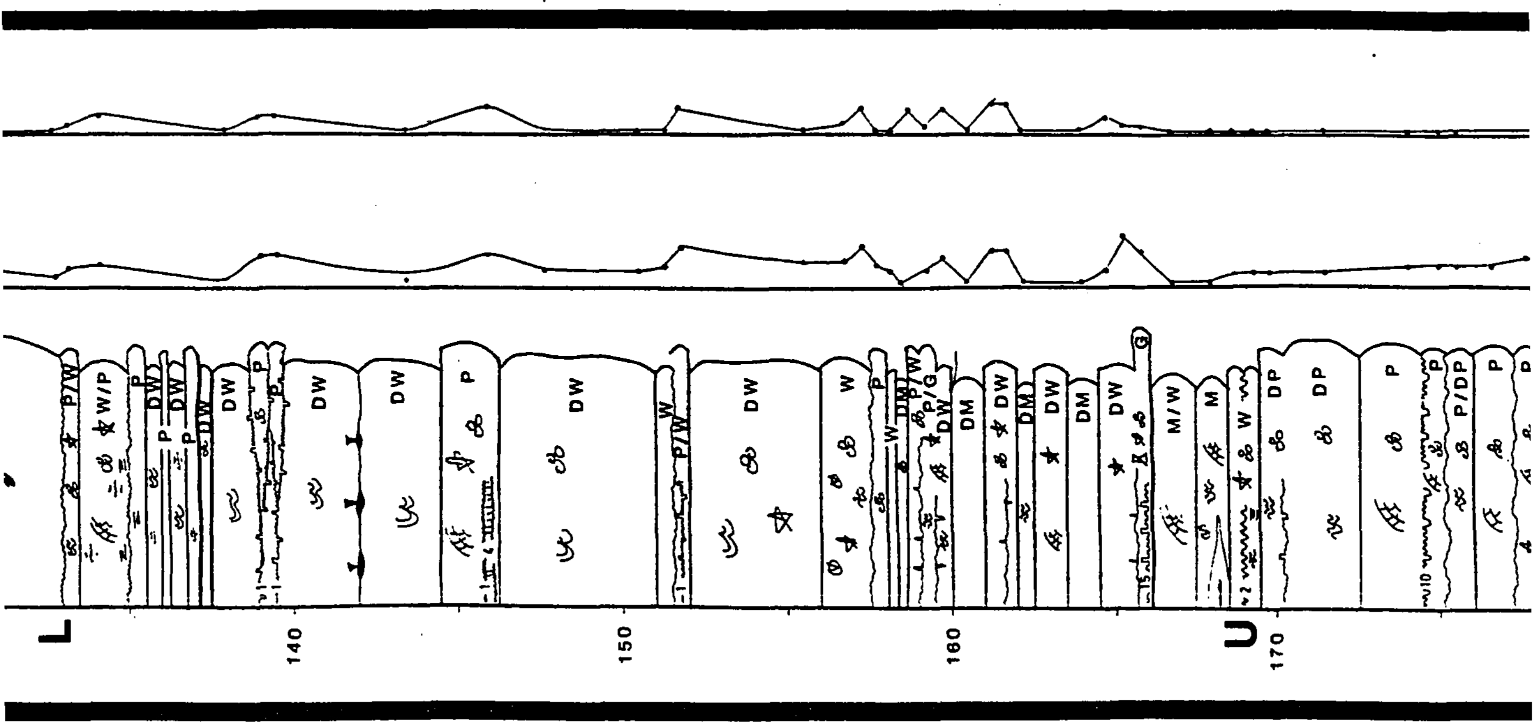
L
140
150
160
U
170

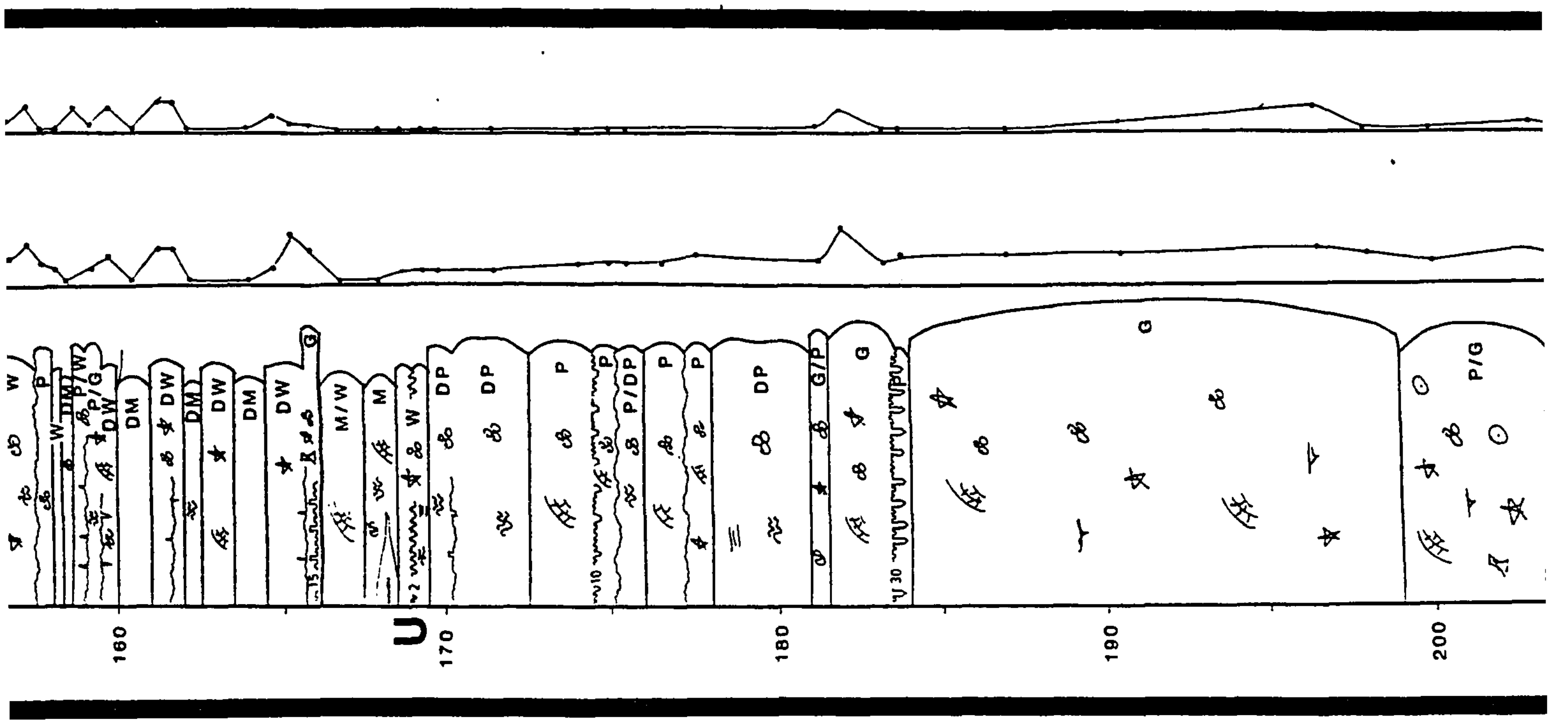
160
170
180
190
200
DM
DW
M/W
DP
P/DP
G/P
G
P/G

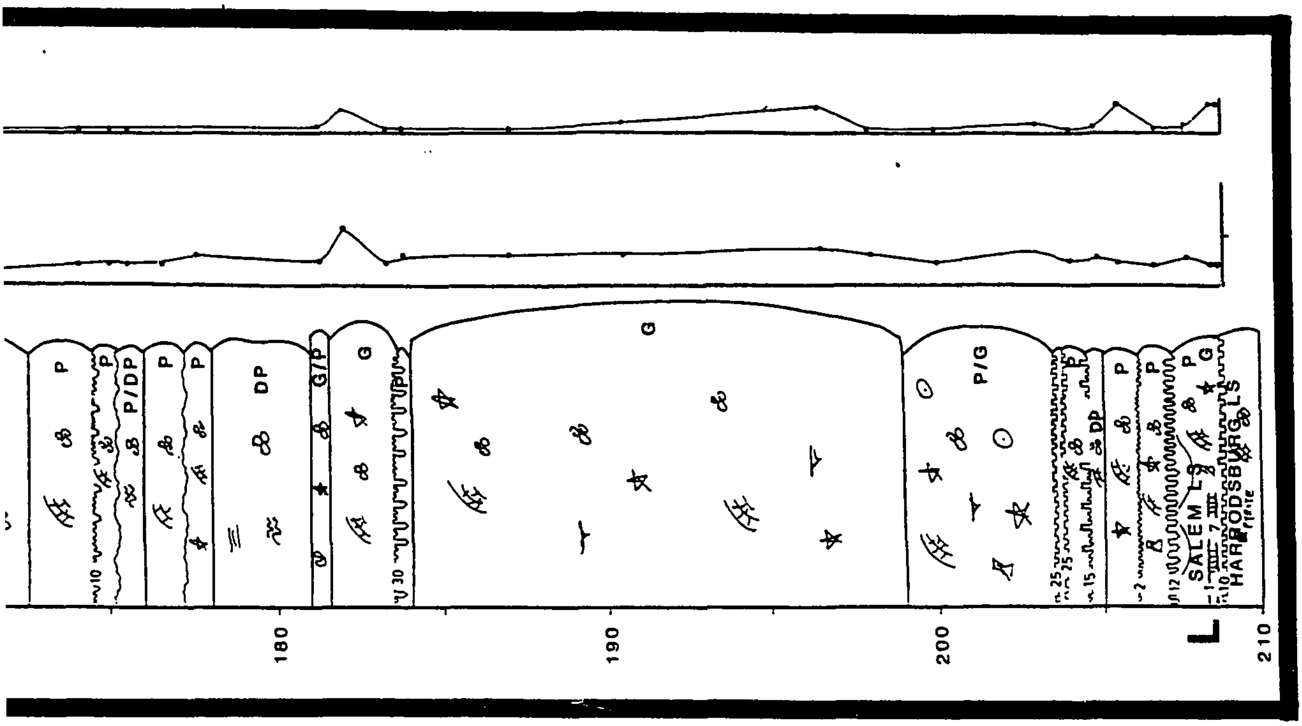
180
190
200
210
SALEM LS
HARRODSBURG LS
P/DP
G/P
P/G
DP

PLATE 9

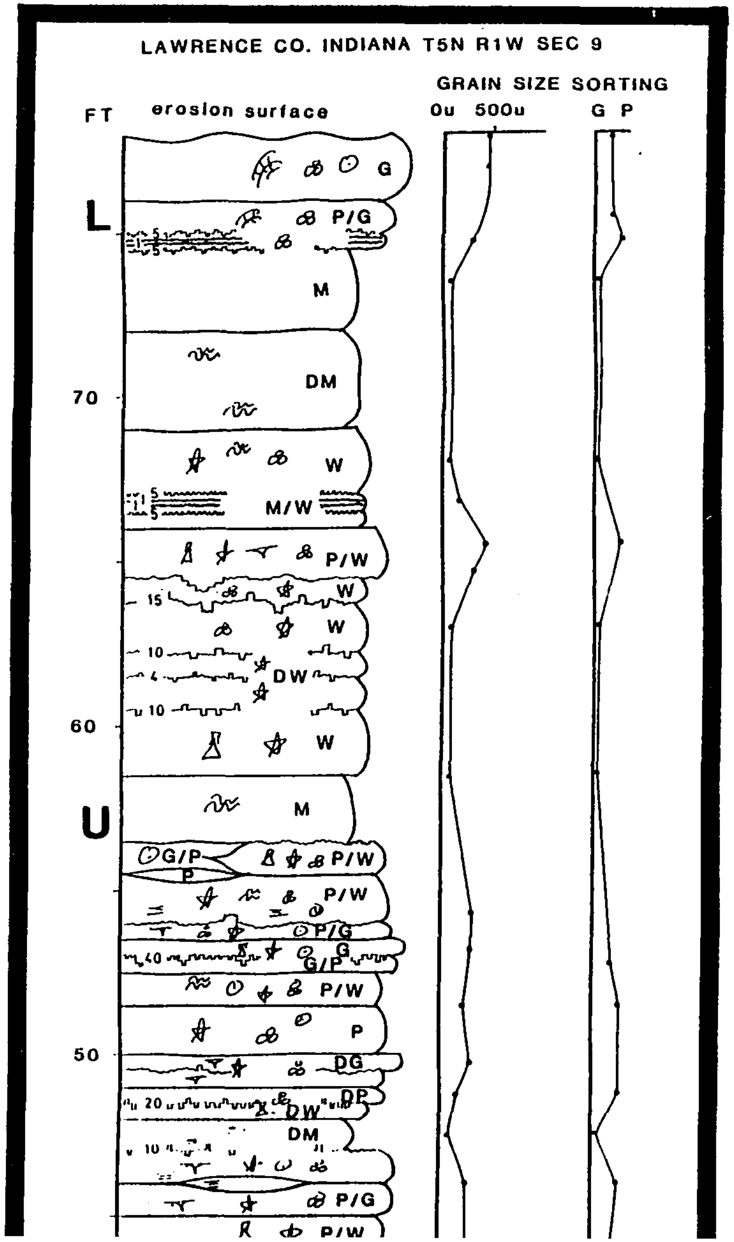
LAWRENCE CO. INDIANA T5N R1W SEC 9
GRAIN SIZE
SORTING
FT
erosion surface
0u 500u
G P
L
U
70
60
50
G
P/G
M
DM
W
M/W
P/W
W
W
DW
W
M
G/P
P
P/W
P/W
P/G
G
G/P
P/W
P
DG
DP
DW
DM
P/G
P/W
15
10
4
10
40
20
10
5
5
5
5

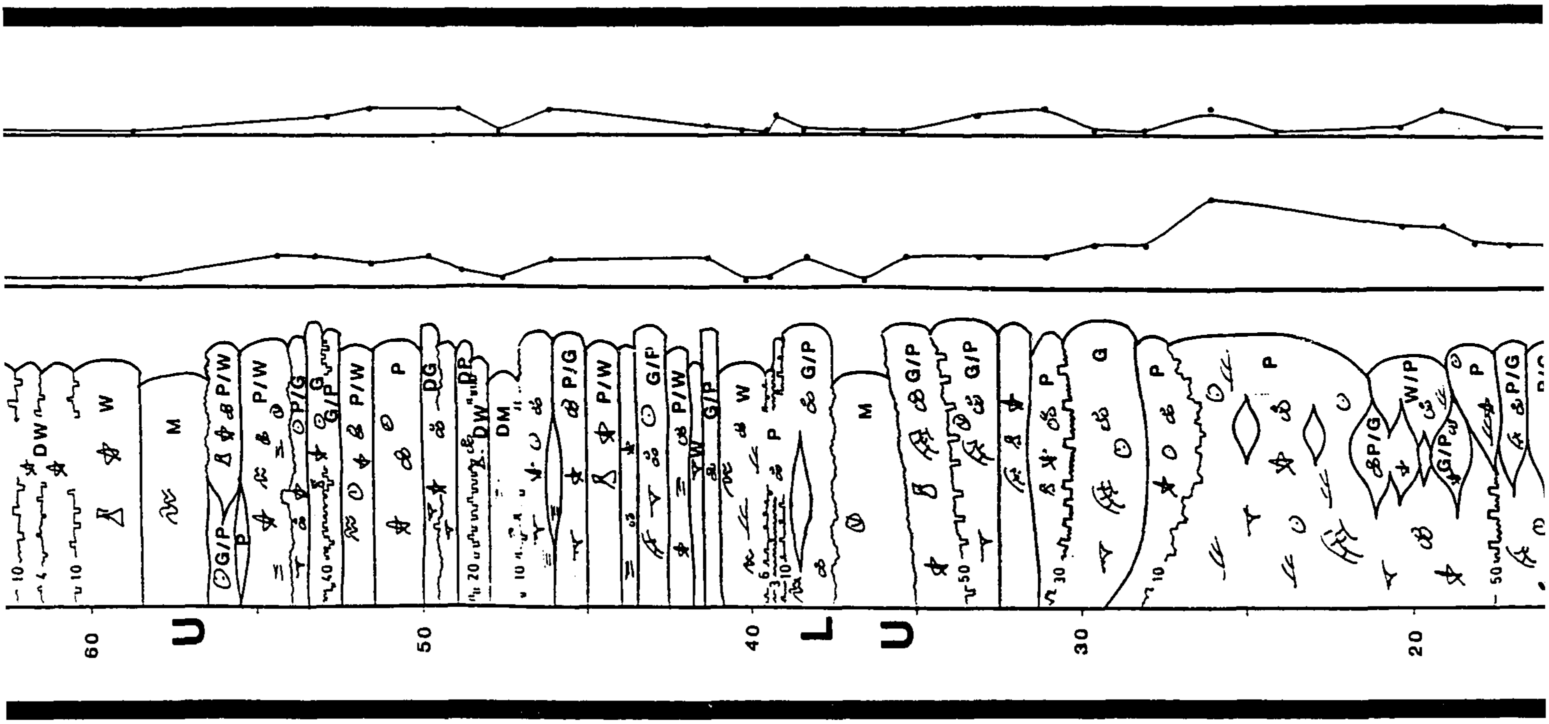
60
50
40
30
20
U
L
U

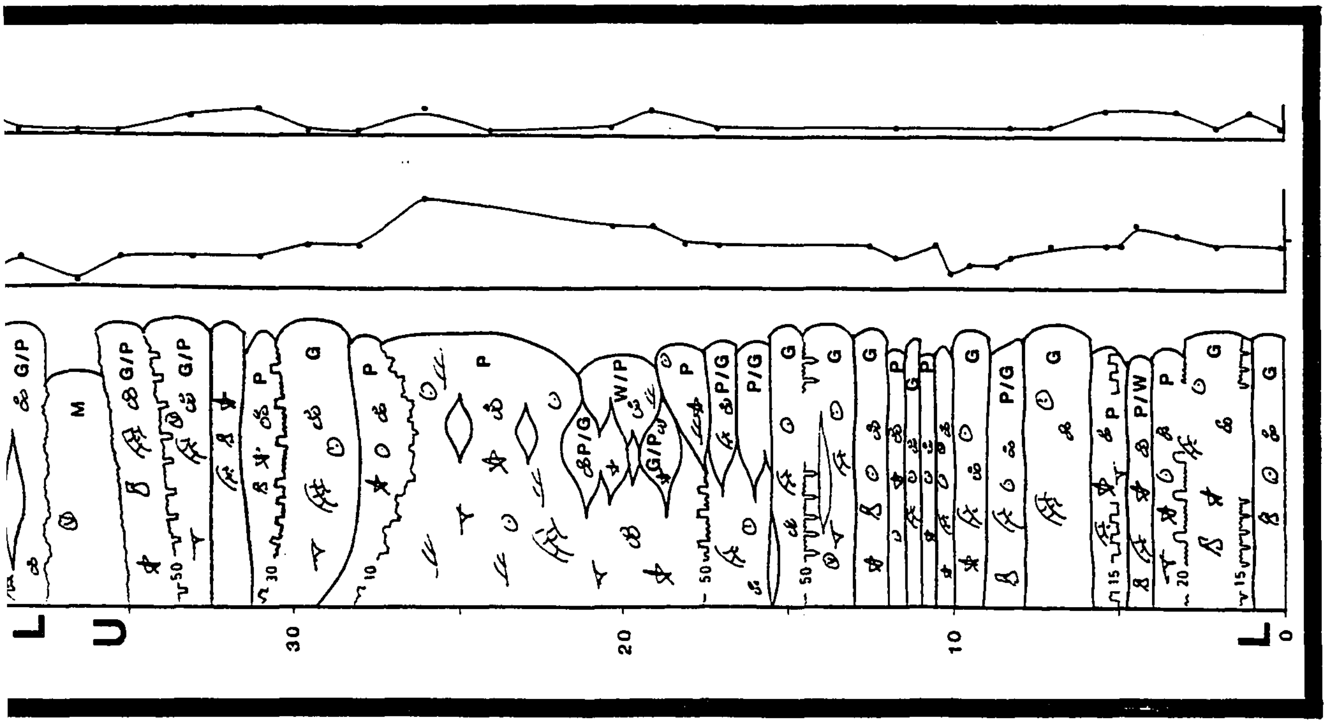

PLATE 10

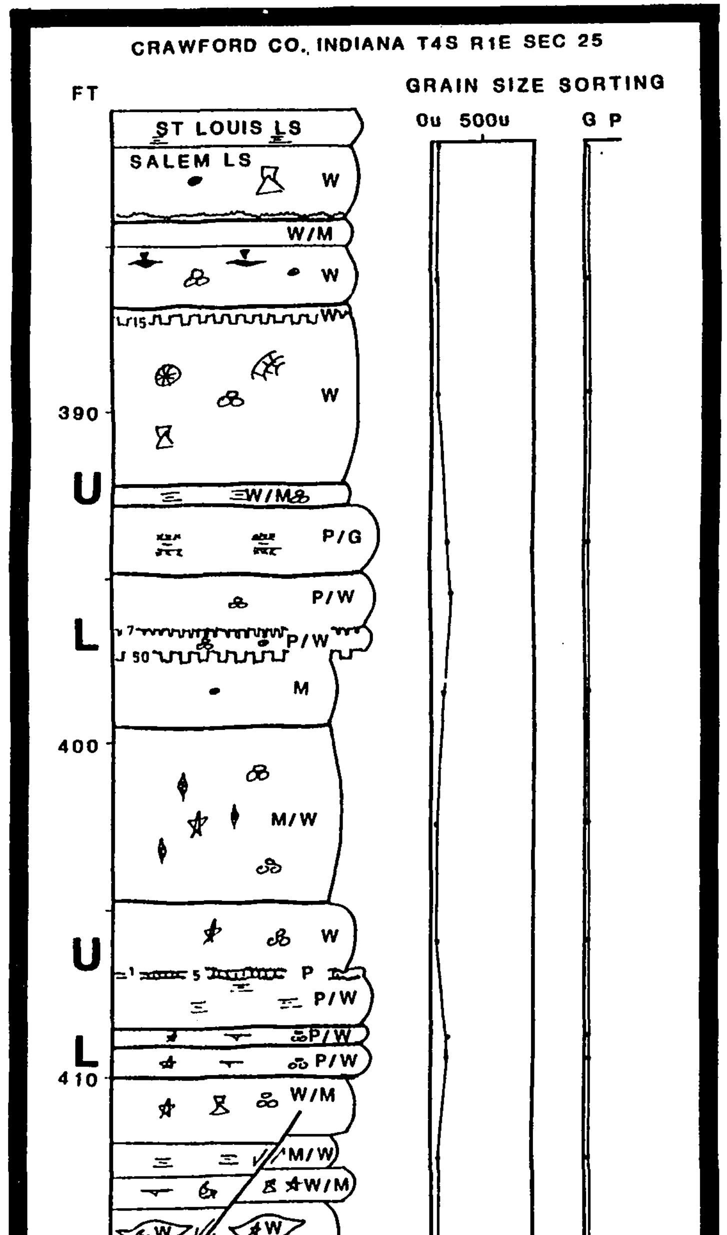

CRAWFORD CO., INDIANA T4S R1E SEC 25
FT
GRAIN SIZE SORTING
0u 500u
G P
ST LOUIS LS
SALEM LS
W
W/M
W
W
390
U
W/M
P/G
L
P/W
P/W
M
400
M/W
U
W
P
P/W
L
P/W
P/W
410
W/M
M/W
W/M
W
W

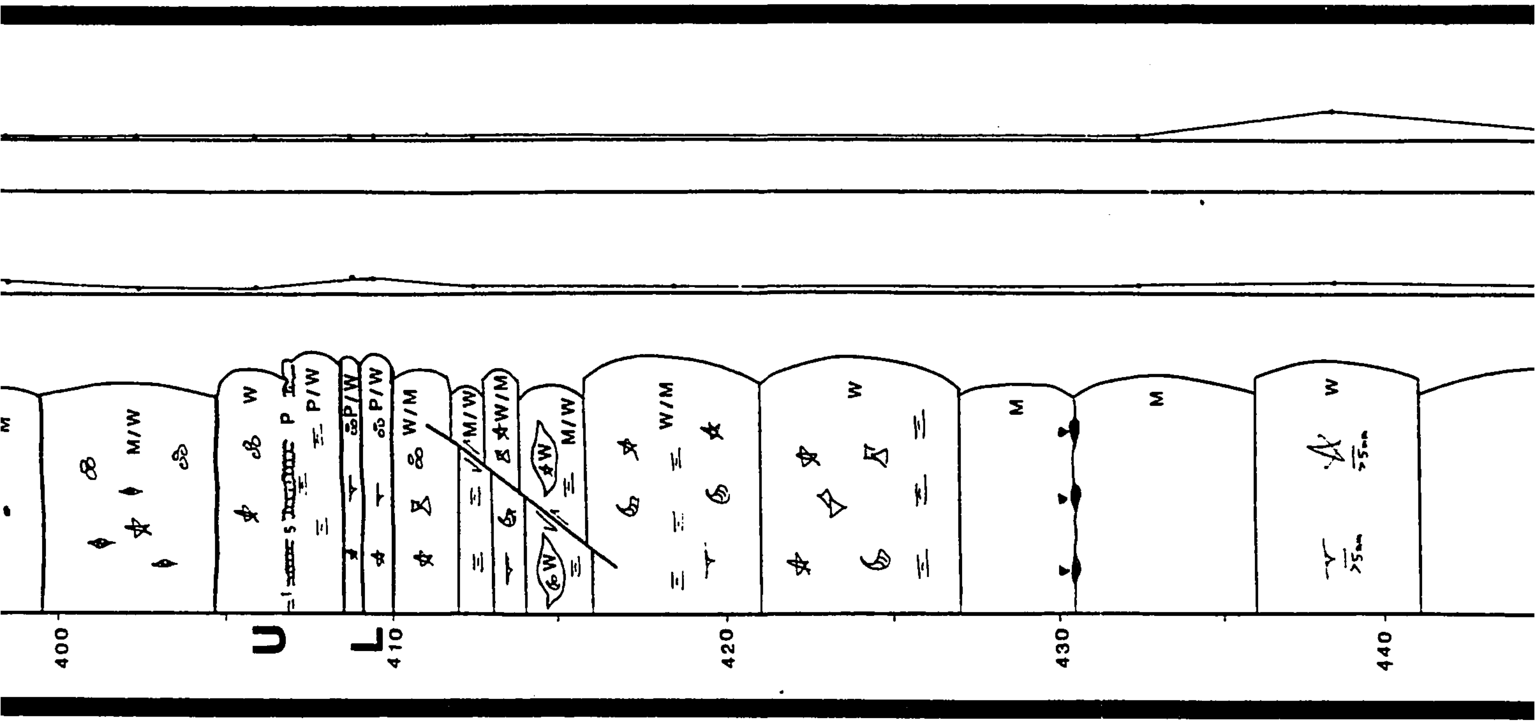
400
U
L
410
420
430
440
M/W
W
P
P/W
W/M
M

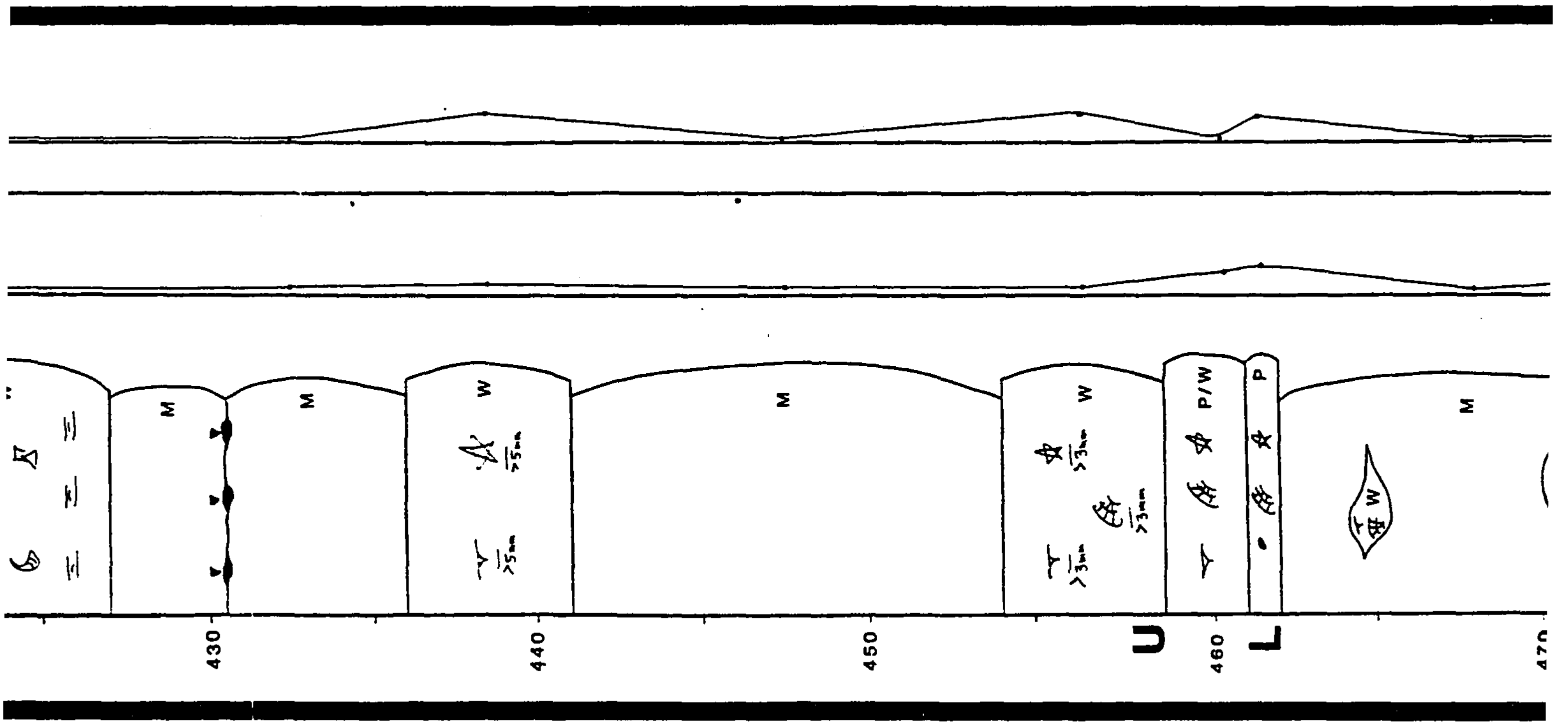
M
M
W
M
W
P/W
P
M
430
440
450
U
460
L

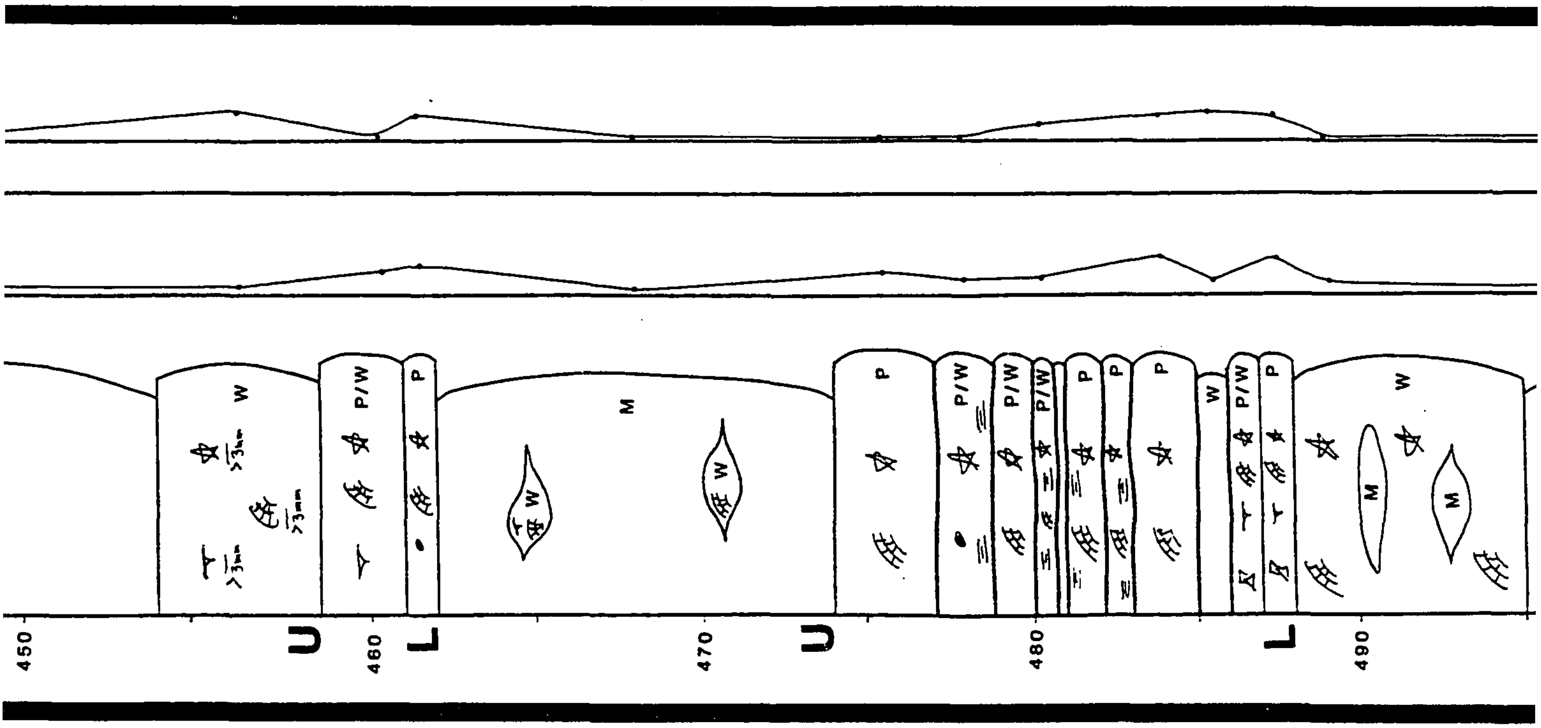

450
460
470
480
490
U
L
U
L
W
P/W
P
M
>3mm

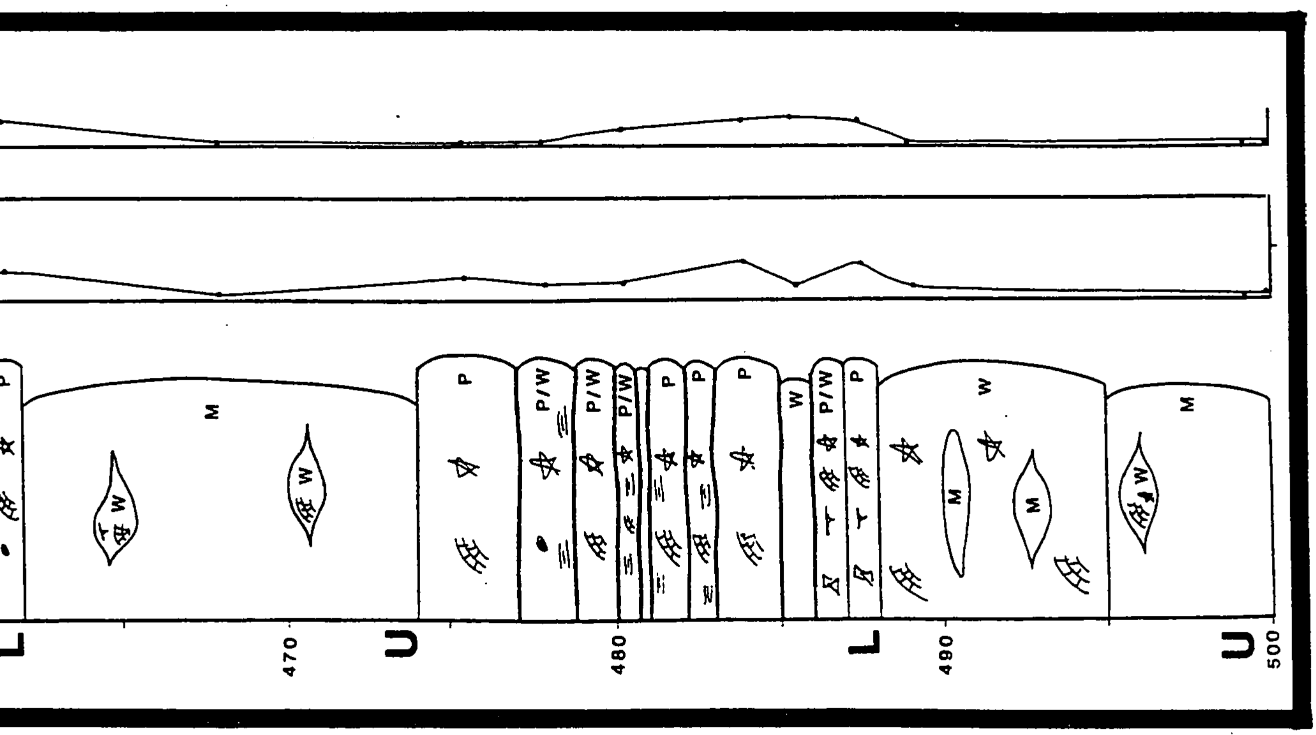

P
M
W
P/W
U
L
470
480
490
500

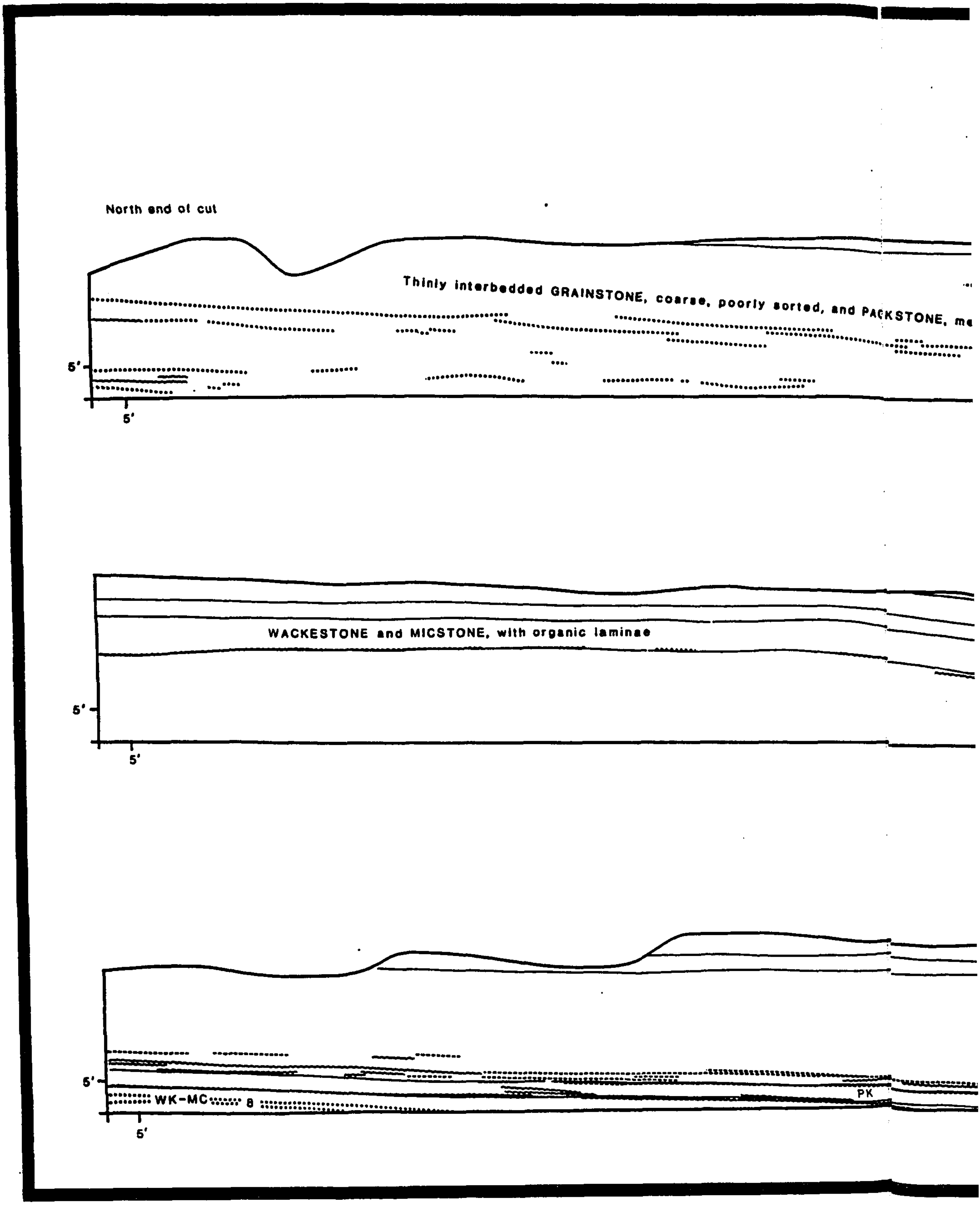
North end of cut
Thinly interbedded GRAINSTONE, coarse, poorly sorted, and PACKSTONE, me
5'
5'
WACKESTONE and MICSTONE, with organic laminae
5'
5'
5'
WK-MC
8
PK
5'

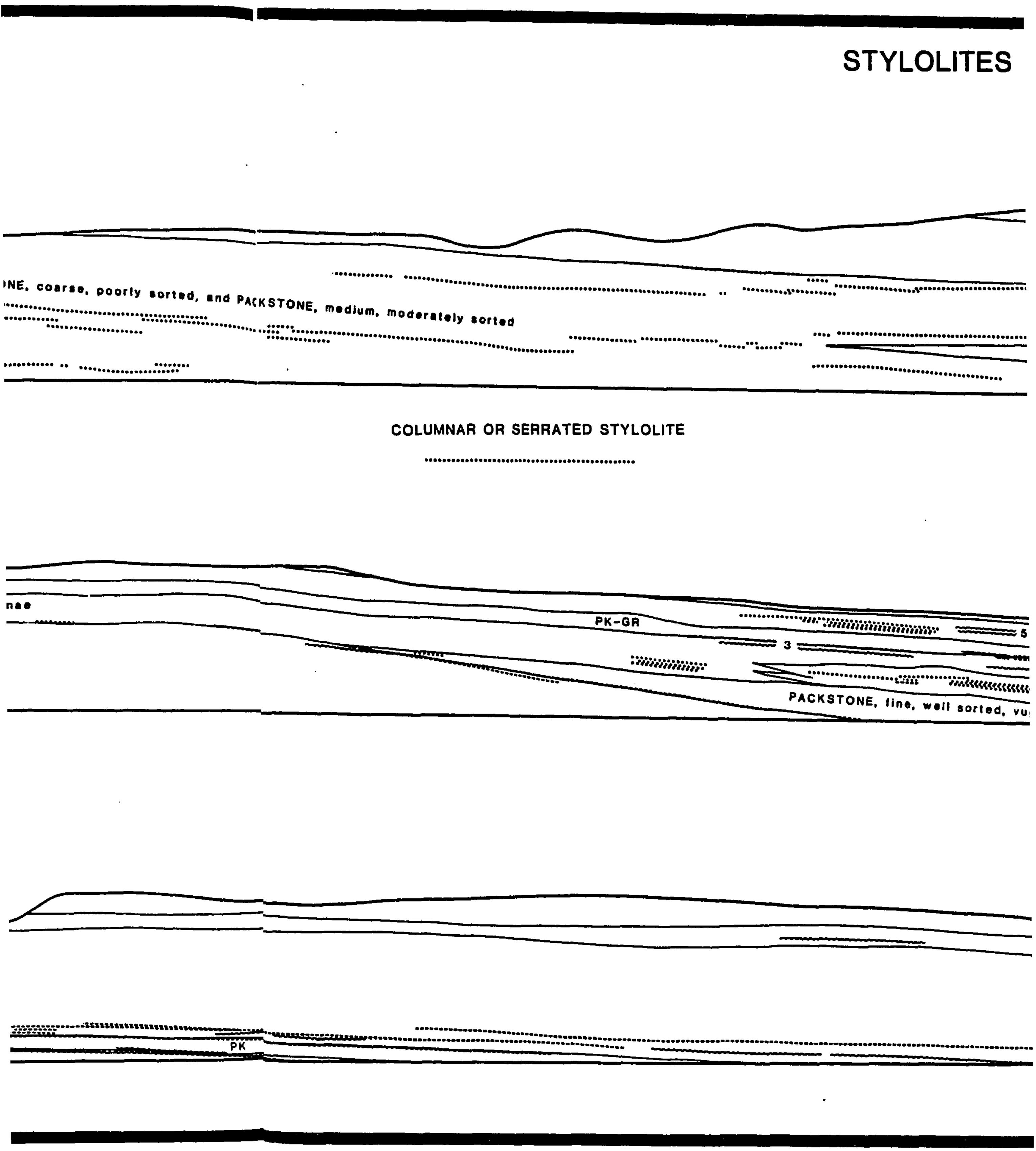
STYLOLITES
NE, coarse, poorly sorted, and PACKSTONE, medium, moderately sorted
COLUMNAR OR SERRATED STYLOLITE
nae
PK-GR
3
5
PACKSTONE, fine, well sorted, vu
PK

PLATE 11

STYLOLITES AND LITHOFACIES IN SALEM LIMESTONE

RC)ADCUT NEAR BEDFORD, INDIANA

Indiana State Route 37, northbound, 1 mile north of Bedford.

R T5N R1W SEC 9, 16

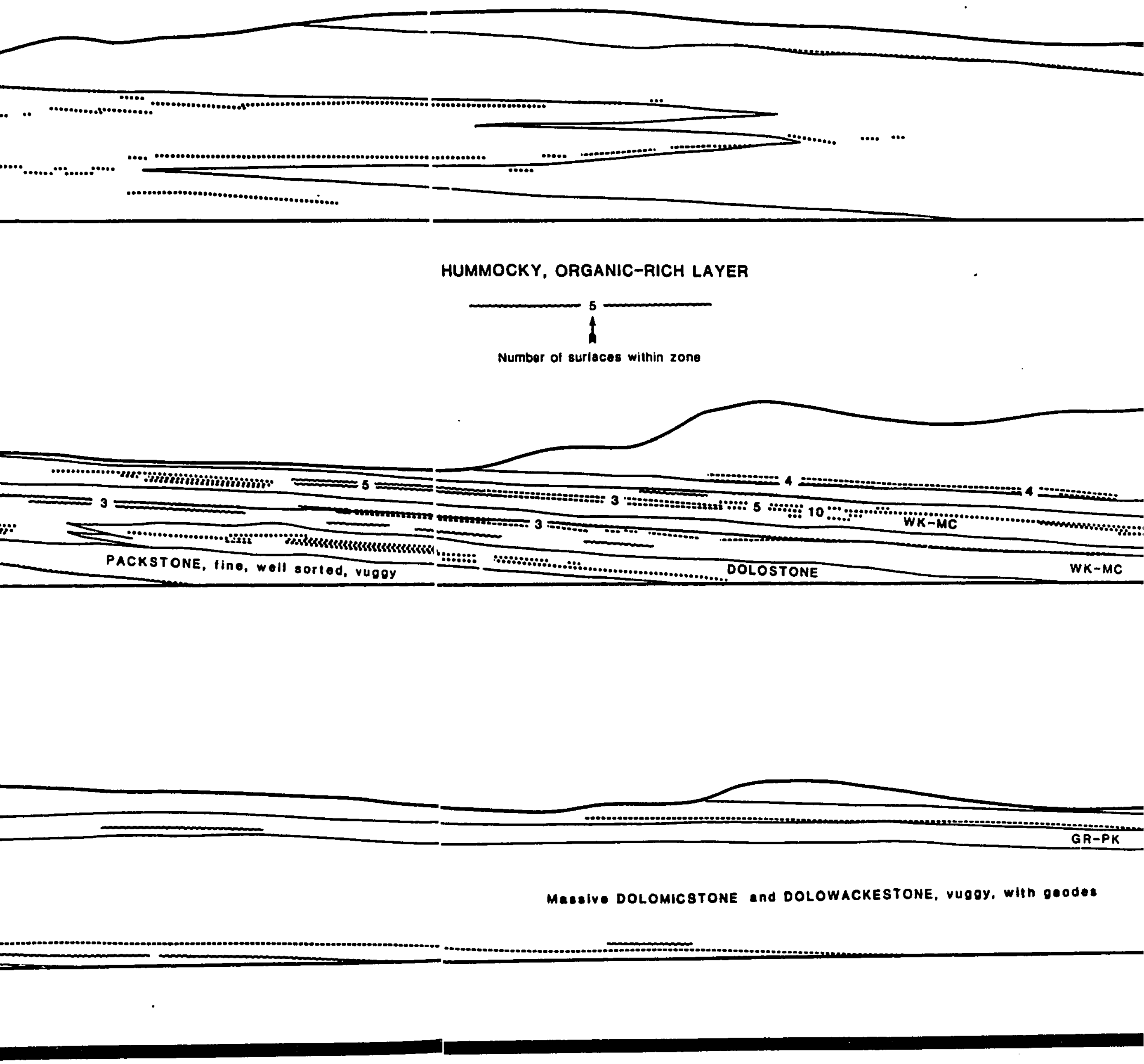

I LIMESTONE

A

dford.

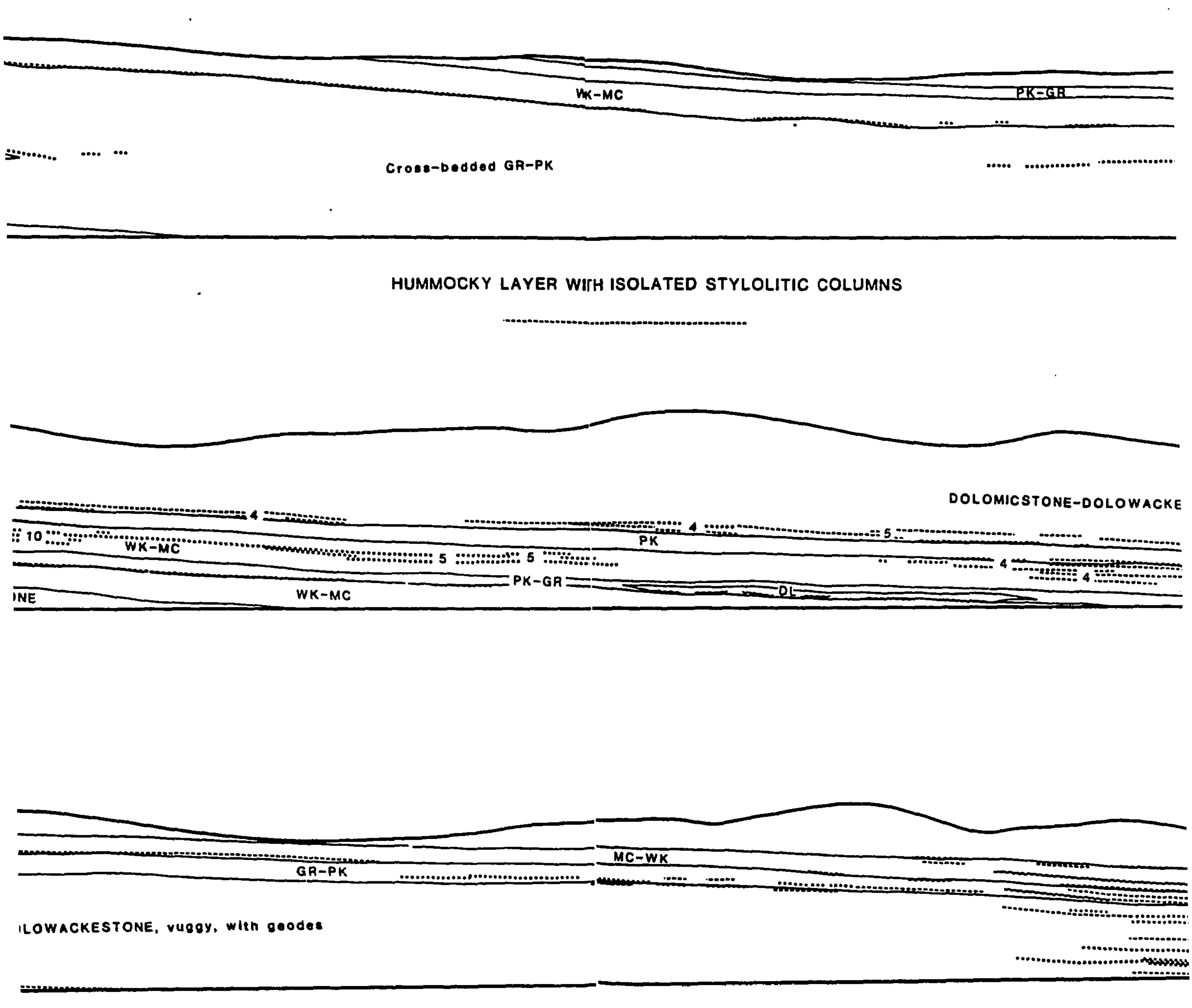

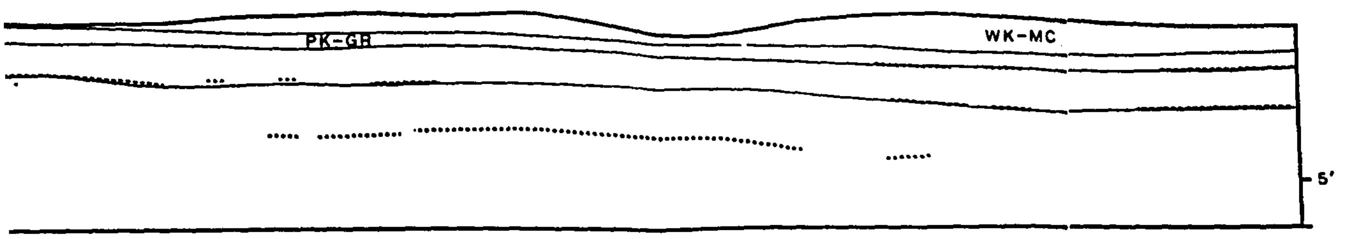
PK-GR
WK-MC
5'

IC COLUMNS

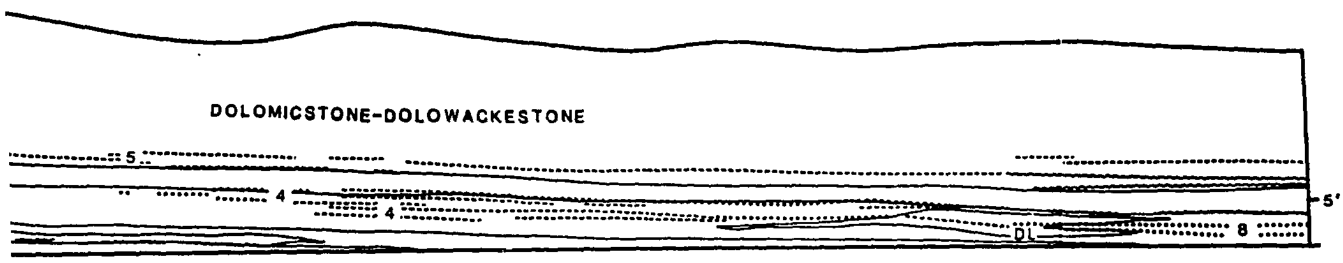
DOLOMICSTONE-DOLOWACKESTONE
5
4
4
DL
8
5'

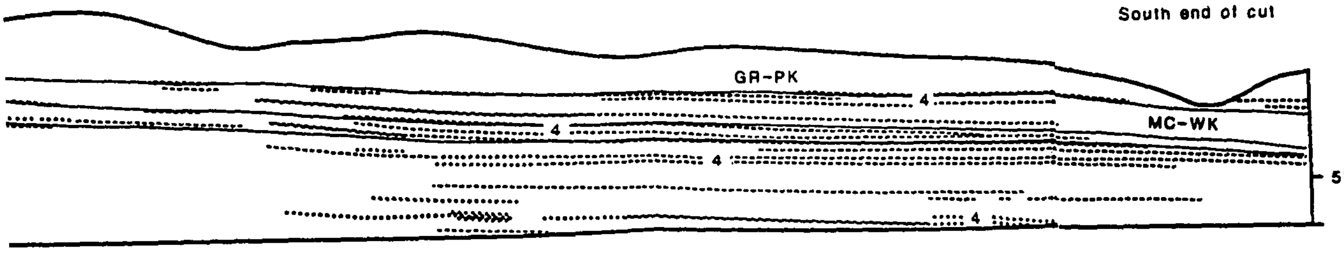
South end of cut
GR-PK
4
4
MC-WK
4
5'
4

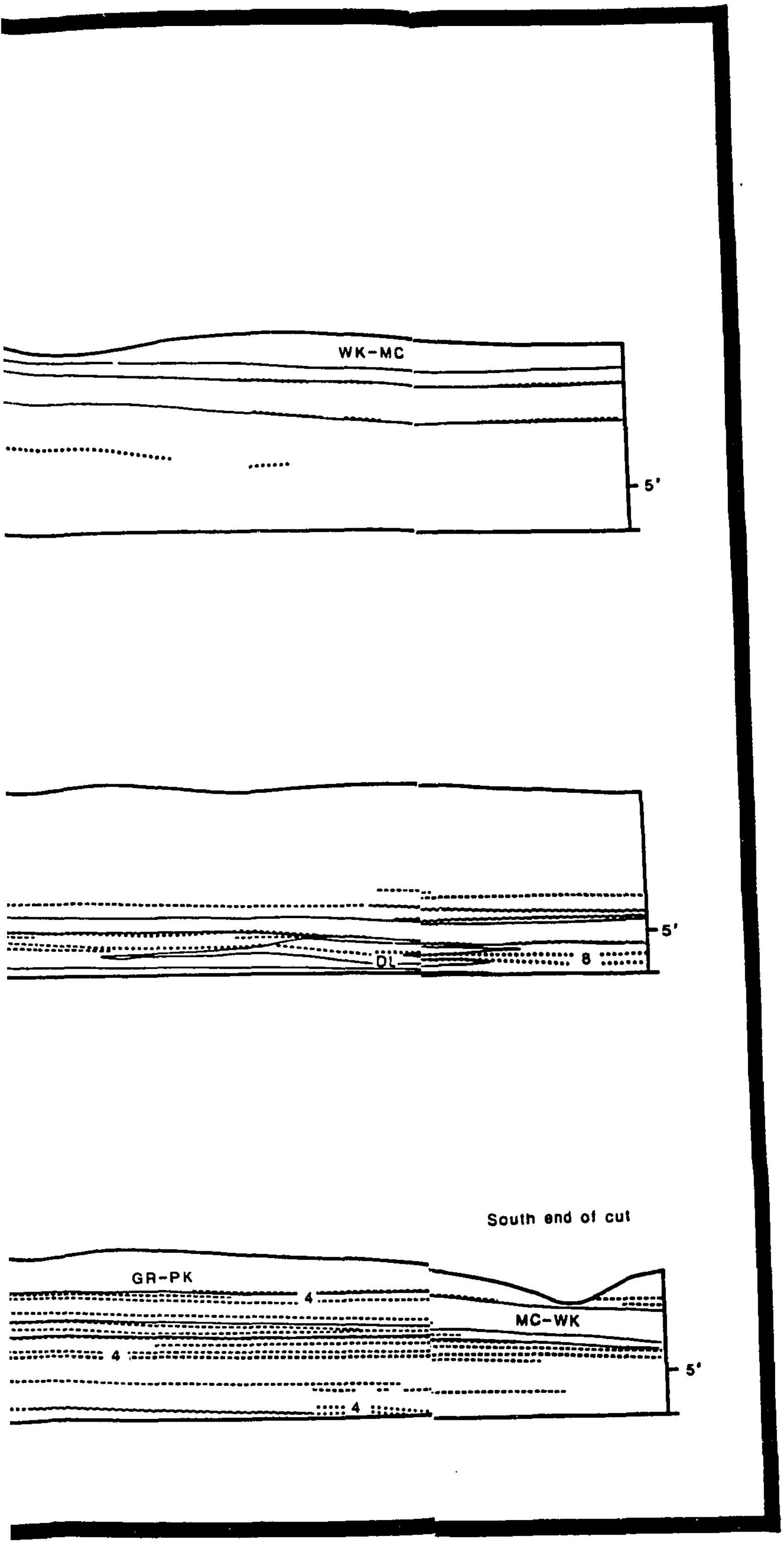
WK-MC
5'
5'
DL
8
South end of cut
GR-PK
4
MC-WK
4
5'
4

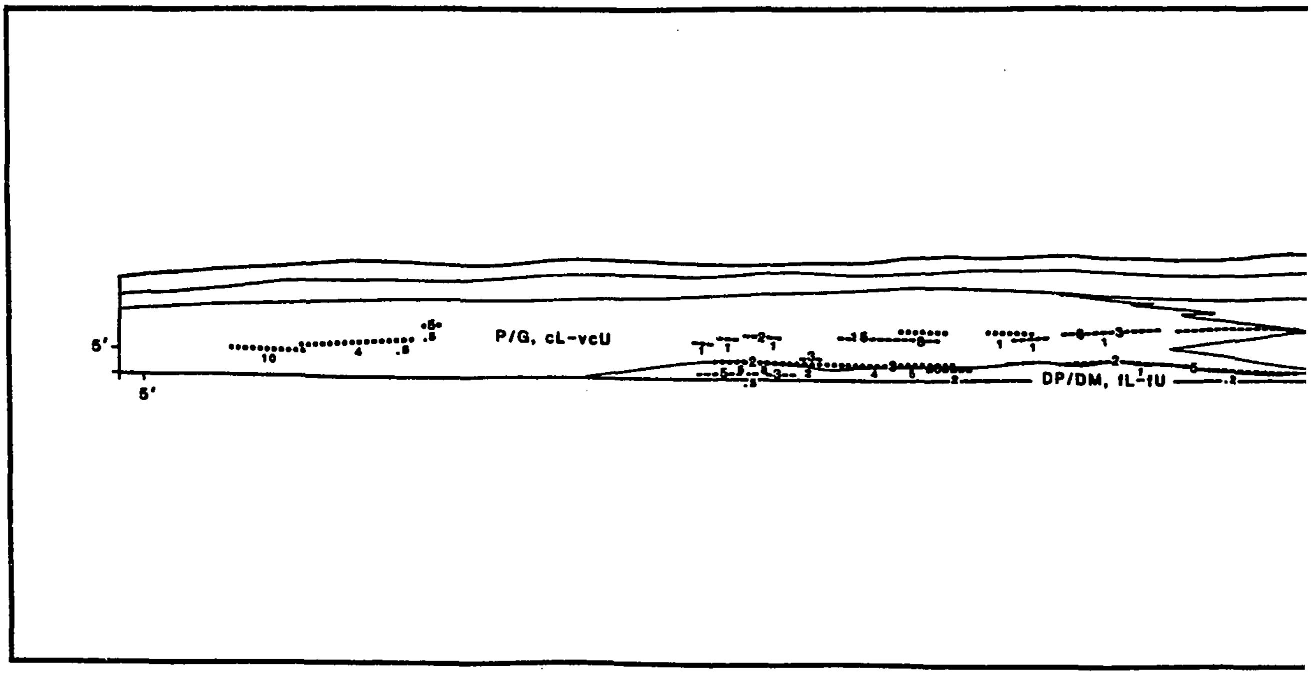
P/G, cL-vcU
DP/DM, fL-fU

PLATE

STYLOLITES AND LITHOFACIE

ROADCUT WEST OF ST.

I-270, northbound, 1 mile

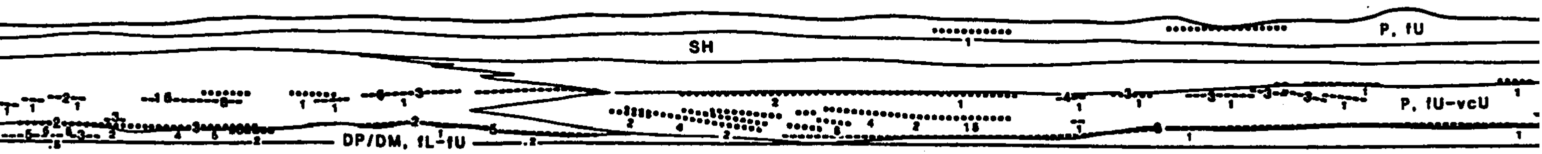

COLUMNAR OR SERRATED STYLOLITE

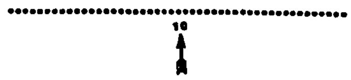

Height of columns, in cm.

PLATE 12

STYLOLITES AND LITHOFACIES IN SALEM LIMESTONE

ROADCUT WEST OF ST. LOUIS, MISSOURI

I-270, northbound, 1 mile south of jct. I-44.

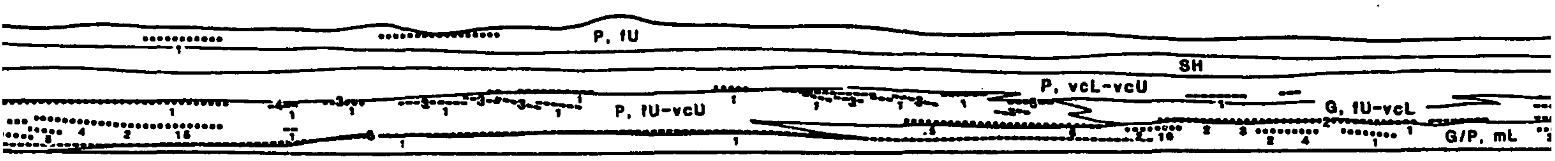

COLUMNAR OR SERRATED STYLOLITE

Height of columns, in cm.

HUMMOCKY SEAM WITH ISOLATED STYLOLITE COLUMNS

Number of seams in zone

EM LIMESTONE

SOURI

4.

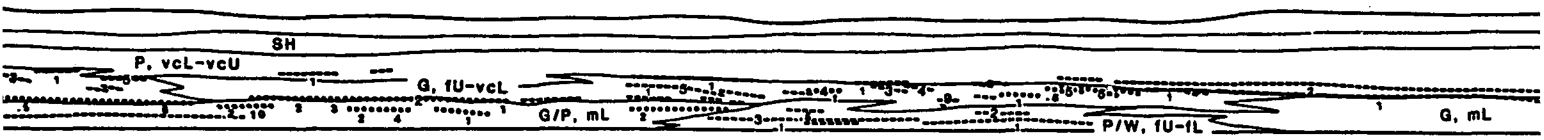

DCKY SEAM WITH ISOLATED STYLOLITE COLUMNS

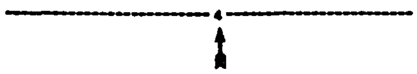

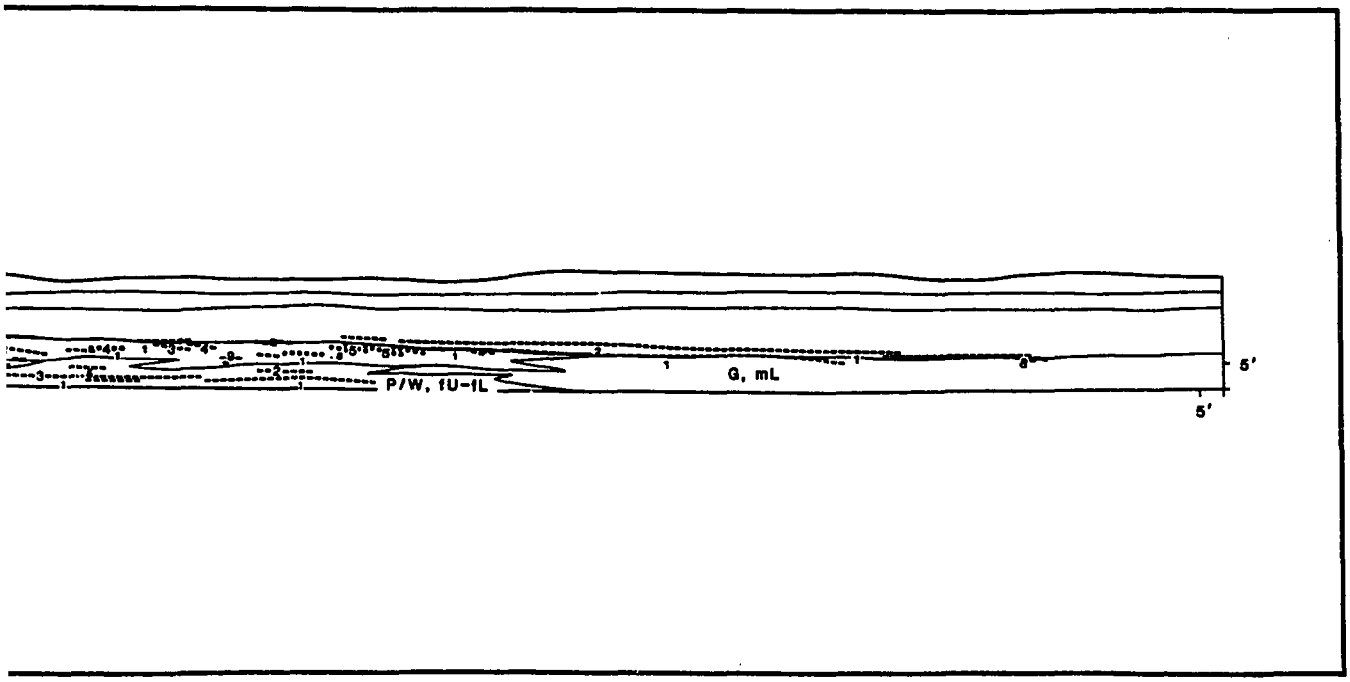
P/W, fU-fL
G, mL
5'
5'

PLATE 13

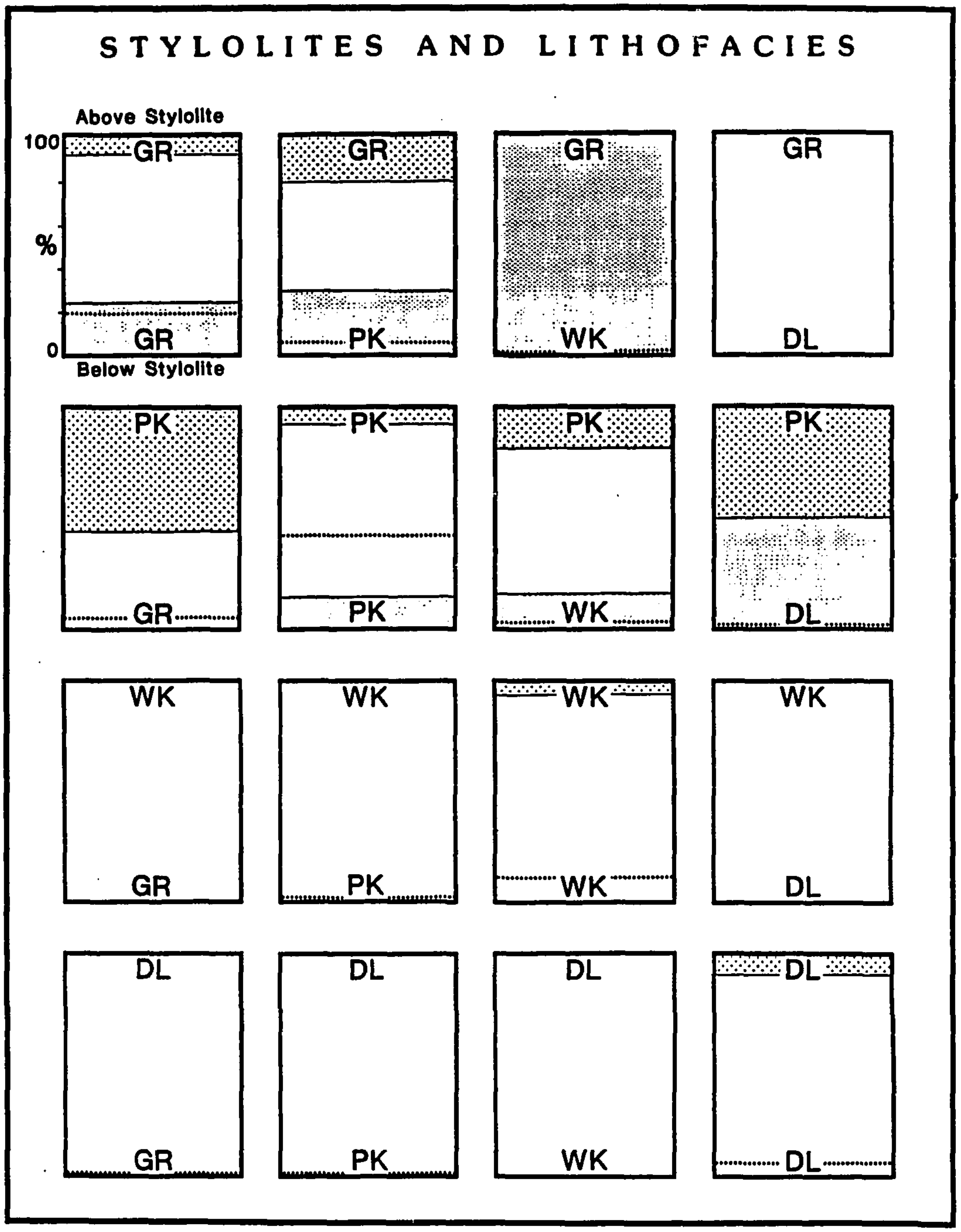
STYLOLITES AND LITHOFACIES
Above Stylolite
100
%
0
Below Stylolite
GR
GR
GR
PK
GR
WK
GR
DL
PK
GR
PK
PK
PK
WK
PK
DL
WK
GR
WK
PK
WK
WK
WK
DL
DL
GR
DL
PK
DL
WK
DL
DL